



# Valorization of by-products and products from agro-industry for the development of release and rejuvenating agents for bituminous materials

Peter Mikhailenko

## ► To cite this version:

Peter Mikhailenko. Valorization of by-products and products from agro-industry for the development of release and rejuvenating agents for bituminous materials. Material chemistry. Université Paul Sabatier - Toulouse III, 2015. English. NNT : 2015TOU30094 . tel-01445294

**HAL Id: tel-01445294**

**<https://theses.hal.science/tel-01445294>**

Submitted on 24 Jan 2017

**HAL** is a multi-disciplinary open access archive for the deposit and dissemination of scientific research documents, whether they are published or not. The documents may come from teaching and research institutions in France or abroad, or from public or private research centers.

L'archive ouverte pluridisciplinaire **HAL**, est destinée au dépôt et à la diffusion de documents scientifiques de niveau recherche, publiés ou non, émanant des établissements d'enseignement et de recherche français ou étrangers, des laboratoires publics ou privés.



# THÈSE

**En vue de l'obtention du**

## **DOCTORAT DE L'UNIVERSITÉ DE TOULOUSE**

**Délivré par :**

Université Toulouse 3 Paul Sabatier (UT3 Paul Sabatier)

---

**Présentée et soutenue par :**

**Peter Mikhailenko**

**le** mercredi 15 juillet 2015

**Titre :**

Valorization of by-products and products from agro-industry for the development of release and rejuvenating agents for bituminous materials

---

**École doctorale et discipline ou spécialité :**

ED MEGEP : Génie civil

**Unité de recherche :**

Laboratoire Matériaux et Durabilité des Constructions

**Directeur/trice(s) de Thèse :**

M. Erick Ringot

**Jury :**

M. Emmanuel Chailleux, Directeur de Recherche, IFSTTAR, Nantes, Rapporteur

M. Christophe Petit, Professeur des Universités, IUT Limoges, Rapporteur

M. Medhat Shehata, Professor and Associate Chair, Ryerson University, Toronto, Examineur

M. Gilles Escadeillas, Professeur des Universités, IUT Toulouse III, Examineur

M. Erick Ringot, Professeur des Universités, Université de Toulouse III, Directeur de thèse

Mme Alexandra Bertron, Maître de Conférences HDR, IUT Toulouse III, Co-encadrant de thèse



# Abstract

---

The growing health and environmental concerns brought on by the use of petroleum based products in the asphalt construction industry have necessitated the development of alternatives. Infrastructure, especially that involving transportation has many uses for petroleum products including, as fuel, as well as in asphalt pavement construction – where petroleum products have traditionally constituted the binder for the mix as well as the rejuvenating agents (for asphalt recycling) – along with various agents used in the construction process including bitumen removers and asphalt release agents. Thus, there is a need to replace petroleum base agents with bio-sourced and biodegradable substitutes.

The present work is part of a project to develop bio-sourced (recycled from agricultural waste) products for the construction industry. This work is dedicated to developing products relating to the asphalt industry. Two types of product applications were envisioned: i) an asphalt release agent (ARA) and ii) an asphalt rejuvenating agent. Additionally, a bitumen remover (BR) developed as part of the work on the ARA.

ARAs prevent asphalt from adhering to tools and equipment used in asphalt production, without producing overly negative side effects with regards to the pavement. Three principal tests methods were developed and optimized for the performance and damage to asphalt of the ARAs. The asphalt slide test was developed to quantify the performance of the ARA by sliding hot asphalt mix down a plate with the ARA applied. The testing of the damage to asphalt from ARAs consisted of testing an asphalt cylinder – in contact with an ARA for seven days – in indirect-tensile strength (ITS). The bitumen degradation test consisted of submerging a bitumen sample in an agent over a certain time and weighing the bitumen that did not dissolve in the agent. This was followed by the observation of the bitumen-ARA chemical interaction by FTIR spectrometry. This test served as an assessment of ARA damage to bitumen as well as of the performance of BRs.

The testing of the commercial ARAs from both the French and USA markets found that they had two primary modes of functioning: i) by softening the bitumen and ii) by forming an interface between the asphalt and the metal surface. While some agents had elements of both, it was found that interface agents are preferable, due to the ability to use a single ARA application for multiple occasions. With this completed, a water-based bio-sourced substrate ARA – based on glycerol derived from agricultural waste – was developed. The



commercially available BRs were tested as well, finding that i) the most effective BRs had the highest ester concentration and ii) that highly concentrated short chained ester (C7-10) were very effective bitumen dissolvers.

The goal of rejuvenating agents is to regenerate the old bitumen from recycled asphalt pavement (RAP) by restoring the original properties and ensuring the stability of these properties over time. This part consisted of the development of methods for bitumen and aging, as well as characterization of the chemical rejuvenation of bitumen by FTIR spectrometry (including imaging) and thermogravimetric analysis. Bio-sourced oleo polyol was evaluated as a rejuvenating agent. For the imaging, a mastic polishing method was developed in order to attain as samples as flat as possible for the analysis.

The bitumen rejuvenation was observed using FTIR spectroscopy analysis. Several peaks (notably  $I_{C=O}$  and  $I_{S=O}$ ) were observed for bitumen oven aged up to 42 days (long term). It was found that an oven aging period of 14 days was roughly equivalent to bitumen aged by a RTFOT+PAV cycle in terms of rheology and penetration. The mastic (aged for 14 days) was then combined with a bio-sourced agent (at 7.5%w of mastic). It was found by FTIR imaging that the oxidation indicator  $I_{S=O}$ , was reduced by the incorporation of the rejuvenating agent.

*Keywords: asphalt release agent (ARA), bitumen remover (BR), asphalt testing, biodegradable, road construction, bitumen aging, FTIR, RAP, rejuvenating agent*



# Acknowledgements

---

School children are often mistakenly taught that scientific progress is the work of this or that individual innovator. The reality is that all research is built upon hundreds of years of scientific advancement before it, and that serious advancement is achieved by the scientist only with the continued mentoring, technical and moral support of those around them.

With that said I would like to thank the ARGIBTP project for giving me an opportunity to work on this exciting and innovative project. I thank all of the members of the ARGIBTP project without who I have had the pleasure to work with and who have made invaluable contributions to my work.

I thank my co-director Alexandra Bertron for her guidance in this the process of planning, interpreting, presenting and writing the work. I thank my director Erick Ringot for his guidance and material support during the project.

I thank Gilles Escadeillas for his role in the project, particularly for his insightful reviews of my work.

I thank my defense jury members Emmanuel Chailleux and Medhat Shehata for their review of my dissertation and the valuable contributions at my defense.

I thank the technical staff at LMDC for their invaluable support and advice during my experimental program. Notably Guillaume Lambare, Bernard Attard, Marc Begué, Sylvain Dos Santos, Yann Bouaskeur, Laurent Boix, Carole Soula, Vanessa Mazzars, Maude Schiettekatte and David Guillouset. I also thank the administrative staff of LMDC for helping me with a whole range of administrative procedures that exist at LMDC, notably Fabienne Lacoste and Ghislaine Dupouey.

I thank the professors, who have helped me with a number of technical questions and also my doctoral colleagues who were there for moral support. Thanks to Youssef, Buchette, Ilgar, Nam, Sylvain, Pablo, Carolina, Laila, Titi, Elsa, Julie A, Célimène, Célestine, Laurent, Marilia, Boubacar, Thomas V, Kahina, Maha, Belal, Isabelle, Thomas M, Khadim, Nuraziz, Remi, Aurelie, Mouss, Oly, Xiaoxiao and Anh Quan. Love and thanks also to my office-mates Hugo, Ndine, Said, Tito, Gael and Ponleu.

Thank you to my housemates for a fun year of living together and for understanding when I was a bit stressed (and absent) during my redaction period.

Thank you to all my friends in Toulouse who made the last three years enjoyable outside of the office notably Robin and Anne-Cecile.

Thank you to all of my Toulouse comrades, you know who you are.

Thank you to all of my friends back in Toronto for continuing a long distance friendship.

Thank you most of all to my family for constantly encouraging me to educate myself and doing everything possible to support me in this regard. See you soon!

# Table of Contents

1	Introduction.....	8
2	Bibliography.....	12
2.1	General aspects of asphalt pavement.....	13
2.1.1	Paving .....	13
2.1.2	Aggregates.....	14
2.1.3	Bitumen chemical composition and structure .....	15
2.1.4	Bitumen properties and testing .....	27
2.1.5	Special types of bitumen .....	30
2.1.6	Conclusions on the general aspects of asphalt .....	31
2.2	Asphalt release agents .....	32
2.2.1	Petroleum based ARAs .....	33
2.2.2	Bio-based ARAs.....	34
2.2.3	Laboratory testing of ARAs.....	35
2.2.4	Bitumen solubility.....	38
2.2.5	Conclusions on ARAs .....	39
2.3	Reclaimed asphalt pavement (RAP) and bitumen rejuvenation .....	39
2.3.1	Bitumen aging.....	40
2.3.2	Recycling methods.....	57
2.3.3	Requirements for using in new asphalt.....	58
2.3.4	Variability of RAP and laboratory manufactured RAP .....	59
2.3.5	RAP blending with virgin binder .....	60
2.3.6	Asphalt recycling agents.....	63
2.4	Conclusions of the bibliographic study.....	69
3	Determination of the performance and damage to asphalt of bio-sourced asphalt release agents and bitumen removers.....	71
3.1	Introduction and objectives of study .....	71
3.2	Materials.....	72
3.2.1	Asphalt release agents and bitumen removers.....	72
3.2.2	Bitumen .....	75
3.2.3	Asphalt.....	76

3.3	Development of test methods for the determination of asphalt release agent (ARA) performance.....	78
3.3.1	ARA Performance Evaluation Apparatus.....	78
3.3.2	Asphalt Slide Test .....	81
3.3.3	Determining asphalt slide test validity and parameter optimization.....	83
3.3.4	Discussion on the development of test methods for ARA performance .....	86
3.4	Development of test methods for the determination of asphalt release agent damage to asphalt and bitumen remover performance.....	88
3.4.1	ARA degradation of asphalt.....	88
3.4.2	Degradation by asphalt release agents and bitumen removers of bitumen and construction materials.....	100
3.4.3	Discussion on the development of test methods to determining the degradation of asphalt by ARAs and BRs .....	103
3.5	Performance and degradation of asphalt by commercial asphalt release agents and bitumen removers .....	105
3.5.1	Test results .....	106
3.5.2	Discussion .....	113
3.6	Bio-sourced formulations as asphalt release agents and bitumen removers asphalt release agents.....	117
3.6.1	Glycerol-based formulations .....	117
3.6.2	Test results .....	122
3.6.3	Discussion on the development of bio-sourced formulations .....	135
3.7	Conclusion for the determination of the performance and damage to asphalt of bio-sourced asphalt release agents and bitumen removers.....	138
4	Physico-chemical characterization of bitumen aging, rejuvenation and remobilization by rejuvenating agent .....	141
4.1	Bitumen remobilization by SEM-EDS analysis.....	142
4.1.1	Materials and methods .....	142
4.1.2	Results and discussion .....	146
4.1.3	Conclusions of the characterization of bitumen remobilization by SEM-EDS.....	153
4.2	Physico-chemical characterization of bitumen aging and rejuvenation .....	154
4.2.1	Materials and methods .....	154
4.2.2	Results and discussion .....	163
4.3	Conclusions on bitumen aging, rejuvenation and remobilization.....	180

5	General conclusions and perspectives .....	182
	Determination of the performance and damage to asphalt of bio-sourced asphalt release agents and bitumen removers .....	183
	Physico-chemical characterization of bitumen aging, rejuvenation and remobilization by rejuvenating agent .....	185
	Perspectives.....	186
	References.....	189
	List of Tables .....	203
	List of Figures.....	205
	Appendix A. Bitumen testing .....	213
	Softening point .....	213
	Penetration index .....	214
	Flash point .....	214
	Viscosity .....	214
	Fraas breaking point .....	215
	Solubility .....	215
	Density / specific gravity .....	216
	Cohesion .....	216
	Ductility test .....	216
	Adherence of bitumen to aggregates.....	217
	Appendix B. Asphalt gradation and fabrication.....	218
	Gradation of asphalt.....	218
	Equipement for the fabrication of asphalt mix .....	219
	Appendix C. Bitumen Flow Test.....	220
	Appendix D. Bitumen Degradation Test FITR-ATR results .....	222
	Commercial agents.....	222
	Candidate formulations.....	226
	Appendix E. Bitumen microscopy.....	232

# 1 Introduction

The global construction industry has had a long history of innovation in order to make construction feasible in various situations. While these innovations in many cases have allowed for faster construction and the use of fewer resources, there have been cases where worker and environmental health have been compromised.

Infrastructure, especially transportation infrastructure, has many uses for petroleum products, including as fuel (Esteban et al., 2012). In asphalt pavement construction, where petroleum products have traditionally constituted the binder for the mix as well as the rejuvenating agents (Romera et al., 2006), along with various agents used in the construction process including bitumen removers (BRs) (Mikhailenko et al., 2015b) and asphalt release agents (ARAs) (Tang and Isacsson, 2006). While many of these products have been shown to be effective in their applications, the health hazards caused by these products to the worker at construction sites have been notable (Acton, 2013; Rosner et al., 1996). There is also substantial evidence that these chemicals are major pollutants of soils, ground waters and any environments where they are used (Marchal et al., 2003; Tang, 2008).

At this time, with growing environmental and workplace health concerns (Acton, 2013; Tang, 2008), there is a need to replace petroleum based agents with biodegradable substitutes. Some of the alternatives to petroleum based products are fatty-oil based products. They are biodegradable and work well at high temperatures. Fatty oils are regarded as environment-friendly, but the health effects of their mist should not be neglected. In the United States, the Occupational Safety and Health Administration (OSHA) has found that exposure to vegetable oil mist can lead to a variety of health and safety hazards, including problems with vision, eye tearing, and skin irritation. In addition, certain additives to ARAs – which can include monocyclic and polycyclic aromatic hydrocarbons, may also present health effects – although less than for petroleum based products (Tang, 2008). There exists the potential to incorporate various recycled bio-oils into the newly formulated products, adding a further environment benefit.

This research was realized in the context of the AGRIBTP collaborative project, which aimed to develop a new branch of industry dedicated to the production of new formulations for the construction industry from the processing products and by-products of vegetable oils and animal fats in South-West France. Four types of product applications were envisioned: (i) release agents for concrete formwork, (ii) curing compounds for fresh concrete, (iii)

asphalt release agents for the protection of tool and equipment from hot mix asphalt and (iv) asphalt rejuvenating agents for the regeneration of aged bitumen in recycled asphalt pavement (RAP).

The first phase of the project aimed to develop (i) molecules that functionalize the raw materials from agricultural resources and (ii) chemical processes for processing the raw materials. More specifically, this aimed to recover glycerol – a chemical present in agro-industrial waste – and to transform this waste in to functional chemicals that could be used in industrial purposes. With regards to the latter, the formulation of products in order to meet preliminary technical specifications was also carried out.

The present work is part of the second phase of this project, and concerned the products dedicated to asphalt – asphalt release agents and rejuvenating agents – for recycling asphalt mix. This part of the study was comprised of several goals:

- to study the effectiveness of the agents;
- to identify how they functioned with construction materials;
- to contribute to the optimization of the product formulas in order to obtain high-performance products.

This required the development of scientific methods to understand, quantify and predict the effectiveness of the products developed at all stages of their usage.

Asphalt release agents (ARAs) are used for spraying surfaces that come into contact with the mixture during the road construction process, such as truck beds, pavers, finishers, tools and various other (usually metal but sometimes plastic) items. The reduction in bitumen adherence is based on the interaction of the bitumen, the ARA and the surface the ARA is applied to.

As opposed to bitumen removers (BRs), asphalt release agents are not intended to break down the bitumen, but rather to protect the equipment used to produce and place the mixture from bitumen residue. Therefore, it is important that asphalt release agents do not cause significant damage to the asphalt pavement when coming into contact with it. BRs on the other hand, are used to clean materials that come into contact with asphalt mix and function best by dissolving the bitumen as efficiently as possible.

As mentioned, diesel had been historically used as an ARA (and BR), but is currently banned for this purpose in many countries such as France due to environmental and health concerns. There have been a number of biodegradable and less volatile alternatives



developed from both bio-sourced and synthetic varieties, from organic esters for example. Unfortunately, some of these alternatives have been either ineffective or damaging to asphalt.

It is necessary to further develop safe biodegradable alternatives that are safe for workers, the environment and the pavement itself. For this, we need to (i) understand the composition of ARAs and BRs and their interaction with the asphalt and (ii) develop the test methods that allow us to characterize the performance and damage to asphalt of these agents.

In order to accomplish this, several test methods were developed in order to evaluate ARA performance and damage to asphalt. In parallel, testing for the performance of bitumen removers was also developed. A number of commercially available ARAs and BRs were tested and these results were used to develop bio-sourced ARAs. This was accompanied by chemical characterization of the interaction between bitumen and the agents with the aid of Fourier Transformed Infrared Spectrometry (FTIR).

The goal of the rejuvenating agent is to regenerate the old bitumen from recycled asphalt pavement (RAP) by restoring the original properties and ensuring the stability of these properties over time. Most rejuvenating agents have been petroleum sourced and bio-sourced agents are relatively recent.

Work on rejuvenating agents consisted of understanding the process of bitumen aging, how to characterize it and with that to characterize the physico-chemical interactions between bitumen and the rejuvenating agent. In particular, the characterization of bitumen aging, along with developing methods for analyzing its remobilization and chemical rejuvenation will be presented, that is, whether rejuvenating agents are able to chemically regenerate the bitumen. This again, necessitated the development of new test methods and was performed in the context of developing a bio-sourced rejuvenating agent.

To begin, oven-bitumen aging was studied as a way of simulating aging in the laboratory. The bitumen was then analyzed by several physico-chemical techniques including FTIR, Thermogravimetric analysis (TGA) and Scanning Electron Microscopy (SEM), in order to determine the optimal techniques for aging and analyzing the aging of bitumen. The rejuvenating agents were incorporated into the aged bitumen and compared with the aged bitumen by itself and unaged bitumen in order to determine the effectiveness of the aging.

Three major chapters will be presented in this manuscript: a bibliographic study (Chapter 2), work on rejuvenating agents (Chapter 3) and work on asphalt release agents and bitumen removers (Chapter 4). The manuscript will end with a general conclusion (Chapter 5).

## 2 Bibliography

The objective of this bibliography is to look at previous research that has been done involving asphalt release agents and rejuvenating agents, and if possible, to improve upon this analysis. To begin however, the properties of asphalt and bitumen will be studied. Of particular interest are the mechanisms of bitumen aging and performance.

The bibliography will be divided into three parts: i) a general overview of asphalt mix focusing on the nature of bitumen, ii) a review of the nature and performance of asphalt release agents (ARA) and the existing methods for evaluating them and iii) a review of bitumen aging and the rejuvenation with rejuvenating agents agents.

ARAs are used to protect the tools and paving equipment that are used for asphalt construction. Performance characteristics consist of their ability to prevent the asphalt from sticking to the equipment. Complications can include causing damage to the asphalt, volatile emissions hazardous to worker's health and being difficult to clean from the equipment. BRs on the other hand, are used to clean materials that come into contact with asphalt and function best by dissolving the bitumen as efficiently as possible.

The change in properties of asphalt over time result in increasing stiffness and cracking that is not favourable to road safety. The aging affects the bitumen almost exclusively, creating chemical and physical changes that drive the need to replace the asphalt (Smith and Edwards, 2001). While replacing the asphalt is costly, there exists the possibility to recycle the asphalt, thereby reducing the amount of virgin materials used along with the cost. Asphalt rejuvenating agents are added to reclaimed asphalt pavement (RAP) in order to facilitate their use in asphalt pavement (manufactured with RAP mixed with new bitumen and new granular). The object of these agents is to rejuvenate the properties of the old bitumen in RAP. The performance characteristics consist of rejuvenating the properties of the old bitumen as improved flowability, adherence to the aggregate and resistance to cracking. Complications can include the recycling agent not being able to interact with the old bitumen (Brownridge, 2010; Chen et al., 2007).

## 2.1 General aspects of asphalt pavement

Bitumen has been used widely in road pavements because of its favourable workability and binding properties. Bitumen is known to have been used in construction since 6,000 BC in the ship-building industry in Sumeria (present day Iraq), which used naturally occurring bitumen found in surface seepage in the area. In the Indus Valley (present day Pakistan-India), there exists a bitumen-stone water tank, which dates back to around 3,000 BC. The stone blocks in the tank's walls are bonded with natural bitumen and there is a vertical bituminous core in the centre of the wall - this same principle is used today in modern dam design (*The Bitumen Industry*, 2011). Historically, asphalt pavement was first known to be used in roads circa 625 BC in Babylon (also present day Iraq). It was found on ancient inscriptions that the road from the palace to the north wall in Babylon was made with asphalt and burned brick. The ancient Greek and Roman civilizations were familiar with asphalt as well. In fact, the word asphalt has its origin in the Greek word “asphaltos” which means “secure”. The development of modern pavements began in Great Britain. Thomas Telford for example, oversaw the pavement of more than 900 miles of roads in Scotland during the years 1803-1821. He developed a method of building roads with broken stones, laid to a depth according to the weight and volume of traffic it would have to carry. Early modern asphalt pavement was also used on the Paris-Perpignan highway in France, which was completed in 1852 and is considered the first modern paved highway (Harrison, 2012; NAPA, 2012).

Today, asphalt is the preferred material in the world for the paving of roads. For example, on the most extensive road network in the world in Europe, spanning 5.2 million km; asphalt accounts for 90% of the pavement material. In France, more than 95% of roads are constructed with asphalt pavement (*The Asphalt Paving Industry*, 2011). Of the 102 million tons of bitumen refined from crude oil every year, approximately 85% (87 million tons) goes toward the construction of asphalt pavement (*The Bitumen Industry*, 2011). In 2007, 1.6 trillion metric tons of asphalt was produced worldwide, with Europe accounting for 435 million tons of this production from about 4000 production sites (*The Asphalt Paving Industry*, 2011).

During hot temperatures and repeated loading, bitumen in asphalt can succumb to permanent deformation or rutting. During cold temperatures, asphalt becomes hard and brittle, and with repeated loading, leading to thermal or fatigue cracking (Atkins, 2003).

### 2.1.1 Paving

Asphalt pavement (CAS #8052-42-4/ EN 13108-4) is typically composed of about 94-96 %w aggregates mixed with generally 4-6 %w bitumen, depending on the performance requirement. EN 13108-4 sets the minimum bitumen content at 3%w. The mixing of the aggregates and bitumen

binder can be performed in batch plants or drum plants. The aggregates are stored on site in piles at ambient temperatures while the bitumen is stored in heated tanks at 150-180°C. In batch mixing, the aggregates are stored and dried in hot bins before they fall through hot air chutes and mix with the bitumen, after which the asphalt is loaded onto trucks. This method is more prevalent in the United States. For drum mixing, the aggregates and bitumen are mixed in the same drum that dries the aggregates, this method being more popular in Europe.

After the bitumen is loaded onto the trucks (the truck beds usually being steel), it is transported a maximum of 30-80 km to the intended construction site. The transportation distance is limited by the temperature that is needed at the site so the outside temperature is a very important factor in the transportation range. Consequently, in some regions the construction of asphalt pavement roads is limited to the summer (hottest) months.



Figure 2-1 Pavement roller

When they arrive at the road construction site, the transportation trucks discharge the hot asphalt mix into a hopper on the paving machine. After the asphalt is placed on the road, it is usually compacted into place by a roller (Figure 2-1). Because the bitumen viscosity changes with temperature, it is important to have the bitumen placed at a sufficiently high temperature to achieve an acceptable content of voids during compaction. The voids acceptable content depends on the type of mixture and the limits can vary from as low as 4 % to as high as 12 % by NF P 98-150-1. Required production and placement temperatures will vary depending on the bitumen grade (*The Asphalt Paving Industry*, 2011).

### 2.1.2 Aggregates

The aggregates compose the vast majority of asphalt (94-96%w). Although reclaimed asphalt pavement is being used more frequently in today's industry as aggregates, the majority is still virgin

mineral rock. The keys to the choice of aggregates are to allow for strength and skid resistance for the asphalt and adhesion to the bitumen (Atkins, 2003).

#### ***2.1.2.1 Type of aggregates***

Aggregates for asphalt are generally comprised of coarse aggregates, fine aggregates and mineral filler as specified by the EN 13108-4 standard for hot rolled asphalt. EN 13108-8 allows for the addition of reclaimed asphalt pavement, although this will be discussed later. The requirements for coarse aggregate, fine aggregate and mineral filler are defined by the EN 13043 norm for aggregates for bituminous mixtures in roads.

#### ***2.1.2.2 Mineralogical composition***

The petrographic composition of the aggregates for asphalt is defined by EN 932-3. The aggregates are divided between magmatic, sedimentary and metamorphic types. An aggregate is defined as one of these types when at least 50% its composition is of the said type.

Asphalt aggregates need to be able to accommodate the adherence of bitumen, so it is important that the aggregates are hydrophobic. Some siliceous aggregates like quartz tend to have an affinity for water due to their negative surface charges, making them inappropriate for use in asphalt as the presence of water reduces the adherence properties of bitumen (Atkins, 2003). Limestone aggregates on the other hand, tend to have positive surface charges, making them ideal for adherence to negatively charged bitumen and more likely to be absorbed by the aggregates (Durrieu, 1977).

Additionally, it has been shown that the aggregate type influences the aging properties of the binder, as some aggregates serve as a catalyst for oxidation reactions, while some serve as inhibitors (Srivastava and van Rooijen, 2000). El Béze et al. (2012) found that calcium carbonate particles in aggregates can accelerate the oxidation of the bitumen.

### **2.1.3 Bitumen chemical composition and structure**

There are various origins of bituminous materials, such as bitumen from lakes, rock deposits and tars obtained from the distillation of coal. The most common source of bitumen is from the distillation of crude oil, this being the form of bitumen used in asphalt pavement (EN 12697-ASTM D 6373). It comes from the last part of the crude oil distillation, after naphtha, gasoline, kerosene, and other fractions have been removed.

What results is a highly complex material that can have hydrocarbon chains up to 150 atoms long. Molar masses of up to 10,000 g/mol can be found although typically, there are relatively few molecules present with molar masses of over 1000 g/mol. Bitumen typically contains around 80% carbon by mass as well as hydrogen, sulfur, small amounts of oxygen, nitrogen and trace amounts of

metals such as iron, nickel, and vanadium. An example of the typical bitumen compositions (by % atoms) is provided in Table 2-1 (Mortazavi and Moulthrop, 1993; *The Bitumen Industry*, 2011).

Table 2-1 Typical bitumen chemical composition for Europe (*The Bitumen Industry*, 2011)

Element	Range	Average
<b>C (%w)</b>	80.2-84.3	82.8
<b>H (%w)</b>	9.8-10.8	10.2
<b>S (%w)</b>	0.9-6.6	0.7
<b>N (%w)</b>	0.2-1.2	3.8
<b>O (%w)</b>	0.4-1.0	0.7
<b>Ni (ppm)</b>	10-139	83
<b>V (ppm)</b>	7-1590	254
<b>Fe (ppm)</b>	5-147	67
<b>Mn (ppm)</b>	0.1-3.7	1.1
<b>Ca (ppm)</b>	1-335	118
<b>Mg (ppm)</b>	1-134	26
<b>Na (ppm)</b>	6-159	63

The classification of bitumen presents difficulties with the large variety of hydrocarbons and structures that compose it. It is difficult to classify because it is not a mixture, but a complex continuum of hydrocarbons. Nevertheless, classification systems and structural models have been developed, such as the SARA classification system and the GEL-SOL model (Lesueur, 2009).

#### 2.1.3.1 *N-heptane separation*

An early method for classifying bitumen was performed by emerging it in n-heptane (NF T60-115-ASTM D 3279).

The asphaltenes are considered as the fraction that is insoluble in n-heptane, with the maltenes composing the soluble fraction. Maltenes are considered the fluid and oily fraction of the bitumen. A simplified model of bitumen composition is shown in Figure 2-2, representing the asphaltenes suspended in a maltene solution.

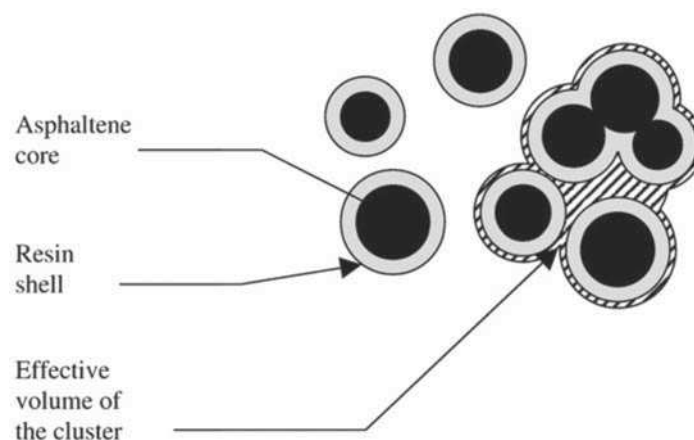


Figure 2-2 Simplified model of bitumen structure (asphaltene suspended in maltenes) (Lesueur, 2009)

### 2.1.3.2 SARA fractions

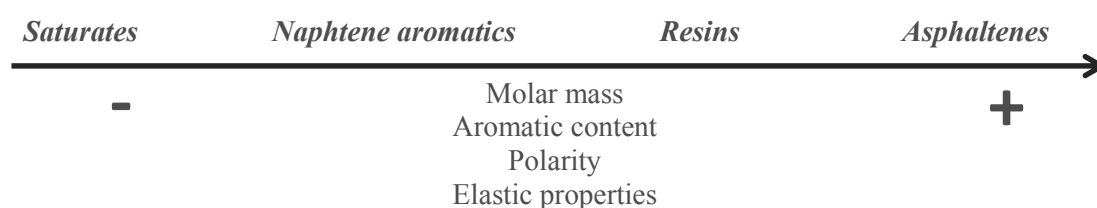
The most commonly used system of classification today for bitumen is known as SARA fractions (or Corbett method - ASTM D 4124) using high performance liquid chromatography (HPLC).

It separates the molecules of bitumen into 4 categories: **Saturates**, **Aromatics**/ naphthene aromatics, **Resins** and **Asphaltenes**.

The chemical properties of the bitumen are dependent on a combination of these constituents. Even though the exact composition of each of these hydrocarbon families depends on the origin of the crude oil and on the experimental set-up, they show similar features and overall properties that do not vary significantly (Dehouche et al., 2012; Lesueur, 2009; *The Bitumen Industry*, 2011).

Effectively, the hydrocarbons can be said to be a chemical continuum with an increase in molar mass, aromatic content and polarity from saturates to naphthene aromatics to resins to asphaltenes as shown in Figure 2-3 (Lesueur, 2009).

Figure 2-3 Trends of bitumen components by aromatic content and polarity



#### 2.1.3.2.1 Asphaltenes

**Asphaltenes** are the heaviest part (750-3500 g/mol) of the bitumen and are the result of the polycondensation of monomer both in the geological processes that form crude oil and the process of distillation and production of bitumen itself.

They compose 5-20% of the bitumen by weight. Asphaltenes form a brown to black powder at room temperature and are responsible for the black colour of bitumen. About 40% of the carbon atoms in asphaltenes are part of aromatic rings, while 90% of the hydrogen atoms are attached to saturated carbons. Asphaltenes are agglomerations of the most highly polar molecules in the bitumen and have been shown to be responsible for its strength, stiffness and the characteristics of the colloidal structure.



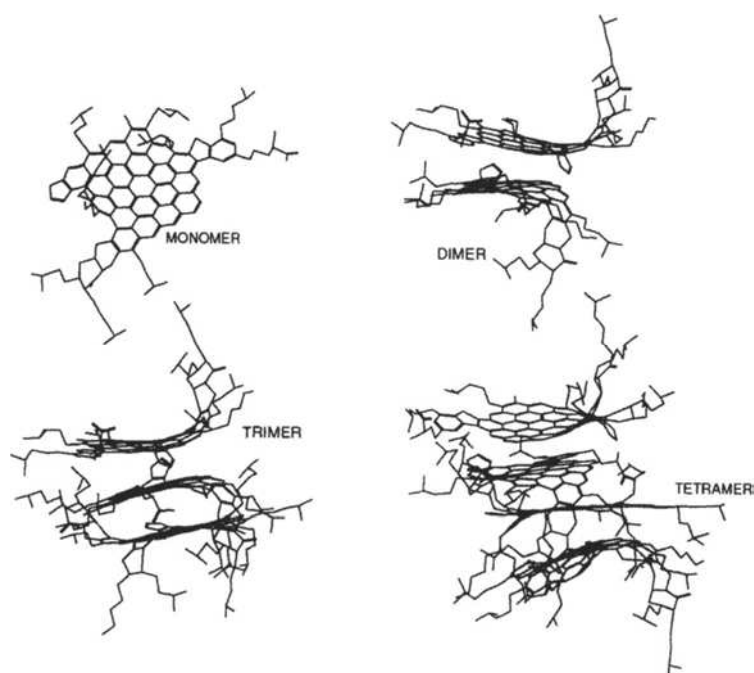


Figure 2-4 Formation of dimer, trimer and tetramer for an asphaltene molecule (Lesueur, 2009)

Due to the polycondensation of the many condensed aromatic rings, asphaltenes form almost planar molecules that can associate through aromatic bonding to form graphite-like stacks (Figure 2-4). The molecules can aggregate to form micelles and the micelles can aggregate to form aggregations as shown in Figure 2-5. This aggregation can be enhanced by the presence of polar interactions between oxygen functional groups. The asphaltene molecules are said to typically consist of between 8 and 20 aromatic rings giving asphaltenes a reported average particle size of 4-10 nm and 15-30 nm for the micelles formed during aggregation of the molecules. (Lesueur, 2009; Olard, 2003; El Béze, 2008; Peralta, 2009; Siddiqui and Ali, 1999a; Tachon, 2008).

Their FTIR analysis shows a relatively strong aromatics peak (around  $1600\text{cm}^{-1}$ ). The presence of a polar peak (around  $3400\text{cm}^{-1}$ ) is significant, while the C-H (around  $2850\text{cm}^{-1}$  and  $2925\text{cm}^{-1}$ ) elongated bands are found to be relatively weaker.

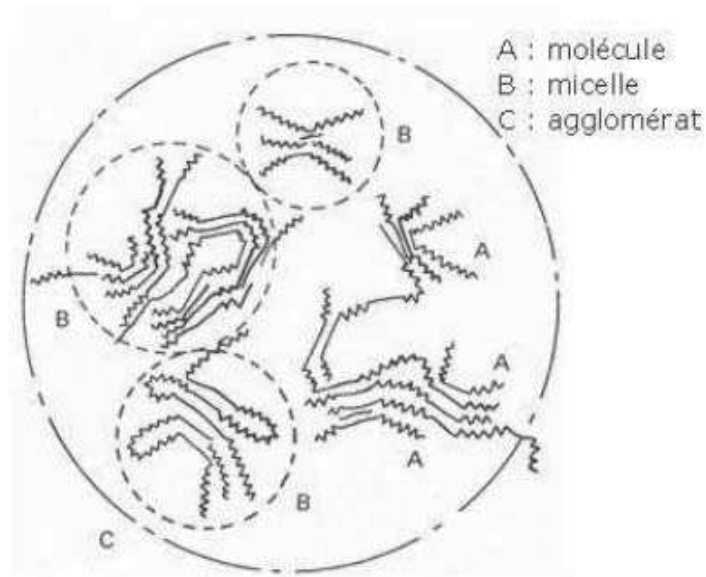


Figure 2-5 Asphaltene molecules, micelles and aggregations [Yuen et al. (1972) cited by El Béze (2008)]

Gawrys and Kilpatrick (2004) observed bitumen with small-angle neutron scattering (SANS) used for deducing sizes of colloidal aggregates, a three dimensional aggregated structure was found for the asphaltenes (Figure 2-6). The asphaltene aggregate size was estimated at 3-4 nm or 12-15 nm, although this depends on the degree of aggregation.

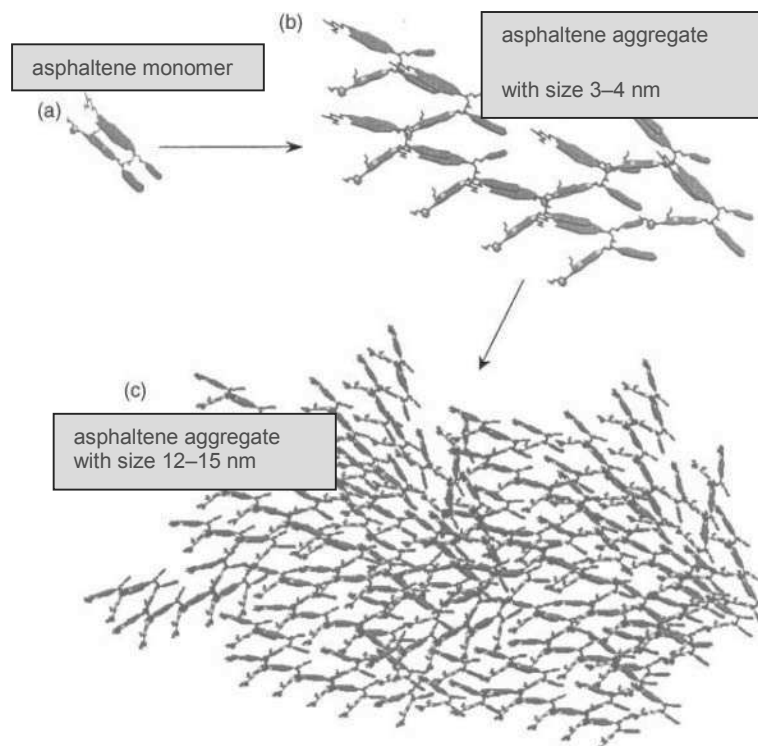


Figure 2-6 Asphaltene aggregates observed by SANS (Gawrys and Kilpatrick, 2004)

Asphaltenes do not show thermal transition at typical asphalt production ranges (up to 200°C), remaining solid. Their density at 20°C is about 1.15 g/cm<sup>3</sup>. Their solubility parameter can be between 17.6 and 21.7 MPa<sup>0.5</sup> but this has been shown to vary based on the level of aggregation.

The solubility parameter in bitumen has been found to decrease as the aggregation of the asphaltenes increases. Compounds with similar solubility parameters are more likely to be miscible (able to form solutions more easily).

The asphaltenes can be further broken down as well into the fractions that are soluble and insoluble in toluene. The insoluble fraction can be further broken down with their solubility and insolubility in carbon disulfide CS<sub>2</sub> into carbenes and carboids, respectively. The carbene and carboid fractions however, make up only 0-2% and 0-0.2% of the bitumen by mass, respectively (Lesueur, 2009; Tachon, 2008).

Lesueur (2009) reviewed literature on the chemical composition of the SARA fractions (Table 2-2). Notably, it shows in that the nitrogen and sulfur components of bitumen are mostly found in the asphaltenes.

Table 2-2 Typical compositions by mass of SARA fractions (Lesueur, 2009)

Fraction	C (%)	H (%)	O (%)	N (%)	S (%)
<b>Saturates</b>	78-84	12-14	<0.1	<0.1	<0.1
<b>Aromatics</b>	80-86	9-13	0.2	0.4	0-4
<b>Resins</b>	67-88	9-12	0.3-2	0.2-1	0.4-5
<b>Asphaltenes</b>	78-88	7-9	0.3-5	0.6-4	0.3-11

As mentioned earlier, maltenes form the part of bitumen soluble in n-heptane. They can be further classified as saturates, resins and aromatics/ naphthene aromatics.

#### 2.1.3.2.2 Saturates

**Saturates** compose 5-15% of bitumen by mass (*The Bitumen Industry*, 2011). They form a colourless or lightly coloured oily liquid when isolated at room temperature. Saturates (Figure 2-7) are hydrocarbons that form long aliphatic chains with very few polar or aromatic compounds present. They are responsible for the function of the maltenes as a flocculating (or dispersing) agent for the asphaltene aggregates.

A FTIR analysis by Tachon (2008) found no aromatic peak while the C-H elongated bands was found to be fairly strong.

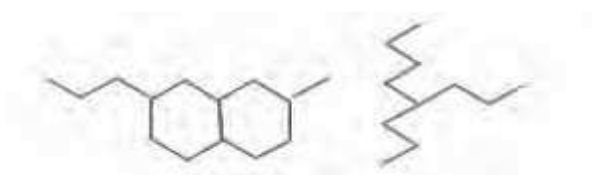


Figure 2-7 Saturate molecules (*The Bitumen Industry*, 2011)

Their average molecular weight has been found to be around 600 g/mol, a density at 20°C of around 0.9 g/cm<sup>3</sup> with a solubility parameter of between 15 and 17 MPa<sup>0.5</sup> (Lesueur, 2009; Peralta, 2009). Saturates can increase bitumen elasticity due to a 'wax' component that crystallizes during low temperatures and causes cracking of the bitumen. Nevertheless, this has been shown not be a factor when the proportion of saturates in the maltenes is not too large (Edwards, 2005; Fritsche, 1994; Soenen and Redelius, 2014).

#### 2.1.3.2.3 Aromatics/ naphthene aromatics

**Aromatics/naphthene aromatics** are molecules with naphthene and aromatic nuclei along with some paraffinic and naphtenic carbons including sulphur elements (Figure 2-8). They are the prevalent fraction, composing 30-60% of the bitumen and have average molecular weights of 500-900 g/mol (Gasthauer et al., 2008; *The Bitumen Industry*, 2011).

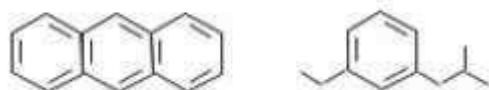


Figure 2-8 Aromatic/ Naphthene Aromatic molecules (*The Bitumen Industry*, 2011)

Their chemical structures are lightly aggregated aromatic rings with short aliphatic chains and when isolated, form a yellow to red liquid at room temperature. Only 30% of the carbons present are found in the aromatic rings and thus, result in a relatively low peak in FTIR analysis for aromatic bands, although there is a small peak at 1500cm<sup>-1</sup> that does not seem to be present in the other fractions. The C-H elongated bands are found to be strong, while the polarity bands are not present in the IR spectrum (Tachon, 2008).

They are responsible for the function of the maltenes as a solvent as they have the ability to dissolve other heavy hydrocarbons. They have a density at 20°C of about 1 g/cm<sup>3</sup> and solubility parameter of between 17 and 18 MPa<sup>0.5</sup> (Lesueur, 2009; Olard, 2003; Peralta, 2009).

#### 2.1.3.2.4 Resins

**Resins** are responsible for the bitumen's ductility and adhesion properties as well as its malleability and plasticity.

Resins can compose 15-55% of the bitumen and have average molecular weights of 800-2000 g/mol (*The Bitumen Industry*, 2011).

They are composed of more cyclic hydrocarbons than the aromatics, including aromatic, naphtenic and heterocycle joined by aliphatic bridges (Murgich et al., 1996). They contain more polar chemical groups that can include oxygen, nitrogen or sulfur atoms (Gasthauer et al., 2008). Resins have a

density at 20°C of about 1.07 g/cm<sup>3</sup> and a solubility parameter of between 18.5 and 20 MPa<sup>0.5</sup> and form a dark red or black semi-solid or at room temperature (Lesueur, 2009).

Like asphaltenes, resins are the aggregation of aromatic rings, but in the case of resins, this is typically only 2-4 rings. In fact, asphaltenes can be considered to be the result of many resin molecules coming together. They function as a barrier phase between the lighter molecules and the asphaltenes, contributing to the stability of the bitumen system (Lesueur, 2009; Peralta, 2009). Resins (Figure 2-9) are composed of mainly polycyclic molecules containing saturated, aromatic and hetero-aromatic rings and heteroatoms in various functional groups (Oyekunle, 2006).

As the case with asphaltenes, their FTIR analysis shows a relatively strong aromatics peak. The presence of a polar function (around 3400cm<sup>-1</sup>) is significant although less than for asphaltenes, while the C-H elongated bands are found to be relatively strong, indicating a condensed structure (Tachon, 2008).

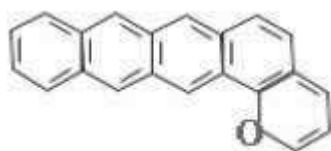


Figure 2-9 Resin molecule (*The Bitumen Industry*, 2011)

#### 2.1.3.3 Classification of bitumen by acidity

While the n-heptane and SARA methods seek to classify the bitumen by hydrocarbon families and their function in the bitumen, the Ion Exchange Chromatography (IEC) method separates the bitumen into strong and weak acids and bases as well as neutral components.

IEC fractioning separates bitumen into six fractions corresponding to strong and weak acids and bases, amphoteric (can function as acids or bases in reactions) and neutral components. This method has more to do with understanding the interfacial and chemical interactions of bitumen than understanding the structure itself.

The fractioning consists of dissolving the bitumen in a solution made of benzene, tetrahydrofuran and ethanol. The sample is then passed through an anionic followed by a cationic ion-exchange resin. The amphoteric content is then found in a separate process using cyclohexane (Lesueur, 2009). It has been suggested that the acid, basic and amphoteric fractions are comparable with the resin and asphaltene fractions from SARA (Mortazavi and Moulthrop, 1993).

#### 2.1.3.4 GEL-SOL microstructural models

There are two commonly proposed models of bitumen colloidal structures: the SOL and GEL models (Figure 2-10, Figure 2-11). Both models follow the SARA fraction classification and the arrangement of higher molecular weight molecules being dispersed in those of lower molecular weight. The SOL

structure has a higher proportion of maltenes (oily compounds), meaning that the asphalt colloids are free to move in the structure, resulting in the bitumen having the properties of a Newtonian fluid and being more ductile.

As mentioned in the previous section, it is the aromatics/naphthene aromatics that are responsible for the solvent capability of the maltenes, and so are responsible for the separating effect of the SOL model. Where aromatics/naphthene aromatics are less present, or where they have less solvating power (relatively high saturate to aromatics/naphthene aromatics ratio) the GEL structure may be applicable, meaning the bitumen has visco-elastic properties and is more fragile (El Béze, 2008; Read and Whiteoak, 2003; Stangle et al., 2006; Tachon, 2008).

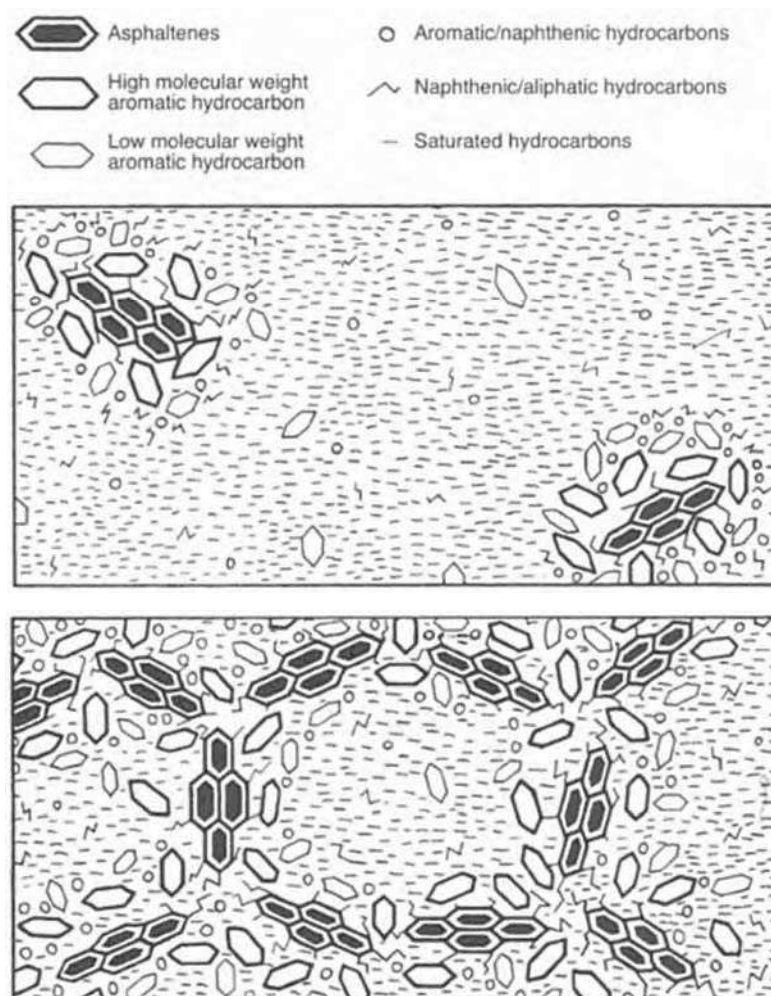


Figure 2-10 SOL (top) and GEL (bottom) bitumen models (Read and Whiteoak, 2003)

The resins also play an important role in these structures. As can be noted from Figure 2-10, in the SOL, the resins surround the asphaltene congregations, thereby preventing the formation of structure of the GEL model (solvating) (Oyekunle, 2006; Tachon, 2008). There have also been studies (Koots and Speight, 1975), showing the role of resins in preventing the asphaltenes from agglomerating. This can also be observed in the bitumen hydrocarbon analysis shown in Table 2-3

where the SOL bitumen has the highest content of resins. Therefore, this dispersion is a function of both a lower content of asphaltenes and a higher content of resins.

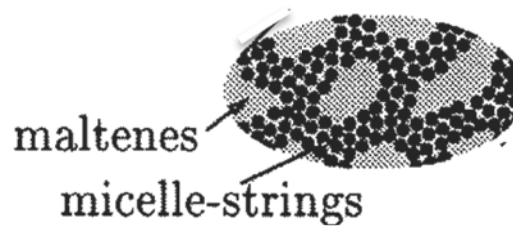


Figure 2-11 GEL bitumen model (Stangle et al., 2006)

Remarkably, it has also been shown that the resins from one crude oil would not necessarily stabilize the asphaltenes sourced from a different crude oil, which may have to do with the various shapes and configurations of the asphaltenes based on their source. This also suggests that there may be some molecular recognition that permits the resins to enter the asphaltene micelles (Koots and Speight, 1975; Murgich et al., 1996). These findings would support the hydrocarbon-continuum hypothesis for bitumen.

Table 2-3 Hydrocarbon compositions by structural model of bitumen (Tachon, 2008)

Model	% Asphaltenes	% Resins	% Saturates and Aromatics
<b>I: GEL</b>	>25	24	50
<b>II: SOL</b>	<18	36	48
<b>III: SOL-GEL</b>	21-23	30-34	45-49

The SOL model is applicable where there is a sufficient amount of resins and aromatics (solvating power) to disperse the asphaltenes congregations. This produces bitumen that follows the physical properties of the maltenes and thus, a viscous model more than an elastic one. The corresponding asphalt would therefore be better able to respond to short-term stresses, but would be more susceptible to long term stresses such as rutting (permanent deformation to asphalt from repeated vehicle loading during service time) due to the structure allowing for greater deformation (Tachon, 2008).

As stated in Read and Whiteoak (2003), both structures normally exist in bitumen concurrently, but not in a homogenous mixture. Lesueur (2009) has cited the X-ray and neutron scattering studies of Bodan (1982), Storm et al. (1993) and Storm et al. (1995) as showing bitumen to be a heterogeneous mixture.

The asphaltene structures of the GEL model are dispersed in the viscous medium of the SOL model. However, Lesueur (2009) notes that this hypothesis would result in a yield stress (plateau of modulus versus temperature and frequency), which has never been observed for pavement grade bitumen.

There have been two indices developed to quantify the stability of asphaltene structures and thereby determine whether the SOL or GEL model may be more relevant to a given bitumen. The colloidal stability of bitumen has been defined by the asphaltene index,  $I_A$ , as shown in Equation 2-1 (Loeber et al., 1998), which takes into account the asphaltene + resin content (as %w) as the most important factor in the stability of the colloids.

Equation 2-1

$$I_A = \frac{\text{Asphaltenes} + \text{Resins}}{\text{Saturates} + \text{Aromatics}}$$

As stated previously, resins and aromatics are said to play an important part in the stability of asphaltenes. This is the basis for the Gaestel (1971) colloidal index,  $I_C$ , as shown in Equation 2-2. For this index, it is the ratio of the asphaltenes and flocculants (saturates) over the solvents (naphthene aromatics/ aromatics + resins).

Equation 2-2

$$I_C = \frac{\text{Asphaltenes} + \text{Saturates}}{\text{Resins} + \text{Aromatics}}$$

When these indices increase, the colloidal stability is said to decrease. This means that the asphaltenic structures or the GEL model are more likely to be present in the bitumen than with the SOL model.

A typical range for  $I_C$  has been reported to be between 0.5 and 2.7 for pavement grade bitumens. Values for  $I_C$  of >1.2 has been observed for bitumens with markedly GEL properties, while the values for bitumens with dominant SOL properties have been found at <0.7 (Lesueur, 2009; Oyekunle, 2006). Contrarily, Le Guern et al. (2010) found that the colloidal index, which increases with aging, does not have a strong correlation with the agglomerate content (GEL). These two indices further demonstrate the dynamic nature of bitumen physics that are still being researched.

#### **2.1.3.5 Microscopic observations of the structure of bitumen**

The GEL structure has been observed by Atomic Force Microscopy (AFM) as shown in Figure 2-12. The structures observed, coined ‘bee’ structures by Loeber et al. (1996), have been measured at 1µm and have attributed the bee structures to the saturates (wax) fraction of the bitumen (Kim, 2014; Loeber et al., 1996; McCarron et al., 2012; Nahar et al., 2013; Zhang et al., 2011).



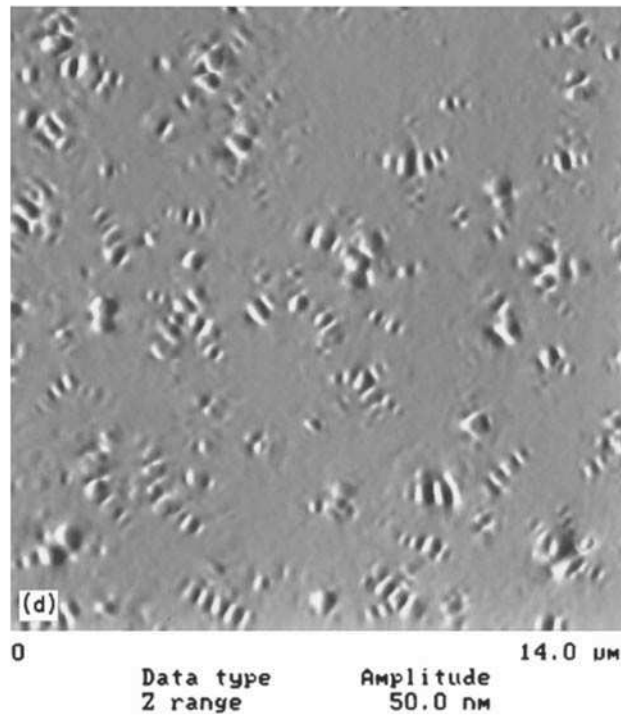


Figure 2-12 GEL bitumen structure observed by AFM (Loeber et al., 1996)

A GEL-like model was observed by environmental scanning electron microscope (ESEM) at magnifications of 250-500 by Loeber et al. (1996), Rozeveld et al. (1997) and Stangle et al. (2006). As shown in Figure 2-13, the melting of the bitumen under SEM observation forms micelle-like structures that resemble the GEL model. This is explained by the authors to be the volatilization of the lighter bitumen fractions by the electron beam locally.

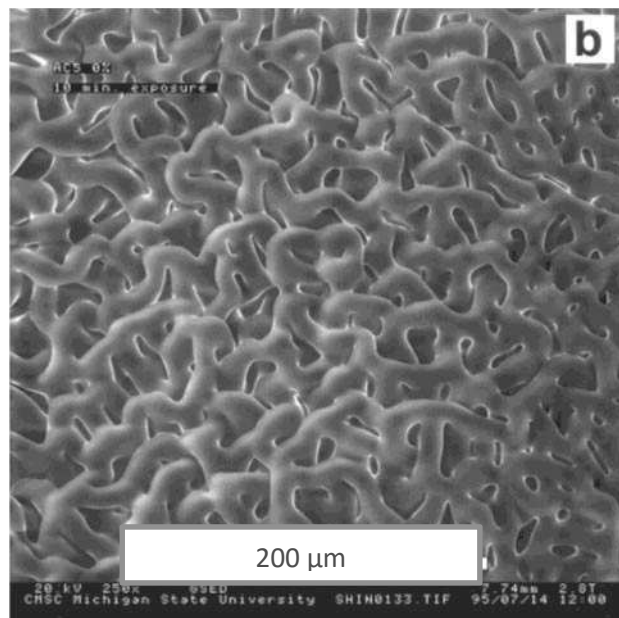


Figure 2-13 SEM observation of bitumen x250 (Rozeveld et al., 1997)

The observation of the separated asphaltene fraction in Figure 2-14 shows an asphaltene structure of 0.2-0.3  $\mu\text{m}$ . Loeber et al. (1996) measures the particle size inside the asphaltenes at 100nm. This is much higher than the estimate of asphaltene micelle size of 20 nm by Altgen and Harle (1975) or aggregate size of 3-4 nm by Gawrys and Kilpatrick (2004).

Rozeveld et al. (1997) indicates that the image in Figure 2-14 could be the clusters of ten or more individual micelles. It is likely that the size of the structure has many variables, including bitumen source, age, testing procedures and how the SARA fractions are defined by the authors.

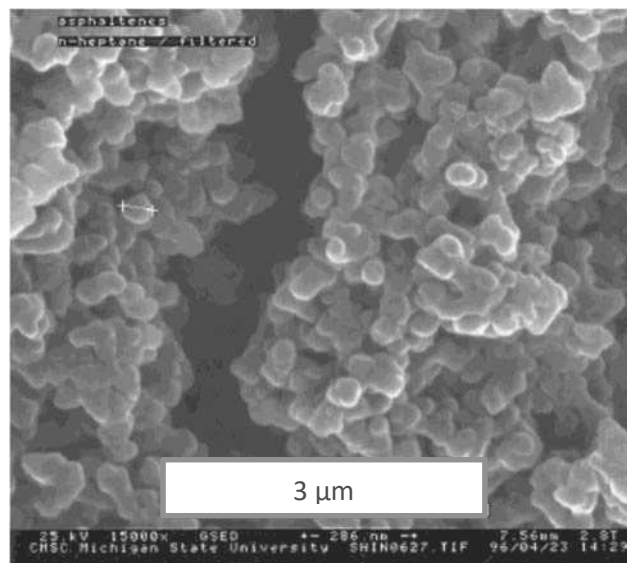


Figure 2-14 SEM observation of asphaltenes x15000 (Rozeveld et al., 1997)

Research by Redelius (2000) and Sirota (2005) has contended that the model of dispersed asphaltene micelles or colloids is incorrect. It was argued that the scattering often attributed to asphaltene colloidal aggregates is the result of ephemeral dynamically fluctuating compositional inhomogeneities similar to those in one-phase liquid mixtures of different molecules.

The chemical and microstructural properties of bitumen all play a role in its physical performance characteristics which are discussed in the following section.

#### 2.1.4 Bitumen properties and testing

There are many different testing procedures available for bitumen. This section will discuss some of these procedures and their relation to the performance of bitumen in asphalt, while others can be found in Appendix A.

The NF EN 12591 norm defines paving grade bitumen for France by several tests while NF EN 12607-1 refers to the tests in order to determine the effects of aging on bitumen, further described in Appendix A.

#### 2.1.4.1 Penetration

The standard penetration test (ASTM D5-EN 1426) is a measurement of the consistency of bitumen at ambient temperatures. The test consists of plunging a standard needle into the bitumen for 5 seconds at a temperature of 25°C and measuring the penetration of the needle. The test is a common identifier for the grade for bitumen, for example, a bitumen sample with a grade of 60/70 would have a penetration value of 6 to 7 mm. This test is used as an identifier because of its simple implementation and repeatability.

#### 2.1.4.2 Viscosity

At sufficiently high temperatures, bitumen is essentially a Newtonian liquid, and can be described by a shear rate independent viscosity value. The viscosity of bitumen refers to the resistance to shear or tensile deformation of bitumen (Lu and Isacsson, 2002). Like penetration, this is a measure of the facility of working with the bitumen on the construction site. The NF EN 12591 standard defines tolerances for dynamic (EN 12596) and kinematic (EN 12595) viscosity.

Dynamic viscosity ( $\mu$ ) is the tangential force per area needed to move one horizontal surface (plate) with respect to the other at a certain velocity when separated at a certain thickness of the fluid in question. The higher the value of the dynamic viscosity for the bitumen, the more force is needed to deform it and thus, the harder it is. It is measured in Pa\*s at 60°C, a temperature typical for road asphalt in the hot summer months. The limit of dynamic viscosity for 35/50 grade bitumen is  $\geq 225$  Pa\*s.

Kinematic viscosity ( $\nu$ ) is the relation of the dynamic viscosity to the density of the bitumen ( $\rho$ ) as is shown in Equation 2-3. It is expressed in mm<sup>2</sup>/s and is measured at 135°C, a temperature typical for the fabrication of bitumen.

Equation 2-3

$$\nu = \mu/\rho$$

The limit of kinematic viscosity for 35/50 grade bitumen is  $\geq 370$  Pa\*s.

The resistance to deformation is kept to a minimum in this case to ensure a stable road and resistance to permanent deformation. However, there is a chance that the aggregates would not be covered if the bitumen during asphalt fabrication viscosity is too low (El Béze, 2008). The viscosity of bitumen is commonly measured by viscometers such as the one in Figure A-2 (Appendix A).

#### 2.1.4.3 Rheology

Bitumen is a viscoelastic material, which can be elastic or viscous in its behavior, depending on temperature and time of loading.

At low temperatures and or short loading times, bitumen behaves more as an elastic solid. As temperature and/or loading time increases, the bitumen becomes more viscous. At sufficiently high temperatures and/or long loading times, bitumen becomes essentially a Newtonian liquid, and can be described by a viscosity value that is independent of the shear rate (Lesueur, 2009; Lu and Isacsson, 2002).

The rheology of bitumen can be measured as a function of the shear stress over frequency and temperature by a rheometer over a range of temperatures from 10-100°C, most commonly by the dynamic shear rheometer (DSR, NF T 66-065) (Eschbach, 1993; Van den bergh and Van de Ven, 2012).

A bitumen sample is placed in the rheometer and oscillated at various frequencies and temperatures. The sinusoidal oscillation induces a delayed response in the bitumen, this delay can be expressed mathematically as a phase angle ( $\delta$ ) is a measure of the plasticity/ elasticity (Porot and Nigen-Chaidron, 2007).

The results of these tests can be plotted on “Black” curves, with the phase angle ( $\delta$ ) versus the complex modulus, which can be further used to understand the bitumen performance in terms of stiffness and the viscous/elastic balance of the bitumen. These graphs give a more dynamic overview of the rheological performance of the bitumen than simply penetration, being at varied frequencies and temperatures (Loeber et al., 1998).

The study by Loeber et al. (1998) of various bitumens while combining SARA analysis (Section 2.1.3.2) rheology and penetration. The results demonstrated from the various bitumens tested with varied SARA fraction contents and penetration, that the performance of bitumen in rheology (a more elastic bitumen would tend to have lower values in  $G^*$  and  $\delta$ ) in Figure 2-15 is less dependent on the penetration and more dependent on the colloidal index (Equation 2-2) as shown in Table 2-4, that is, the ratio of asphaltenes relative to the “solvents” (aromatics + resins). Bitumen #3, despite having a relatively high penetration, had a Black curve similar to bitumen #2, which was graded at 10/20 mm, due to the elevated asphaltenes content of bitumen #3.

Soenen and Redelius (2014) also found that the presence of larger polyaromatic structures in bitumen (i.e. asphaltenes) corresponded to a higher rheology via the DSR.

Table 2-4 SARA composition and penetration values for bitumens corresponding to Figure 2-15 (Loeber et al., 1998)

Bitumen	Markers	Penetration	Saturates	Aromatics	Resins	Asphaltenes
1	+	70/100	2.1	71.0	9.4	17.6
2	o	10/20	6.8	59.7	15.1	18.4
3	x	70/100	4.0	55.5	15.1	25.4

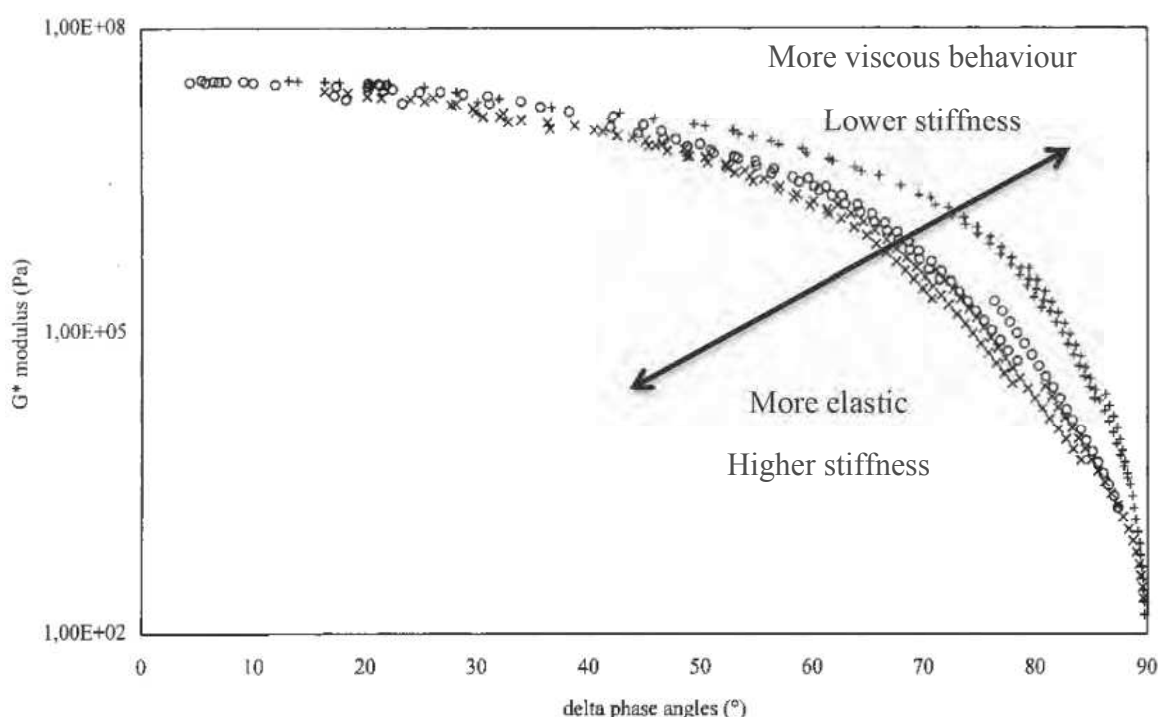


Figure 2-15 Black curve representation of different bitumens, varying in composition from testing with rheometer from frequencies 0.06-10Hz at 5 to 60°C (Loeber et al., 1998)

## 2.1.5 Special types of bitumen

### 2.1.5.1 Cutback and emulsified bitumens

Cutback bitumen refers to a process of mixing normal grade bitumen with lower viscosity distillates. This allows the bitumen to be mixed in asphalt at lower temperatures, allowing for the production of asphalt in lower temperature climates or with less energy consumed for heating. The distillates used for cutback bitumen include petrochemicals such as naphtha, kerosene, diesel oil, and furnace oil (Mathew, 2009; *The Bitumen Industry*, 2011).

The reduction in the viscosity of bitumen can also be achieved by emulsification. Bitumen emulsions are generally considered more environmentally sound than cutback bitumen because they do not involve the addition of volatile and polluting low-viscosity petrochemicals. The use of bitumen at

lower temperatures also reduces the environmental impact of VOCs (volatile organic compounds) from the bitumen. Bitumen emulsions involve the mixing of bitumen with water and one or more emulsifiers (surfactants). The emulsion process disperses (by shear force) the bitumen in the water, forming bitumen drops with diameters of 0.1 to 100  $\mu\text{m}$ . These are kept dispersed by electrostatic charges from the drops and stabilized by the emulsifiers, greatly reducing the viscosity of the bitumen at ambient temperatures.

Various bio-based products have been shown to be adequate bitumen emulsifiers such as tallow (beef/mutton fat), sunflower, corn oil, residues from fatty-acid distillation, rosin acids, hydroxystearic acid and lignin sulphonates (Read and Whiteoak, 2003; Rodríguez-Valverde et al., 2008; Tachon, 2008).

France has had a standard for bitumen emulsions used in asphalt construction since 1993 and today it is covered under EN 13808 (ASTM D 977, ASTM D 3628). Of particular importance are the viscosity and cohesion properties of the emulsions.

#### ***2.1.5.2 Polymer modified bitumen***

Polymer modified bitumen (PmB) refers to the addition of polymer additives to bitumen in order to attain various properties (EN 14023-ASTM D 6154). Polymers are added (by mixing or chemical reaction) to the bitumen during the production of asphalt at high temperatures. Examples of the polymers that can be used include recycled rubber, polyethylene, ethylene vinyl acetate (EVA) and most commonly, styrene–butadiene–styrene (SBS).

Improved properties from PmBs can include susceptibility to temperature variations, resistance to deformation at high temperatures, resistance to aging and loading, adhesion to the aggregates, stripping and cracking.

The magnitude of the improvements depend on the amount added (3-7 % by weight of bitumen), nature of bitumen and the mixing method (Dehouche et al., 2012; Mathew, 2009; Mouillet et al., 2008).

#### **2.1.6 Conclusions on the general aspects of asphalt**

Asphalt is composed of aggregates and bitumen. The aggregates consist of crushed coarse aggregates, sand and limestone filler. Aggregates with a higher proportion of calcium have a stronger adhesion to the binder due to their surface energy relative to the bitumen.

Bitumen is the binder that keeps the asphalt mix in cohesion. Bitumen is a continuum of hydrocarbons, derived from the bottom portion of the distillation process of crude oil. The hydrocarbons can be classified into four principle categories, listed in descending order for molar

mass, polarity and aromatic content: asphaltenes, resins, naphthene aromatics/ light aromatics and saturates. The asphaltenes fraction has been linked to the mechanical behavior of asphalt.

The SOL-GEL model describes the bitumen as a heterogeneous mixture, one part being dominated by asphaltene structures (GEL), while the other, has the asphaltene-resins suspended in a saturates-light aromatics solution (SOL).

## **2.2 Asphalt release agents**

The most important component of an asphalt mixture is bitumen, which through adhesion keeps the aggregates together and the asphalt mix cohesive. These same adhesion properties can make it very difficult to clean surface of equipment that has been used to work or transport asphalt mixtures intended for road construction. In the case of the truck beds used for transporting the asphalt mix for example, the adhesion prevents the mixture from smoothly sliding out of the bed as the truck attempts to discharge its load (Crum, 2008; Scardina, 2007). In such cases, workers must spend time and effort to manually coax the residual mixture out of the truck bed, while exposing themselves to volatile organic compounds (VOCs) from the mixture (Tang, 2008). This issue is even more significant for polymer modified mixtures (PMA), which tend to be more adherent than conventional asphalt mix (Lavin, 2003).

Asphalt release agents (ARAs) are used for spraying surfaces that come into contact with the mixture during the road construction process, such as truck beds (Figure 2-16), pavers, finishers, tools and various other (usually metal but sometimes plastic and rubber) items. The reduction in bitumen adherence is based on the interaction of the bitumen, the ARA and the surface the ARA is applied to (Bymaster and Smith, 2009; Tang and Isacsson, 2006). As opposed to bitumen removers (BRs), asphalt release agents are not intended to break down the bitumen, but rather to protect the equipment used to produce and place the mixture from bitumen residue. Therefore, it is important that asphalt release agents do not cause significant damage to the asphalt pavement when coming into contact with it. BRs on the other hand, are used to clean materials that come into contact with asphalt mix and function best by dissolving the bitumen as efficiently as possible (Mikhailenko et al., 2014).

The product traditionally used for this purpose was diesel, but diesel is toxic to workers (Kriech et al., 2011; Sobus et al., 2009) and the environment (Acton, 2013; Tang and Isacsson, 2006, 2005), and can cause damage to the asphalt (Lavin, 2003; Martin, 1978; Zaki and Troxler, 2013). Since then a number of bio-sourced alternative products have been developed, some of them have proven to be damaging to the asphalt, ineffective or both (Bymaster and Smith, 2009; Mahr et al., 2003; Tang, 2008).



Figure 2-16 Application of ARA on truck bed (left); part of field Trial showing effectiveness of two ARAs (right) ("SITTM Asphalt Release Agent Field Trial," 2010)

Tang (2008) has classified ARAs into three categories according to their chemical composition:

- petroleum based (Scardina, 2007),
- fatty-oil based (Artamendi et al., 2012; Ballenger and Light, 1993; Bymaster and Smith, 2009; Chesky, 2001; Davies, 2005; Dituro et al., 2002; Kinnaird, 2000; Kodali et al., 1997; Kultala, 2000; Lockwood et al., 1999; Olson et al., 1999; Zanzotto, 2003),
- non-oil based formulations (DeLong, 1994; Mahr et al., 2003; Martin, 1978; Martin and Coffey, 2000; Salmonsens et al., 1999; Zaki and Troxler, 2013).

This portion of the bibliography will cover the type of ARAs that have been developed and the performance characteristics that may be associated with their chemistry. Additionally, the test methods developed thus far in testing their performance and damage to asphalt will also be studied.

### 2.2.1 Petroleum based ARAs

Petroleum-based ARAs and BRs, such as diesel fuel, have been used for years as they are inexpensive, available on most construction sites and adhere to most surfaces due to their low viscosity. They function by softening the bitumen on the surface, that is, reducing its viscosity, cohesiveness, and thereby the adherence to the surface (Davies, 2005; Dituro et al., 2002; Mahr et al., 2003; Scardina, 2007).

Petroleum products such as diesel fuel however, are skin irritants and emit volatile compounds harmful to human health, while also causing environmental problems in the area around the construction site by leaching into the soil and groundwater. Diesel oil based agents generally contain aliphatic, olefinic, cycloparaffinic and aromatic hydrocarbons in different portions, as well as additives to improve the engineering performance. Among these compounds, the monocyclic aromatic hydrocarbons (MAHs) and polycyclic aromatic hydrocarbons (PAHs) are well-known contaminants, which have shown to be mutagenic and potentially carcinogenic.



This can lead to health problems in both the short and long term (Tang, 2008; Tang and Isacsson, 2006, 2005).

Petroleum based ARAs are flammable, and when they come into contact with the new asphalt in high concentrations on the asphalt truck bed or by an accidental spill, may cause damage to the bitumen leading to soft spots that reduce the structural integrity of the roadway (Ballenger and Light, 1993; Tang and Isacsson, 2006, 2005). The deterioration effect is exacerbated with increasing heat, light and time of contact with the bitumen (Acton, 2013; Kodali et al., 1997; Martin, 1978).

Due to their high volatility, there is also the issue of them evaporating during particularly long voyages, leading to a loss in functionality (Mahr et al., 2003). For this reason, the U.S. Department of Transportation as well as many state departments have restricted the use of diesel fuel as an asphalt release agents as part of the Oil Pollution Act of 1980, defining ARAs as “biodegradable while not posing a health risk to workers or an impact on the environment” (Acton, 2013; Zaki and Troxler, 2013). This has necessitated the development of alternative biodegradable ARAs and BRs.

### **2.2.2 Bio-based ARAs**

There have been a variety of bio-sourced ARAs developed during the past two decades. For example French market, has a number of C18 ester ARAs available.

#### **2.2.2.1 ARA composition**

Alternative ARAs include bio-sourced fatty-oil based agents. They can be composed of lecithin dispersed in an ether (Kodali et al., 1997; Olson et al., 1999), tall oil (Kultala, 2000) fatty acids diluted in water (Kinnaird, 2000), glycerol (Artamendi et al., 2012; Dituro et al., 2002; Lockwood et al., 1999; Zanzotto, 2003), soybean, cottonseed, canola, peanut, sunflower and palm oils, (Ballenger and Light, 1993; Davies, 2005).

Other biodegradable agents can be organic, inorganic or a mixture of both. These agents can be composed of water based mixtures with polycycloaliphatic amines, polyalkylene glycols (Salmonsens et al., 1999), polysiloxane in emulsion (Mahr et al., 2003; Martin and Coffey, 2000; Zaki and Troxler, 2013), water-based solutions of magnesium or calcium chloride (DeLong, 1994) and organic esters (Mikhailenko et al., 2015b) among others.

#### **2.2.2.2 ARA performance and interaction with asphalt**

All of the above agents are claimed to be biodegradable and to work as a surfactant by reducing the interfacial tension between bitumen and the contact surface as well as the friction, forming a separating layer or substrate that does not damage the asphalt. However, this has been shown to not always be the case.

There has also been damage to asphalt observed from the use of certain bio-sourced ARAs such as ester (C18) based formulations (Figure 2-17). Escadeillas et al. (2011) mixed diesel and a vegetable-based ARA with bitumen and observed the changes in penetration (ASTM D5-EN 1426) and softening point (ASTM D36-EN 1427). It was found that the penetration increases significantly with diesel and ARA addition while the softening point decreases. These were strong indications of the diesel and the vegetable-based agent deteriorating the bitumen in a similar manner.



Figure 2-17 Damage to asphalt observed from the use of vegetable based ARA on new pavement

Alternative biodegradable ARAs and BRs have often been found to be less effective than diesel (Bymaster and Smith, 2009; Mahr et al., 2003; Tang, 2008), although this has begun to change in recent years (Scardina, 2007). The agents may have less power to damage the bitumen than petroleum-based ARAs, but will stay in contact with the asphalt for a longer time due to their higher evaporation temperatures (Zaki and Troxler, 2013).

Additionally, bio-sourced chemicals can also possess an unpleasant odor, attracting insects such as flies and therefore presenting a nuisance and even health hazard to the surrounding area (Lockwood et al., 1999).

### 2.2.3 Laboratory testing of ARAs

The American Association of State Highway and Transportation Officials (AASHTO) National Transportation Product Evaluation Program (NTPEP) for asphalt release agents (NTPEP, 2014) has two tests for evaluating ARA performance and one for safety. However, their results are pass/fail and the tests are subjective in their implementation. There are many US departments of transportation that have similar rating systems. There is no known testing for BRs.

Asphalt release agents are widely used to protect tools and truck beds from the residue of asphalt; however, the study of their performance or of the damage that they can cause to asphalt has been minimal due to the fact that ARA manufacturers – in the cases where they test their products before

filing patents or putting the products on the market – do not publish the results of these studies (Tang, 2008). Studies or patents on BRs appear to not exist, most likely due to the fact that BRs function simply as bitumen solvents and thus, need to meet less performance criteria than ARAs. The only information available on most ARAs and BRs are generally material safety data sheets (MSDS), which do not present the full compositions of the products.

The only peer reviewed articles (Tang and Isacson, 2006, 2005) on ARAs test them only for the chemicals that can be harmful to worker health (VOCs), which although very important but not a main objective of this study. Some preliminary work has been done on ARAs by (Escadeillas et al., 2011; Nivet and Alliot, 2011; Randrianarimanana, 2010), although with little in the way of tangible results.

#### ***2.2.3.1 CBR test for determining ARA damage to asphalt***

Escadeillas et al. (2011) attempted to quantify the damaging effects of different types ARAs on the asphalt. Asphalt samples ( $\varnothing 200$  mm x 100 mm) were produced using proctor compaction (EN 12697-30) and EN 13297-30 proctor moulds (Figure 2-18). Several vegetable-based ARAs were tested in addition to diesel fuel.

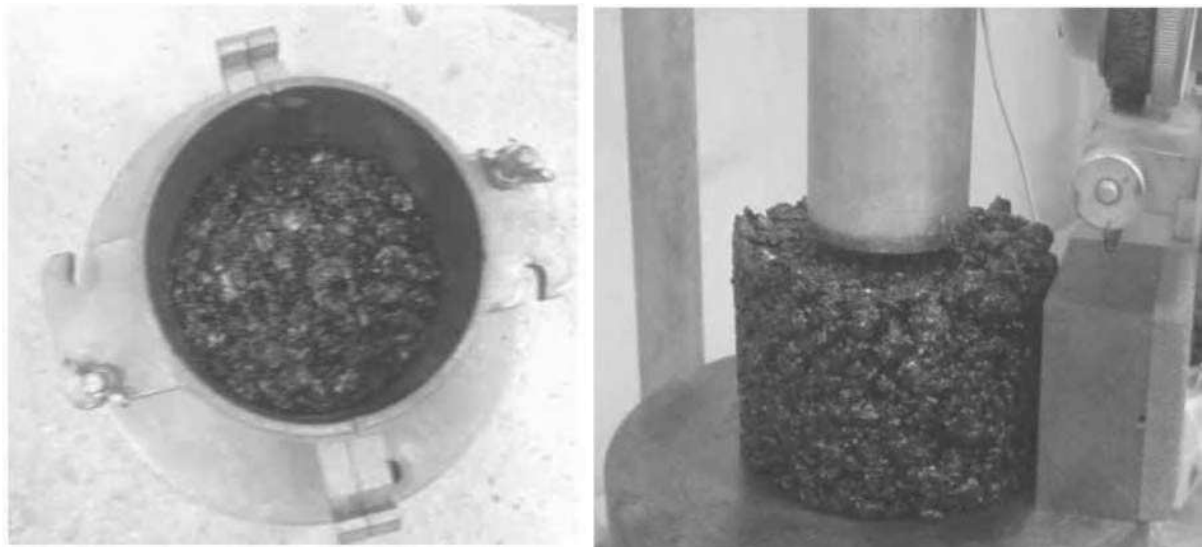


Figure 2-18 Asphalt in EN 13297-30 proctor moulds after compaction (left) and CBR test on asphalt sample (right)

The ARAs were applied to the asphalt at temperatures of 20, 90 and 140°C. The samples were then tested via the CBR test, which measures the resistance of the center of the sample to compression from a  $\varnothing 100$  mm piston at 1.47 mm/min (Figure 2-18). The samples were tested at 1 and 7 days after the application of the ARA.

It was found that for samples with gasoil, the resistance to the CBR increased somewhat with the decrease in application temperature. This is due to a relatively low temperature of is increased. This

was also the case for the vegetable-based ARAs with lower evaporation temperatures as, where this effect was even more significant.

Gasoil did not show a significant reduction lowering the strength of the sample, at 1 or 7 days. On the contrary, many of the vegetable based agents caused a significant decrease in strength. The decrease in strength at 1 and 7 days from the vegetable ARAs varied, with some showing a significant disparity between 1 and 7 day results, while other ARAs did not appear to reduce the strength of the asphalt at 7 days compared to 1. This was an indication of variable time dependency for the interactions between the ARAs and the bitumen. Different chemicals in the ARAs will have different interactions with the bitumen that will also be dependent on time of contact.

#### ***2.2.3.2 NTPEP Evaluation of Asphalt Release Agents***

The AASHTO norms for “NTPEP Evaluation of Asphalt Release Agents” (2014) have been developed in the United States in the 2000s as a means of evaluating asphalt release effectiveness, and safety. ARA manufacturers in the United States need to submit their products to these testing protocols before they are approved to be used in highway construction projects. This submission could be on a national level to AASHTO or to the various state departments of transportation, who may or may not have their own versions of the testing procedures. The 3 principle tests described in AASHTO consist of a 7-day stripping test, an asphalt slide test and an asphalt performance test. The first one is a test of the damage from the ARA on the bitumen and the latter two are measures of ARA performance.

##### **Asphalt slide test**

The Asphalt slide test is designed to replicate the event of the ARA asphalt on a truck-bed in a laboratory. The test begins by spraying an ARA on a steel plate and placing 0.5 kg of hot asphalt (143°C) on top of it. A hot bucket of sand is then placed on top of the asphalt, simulating the pressure on the asphalt at the bottom of the truck for 1h.

The plate is then tilted at 45° in order to let the asphalt slide off. The plates are then tilted up to two more times, if the asphalt did not slide off the first time. The effectiveness of the ARA is taken as a measure of the amount of binder left on the plate, with less binder indicating a more effective agent.

##### **Asphalt performance test**

The asphalt performance test determines the susceptibility of hot asphalt binders adhering to plant and paving equipment, rakes, shovels, etc. when using ARAs. The test begins by spraying an ARA on a steel plate and placing 20g of hot bitumen (143°C) on top of it. The binder is allowed to cool for 5 min, after which, the tester attempts to remove the bitumen with a spatula in one continuous pull.

The effectiveness of the ARA is taken as a measure of the amount of %w binder left on the plate. Unfortunately, the removal of the bitumen with a spatula makes this test very subjective due to the potential variations in the strength and skill of the tester.

#### **7-day stripping test**

The AASHTO 7-day stripping test submerges a hot sample (143°C) of asphalt (about 50 g) into an ARA in a glass jar. After a 7-day period, the sample is observed visually for stripping around the aggregates. The stripping is evaluated on a 4-tier scale ranging from no stripping to severe stripping which consists of discoloration along with stripping of the coarse and fine aggregate. While this test observes the effect of the ARA on the bitumen, it is at the same time subjective and dependent on the opinion observer.

The NTPEP provides a base for ARA evaluation and there are many US departments of transportation that have similar rating systems. However, their results are pass/fail and the tests are subjective in their implementation. Additionally, there are no known tests or testing programs for BRs.

#### **2.2.4 Bitumen solubility**

An important factor in the performance of BRs is their ability to dissolve bitumen residue on tools. The capability of a solvent to dissolve bitumen can be defined by the Hansen solubility parameter (Ra). The parameter takes into account the dispersion forces (D), the energy from dipolar intermolecular force (P) and the energy from hydrogen bonds (H) between molecules of the solvent. An interaction radius is assigned to the matter being dissolved (R<sub>0</sub>). To define whether the matter will be dissolved by the solvent relative energy difference (RED) is given as in Equation 2-4, will a lower value indicating the bitumen is more likely to be dissolved (Hansen, 2012).

Equation 2-4

$$RED = \frac{Ra}{R_0}$$

Where, if RED < 1 the molecules are alike and will dissolve

RED = 1 the system will partially dissolve

RED > 1 the system will not dissolve

A list of solvents according to their HSD values is shown in Figure 2-19.

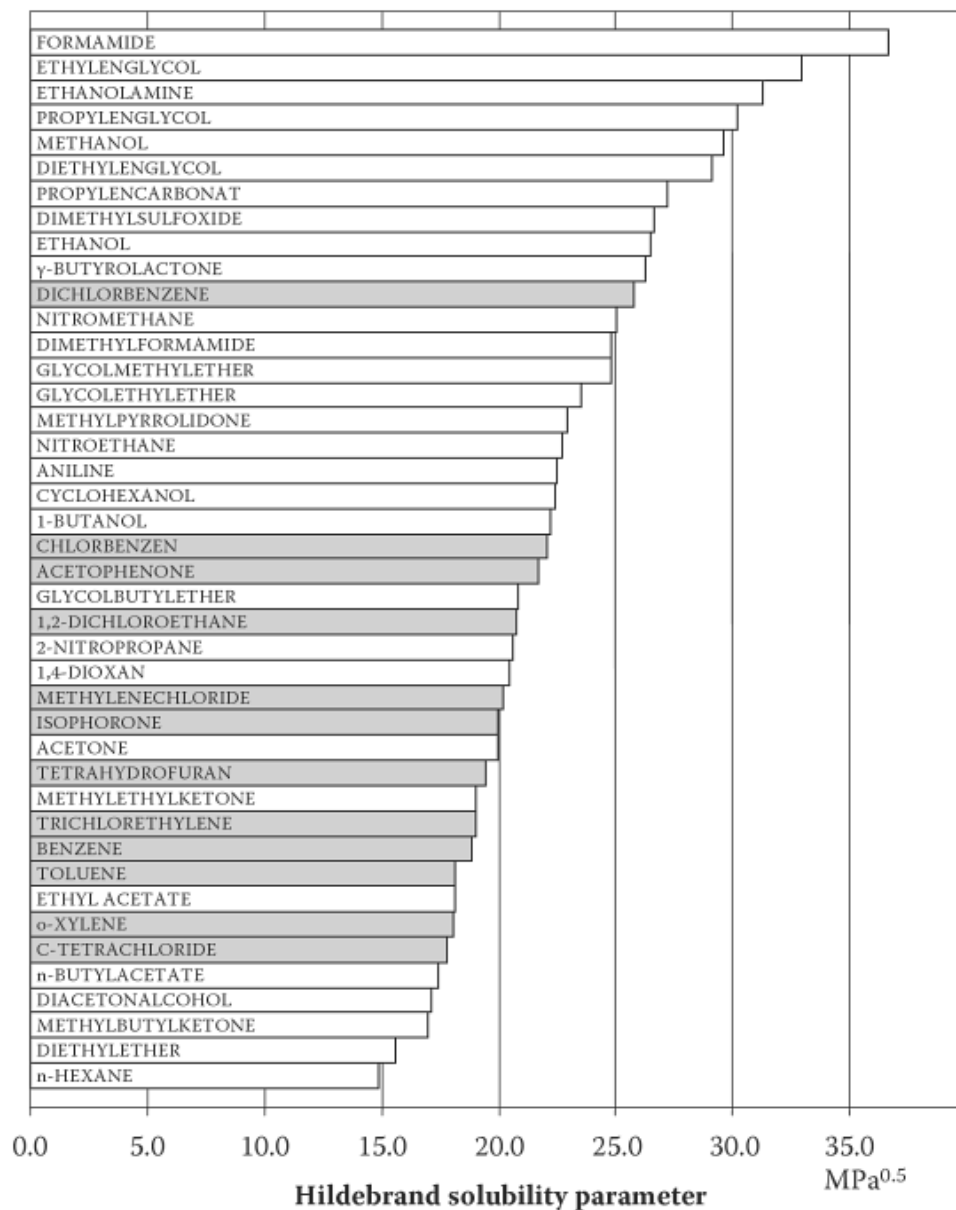


Figure 2-19 Various solvents according to their HSD values with good solvents shown in grey (Hansen, 2012)

### 2.2.5 Conclusions on ARAs

ARAs are used in the protection of asphalt tools from bitumen residue. Traditionally, diesel fuel has been used as an ARA, however, since it is currently banned for this use, several bio-sourced agents have been developed. These agents however, are sometimes not as effective as diesel.

There have been two test developed by AASHTOO for testing ARA performance, and one for the degradation of asphalt. However, these tests are subjective and quantitative methods need to be developed.

## 2.3 Reclaimed asphalt pavement (RAP) and bitumen rejuvenation

With the aging of asphalt pavement roads around the world, their need for replacement can create enormous waste disposal problems. While surface rejuvenation can extend the service life of a

pavement, the mechanical changes from bitumen aging makes it inevitable that the asphalt will need to be replaced. When the price of oil (and bitumen) was relatively low, recycling asphalt was not considered economically necessary. Recently however, as this situation is changing, recycling asphalt is becoming more widespread (Brownridge, 2010; Davidson et al., 1978; Zargar et al., 2012).

As of 2013, the industry in France has the capacity to recycle 7-8 million tons of RAP per year, compared to the yearly asphalt production in France being around 40 million tons (IDRRIM, 2013).

The recycling of asphalt is a process where old pavement is broken up (Figure 2-20) and used as reclaimed asphalt pavement in new asphalt pavement. RAP is defined as “asphalt reclaimed by milling of asphalt road layers, by crushing of slabs ripped up from asphalt pavements or lumps from asphalt slabs and asphalt from reject and surplus production” by EN 13108-8. Some RAP can be characterized as “black rock”, that is, bitumen will not be able to act as a binder for asphalt with conventional mixing procedures, but most RAP is able to recover a part of its adhesive abilities (Chen et al., 2007).

In addition to the cost benefits of being able to produce new asphalt from old, there is also the advantage of reducing the carbon footprint of the construction significantly by reducing the emissions in the transportation of raw materials as well as the reduction in the extraction of virgin aggregates. Additionally, this allows for the clean and relatively easy removal of a waste product in old asphalt. On the other hand, VOCs from bitumen volatilization have been found to increase with recycling rate (Jullien et al., 2006; Schvallinger, 2011).



Figure 2-20 Breaking up of old asphalt slabs for use as RAP (bitumen.info, 2009)

### 2.3.1 Bitumen aging

As all building materials, asphalt pavement has a service life, and at some point in its life, needs to be replaced, due to the bitumen aging. The bitumen gets hard and brittle over time, leading to cracking in the pavement. This makes the road less safe for vehicles as it reduces the stability of the road.

The replacement of the road depends on the degree of aging, the importance of the road traffic in terms of overall traffic and economically, as well as the financial conditions of the governing body responsible for maintaining, rehabilitating and replacing the road (Finlayson et al., 2011; Wang et al., 2014).

The quality over time of asphalt pavement can depend on many factors including the traffic loading, the environment, the drainage and the quality of construction. While regular maintenance cycles can mitigate the aging effects, the long-term aging effects on the bitumen will eventually lead to surface cracks that require the pavement to be rehabilitated or replaced (Smith and Edwards, 2001).

The initial hardening of the bitumen is largely due to the evaporation of the lighter aromatics, naphthene aromatics during bitumen storage (160-180 °C), along with mixing (160 °C) while the long-term aging is due to the oxidation over the in-service time (Chávez-Valencia et al., 2007; Siddiqui and Ali, 1999a). Another possible contributor to aging is ultraviolet (UV) radiation from exposure to the sun (Durrieu et al., 2007).

The effect of time on bitumen leads to a progressively more stiff and brittle material. It was found that the more volatiles were lost for a certain bitumen after RTFOT aging (around 0.3-0.6 %w), the stiffer the bitumen became (Siddiqui and Ali, 1999a). The factors affecting bitumen ageing include characteristics of the bitumen and its content in the mix, nature of aggregates and particle size distribution, void content of the mix, production related factors, climate, temperature and time (Atkins, 2003; Chen et al., 2007; Farcas, 1996; Fernández-Gómez et al., 2013).

Bitumens that are either aged in the field or pre-oxidized, or rich in asphaltenes are more likely to exhibit characteristics of the GEL model. As explained earlier, the GEL model constitutes a three-dimensional continuous structure that exhibits an elastic behavior. As such, this augments the stiffness of the bitumen and has an effect on the resulting asphalt. While the asphalt would be more resistant to rutting with the GEL model, the cracking of the bitumen is also more likely leading to a need for road replacement (Tachon, 2008).

In order to be able to replicate these changes in a laboratory environment, there have been several laboratory aging methods developed including thin film oven and convection oven based methods. Concurrently, there have been several analysis techniques developed to better understand the chemical changes in bitumen and to allow for the identification of aged bitumen. These methods include FTIR, FTIR microscopy, SEM, TGA Raman spectrometry and other techniques. These are often combined with rheological testing of bitumen.

The objective of this part of the review is to understand the bitumen aging process and how to be able to best replicate in our laboratory. That is, the study of the performance and chemical effects of bitumen aging, along with the most current techniques for being able to perform and analyze



bitumen aging a laboratory environment. This understanding of bitumen aging will aid the study of bitumen rejuvenation by bio-sourced rejuvenating agents, which will be discussed in Section 2.3.6.

### **2.3.1.1 Accelerated aging methods**

Due to the fact that the life cycle of asphalt is many years, several accelerated laboratory aging methods have been developed in order to simulate the effects of in-field aging and oxidation on bitumen for a shorter period of time. Nevertheless, these methods vary in one way or another compared to in-field aging, depending on the bitumen characteristic that is being evaluated (oxidation, penetration...).

This can be separated into short-term and long-term aging:

- Short-term aging refers to the change in properties of asphalt during storage at the plant and conventional hot-mixing (both around 160°C) in terms of viscosity, penetration, or ductility measurements. Most of the volatilization occurs during short term aging.
- Long term aging is the bitumen oxidation during the service-life of the asphalt before it would need replacement (Fernández-Gómez et al., 2013).

#### **2.3.1.1.1 Thin Film Oven Test and Rolling Thin Film Oven Test**

**Short-term aging** can be simulated in a laboratory by the thin film oven (TFOT – EN 12607-1 or ASTM D 1754) test which ages a thin strip of asphalt at 163°C for 5 hours. This can also be simulated with the rolling thin film oven (RTFOT - EN 12607-2 or ASTM D 2872) test as shown in Figure 2-21, which is performed at 163°C for 85 min while in rotating motion.

There is some opinion that the RTFOT is actually more severe than asphalt plant conditions (Mouillet et al., 2008).



Figure 2-21 Rolling Thin Film Oven Test (Jet Materials)

#### 2.3.1.1.2 Pressurized Aging Vessel

**Long term aging** can be performed by PAV (ASTM D 6521), which is intended to simulate the effects of oxidation for several years, although the precise duration is still up for debate. Farcas (1996) estimated the real age at 4 years, while it was estimated to be 5-10 years by (Litzka et al., 1998).

The PAV accelerates the aging (oxidation) of asphalt binders by means of pressurized air and elevated temperature (Figure 2-22). The PAV is designed to be conducted on the asphalt samples after the RTFOT (from the residue of the same sample). The samples (50 g) are vacuum de-gassed and placed inside the PAV at a temperature of 109°C. An air pressure of 2.1 MPa is applied through a compressed air cylinder and maintained for 20 h. The pressure is slowly released before the end of the test.

This is intended to simulate the type of changes which occur in asphalt binders during in-service oxidative aging, but may not accurately simulate the relative rates of aging. For bitumen binders of different grades or from different sources, there is no unique correlation between the aging time/temperature in the PAV and in-service pavement age and temperature. Therefore, for a given set of in-service climatic conditions, it is not possible to select a single PAV aging time and elevated temperature and pressure that will correspond to the properties or the relative performance of all asphalt binders.

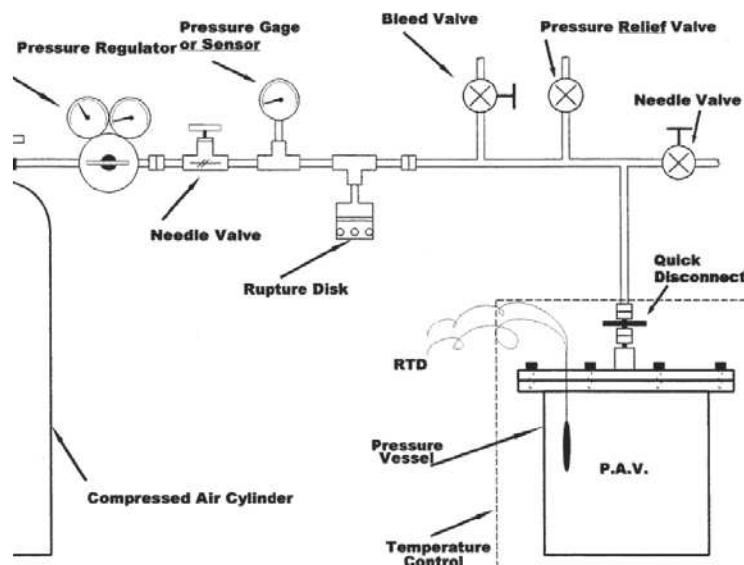


Figure 2-22 Example of Pressurized Aging Vessel (ASTM D 6521)

#### 2.3.1.1.3 Ventilated Oven

Aging by ventilated oven is also a popular method of simulating the aging of bitumen.

The convenience of this method is that it can be performed in almost any laboratory as ventilated ovens are common place. The oven needs to be well ventilated for the test to provide a consistent

supply of oxygen to the sample, which should be made as thin as possible in order to provide more surface area for the oxidation.

There are varied temperatures suggested for these methods such as 60°C by Durrieu et al. (2007) or 60, 80 and 100°C for 24, 36 and 48 days by Chávez-Valencia et al. (2007). De la Roche et al. (2013) conducted the aging of asphalt in two stages; the first at 135°C for 4 h and the second at 85°C for 9 days.

Chávez-Valencia et al. (2007) found that 24-36 days over oven aging at 100°C can be correlated with approximately 1-2 year of aging in the field for certain properties but not others.

It is important to note, that the oxidation conditions present during high-temperature oven aging have been shown to be different from the ones present in the field. De la Roche et al. (2013) found that plant and laboratory manufactured asphalt ages differently in terms of certain indicators. The asphalt in the field for example, would not lose as many volatiles compounds as during high temperature oven aging (Tahirou, 2009). This is because some of the volatiles for their in-field conditions would never achieve their volatility temperature.

When the aging is conducted for a few hours, it is sometimes known as short-term oven aging (STOA). This method was conducted by Kandhal and Chakraborty (1996), Lee et al. (2008) at 135 and 154°C for 2-4 h, respectively. This method appeared to show slightly more profound effects than RFTOT in terms of aging (Lee et al., 2009).

#### 2.3.1.1.4 UV aging

There also exists the possibility of laboratory UV aging as performed by Durrieu et al. (2007), Lins et al. (2008) and Naskar et al. (2013).

The goal of UV aging is to simulate the effects of high energy cosmic radiation from the sun on bitumen that are not simulated with conventional laboratory aging.

Durrieu et al. (2007) performed this on bitumen after RTOFT aging where the samples are placed in a special chamber and subjected to UV radiation at a temperature of 60 °C for 170 h. Lins et al. (2008) used a weathering chamber that mixed UV light with water spray for 500, 1000, 1500, and 2000 h. Naskar et al. (2013) placed the samples two Teflon sheets for 1 min at 80°C and a pressure of 5 tons in an electrically heated hydraulic press to obtain 2 mm thick bitumen film for UV exposure. The bitumen film placed on an aluminum sheet was kept in the UV chamber at a 500 mm distance from the lamp. The film was kept for 30 min in the UV chamber maintained at room temperature.

#### 2.3.1.1.5 Other methods

There has also been a simulated oxidation method developed by Lamontagne et al. (2001b) to study the oxidation of polymer-modified bitumen (PmB) while observing the samples with a Fourier

transform infrared (FTIR) microscope. The aging was determined from the evolution the PmB's microstructures, corresponding to and FTIR spectra band (Mouillet et al., 2008).

It is possible to age asphalt in service as well (Chávez-Valencia et al., 2007; Hofko et al., 2014; Jung, 2006; Lamontagne et al., 2001a). The asphalt samples can be recovered in accordance with the ASTM D 5404 Standard Practice for Recovery of Asphalt from Solution Using the Rotary Evaporator, which separates the bitumen from the aggregates by a solvent, where the bitumen is then recovered by a rotary evaporator. The test is generally conducted over years and is difficult to correlate with lab testing because of climatic variability.

### ***2.3.1.2 Physical and performance effects of bitumen aging***

As RAP is derived from old asphalt, its performance characteristics are determined largely by the aging of the bitumen. The resulting characteristics include a decrease in penetration, increase in softening point, increase in viscosity, decrease in ductility, cohesion, and adhesion of aggregates and bitumen, along with a decrease in thermal resistance for asphalt (Al-Qadi et al., 2007).

In terms of rheology, the elastic behavior of the RAP binder is much higher than for virgin binder, the difference being highly dependent on the RAP source (Jamshidi et al., 2012). The capacity of the asphalt to heal itself is also decreased (Van den bergh and Van de Ven, 2012). In addition to these negative effects, the rutting and fatigue resistance are sometimes increased due to the bitumen becoming harder, although this is not always the case, and the performance can also be equal or worse in these two parameters compared with asphalt without RAP addition. In the final analysis, the performance of the RAP asphalt will depend heavily on the quality of the RAP aggregates (Al-Qadi et al., 2007; Aravind and Das, 2007).

#### ***2.3.1.2.1 Penetration***

Siddiqui and Ali (1999a), Durrieu et al. (2007), Mouillet et al. (2008), Le Guern et al. (2010), Firoozifar et al. (2011) and El Béze et al. (2012) found that after RTFOT and PAV aging, the penetration decreases, as the bitumen ages and becomes stiffer. This loss of penetration becomes more severe as the intensity of the aging increases such as with PAV aging (Section 2.3.1.1). Mastrofini and Scarsella (2000), Peralta (2009) and Dehouche et al. (2012) found a decrease after RTFOT aging and so did Chávez-Valencia et al. (2007) after both oven and in-field aging.

#### ***2.3.1.2.2 Softening point***

It was found that after RTFOT and PAV aging the softening point temperature increases as the bitumen ages and becomes stiffer (Siddiqui and Ali (1999a), Durrieu et al. (2007), Mouillet et al. (2008), Le Guern et al. (2010) and Firoozifar et al. (2011) and El Béze et al. (2012)). The softening point becomes higher as the intensity of the aging increases such as with PAV aging.

#### 2.3.1.2.3 Viscosity

As the bitumen ages, it becomes harder and more resistant to shear deformation the values for dynamic viscosity of the bitumen increases with aging (Siddiqui and Ali (1999a), Mastrofini and Scarsella (2000), Jung (2006), Vargas et al. (2008), Lee et al. (2008), Lee et al. (2009), and Firoozifar et al. (2011)).

In Siddiqui and Ali (1999a), the bitumen that had the lowest increase in viscosity from aging was the bitumen that lost the least mass with aging in had the lowest change in the naphthene aromatics fraction. They also found that the increase in asphaltenes was directly correlated to an increase in viscosity (Fernández-Gómez et al., 2013).

#### 2.3.1.2.4 Rheology

In terms of rheology, the bitumen becomes stiffer with aging as the bitumen adapts more GEL like characteristics and becomes more elastic. This increase is strongly temperature dependent as at medium-high temperature, the aged (RTFOT) samples have higher stiffness and elasticity, while at low temperatures, the difference in rheology is far less severe (Lu and Isacsson, 2002; Mastrofini and Scarsella, 2000).

#### 2.3.1.2.5 Ductility

During aging, the bitumen not only becomes harder, but more brittle as well. Therefore, there is a loss of ductility that occurs during aging (Atkins, 2003). Jung (2006) found that the ductility of bitumen increases significantly after RTOFT and PAV aging. This results in the embrittlement of asphalt paving and fatigue cracking (Fernández-Gómez et al., 2013; Petersen, 2009)

#### 2.3.1.2.6 Bitumen cohesion and adherence to aggregates

Aging effects reduce the adherence of bitumen to aggregates due to the bitumen becoming more hydrophilic with time. This mechanism leads to the formation of cohesively weak boundary layers between the bitumen and aggregates (Airey, 2003; Tahirou, 2009).

### 2.3.1.3 *Chemical changes to bitumen during aging*

The chemical changes in bitumen during aging can be observed by several techniques, which will be discussed in the following section.

#### 2.3.1.3.1 Elemental of bitumen composition after aging

Elemental analysis (EA-ASTM D 5291) of three asphaltene fractions (the bitumen A having the highest penetration and C the lowest) after RTFOT by Mastrofini and Scarsella (2000) is shown in Table 2-5. The elemental ratios change noticeably, indicating the loss of some elements by chemical transformation or volatilization. The O to C ratio of the asphaltenes is increased as the bitumen

experiences oxidation during aging. The H to C ratio is said to decrease due to the dehydrogenation reaction during the oxidation of asphalt.

Table 2-5 Elemental analysis (ASTM D 5291) by weight of asphaltene fractions after RTFOT aging (Mastrofini and Scarsella, 2000)

Asphaltenes	Penetration of bitumen 25°C (1/10mm)	C (%)	H (%)	O (%)	N (%)	S (%)	H/C	O/C
A-new	68	82.6	7.6	1.3	1.0	6.8	1.104	0.012
A-RTFOT	37	83.4	7.2	1.4	1.0	7.0	1.022	0.013
B-new	59	84.6	7.5	1.8	0.6	5.5	1.064	0.016
B-RTFOT	34	85.1	7.3	2.1	0.7	4.8	1.029	0.018
C-new	38	83.0	6.3	2.6	0.8	7.2	0.911	0.023
C-RTFOT	17	84.2	5.8	3.2	0.8	6.0	0.827	0.028

#### 2.3.1.3.2 SARA Fractions after aging

It terms of bitumen aging, SARA classification – also referred to as Corbett Method, High Performance Gas Chromatography (HPLC), Thin-Layer Chromatography with Flame Ionization Detection (TLC-FID, also known as IATROSCAN) – allows the quantification of chemical changes in the bitumen. As described in Section 2.1.3.2, the SARA classification using HPGC can categorize the hydrocarbons of asphalt based on their properties into asphaltenes, resins, saturates and aromatics/naphthene aromatics.

A study by Siddiqui and Ali (1999a) used Corbett method (with RTFOT and PAV aging) to observe that there is a relative increase with aging in the asphaltene and resin fractions and a decrease in the naphthene aromatic fraction. There was also a small increase in the saturate fraction following oxidation for some of the bitumens, but this was not considered as significant. These proportional changes were combined with a loss in mass of from the bitumen after RTFOT aging, indicating volatilization, likely of the aromatics fraction. This is combined with a chemical transformation of the bitumen, which the authors indicated favouring the transformation of naphthene aromatics to asphaltenes due to the increase in the Gaestel index. The authors hypothesize that some of these reactions may have been condensation with ester formation, polymerization or isomerization, dehydrogenation, aromatization, and dealkylation as shown in Figure 2-23 (Siddiqui and Ali, 1999b).

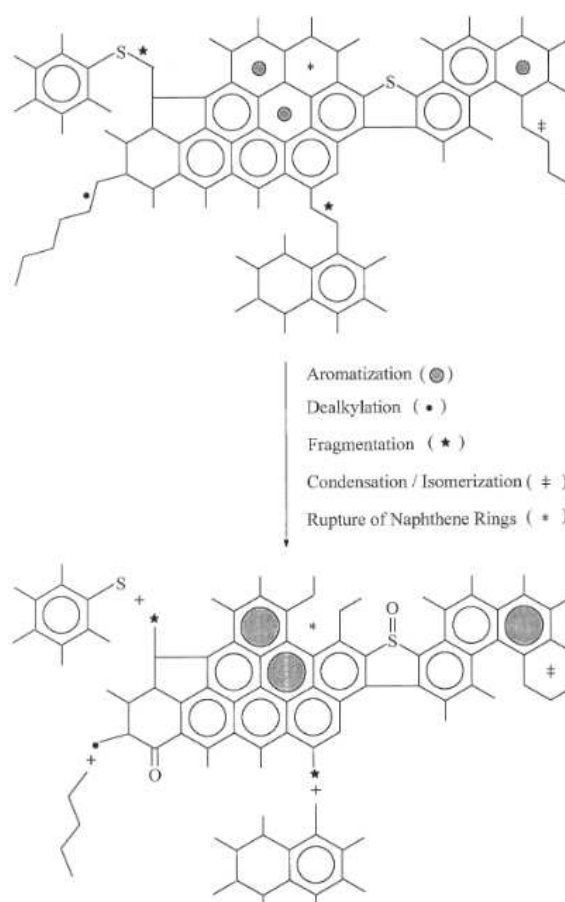


Figure 2-23 Possible representation of reaction types in a hypothetical asphalt structure on laboratory aging (Siddiqui and Ali, 1999b).

Lu and Isacson (2002) examined the aging of 7 types of bitumen (with TFOT and RTFOT aging) with TLC-FID. The results showed a reduction in the content of aromatics fraction after aging in all of the bitumens. Aging was found to have a significant effect on the increase of resins and asphaltenes.

The aromatics were reduced with aging while saturates proportion would stay the same, or change to a small degree. Since the fractioning of bitumen is mainly based on molecular polarity, the compositional changes are attributed to the transformation of different fractions as in the aromatics to resins and resins to asphaltenes.

It is interesting to note that TFOT appears to promote the increase of the resin fraction while reducing the aromatics fraction more significantly. RTFOT on the other hand, seems to favour the increase of the asphaltene fraction (Lu and Isacson, 2002). This could be an indication that the aromatics to resins transformation is favoured by longer exposure to high temperatures (5h duration for TFOT versus 85min for RTFOT) while the formation of asphaltenes is favoured by more exposure to oxygen (rotation in oven).

Le Guern et al. (2010) examined the aging of 5 types of bitumen (with RTFOT and PAV aging) with TLC-FID. The results were the same as for Lu and Isacsson (2002), except with a more profound effect due to PAV aging. The resin and asphaltene fractions increased with aging while the aromatics saw a significant drop. The saturate fraction saw a small increase for 4 of the bitumens with a small decrease for the other one. Using only RTFOT aging, Dehouche et al. (2012) found similar results except that the saturates had small decreases for the bitumens observed while El Béze et al. (2012) saw the saturates stay constant.

Gasthauer et al. (2008) however, also found through GC-MS analysis of a presence of saturates in bitumen fumes, although the volatilization of naphthene aromatics was greater at higher temperatures, and that the asphalt temperature was the key element in predicting the nature of the emissions. It has been reported that an increase of 10-12°C in temperature can increase the volatile emissions two fold (Fernández-Gómez et al., 2013; Read and Whiteoak, 2003)

Proportionally, there is a trend toward the increase of resins and asphaltenes among the SARA fraction as well as a decrease in aromatics. As mentioned previously, the aromatics, resins and asphaltenes are very closely related, and as such, the aromatics oxidation tend to agglomerate to form resins and asphaltenes, while the resins agglomerate to form asphaltenes. This is combined with the volatilization for the lighter aromatics fraction or saturates. Kuszewski et al. (1997) found indications that naphthene aromatics can be characterized into two fractions; one being more susceptible to oxidation than the other. There is not clear trend with saturates with regards to aging.

#### 2.3.1.3.3 Fourier transform infrared spectroscopy

Fourier transform infrared spectroscopy (FTIR) can be used to obtain infrared spectrum of material while collecting a wide spectral range. The spectra correspond to vibrations of various chemical liaisons, allowing for them to be characterized. FTIR generally is able to observe spectra of between 200 and 4000  $\text{cm}^{-1}$  and can observe the relative changes in the bonds over time. The oxidation of hydrocarbons is associated with the increase of C=O and S=O bonds (Siddiqui and Ali, 1999a).

Spectrometry by transmission (FTIR-T) allows for the analysis of the liquid sample or of the sample dissolved in a substance that is invisible to IR spectrometry. While the FTIR-T sample has to be placed in a chamber, the attenuated total reflectance (FTIR-ATR) mode allow for analyzing the sample in liquid or powder form directly on a crystal (Farcas et al., 2009). Nevertheless, although the FTIR-ATR analysis is easier to implement, FTIR-T generally provides more intense (precise) spectra. FTIR microscopy allows for a cartography of the distribution of the spectra in the asphalt, that is, in relation to the position of the bitumen and the aggregates (El Béze, 2008).



The oxidation (aging) of bitumen can be observed with the change in C=O absorbances (around 1700 cm<sup>-1</sup>) and S=O absorbances (around 1030 cm<sup>-1</sup>). Mouillet et al. (2008) considers the S=O bands to represent the short term aging during asphalt manufacturing and the C=O bands to represent the long-term aging during the service life of the asphalt, while Siddiqui and Ali (1999a) consider both for short and long term aging.

There are several ways to prepare a sample for FTIR-T analysis. The “dry-plate technique” for example, dissolves the sample in dichloromethane as it lays on a potassium bromide (KBr) thin plate. The solvent is then evaporated under a nitrogen flow to avoid interference in the obtained spectra and a film thickness of about 20 µm is obtained (El Béze et al., 2012; Durrieu et al., 2007; Lamontagne et al., 2001a). It is also possible to prepare the bitumen with 5 %w solutions of in carbon disulfide (Edwards, 2005).

The carbonyl index (%) can be defined as in Equation 2-5 with a higher value indicating relatively more C=O bonds consisting of ketones, anhydrides formed during aging and carboxylic acid increasing during aging. The ketones are formed on the asphaltenes and resins where the benzylic carbons are concentrated (Siddiqui and Ali, 1999a).

Performing laboratory aging with TFOT, RTFOT and PAV, it was found a significant increase in C=O bonds, indicating a higher degree of oxidation (Araújo et al., 2011; Béze et al., 2012; Chávez-Valencia et al., 2007; Durrieu et al., 2007; Jung, 2006; Lamontagne et al., 2001b; Le Guern et al., 2010; Lu and Isacsson, 2002; Mouillet et al., 2008; Vargas et al., 2008; Yao et al., 2013). The rapid increase of I<sub>C=O</sub> after early aging can be attributed to formation of carboxylic acids, ketones, and anhydrides while the less rapid long term increase can be attributed to dehydrogenation and aromatization (Siddiqui and Ali, 1999a). This trend was confirmed with in-situ aging on asphalt roads (Chávez-Valencia et al., 2007; Jung, 2006; Lamontagne et al., 2001a). Durrieu et al., (2007) found that UV radiation plays a significant role in the increase of the C=O peak.

Equation 2-5

$$I_{C=O} = \frac{A_{1700cm^{-1}}}{A_{1460cm^{-1}} + A_{1376cm^{-1}}}$$

Where, A is the area around the specific absorbance. 1700cm<sup>-1</sup> is the absorbance for C=O while 1460cm<sup>-1</sup> and 1376cm<sup>-1</sup> are the absorbances for the deform CH<sub>2</sub> and CH<sub>3</sub> groups, which serve as baselines for the analysis as they stay relatively constant during aging (El Béze, 2008).

Chávez-Valencia et al. (2007) were able to derive an Arrhenius equation from this trend for the lab asphalt (A<sub>1</sub>), which shows the relationship of the C=O formation for this asphalt with temperature and time (Equation 2-6).

Equation 2-6

$$r_c = 0.0196e^{-2004/T} [d(C=O)/dt] \text{ (mol/day)}$$

Where, T is the temperature in °C, t = aging time in days.

Through this, the authors were able to calculate the activation energy for the asphalt oxidation, that is, the energy required for the reaction to occur. This was only done for the lab samples since it requires a range of temperatures. This could be a useful feature for the computer modeling of bitumen oxidation.

Liu et al. (1997) derived a relationship between the area under the C=O curve from FTIR analysis CA, and the change in viscosity  $\eta$ , over time  $t$ , as in Equation 2-7. It is not a measure of how fast an asphalt oxidizes, but it is a measure of its tendency to harden when it oxidizes, with lower values indicating a slower hardening (Madrid et al., 2000).

Equation 2-7

$$\frac{\delta \ln \eta}{\delta t} = \frac{\delta \ln \eta}{\delta CA} \frac{\delta CA}{\delta t}$$

The sulfoxide index (%) can be defined as in Equation 2-8 with a higher value indicating relatively more S=O bonds, which are formed during the oxidation of sulfide moieties (Siddiqui and Ali, 1999a). As with C=O, a significant increase in S=O absorbance was found with aging (Lamontagne et al. (2001a), Lu and Isacsson (2002), Chávez-Valencia et al. (2007), Mouillet et al. (2008), El Béze et al. (2012) and Yao et al. (2013) (Béze et al., 2012; Chávez-Valencia et al., 2007; Lamontagne et al., 2001a; Lu and Isacsson, 2002; Mouillet et al., 2008; Yao et al., 2013). Lamontagne et al. (2001a) and Chávez-Valencia et al. (2007) confirmed this trend with field-aging.

Equation 2-8

$$I_{S=O} = \frac{A_{1030cm^{-1}}}{A_{1460cm^{-1}} + A_{1376cm^{-1}}}$$

Where, A is the area around the specific absorbance. 1034 $cm^{-1}$  is the absorbance for S=O while 1460  $cm^{-1}$  and 1376  $cm^{-1}$  are the absorbances for the deform  $CH_2$  and  $CH_3$  groups (El Béze, 2008).

Aromaticity (at 1600  $cm^{-1}$ ) is the measure with FTIR of the relative contents of aromatic C=C bonds, respectively. This could be an indication of volatile naphthene aromatics and heavier particles such as resins and asphaltenes as well. It was found by Lamontagne et al. (2001b) and Mouillet et al. (2008) that the aromaticity of bitumen tends to increase somewhat with aging in both lab and field environments as the heavier and less volatile chemicals in bitumen, notably resin and asphaltene, tend to be more aromatic. This increase in the long term could be due to the dehydrogenation of naphthenic clusters with cleavage of short aliphatic side chains and increased condensation (Siddiqui and Ali, 1999a). Tachon (2008) found that the aromatics peak was strongest in the resin and

asphaltene fractions, weaker in the aromatics and not present with the saturates. In the previous section, it was demonstrated that aging has a strong correlation with the increase of asphaltene and resin fractions.

Tachon (2008) found that a strong peak associated with polarity (around 3450 cm<sup>-1</sup>) is present in only the resin and asphaltene fractions. Although this was not correlated with bitumen aging, it is possible that there could be a considerable depending on the aging regime. Araújo et al. (2011) observed this as well with RTFOT-aged bitumen.

It was also found that the peaks for aliphatics stretches around 2925 and 2853 cm<sup>-1</sup> were the least significant in the asphaltene fraction (Tachon, 2008). The FTIR analyses of RTFOT aged bitumen appear to show a decrease in these peaks with aging, indicating that they could possibly be indicators of aging (Lins et al., 2008; Yao et al., 2013). The change of key FTIR bands as a result of bitumen aging is summarized in Table 2-6.

Table 2-6 FTIR bands with bitumen aging

Chemical Group	Bond	Approximate Wavenumber (cm <sup>-1</sup> )	Change with aging	Intensity	Expression	References
<b>Sulphoxide</b>	S=O	1030	Increases in short-term	Weak	$\frac{A_{1030}}{A_{1460} + A_{1376}}$	Lamontagne et al. (2001a) Lu and Isacsso (2002)
<b>Carbonyl</b>	C=O	1700	Increases in long-term	Weak to medium	$\frac{A_{1700}}{A_{1460} + A_{1376}}$	Chávez-Valencia et al. (2007)
<b>Aliphatics (deform)</b>	C-CH <sub>3</sub>	1460, 1376	Relatively constant to small decrease	Medium	$\frac{A_{1460} + A_{1376}}{\Sigma A^1}$	Mouillet et al. (2008) El Béze et al. (2012) Yao et al. (2013)
<b>Aromatics</b>	C=C	1600	Relatively constant to increase	Medium	$\frac{A_{1600}}{\Sigma A^1}$	Lamontagne et al. (2001b) Mouillet et al. (2008) Tachon (2008) <sup>2</sup>
<b>Aliphatics (stretch)</b>	CH <sub>2</sub> , CH <sub>3</sub>	2923, 2853	Relatively constant to small decrease	Medium to strong	$\frac{A_{2923} + A_{2850}}{\Sigma A^1}$	Tachon (2008) <sup>2</sup> Lins et al. (2008) Yao et al. (2013) <sup>3</sup>
<b>Polarity</b>	O-H	3450	Increases	Strong	$\frac{A_{3450}}{\Sigma A^1}$	Tachon (2008) <sup>2</sup> Araújo et al. (2011)

<sup>1</sup>  $\Sigma A = A_{1700} + A_{1600} + A_{1460} + A_{1376} + A_{1030} + A_{864} + A_{814} + A_{743} + A_{724} + A_{(2953, 2923, 2862)}$  (Lamontagne et al., 2001a) or  $\Sigma A = A_{2000} + A_{600}$  (Yao et al., 2013)

<sup>2</sup> Hypothesized from results of FTIR analysis of SARA fractions by Tachon (2008)

<sup>3</sup> Observed from results of FTIR analysis of SARA fractions by Yao et al. (2013)

#### 2.3.1.3.4 Thermogravimetric analysis

Thermogravimetric analysis (TGA) is a chemical analysis technique based on the heating of materials progressively while measuring the change in mass with temperature. Various compounds will breakdown at different temperature, allowing us to identify and quantify these compounds. The differential of the change in mass with temperature are known as differential thermogravimetric (DTG) curves. The samples generally weigh less than one gram; therefore, the machine needs to be very precise in its measurements in order to allow for accurate quantification (Mikhailenko, 2012). The study of the thermal decomposition of bitumen is very difficult due to the presence of many varied and complex molecules along with their parallel and consecutive reactions (Benbouzid and Hafsi, 2008).

Kuszevski et al. (1997) observed the four SARA fractions of various bitumens under TGA at 163°C for up to 80h, exposing the bitumen to high temperatures for a long period of time. It was found that for the 20 bitumens tested, there were considerable differences in volatility depending on the bitumen origin. While around half of the asphalt showed volatility at 20h, nearly all of the bitumens lost at least half their mass at 80h of heating. Naphthene aromatics and polar aromatics were reduced with heating, with the reduction being significant at 80h. The asphaltenes fraction experienced an increase during the first parts of aging, due to the oxidation of polar aromatics and resins. At 80h, the asphaltenes decreased significantly, which is attributed to their consolidation into insoluble carboids. It was remarked that the presence of heteroatoms in the asphaltenes provided with distinct combustion characteristics. Firoozifar et al. (2011) found that a higher asphaltenes content decreased the decomposition temperature.

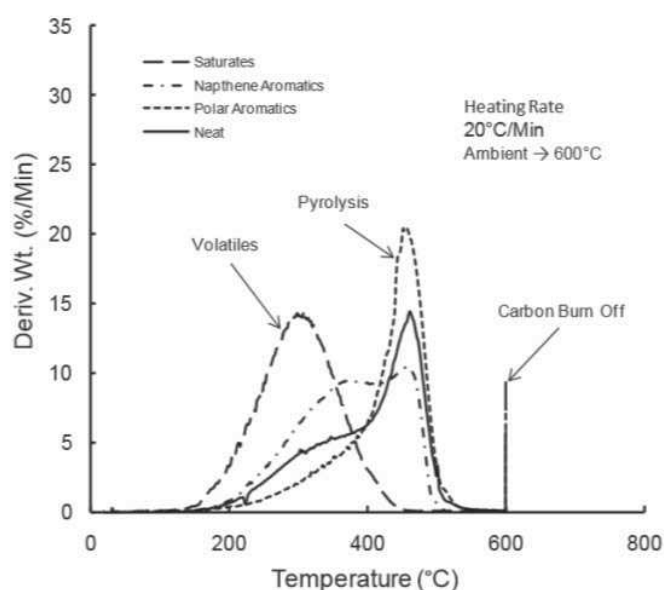


Figure 2-24 DTG curve for SARA fractions of bitumen (Pauli, 2014)

Pauli (2014) also observed the SARA fractions in TGA/ DTG, heating up to 600°C in inert Argon gas Figure 2-24. The saturates volatilized with a single peak from 200-400°C. Naphtene aromatics and asphaltenes appeared to produce two peaks at around 200-400°C and another larger peak at 400-550°C. Resins produced one large peak at 200-550°C centered around 450°C.

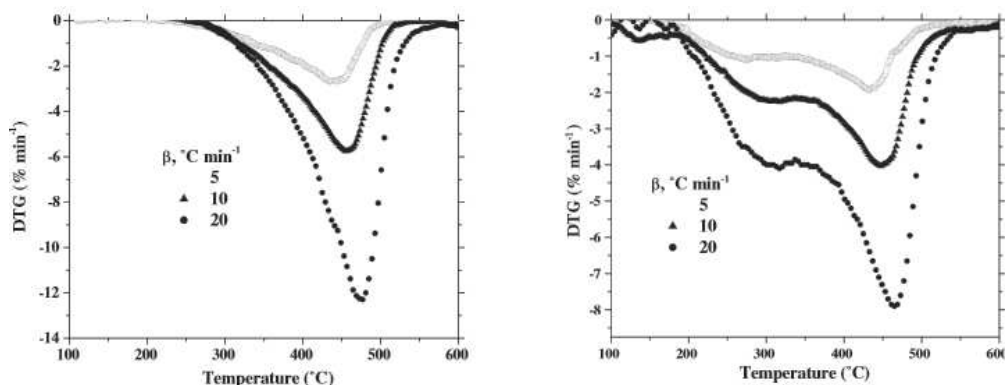
The thermal decomposition of organic materials such as bitumen is known as pyrolysis. It can be represented the relationship between the heating rate, and the volatile and solid byproducts that result from the heating as in Equation 2-9 (Benbouzid and Hafsi, 2008). Nomura et al. (1999) noted lighter liquid and gaseous products in bitumen as those volatilized before 310°C.

Equation 2-9



Benbouzid and Hafsi (2008) looked at the behavior of bitumen under TGA at up to 600°C at varied heating rates, before and after oxidation, finding two stages of deconvolution in oxidized (at around 200°C) bitumen as opposed to one stage in the unoxidized bitumen (Figure 2-25). The sole stage (at around 475°C) in the unoxidized bitumen corresponded to a stage present at the same temperature for the oxidized bitumen. The first stage in the oxidized bitumen is attributed by the authors to the decomposition of oxidation reagents.

Figure 2-25 DTG curves for unoxidized (40/50, left) and oxidized (20/30, right) bitumen (Benbouzid and Hafsi, 2008)



Mouazen et al. (2013) performed TGA on 50/70 bitumen up to 600°C in a nitrogen environment. The small mass loss (<3%) at 200-300°C was attributed to emissions of H<sub>2</sub>, CH<sub>4</sub> and CO/CO<sub>2</sub> as by Cataldo et al. (2004). The principal material decomposition was found in one stage beginning at 300°C and centered around 484°C on the DTG curve, which can be attributed to hydrocarbon decomposition (Qing et al., 2007).

Sonibare et al. (2003) found 3 stages of deconvolution with oil sands heated up to 600°C in air. The first stage at 25-335°C was attributed to light hydrocarbons. The second stage (335-480°C) was attributed to hydrocarbon combustion with thermal cracking reactions, with the formation of a

carbon rich residue. The final stage (480-540°C) included the combustion of the remaining hydrocarbons and carbon residue.

Lucena et al. (2004), Zhang et al. (2008), Martín-Alfonso et al. (2009), Aguiar-Moya et al. (2013) used TGA to observe PmBs, with the latter using TGA to determine whether PmB degrade at a temperature below that of bitumen.

#### 2.3.1.3.5 Mass spectrometry

Mass spectrometry (MS) is an analytical chemistry technique where a material is ionized by bombarding it with electrons in order to measure the mass-to-charge ratio and the abundance of gas-phased ions. The hydrocarbons with the higher atomic mass tend to be found on the right side of the spectra, that is, corresponding to higher  $m/z$  (mass-to-charge ratio). Generally combined with other techniques such as Gas Chromatography (GC-MS) and High-Performance Liquid Chromatography (HPLC-MS), it is useful in performing qualitative analysis of hydrocarbons (Barman et al., 2000; Lee, 2012; Mathews et al., 1999).

Flego et al. (2013) used direct insertion probe – mass spectrometry (DIP-MS) to observe the differences in the nature of the volatiles for various bitumens. The analysis was able to differentiate between lighter and heavier hydrocarbons, showing that the volatilized molecules were heavier, the higher the temperature the bitumen was subjected to. Gasthauer et al. (2008) and Tang and Isacson (2006) used GC-MS to identify the volatile compounds in bitumen and bio and petrol sourced asphalt release agents, respectively.

#### 2.3.1.3.6 Bitumen characterization by Raman spectroscopy

Raman spectrometry was used by Bergmann et al. (2000) in order to characterize asphaltenes extracted from petroleum. The advantage of the Raman technique is that it is less sensitive to issues with the surface of the sample such as contamination or oxidation that can occur with soft X-Ray absorption techniques. Compared to paraffin (saturated hydrocarbons), the asphaltene showed a lower intensity. It remains to be seen if this can be correlated with the higher proportion of asphaltenes in aged bitumen (Section 2.3.1.3.2), or if bitumen by itself can be analyzed.

#### 2.3.1.4 *Changes to microstructure*

Small samples of bitumen, polymer modified (PMB) bitumen and asphalt have been observed under ESEM (Environmental Scanning Electron Microscope) (Rozeveld et al., 1997; Stangle et al., 2006) as shown in Figure 2-26 and Figure 2-27. For the SEM settings Rozeveld et al. (1997) used a 20kV accelerating voltage, 267 Pa pressure at ambient temperature and Stangle et al. (2006) used a 20kV accelerating voltage, 80 Pa pressure also at ambient temperature.

The electron beam of the SEM has been found to heat and melt bitumen after several minutes, even when observed under ambient temperatures. The melting of the bitumen under SEM observation forms micelle-like structures that may resemble the GEL model. The depth of penetration by the electron beam was estimated to be between 0.01  $\mu\text{m}$  and 10  $\mu\text{m}$ . Observations by Golubev et al. (2008) of various fractions of bitumen by SEM showed similar structures.

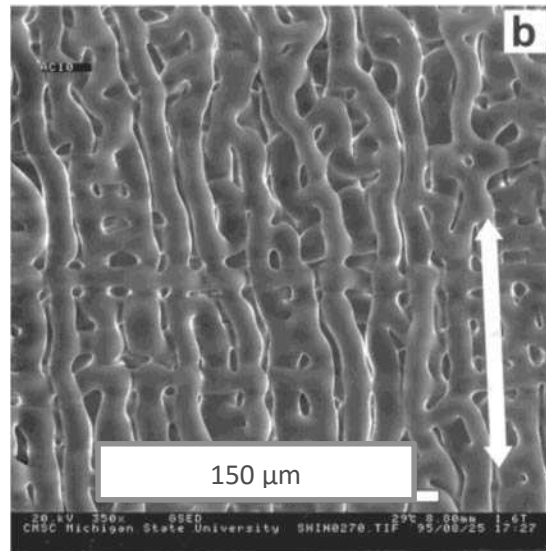


Figure 2-26 SEM observation of bitumen x350 (Rozeveld et al., 1997)

The structure varied with the composition of the bitumen, indicating a structure inherent to the bitumen and not a phenomenon solely of the electron beam. The modification of bitumen by tensile strain, corresponded with a deformation in the microstructure (fibrils), indicating that the structure observed is at least partly responsible in the tensile strength and cohesive properties of the bitumen. The structure was also thicker after aging (Figure 2-27), with a fibril diameter increase of 50% in both studies. This supported the hypothesis that the structure is composed of the asphaltene and resin fractions as their structures tend to be more robust than those of aromatics. This thickening also corresponded with a relative increase in the asphaltene fraction (determined by SARA fractioning) of the bitumen (Stangle et al., 2006).

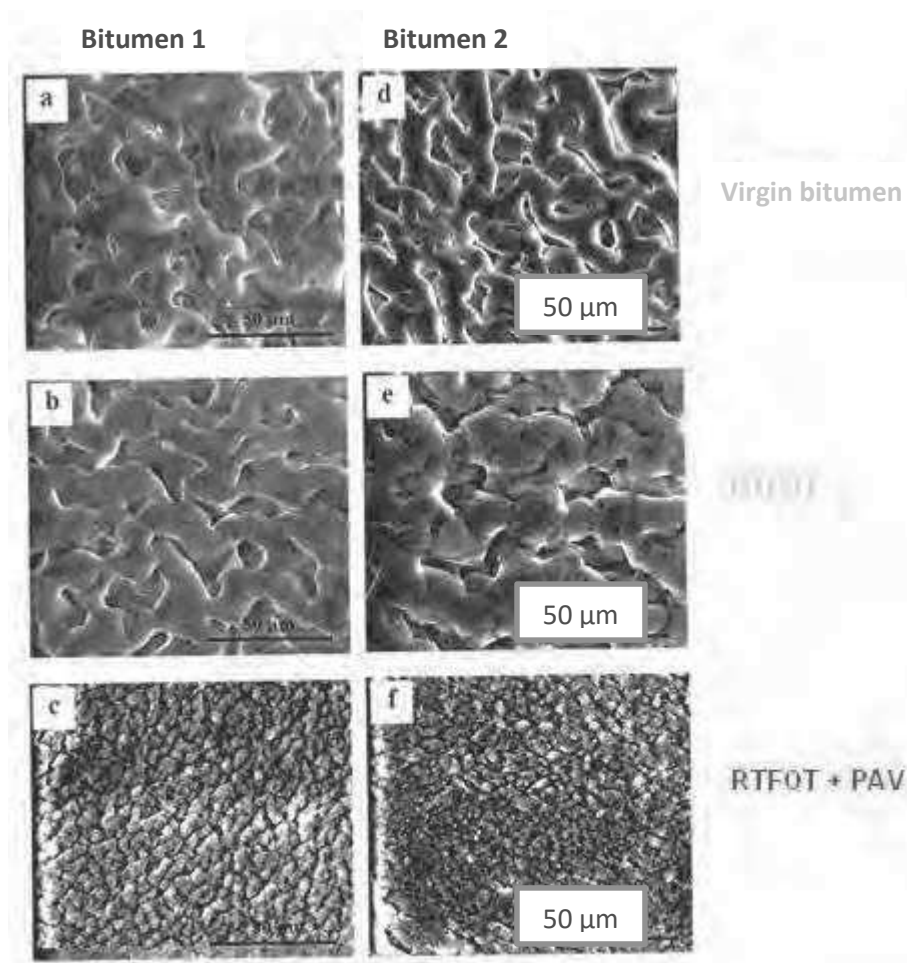


Figure 2-27 SEM observation of 50/70 bitumen a-new/ b-RTFOT aging / c-RTFOT + PAV aging (Stangle et al., 2006)

#### 2.3.1.5 Conclusions on bitumen aging

Bitumen aging results from the heating process during storage and asphalt pavement fabrication for the short term aging, along with oxidation and weather effects for the long term aging. The aging results in the bitumen becoming harder, more brittle and cracking, which results in the need to replace in in order to maintain the road safety. The viscosity and the penetration of the bitumen decreases with aging.

There are several technics to replicate aging in the laboratory including RTFOT and convection oven. There are several techniques that can observe the aging of bitumen chemically including MS, TGA and Raman. Oxidation can be analyzed by FTIR techniques through the C=O and S=O bands.

#### 2.3.2 Recycling methods

There are several methods by which the RAP can be recycled and used in new bitumen. These include *in-plant* recycling where the RAP is stored on the asphalt plant and then added as a constituent of new asphalt pavement. Conversely, RAP can be used to produce new asphalt *in-place* as it is being recuperated from old pavement. The two methods have a market share of about 50%



each in France (IDRRIM, 2013). A recycling agent can be added to the RAP to facilitate its integration in the new asphalt (Smith and Edwards, 2001). The average recycling rate for RAP in France is around 30-35%, with facilities capable of recycling rates of more than 60% RAP accounting for less than 2% (IDRRIM, 2013).

The hot in-plant method consists of storing the RAP at the plant and then combining it with asphalt and recycling agents to produce new asphalt. The % of RAP allowed in the mix is generally limited for this type of procedure (Santucci, 2007). The RAP (30-50 %w) is typically mixed with virgin aggregates (45-65 w%) and sometimes some kind of recycling or rejuvenating agent (5-10 %w). These can be preheated on their own before mixing, or combined cold before mixing at high temperatures (160°C+) (IDRRIM, 2013).

Hot in-place recycling consists of heating, scarifying, mixing, placing and compacting the upper layer of an existing asphalt pavement on site. Although virgin aggregates, new bitumen and rejuvenating agents are also added, a much higher RAP content can be used with this process (70-100%). This approach requires several pieces of equipment such as pre-heaters, heaters, scarifiers, mixers, pavers, and rollers, producing what is called a “train” (Santucci, 2007).

For cold mix recycling, the bitumen is most often emulsified in order to reduce its viscosity at cold temperatures or a very high viscosity recycling agent is added. New aggregates are sometimes added to the mixing, which is done at a portable mixing site (De Bock and Goncalves, 2006; Santucci, 2007). The advantage of cold mixing is that while reducing energy cost, it also provides a better environmental performance for the pavement fabrication because it emits less volatiles (Schvallinger, 2011).

### 2.3.3 Requirements for using in new asphalt

RAP is essentially granular covered with old and hard bitumen (Figure 2-28). The aged bitumen is a very hard material that has difficulty in adhering to new aggregates partly due to its elevated softening point.

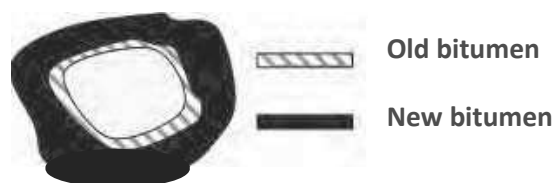


Figure 2-28 RAP in contact with new bitumen (El Beze, 2008)

The adhesion of the binder on the RAP aggregates can be tested for by EN 12697-37 (De Bock and Goncalves, 2006). The requirements of asphalt mixtures by EN 13108 with or without RAP are the same. The requirements by the French NF EN 13108-8 for RAP are a minimum 5 mm for average penetration and a maximum of 77°C for softening point. It allows for RAP addition of up to 40%

provided its binder content variability is less than 1% (up to 10% RAP if the variability is higher) (de la Roche et al., 2013).

#### **2.3.4 Variability of RAP and laboratory manufactured RAP**

RAP not recycled on site is stored in large piles at asphalt plants. Because of the outdoor conditions, the RAP will be exposed to water at variable rates, although some plants will even add water to their RAP piles in order to prevent the piles from conglomerating. The RAP at the top of the piles tends to form a crust which protects the material underneath it. This material in the crust needs to be removed and conditioned before it is reused in the asphalt.

While the grain size of the RAP can be controlled through the crushing process, due to the diverse conditions of fabrication and for the original asphalt of RAP, its properties will have a high variability potential from one source to the next. In addition to this, one source of RAP may have a high variability within it depending on where the aggregates were positioned in the road (depth, near water sources, amount of sun exposure). The bitumen in the top few millimeters of the surface can have a significant increase in viscosity relative to the rest of the pavement (Smith and Edwards, 2001). Thus, there exists a need for lab-manufactured RAP in order to provide a homogeneous material for testing.

El Béze (2008) and Navaro (2011) attempted to avoid these difficulties by manufacturing and aging RAP in a lab environment. El Béze (2008) fabricated asphalt mortar composed of 0.315-0.5mm graded limestone (80%) and bitumen (20%) subjected to RTFOT and PAV aging (for 4 and 8 days) mixed at 180°C for 2-5min. The aggregates were graded in order to eliminate fine particles in the bitumen fraction, causing interference with the chemical analysis of the image. The samples were polished to flatten the surface.

Navaro (2011) made asphalt with two different types of aggregates (limestone and siliceous), aging the asphalt with the limestone to produce RAP and mixed the siliceous aggregates and virgin binder with the RAP to produce new asphalt. The mixing times were varied from 20s to 10min and the mixing temperatures from 110-160°C in order to see their effects on reducing RAP clusters, thus making the mixture more homogenous. The samples were compacted into an 80mm diameter cylinder, cut and polished under pressure with an increasing speed from 1.2-60kN/s (Navaro et al., 2012).

De la Roche et al. (2013) produced a method for aging asphalt with a ventilated oven. The asphalt is produced according to EN 12697-35 and then subjected to short and long term aging. For the short term aging process, 35 kg of the asphalt is divided in two steel boxes, where the height of the asphalt is maintained at between 5 and 6 cm by a movable flange. The samples are placed in the ventilated oven at 135°C for 4 h, making sure to stir the asphalt each hour for homogenization.

For the long-term aging, 24 kg of the same sample is mixed together and split into the two boxes again so that the height of the asphalt is maintained at between 5 and 6 cm. The boxes are placed in the oven again at 85°C for 9 d, the asphalt being stirred for homogenization after 2, 5, 7 and 9 d (de la Roche et al., 2013).

Van den bergh and Van de Ven (2012) produced asphalt mortar (mastic) for testing the self-healing properties of asphalt with RAP. The aggregates were 0-0.5 mm diameter mixed with virgin binder at 180°C for 1-3 min. The mortar was aged with the RCAT device (EN 15323) by short term (4 h at 163°C using air flow) and long term ageing (168 h at 90 °C using oxygen flow).

### **2.3.5 RAP blending with virgin binder**

The blending of RAP with virgin binder is a key element in the quality of RAP mixtures. To understand the physical and chemical processes of interaction between the new bitumen and the old RAP, microscopy combined with chemical analysis were implemented in several studies.

#### ***2.3.5.1 RAP blending through microspectrometry imaging***

El Béze (2008) used three microspectrometry techniques in order to observe the blending mechanisms of RAP mixtures. They included X-ray fluorescence microspectrometry for quantifying quantity of vanadium and manganese; X-ray absorption microspectroscopy (XANES) for the degree of oxidation of sulfur and vanadium; and FTIR-ATR microscopy imaging for the quantifying of the S=O bonds. The RAP aggregates were manufactured in lab using RTFOT and PAV aging on asphalt made of virgin bitumen and limestone aggregates.

For the X-ray fluorescence microspectrometry and XANES, sulfur, vanadium and manganese were used as the tracers. Sulfur is already present in bitumen in significant quantities at 0.9-6.6%. Vanadium and manganese are also present in bitumen in small amounts (Table 2-1), with vanadium known as an indicator of the oxidation of bitumen. In order to observe qualitatively, the remobilization of the old bitumen in RAP, El Béze (2008) used tracers to estimate the degree of interaction between the new bitumen and the bitumen from RAP, and thereby, the homogeneity and degree of the remobilization. The laboratory produced RAP was then mixed with new bitumen and aggregates to make model RAP asphalt.

Sulfur was found to be a good indicator of the bitumen oxidation by XANES cartography as shown in Figure 2-29 where the old bitumen is around the RAP (blue) has a higher S=O content (red). It was also found that the oxidation could never be homogenous due to the aging affecting the surface of the sample more than the interior.

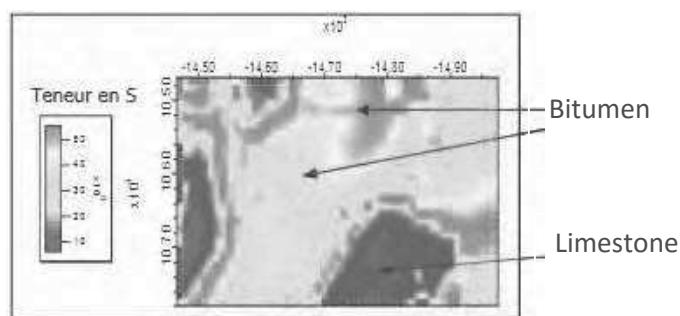


Figure 2-29 XANES cartography of S=O content in RAP asphalt (El Béze, 2008)

The goal of the vanadium and manganese tracers was to show how far new bitumen (with tracers mixed in) added to the RAP could mix with and remobilize the old bitumen. Observing the vanadium by X-ray fluorescence spectrometry cartography, a line analysis was made between two aggregates in the asphalt sample. Measurements of the vanadium content were made along 22 points between the two aggregates. However, it was found that vanadium was not an ideal tracer of bitumen oxidation due to its role as a catalyst of bitumen oxidation. It is therefore not ideal for being able to distinguish new and old bitumen. Manganese was also found to not be an ideal tracer due to the manganese particles remaining between the aggregates and not penetrating the RAP bitumen at all. The FTIR-ATR microscopy involved pressing the ATR germanium crystal against the laboratory made RAP mortar sample for an analysis depth of 1-3  $\mu\text{m}$ . The samples were polished beforehand in order to flatten their surface and reduce discrepancies in the contact between the crystal and bitumen, although the lack of surface flatness caused significant problems in this form of testing. As mentioned in Section 2.3.1.3, FTIR spectroscopy is a proven method for the detection of bitumen aging and oxidation. Limestone aggregates were appropriate for this method as their signature ( $864\text{ cm}^{-1}$ ) does not conflict with the principal indicators of bitumen oxidation at  $1700\text{ cm}^{-1}$  and  $1030\text{ cm}^{-1}$  for C=O and S=O, respectively, making them easily distinguishable from the bitumen. The presence of the oxidation indicators is defined by the area of their peaks relative to the asymmetric aliphatic peaks at  $1460\text{ cm}^{-1}$  and  $1376\text{ cm}^{-1}$ . Some results of this cartography are shown in Figure 2-30, indicating a difference in the aging indicators in the bitumen at two points. The oxidation indicators appear to be higher close to the aggregate grain, although their distribution in the middle points of the bitumen was heterogeneous (El Béze et al., 2012; El Béze, 2008).

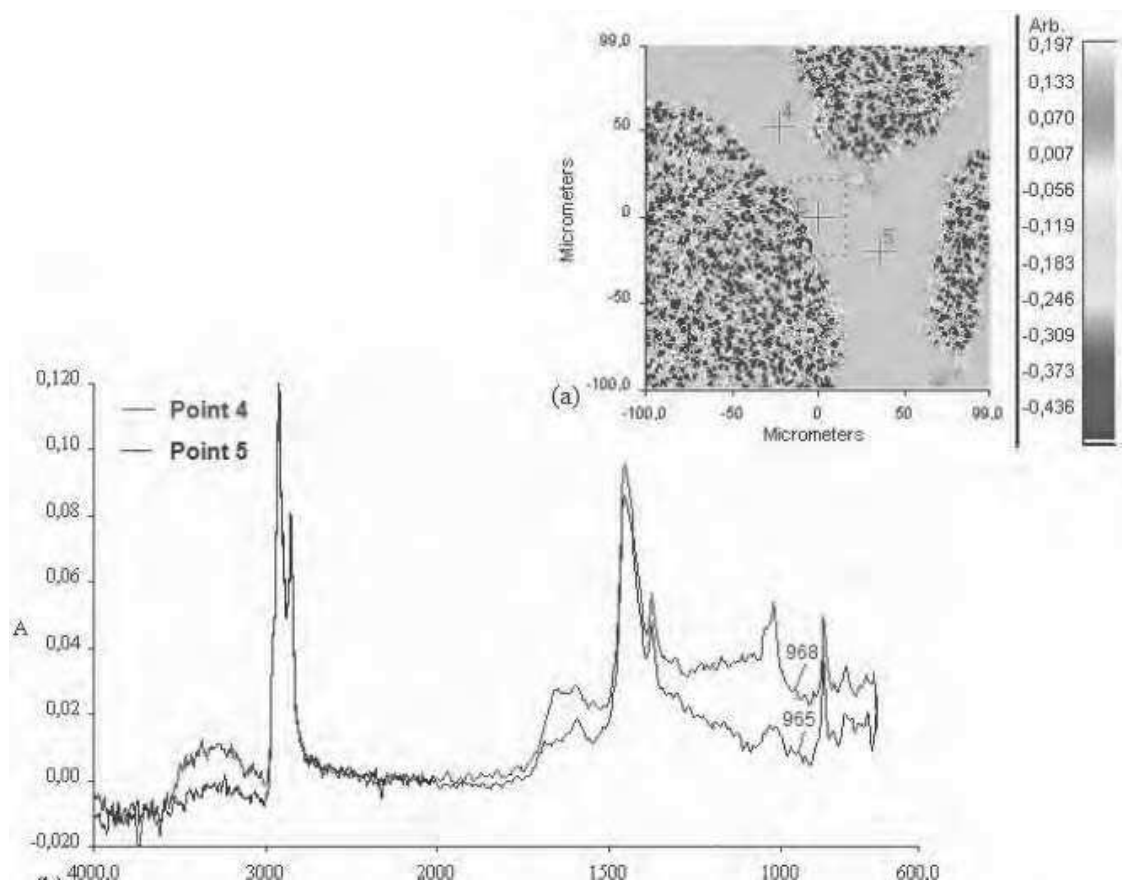


Figure 2-30 FTIR-ATR imaging of bitumen – limestone sample (El Béze, 2008)

### 2.3.5.2 RAP blending through AFM

Nahar et al. (2013) studied the interaction between extracted RAP binder with virgin binder while heating them both on a plate and observing them through peak-force tapping mode AFM cartography. As is shown in Figure 2-31, the new binder structure was significantly more robust than for the aged binder, and the two binders have very distinct structures. The blending zone was formed as the aged and unaged binder melted side by side on a heated plate at 100°C for 30s, then inside an oven at 100°C for 60 min. It was found that the blended zone contained both aged and unaged binder, as well as a newly formed blended binder that had modified properties that were both related to and independent of the parent binders. That is, the rheology of the bitumen in the blending zone was between those of the aged and unaged binder, showing that the bitumen in RAP is capable of some blending, the extent of the blending depending on the contact time and temperature. However, the microstructure appeared to be that of a new material, showing signs of “colloidal rearrangement”.

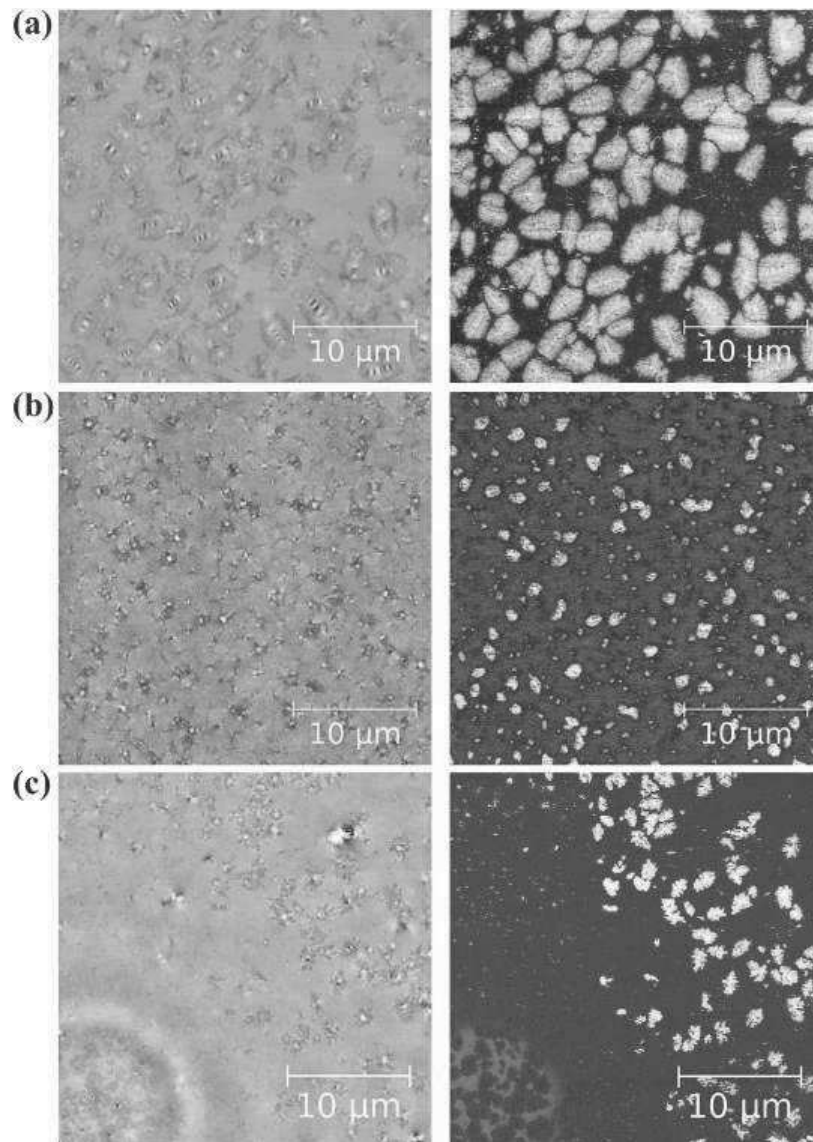


Figure 2-31 AFM tapping mode for topography (left) and phase (right) revealing the microstructure morphology of (a) virgin bitumen (b) RAP-binder and (c) blending zone of virgin and RAP-binder (Nahar et al., 2013).

### 2.3.5.3 Conclusions on RAP

RAP has seen increased research and use in recent years, as oil has become more costly. RAP has high variability, even the RAP extracted from the same source. Most European standards allow for the use of RAP in new asphalt at up to 50%. RAP can be incorporated into new asphalt after being stored at a site and mixed in-plant, or recycled in-situ by being directly incorporated into the new asphalt it is replacing in the new. The blending of RAP bitumen and new bitumen has been observed by FTIR and AFM cartography.

### 2.3.6 Asphalt recycling agents

Asphalt recycling agents or rejuvenators have been known since the 1950s (Brownridge, 2010). Without the recycling agents, the % RAP that can compose the new pavement is much more limited.

It is important that the recycling agent be compatible with the given RAP that is, being able to contact and interact with the old bitumen (Chen et al., 2007).

### **2.3.6.1 Composition**

There have been several types of recycling agents used with RAP. Some examples include lubricating and extender oils, which contain high proportions of maltenes (Terrel and Epps, 1989). The compatibility of the agent with bitumen can be an issue. Recycling agents with high aromatic and low saturate contents are usually more compatible with RAP bitumen (Dunning and Mendenhall, 1978; Wood, 1978). The development of bio-sourced agents is still relatively novel, although this is changing with the drive to replace petroleum products with renewable ones in the construction industry in general (Hajj et al., 2013; Kim, 2014; Reinke et al., 2014; Zargar et al., 2012).

#### **2.3.6.1.1 Petroleum-based recycling agent classification by Rostler Method**

The Rostler method (AZTM D 2006) is a method for classifying recycling agents originally developed in 1970 that is used in the United States. As with the SARA analysis, the categories of asphaltenes and saturates are included. Asphaltenes are taken as the portion of bitumen insoluble in n-pentane with the soluble portion being classified into 4 fractions. The polar compounds are taken as the material soluble in pentane and that reacts with 85% sulfuric acid. The rest of this fraction is broken down into saturates, first acidaffins and second acidaffins.

#### **2.3.6.1.2 Bio-sourced asphalt release agents**

There have been several bio-sourced agents used relatively successfully in the rejuvenation of asphalt, including those sourced from waste cooking oil (Zargar et al., 2012; Zaumanis et al., 2014), waste cooking grease and distilled tall oil (Zaumanis et al., 2014). The bio-oils tended to have a high maltenes content at around 90% (Zaumanis et al., 2014), similar to petroleum based agents.

### **2.3.6.2 Introduction of recycling agents to RAP**

Common practice for hot recycling is to mix the RAP with virgin bitumen, virgin aggregates and a recycling agent. The agent can be introduced to the asphalt mix i) by itself, ii) with the new bitumen or iii) sprayed on the RAP just before final mixing.

There are also the options of having hot or warm mixes depending on whether the effectiveness of the agent in reducing the RAP viscosity in both the short and long term (De Bock and Goncalves, 2006; Santucci, 2007). The can be used in hot (ASTM D 4552 or D 4887) and cold (with emulsions- ASTM D 5505) asphalt recycling. It has also been found that the rejuvenating process can take some time, with the agent initially surrounding the aged bitumen and then interacting with it over an extended period (Carpenter and Wolosick, 1980).

### 2.3.6.3 Changes to the physical properties of bitumen by recycling agents

The goal of recycling agents is to reintroduce the properties lost in bitumen and asphalt during aging such as penetration, softening point, viscosity, ductility, cohesion and adherence to aggregate for bitumen and fatigue, rutting, and thermal resistance for asphalt (Al-Qadi et al., 2007). According to the ASTM D 4552 classification for hot-mix recycling agents, these properties are given as flash point (handling), weight percent of saturates (compatibility, that is, the ability to blend with the bitumen), selected properties of the RTFOT or TFOT oven residue (durability), and specific gravity.

Madrid et al. (2000) found that recycling agents heavy in light aromatics and saturates helped reduce the viscosity of aged bitumen more effectively. Aromatics-heavy oils and to a lesser extent AC-10 (ASTM D 3381 specification for viscosity-graded asphalt cement for use in pavement construction) bitumen worked particularly well. Chen et al. (2007) tested 3 products as softening agents including 2 types of bitumen classified as AC-5 and AC-10 (ASTM D 3381) and a fuel oil commonly used for softening bitumen (Table 2-7). Two rejuvenating agents were also tested that were classified as RA-75 and RA -250 by ASTM D 4552. The agents were added to recovered RAP binder by “melt blending” at 155°C for 5 min and a mixing speed of 150 rpm.

Table 2-7 SARA Classification of recycling agents used in Chen et al. (2007)

	Specific gravity	60°C viscosity (poise)	Flash point (°C)	Asphaltene (wt%)	Saturate (wt%)	Aromatic (wt%)	Resin (wt%)
AC-10	0.99	1,010	256	12.6	23.5	38.6	25.3
AC-5	0.99	560	236	10.5	31.5	40.2	17.8
Fuel oil	0.92	4	138	1.8	68.8	13.8	15.6
RA-75	0.96	63	225	2.3	7.1	82.7	7.9
RA-250	0.99	319	230	3.2	12.4	72.2	12.2

Romera et al. (2006) tested an aliphatic-aromatic commercial oil 17 wt% (CO), a recycled motor oil at 20 %wt (RO), and a 150/200 penetration grade bitumen 73 wt% (B150). The bitumen was mixed with the recycling agent at a temperature of 160°C. Silva et al. (2012) used two different chemicals as rejuvenators in this study; ACF Iterlene 1000 (ACF) and a used motor oil (OIL) at 3, 6 and 12 %wt. ACF was an alkylamidopolyamine mix with a density of 0.91 g/cm<sup>3</sup> at 20°C, viscosity of 60 ± 10 cP at 25°C and flash point of 180°C. It is claimed by the manufacturer to act as a regenerator, anti-oxidant agent, adhesive, plasticizer, dispersing and diluting agent.

Zargar et al. (2012) tested used cooking oil as a rejuvenating agent, composed primarily of oleic acid (C18:0) and palmitic acid (C16:0). The penetration and maltenes content increased while the softening point viscosity and phase angle decreased. However the FTIR analysis of the virgin, aged and rejuvenated bitumen (with 3-4%w agent) proved inconclusive in terms of the C=O and S=O



indices. The rejuvenated binder was found to age less severely than virgin 80/100 binder, which was attributed to the lower volatility of the bio-oil (Reinke et al. 2014).

#### 2.3.6.3.1 Penetration and softening point

Romera et al. (2006) and Silva et al. (2012) found that recycling agents have the ability to significantly increase the penetration and decrease the softening of aged bitumen. However, there was also an indication in Silva et al. (2012) that the rejuvenated binders were also more affected by aging than the normal binders in terms of losing their “rejuvenated properties”, when subjected to further aging.

The softening of the RAP can be characterized by the physical penetration of the recycling agent into the matrix of the aged bitumen surrounding the RAP aggregates. This involves reducing the viscosity of the aged bitumen in the short or long term (ASTM D 4887; ASTM D 4552).

#### 2.3.6.3.2 Viscosity

In ASTM D 4887, the required amount of recycling agent is defined as the amount needed to bring the bitumen to a certain viscosity at 60°C (Figure 2-32).

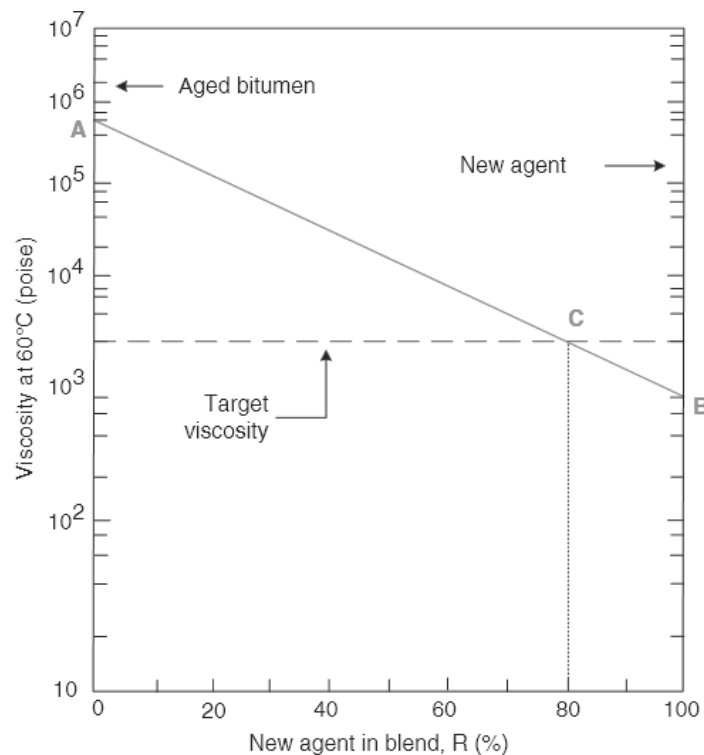


Figure 2-32 Asphalt recycling agent blending guide according to ASTM D 4887 (Chen et al., 2007)

Romera et al. (2006), Silva et al. (2012) and Zaumanis et al. (2014) found that recycling agents have the ability to significantly decrease the dynamic viscosity of aged bitumen.

Silva et al. (2012) found that dynamic viscosity results of the unmodified RAP binder appeared to be much more influenced by additional aging than those of the recycled mixtures with rejuvenators.

Moreover, it was observed that the dynamic viscosity ratios measured. Both results were attributed to the changes in the structure of the binder after aging. The agglomeration of molecules during aging is said to be opposed by their higher dispersion at higher temperatures, thus reducing the dynamic viscosity ratios. This occurs more profoundly at higher temperatures (180°C) and in the binders with higher maltene contents such as those with rejuvenating agents.

#### 2.3.6.3.3 Rheology

Rejuvenating agents have shown the ability to reduce the elastic properties of RAP binder to varied degrees depending on the nature and dosage of the rejuvenating agent. The bitumen will gain more viscous characteristics and will have reduced stiffness with the increasing quantity of rejuvenating agent. (Hajj et al., 2013; Porot, 2007; Reinke et al., 2014; Zargar et al., 2012).

#### 2.3.6.3.4 Low-temperature cracking

Asphalt pavement cracking is one of the primary reasons for pavement replacement. Rejuvenating agents have shown a significant ability in reducing low-temperature cracking (Zaumanis et al., 2014).

#### 2.3.6.3.5 Changes according to SARA fractions

As discussed in Section 2.3.1, it is the lighter fractions of the bitumen that are lost during aging, namely, the lighter aromatics and saturates. These relatively light molecules tend to volatilize at hot temperatures. At the same time, parts of the light aromatics transform into resins and asphaltenes during the oxidation process, and in turn, resins transform into asphaltenes. This process makes the bitumen harder and more brittle.

The recycling agents can function in two ways:

1. To flux the RAP as a softening agent (Section 2.1.5.1),
2. To regenerate the bitumen by replacing the chemicals lost during aging in the RAP bitumen, thereby acting as a rejuvenator (Figure 2-33).

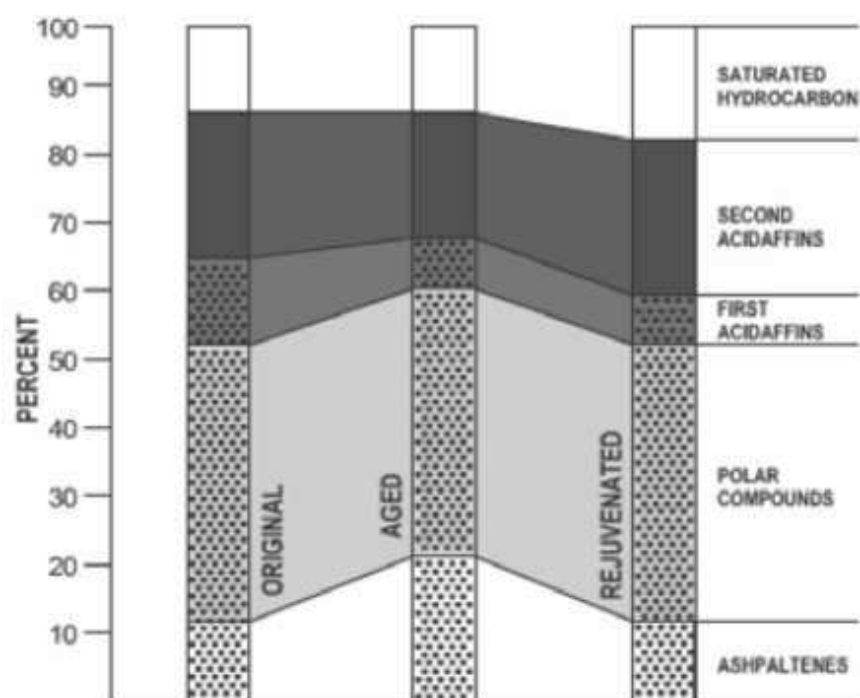


Figure 2-33 Typical changes in chemical composition via the Rostler method with aging of a typical asphalt pavement (Brownridge, 2010)

Chen et al. (2007) subjected recycling agents to SARA via the Rostler Method classification as in Table 2-7. The fuel oil was high in saturates while the RAs were high in light aromatics, with all being low in asphaltenes. The content of saturates in fuel oil exceed the maximum limit of 30 %w specified in ASTM D 4552, where they are limited due to compatibility issues. Indeed, there was significant segregation found when fuel oil was mixed with RAP experimentally. An agent commonly used in Canada had a saturates content limited to 28% because of the same reasons while the asphaltene content was limited to 1.5% (Finlayson et al., 2011).

Romera et al. (2006) found that the addition of recycling agent (17-20%) to RAP bitumen with 30% asphaltenes reduced the proportion of asphaltenes by about 2.5%. However, the content of asphaltenes in the RAP bitumen with recycling agent was still somewhat larger than in the new bitumen at the same penetration values. Furthermore, most of the asphaltenes reduction was from dilution of the aged bitumen by the recycling agent. (Durand et al., 2010a) has also found that the ability of the agent to restore properties to the RAP binder is dependent on the ability of the agent to modify the asphaltenes fraction of the RAP.

#### 2.3.6.3.6 Changes in oxidation peaks

Zargar et al., (2012) analyzed the virgin, aged and rejuvenated (with cooking oil) bitumen in FTIR. It was found that while the C=O and S=O peaks increased with bitumen aging, the rejuvenation reduced the C=O peak someone, while the S=O peak stayed constant.

#### **2.3.6.4 Conclusions of RAP and asphalt rejuvenation**

RAP can be incorporated into new asphalt by in-plant or in-situ methods. The incorporation of RAP into new asphalt presents challenges in terms of a decrease in penetration, increase in softening point, increase in viscosity, decrease in ductility, cohesion, and adhesion of aggregates and bitumen, and an increase in elasticity of the bitumen. This can make the asphalt hard and susceptible to cracking. For this reason, the RAP addition to new asphalt is generally limited to 50%.

An important component of RAP asphalt is the interaction of the RAP and new binder. This can be observed by AFM and FTIR cartography methods.

Rejuvenating agents can help restore properties lost during aging, including penetration, softening point and viscosity. They have shown to be most effective when acting on the asphaltenes. Their effectiveness is ultimately characterized by the long-term performance of the rejuvenated bitumen in the asphalt in terms of its ability to retain the rejuvenated properties.

### **2.4 Conclusions of the bibliographic study**

Asphalt pavement is composed of bitumen and aggregates. It is mixed and placed at hot temperatures at around 160°C, and is compacted by a roller. For the aggregates, crushed limestone is optimal due to its ability to adhere to bitumen by surface energy. The most important part of the asphalt is the bitumen, which hold the aggregates together, and so the properties of asphalt pavement are dependent on the nature of the bitumen.

Although bitumen comes from petroleum source, it is not the only petroleum product used in the construction of asphalt pavement. Many of the supporting products on construction sites have in the past used diesel for ARAs and BRs. Due to the problems caused by petroleum products to workers health and the environment, bio-sourced alternatives have begun to be developed.

ARAs are sprayed on surfaces used in asphalt construction (truck beds, pavers, finishers, tools) in order to prevent bitumen from sticking to them. For ARAs, the traditional agents, diesel fuel, has seen a significant reduction in its use, and the development of new bio-sourced agents. These ARAs are said to function as surfactants, creating a barrier between the asphalt and the surface of application. While these agents have been shown to be less harmful than diesel to the environment, they have been found at times to be less effective than diesel in reducing the adhesion of bitumen to surfaces. ARAs that have been based on organic C18 esters are seeing wide use in France. While the damage to the asphalt that they can has been shown to be less than that for diesel, the results have been varied, with some agents causing significant bitumen degradation.

While there does exist a testing program for the performance and damage to asphalt for ARAs (NTPEP, 2014), its results are subjective. For bitumen removers, no such testing program exists for

BRs. It is therefore necessary to develop a testing program for the performance of ARAs and BRs than can provide qualitative results, with the further goals of the classification of the agents available on the market and the development of superior performing agents.

The bitumen, which is classified by its penetration value, is affected by aging. The aging of bitumen occurs in the short term during its storage and mixing in asphalt pavement, and long term, through oxidation and exposure to outdoor conditions. This makes the bitumen hard and brittle, forming cracks in the road and necessitating the road replacement. This road can further be recycled to form RAP, which can in turn be incorporated into asphalt pavement.

The laboratory aging of bitumen can be performed with thin-film oven and convection oven methods. The aging can be observed through several physical and mechanical techniques. The principle mechanical properties of bitumen affected by aging are penetration, viscosity, rheology, ductility and low-temperature cracking the same properties that are affected in the hardened bitumen of RAP aggregates. The performance of the RAP-bitumen relative to these properties are improved with the use of rejuvenating agents, which can be sourced from petroleum or bio-based.

There are several techniques for chemically observing bitumen aging. These include FTIR, SARA classification and AFM. FTIR imaging is of particular interest relative to RAP in bitumen due to the possibility of observing bitumen oxidation signatures relative to the position of the binder and the aggregates. It remains to be seen if FTIR can also be applied to bitumen rejuvenation. This research project aims to further develop these techniques.

### **3 Determination of the performance and damage to asphalt of bio-sourced asphalt release agents and bitumen removers**

#### **3.1 Introduction and objectives of study**

Asphalt release agents prevent the asphalt from adhering to tools and equipment for asphalt production without resulting in damage (at least in theory) to the asphalt. The product traditionally used on site for this purpose was diesel, but diesel is toxic to workers and the environment, and can cause damage to the asphalt. Although a number of bio-sourced alternative products have been developed, some of them have proven to be damaging to the asphalt, ineffective or both (Mikhailenko et al., 2015b). The purpose of this part of the study is to develop experimental methods to evaluate diesel, commercially available release agents and those developed for this project. These methods will then be used to evaluate the performance and damage to asphalt of the ARAs. A bitumen remover – a product designed to clean asphalt – will also be developed in this part, along with the means of characterizing its performance.

The purpose of this study is the develop methods for determining ARA and BR performance and the degree to which ARAs may damage the asphalt. The study of ARA performance and damage to asphalt pavement has been rare and the study of BRs appears to be non-existent. Although there are norms for testing ARAs provided via the AASHTO NTPEP for asphalt release agents (NTPEP, 2014) – providing three principal test methods – the testing is rather subjective than quantitative as discussed in Section 2.2.3.

The objectives of the test development are to provide testing that (i) reflects as much as possible the on-site conditions, (ii) can differentiate between various ARAs, (iii) can provide new insight into the mechanisms of interaction between ARAs, BRs and asphalt and (iv) that are relatively simple and cost effective to implement.

The ARAs are characterized by two main criteria:

1. Damage to asphalt – the damage to the asphalt caused from contact with ARAs;
2. Performance – The ability of the ARAs to reduce the adherence between the asphalt and the surfaces (usually steel) of the tools and machinery used for asphalt fabrication.

The testing of ARA performance was done by the asphalt slide test. The testing of the damage to asphalt of the ARAs consisted of CBR resistance, indirect-tensile strength and bitumen degradation testing. The bitumen degradation test is also intended as a means of determining the most effective BR.

The products tested included diesel oil, 4 bio-sourced ester based ARAs, 1 synthetic biodegradable ARA, 4 bio-sourced ester based BRs, 1 synthetic biodegradable BR and 8 formulations of varying

chemistries in order to study the role of chemical composition in ARA and BR performance mechanisms and to attempt to develop better formulations. This was done with the aid of analysing the agents with Fourier Transformed Infrared Spectrometry (FTIR) and Gas Chromatography (GC).

## 3.2 Materials

### 3.2.1 Asphalt release agents and bitumen removers

The ARAs and BRs tested consisted of biodegradable commercial agents available currently used, agents that were used historically, as well as new formulations developed for this project.

#### 3.2.1.1 Commercial Asphalt release agents and bitumen removers

The asphalt release agents tested consisted of four bio-based ARAs available on the French market, with the addition of one synthetic bio-degradable ARA from the United States market. Additionally, diesel fuel, a petroleum product historically used as an ARA and BR in the past was also tested. Although this product is currently not permitted for use as an ARA or BR on construction sites (Acton, 2013), it was nevertheless tested as a reference due to its performance characteristics.

Four vegetal-based BRs and one synthetic bio-degradable BR were also tested, with technical information for these products is shown in Table 3-1.

The density of the bio-based products was around 0.89kg/L, slightly higher than the density of diesel. The viscosity at 40°C was 5-14mm<sup>2</sup>/s for the bio-based products while being much lower at 3 mm<sup>2</sup>/s for diesel. It is possible for lower viscosity product to penetrate into the mixture further, possibly resulting in a higher degree of damage.

The evaporation point of the bio-based ARAs was much higher than for the diesel, on one hand being less volatile and nauseating, but on the other hand, staying in contact with the asphalt for a longer time, possibly causing more damage.

The ester-based agents ARA 1, ARA 2, ARA 3, BR 1, BR 2, BR 3, BR 4 and BR 5 were analyzed by Gas Chromatography (CG) performed by a HP 5890 gas chromatograph in order to find the ester content and nature of the products. The chemical composition is given in Table 3-2.

The ester-based agents consisted primarily of C18:1 (12-65%) and 18:2 (4-42%), with notable quantities of C16:0, C18:0 and C18:3. BR 1 contained significant quantities of short chain esters C10 and C12, while BR 5 was composed primarily of C10. The average length of ester chains composing the BR products was shorter than that of ARAs, while the ester content was higher.

ARA 4 was a silicone oil-in-water emulsion stabilized by an alkoxylated polysiloxane surfactant (Zaki and Troxler, 2013). It was found to be 90% water.

Diesel fuel is petroleum based, consisting of 30% aromatics, 46% cycloalkanes and 24% n-alkanes.

Table 3-1 General information and physical properties for commercial ARAs and BRs

Product	Origin	Density at 20°C (kg/L)	Evaporation point (°C)	Kinematic viscosity at 40°C (mm <sup>2</sup> /s)
Diesel fuel	Petroleum	0.82-0.86	60	3
ARA 1	Bio-sourced	0.88	250	11
ARA 2		0.89*	250	14
ARA 3		0.86-0.90	350	12.5
ARA 4	Synthetic biodegradable	0.905	-	-
BR 1	Bio-sourced	0.88	170	10-11
BR 2		0.895*	250	10.5
BR 3		0.89*	250	5
BR 4		0.88	-	-
BR 5	Synthetic biodegradable	0.905	-	-

\*Density at 25°C

Table 3-2 Chemical composition for commercial ARAs and BRs

Product		Chemical composition										
Diesel fuel	30% aromatics, 46% cycloalkanes, 24% n-alkane											
ARA 4	silicone oil-in-water emulsion, which is stabilized by an alkoxylated polysiloxane surfactant, 90% water											
Ester chain as % of total ester content												
	% ester	C8	C10	C12:0	C16:0	C16:1	C18:0	C18:1	C18:2	C18:3	C20	C22:0
ARA 1	41.3				4.5	0.1	1.5	64.8	19.5	7.9	1.6	
ARA 2	38.0				12.8	0.6	11.8	33.2	30.9	9.0	1.7	
ARA 3	74.5				5.3	0.3	1.5	63.1	19.7	7.9	2.2	
BR 1	68.9		17.9	14.8	12.5		4.5	46.1	3.7	0.4		
BR 2	38.1			0.3	10.7		9.8	37.8	34.0	6.3	0.9	0.6
BR 3	72.8				10.9	0.1	12.5	31.5	41.8	0.5	1.1	1.6
BR 4	81.8				5.6	0.3	1.5	63.0	19.4	9.1	1.1	
BR 5	86.0	1.3	73.5	1.2	2.3	0.4	0.7	12.3	8.6	0.8		

### 3.2.1.2 ARA and BR candidate formulations

One of the principal objectives of this project is the development of bio-sourced ARAs with the goal of (i) improving their performance, (ii) reducing their damage to asphalt and (iii) while reducing their environmental impact. BR products were also developed using the ARA test methods and some candidate formulations. In order to propose new formulations understand these interactions, a number of candidate agents (Most as ARAs and some as BRs) were tested.

General information and physical properties for the candidate formulations – marked RD1 to RD7, C7, MUG and MUDG – are shown in Table 3-3. Among these, only RD 4 was not a bio-sourced product.



The ARA candidates RD 4 and RD 5 have low viscosities, indicating that they would have relatively better coverage of the surface (spread easily like diesel, Mikhailenko et al., 2015b), compare to RD 1 and RD 2, which have higher viscosities.

Of the three agents where the evaporation temperature was available, all had evaporation temperatures over 200°C, well over the asphalt production temperature of 160°C.

Table 3-3 General information and physical properties for the candidate formulations

Product	Origin	Density at 20°C (kg/L)	Evaporation point (°C)	Kinematic viscosity @ 40°C (mm <sup>2</sup> /s)
<b>C7</b>	Bio-sourced	0.84	222	9
<b>RD 1</b>		0.91	-	78
<b>RD 2</b>		0.92	-	83
<b>RD 4</b>	Petroleum	0.81	-	10
<b>RD 5</b>	Bio-sourced	0.88	-	15
<b>RD 6</b>		0.95	-	29
<b>RD 7</b>		0.90	-	42
<b>MUG</b>		1.26	290	-
<b>MUDG</b>		1.28	205	-

The 9 candidate formulations fall into 6 main categories with regards to their chemical properties shown in Table 3-4, which were determined with the aid of GC analysis:

- i) C7 and RD 6 are highly concentrated short chain esters with hydrocarbon lengths ranging from 7-10;
- ii) RD 1 and RD 2 are colza oil with unsaturated fatty-acid content at 39% and 3%, respectively;
- iii) RD 4 is a commercially available oil (nominally as a lubricant), it is highly saturated with a high degree of iso-paraffinic structures;
- iv) RD 5 is a highly concentrated ester with a similar chemical composition to the commercial BRs BR 1, BR 3 and BR 4, composed primarily of C18:1 (39%) and C18:2 (32%);
- v) RD 7 is a mixture of RD 2 and RD 5 at 50:50 in order to observe the combined effects;
- vi) MUG and MUDG are derivatives of the glycerol chemistry.

Glycerol is a compound derived from agricultural waste in the process of biodiesel production (transesterification, Figure 3-1), which produces biodiesel and glycerol (G) as a waste product. Diglycerol DiG is then produced from the etherification of glycerol using a catalyst.

Glycerol undecenoates (MUG) and diglycerol undecenoates (MUDG) are glycerol based and diglycerol based compounds, respectively prepared by reacting them with

undecylenic acid (C11) that transforms glycerol and diglycerol into by-products with surfactant properties.

The byproducts for the transformation of glycerol are glycerol monoundecenoate (G MonoC11), glycerol diundecenoate (G DiC11), glycerol triundecenoate (G TriC11) and residual undecylenic acid (C11). For the transformation of diglycerol, the by-products consisted of diglycerol monoundecenoate (DiG MonoC11), diglycerol diundecenoate (DiG DiC11) and triundecenoate (DiG TriC11) along with residual undecylenic acid (further elaborated in Section 3.6.1).

These are the products specifically formulated for this project by the AGRIBTP partner LCA laboratory (Boussambe, 2015), with the aim of transforming recycled chemicals in to high performance products for the construction industry. Thus, they are the principle ARA candidates for this study.

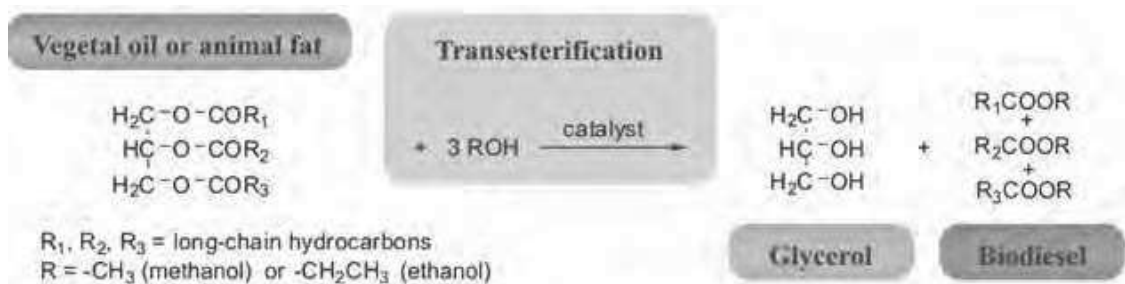


Figure 3-1 Schema for deriving glycerol from biodiesel production (Leoneti et al., 2012)

Table 3-4 Chemical composition of candidate formulations

Product	% of hydrocarbon chain in composition											
	% ester	C7	C8	C10	C12:0	C14:0	C16:0	C16:1	C18:0	C18:1	C18:2	C20:0
<b>C7</b>	92	100										
<b>RD 1</b>	-						13.1		3.8	54.3	24.6	4.3
<b>RD 2</b>	-						13.1		0.1	51.9	23.5	11.4
<b>RD 4</b>	0	Highly saturated with a high degree of iso-paraffinic structures										
<b>RD 5</b>	-					1.7	19.7	2.1	5.7	39.0	31.9	
<b>RD 6</b>	99		58.8	41.1	0.1							
<b>RD 7</b>	-					0.9	16.4	1.0	2.9	45.4	27.7	5.7
<b>MUG</b>	C11 6.9%, G Mono C11 66.0%, G Di C11 26.0%, G Tri C11 0.9%											
<b>MUDG</b>	C11 6.4%, DiG Mono C11 64.2%, DiG Di C11 24.9%, DiG Tri C11 4.4%											

### 3.2.2 Bitumen

The bitumen used in this study, by itself and in the asphalt mixture was Total 35/50 as classified by NF EN 12591, indicating a penetration (ASTM D5-NF EN 1426) value of between 3.5 and 5.0 mm. The

bitumen had to be heated before becoming melted enough to be tested and it was taken care not to heat each specimen of bitumen more than twice due to the volatiles that are lost by the bitumen during the heating process.

### 3.2.3 Asphalt

The asphalt mixes (BBSG 0-10 class 3 by NF EN 13108-1) were manufactured in accordance with NF EN 12697-35+A1 with Total 35/50 bitumen and limestone/silica aggregates. The aggregates, as shown in Table 3-5, consisted of coarse aggregates, fine aggregates and limestone filler that were graded in accordance with NF EN 13108-2. The asphalt was either i) fabricated with a M&O Type 182 mixer in 40 kg batches, stored and re-heated for the preliminary testing or ii) was manufactured directly before the test using a 3R heated asphalt mixer. More information on the asphalt fabrication and the aggregate size distribution (EN 13043) can be found in Appendix B.

Table 3-5 Typical composition of asphalt mixture

Material	(% by mass)
Sand 0/2 mm	23.7
Aggregates 2/6.3 mm	23.3
Aggregates 6.3/10 mm	45.0
Limestone filler (< 80 µm)	2.6
Bitumen Total 35/50	5.6
<b>Total Mass</b>	100

- Bitume Total 35/ 50
- Aggregates (grading according to EN 13043)
  - Sable 0/2 mm crushed sand
  - 2/6.3 mm crushed stone
  - 6.3/10 mm crushed stone
  - Limestone filler (< 80 µm)

Asphalt mixing procedure: NF EN 12697-35

1. Aggregates heated for 8h at 160°C;
2. Bitumen is heated at 110°C for 7 h in a closed metal pot, and then at 160°C for 1 h;
3. The aggregates are weighed ( $\pm 1$  g) and placed in the mixing bowl. First the 6.3/10 and 2/6.3 aggregates, followed by the sand and filler. This is mixed for 3 min (Figure 3-2);



Figure 3-2 M&O Type 182 asphalt mixer

4. The bitumen is weighed and poured in the center of the bowl on the aggregates and are mixed for 10 min (Figure 3-3);



Figure 3-3 Addition of bitumen (at 160°C) to aggregates in mixer (left) and asphalt after mixing (right)

5. After the mixing, the asphalt is distributed in the aluminum containers (at +1 kg per sample) and covered with the cardboard covers. They are stored at room temperature until they are needed for testing (Figure 3-4);



Figure 3-4 Asphalt after being placed into aluminum containers for storage

### 3.3 Development of test methods for the determination of asphalt release agent (ARA) performance

The objective of ARA performance testing is to measure the ability of the ARA to reduce the adherence of bitumen to tools and machinery for asphalt construction (generally metal surfaces). The challenge in this testing is to develop a qualitative analysis that best represents the conditions in the field and that is as cost and time effective as possible to implement.

#### 3.3.1 ARA Performance Evaluation Apparatus

The ARA Performance Evaluation Apparatus (ARA-PEA) is a device co-developed by LR Vision of Castanet-Tolosan and LMDC of Toulouse for evaluating the performance of ARAs in reducing the adhesion between bitumen and construction materials (Figure 3-5 and Figure 3-6). The device consists of an interchangeable plate (usually steel) that can be adjusted to an incline from 0-70°. The principle of the device is that when an ARA is applied to the plate, sliding asphalt or bitumen (see Appendix C) from the top of the plate can allow us to observe the performance of the ARA as the asphalt slides or bitumen flows down the incline. In order to facilitate this, a heating mechanism is installed beneath the plate that is capable of heating it to over 200°C.

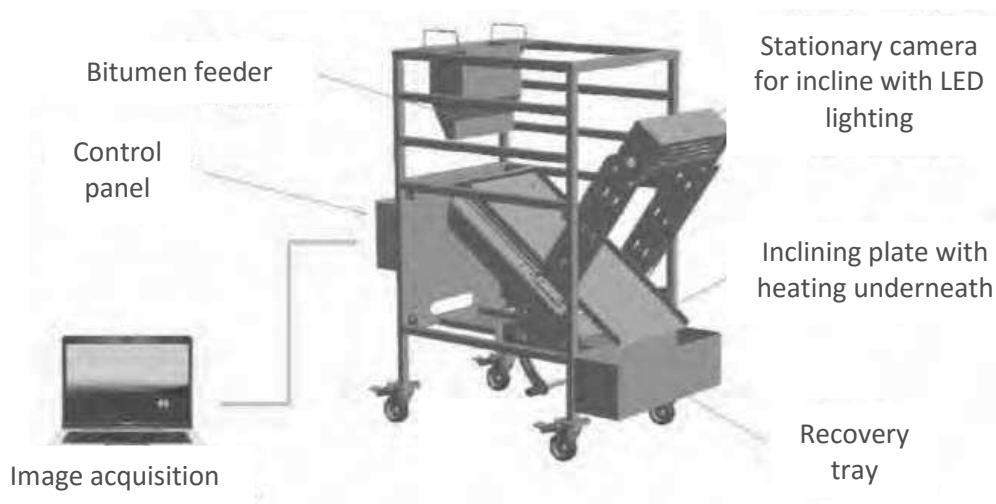


Figure 3-5 ARA Performance Evaluation Apparatus (ARA-PEA)

In order to allow for the quantification of the asphalt release agent performance, there are several measurement devices installed on the apparatus (Figure 3-7), although not all of these may be useful for our study as of yet:

- Gage for setting the angle of inclination ( $0-70^{\circ}$  from horizontal);
- Temperature gage ( $\pm 0.1^{\circ}\text{C}$ ) for adjusting the heating underneath the plate;
- Laser temperature sensor ( $\pm 0.1^{\circ}\text{C}$ ) over the plate to measure the temperature of the asphalt/bitumen;
- Camera in order to film the flow of the bitumen, allowing for the measure of its speed and the observation of the shape of the bitumen flow, along with image analysis of asphalt residue;
- Laser thickness sensor in order to measure the thickness of the bitumen flow on the plate ( $\pm 0.1\text{ mm}$ ).



Bitumen Feeder

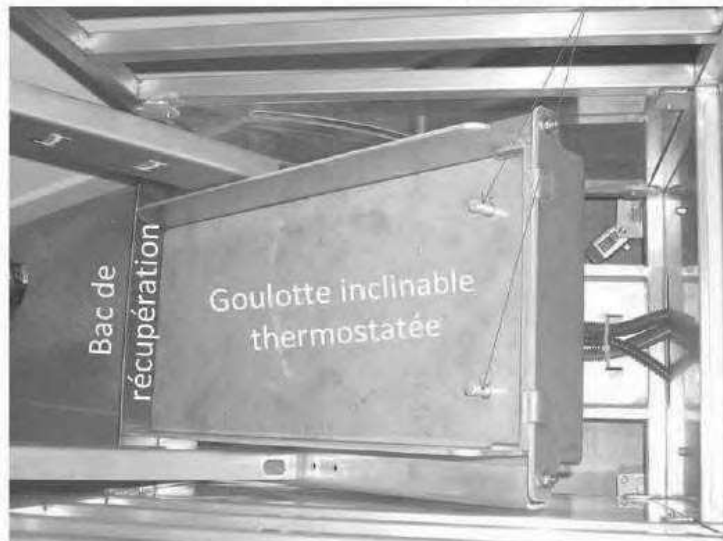
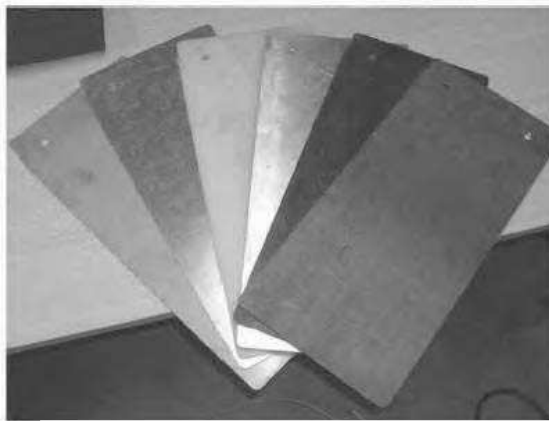


Plate Holders



Changeable Plates 530x240 mm

**Materials for plate (left to right):**

- Aluminum
- PVC
- Galvanized steel
- Stainless steel
- Rubber

Figure 3-6 Details on the ARA Performance Evaluation Apparatus (ARA-PEA)

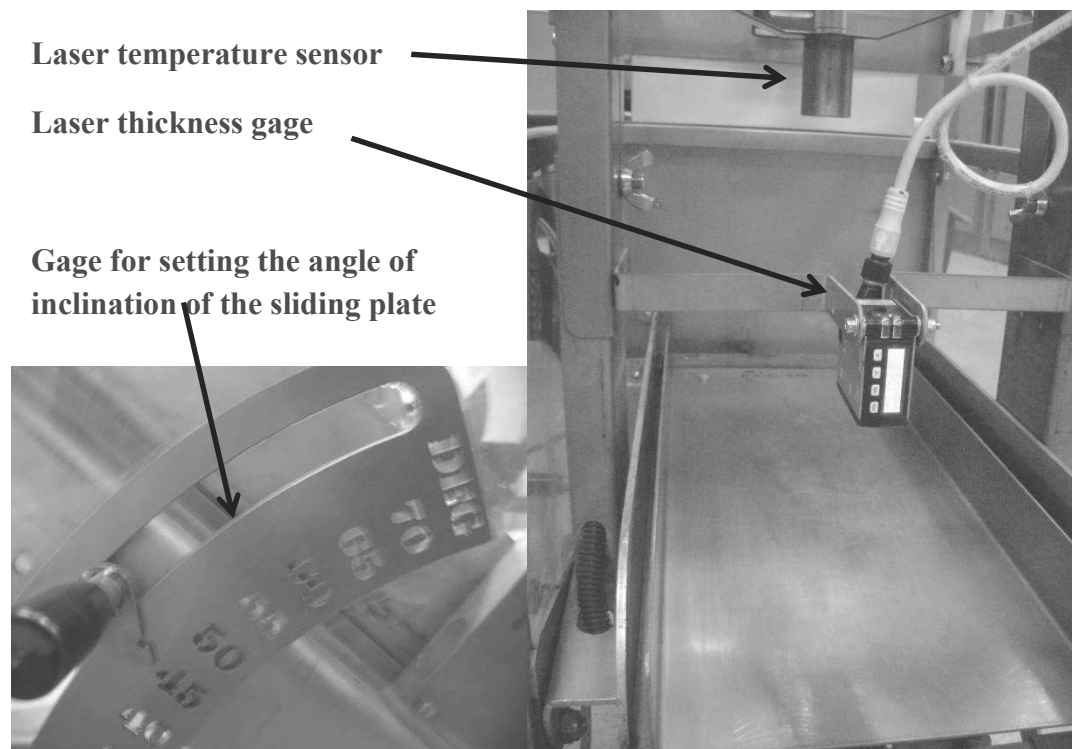


Figure 3-7 Features of ARA-PEA: laser temperature sensor; laser thickness sensor; gage for setting the angle of inclination

### 3.3.2 Asphalt Slide Test

The mixture slide test is part of AASHTO program for asphalt release agents (NTPEP, 2014). The test developed in this study follows some of the same principles as the AASHTO one, while adding the ability to quantify ARA performance. The purpose of the test is the performance of an ARA on a scaled version of an asphalt truck bed using the ARA-PEA presented in the previous section.

The test (Figure 3-8) involves spraying an ARA over an area of 21x40 cm on the steel plate (Figure 1-2) resting horizontally. This is followed by placing  $1200 \pm 10$  g of hot asphalt ( $150 \pm 10^\circ\text{C}$ ) on the surface of the plate, so that it is spread out as evenly as possible. The plate is maintained horizontal and a sheet of wax paper is placed on top of the asphalt to prevent sticking, followed by a wooden board (21x40 cm, 883 g). On top of the board, a load of 20 kg is placed creating a distributed pressure on the asphalt of 2.5 kPa. This simulates the transportation of the asphalt where there is a pressure on the asphalt in contact with the truck bed from the asphalt resting on top. The plate rests horizontally for a certain period of time (0.5-1 h), after which it is placed on the ARA-PEA and immediately inclined at a certain angle ( $0-70^\circ$ ), simulating the discharge of the asphalt from the truck. It is also possible to heat the plate from below when it rests on the device, which simulates the contact temperature between the asphalt, the agent and the plate from the mass effect of the asphalt load.





Figure 3-8 Asphalt Slide Test: 1) applying ARA, 2) asphalt spread on the plate, 3) load of 2.5kPa distributed on top of the asphalt and 4) the inclination of the plate on ARA-PEA at 45°

With the application of an ARA, the asphalt slides down the plate, and from this action, the following data can be taken for judging the performance of the ARA:

- The mass of asphalt residue left on the plate (weighed by a balance precise to 0.01 g);
- The time that the asphalt takes to slide down after the plate is inclined (through a chronometer precise to 1s);
- The area of asphalt residue left on the plate (by image analysis, not further developed).

### 3.3.3 Determining asphalt slide test validity and parameter optimization

A number of parameters were used in developing the asphalt slide test in order to find the ones that can lead to the most indicative results. Five series of testing were performed; they are summarized in Table 3-6.

Table 3-6 Parameters for Asphalt Slide Test

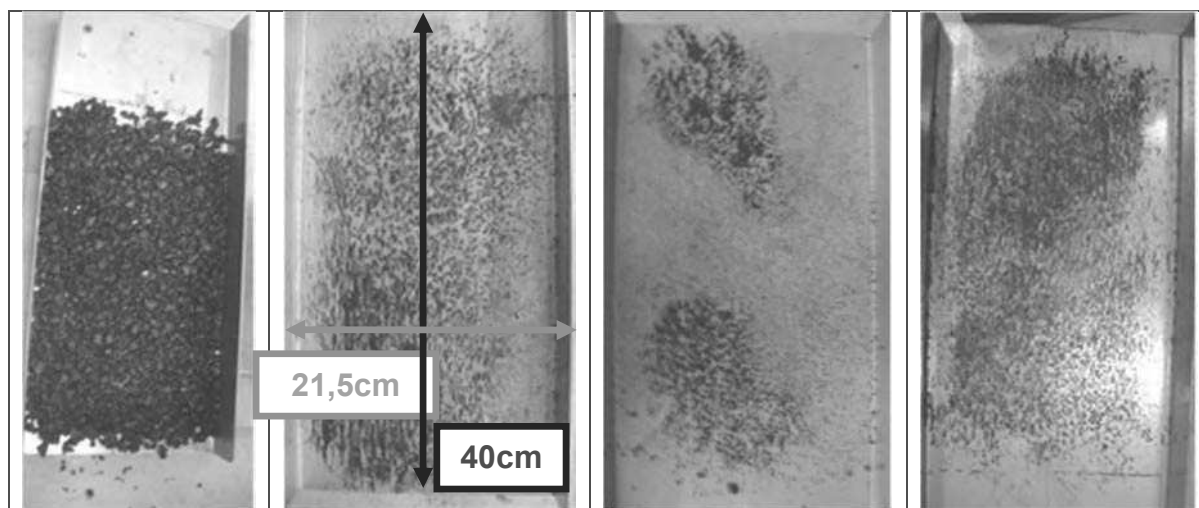
Test No	Quantity of ARA (mL/m <sup>2</sup> )	Quantity of asphalt (g)	Cooling time	Plate heating (°C)	Inclination angle (°)
1	20	1000±10g	1h	-	45-70
2	20	1000±10g	30min	70	45
3	25	1000±10g	30min	variable	45
4	25	1000±10g	30min	60	45
5 - Final	65	1200±10g	30min	60	45

For test No. 1, the ARA was applied at 20±1 mL/m<sup>2</sup>, the plate was not heated during the test while the cooling time was 1 h. The asphalt did not move from the plate when inclined, requiring the top of the asphalt to be pushed lightly before the start of the sliding, even at the maximum possible inclination of 70°. The light pushing did not appear to move the control sample (Table 3-7), nevertheless, the pushing invalidated the test from an objectivity perspective. The results show that the residual mass is small but not insignificant and changes depending on the agent applied (Table 3-7, For test No. 2, the ARA was applied at 20±1 mL/m<sup>2</sup> and the plate was heated to around 70°C before ARA application and was heated during the inclination part of the test at 70°C. This time, the asphalt slid after inclination, indicating the necessity of heating the plate before the asphalt slides. With the perspective of reducing the overall test time while staying within a reasonable timeframe for asphalt transportation from plant to site, a cooling time of 30 min was found to be adequate for the asphalt to develop some adherence to the plate. There was a certain delay between when the plate was inclined and when the asphalt slid, allowing for the measuring of time to the beginning of the slide after the inclination (at 45°) as a performance characteristic for the ARAs. An angle of inclination of 45° was found adequate for the sliding as well. While these parameters produced satisfactory results, further modifications were considered in order to simplify the test.

Table 3-8).

Table 3-7 Images of plates after Asphalt Slide Test No. 1

Control	ARA 1	ARA 2	ARA 3
---------	-------	-------	-------



For test No. 2, the ARA was applied at  $20 \pm 1 \text{ mL/m}^2$  and the plate was heated to around  $70^\circ\text{C}$  before ARA application and was heated during the inclination part of the test at  $70^\circ\text{C}$ . This time, the asphalt slid after inclination, indicating the necessity of heating the plate before the asphalt slides. With the perspective of reducing the overall test time while staying within a reasonable timeframe for asphalt transportation from plant to site, a cooling time of 30 min was found to be adequate for the asphalt to develop some adherence to the plate. There was a certain delay between when the plate was inclined and when the asphalt slid, allowing for the measuring of time to the beginning of the slide after the inclination (at  $45^\circ$ ) as a performance characteristic for the ARAs. An angle of inclination of  $45^\circ$  was found adequate for the sliding as well. While these parameters produced satisfactory results, further modifications were considered in order to simplify the test.

Table 3-8 Results for Asphalt Slide Test No.1

Produit	Asphalt ( $^\circ\text{C}$ )	Quantity ARA ( $\text{mL/m}^2$ )	Residual mass ( $\text{g/m}^2$ )
Control	160	-	1189.68
ARA 1	150	20.48	3.41
ARA 2	160	20.77	0.42
ARA 3	160	21.17	2.17

Table 3-9 Results for Asphalt Slide Test no. 2

Product	Asphalt ( $^\circ\text{C}$ )	Quantity ARA ( $\text{mL/m}^2$ )	Time to beginning of slide (s)
Control	160	-	-
ARA 1	160	20.90	13
ARA 2	160	21.41	1

For test No. 3, the ARA was applied at  $25 \pm 1 \text{ mL/m}^2$  the cooling time was set at 30 min and the angle of inclination at  $45^\circ$ . The plate was not heated before the asphalt was applied; however, the ARA-

PEA was heated at varied temperatures before the inclination in order to determine an optimum for the test. It was found that for a temperature of 60°C at inclination, the samples with ARAs slid, but the control samples did not. A temperature of 60°C was therefore was thereby determined to be adequate for this test and did not need to be optimized further.

For test No. 4, the test was conducted with diesel, ARA 1 and ARA 2. The photos of the plates after the test are shown in Table 3-10 and the results of the test in terms of residual mass and time to beginning of slide are shown in Table 3-11. While the test with these parameters was shown to be repeatable in terms of residual bitumen ( $\sigma$  of 0.11-0.87 g/m<sup>2</sup>), the variability of the time to start of slide was found to be elevated ( $\sigma$  of 0-60 s). As source of this could have been the inconsistency with the contact between the asphalt, the agent and the plate over the plate area. The application of the ARA by spraying as well as the asphalt mix can leave some parts of the plate with thicker layers of ARA than others. This was confirmed by the low time to beginning of slide for diesel, which corresponds to diesel having the most even coverage on the plate visually (Table 3-10).

Table 3-10 Images of plates after Asphalt Slide Test no. 4

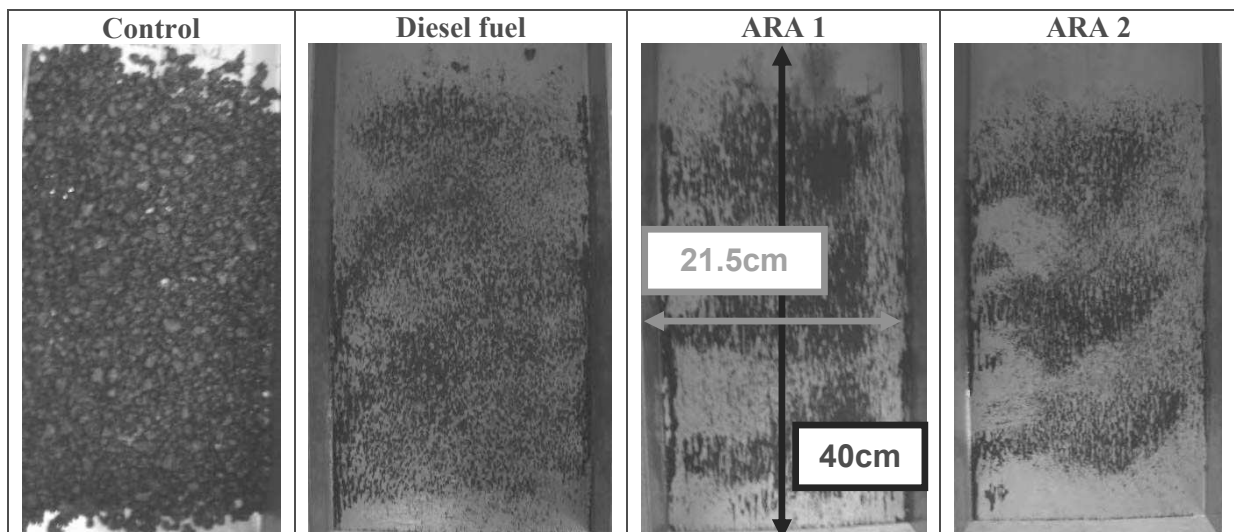
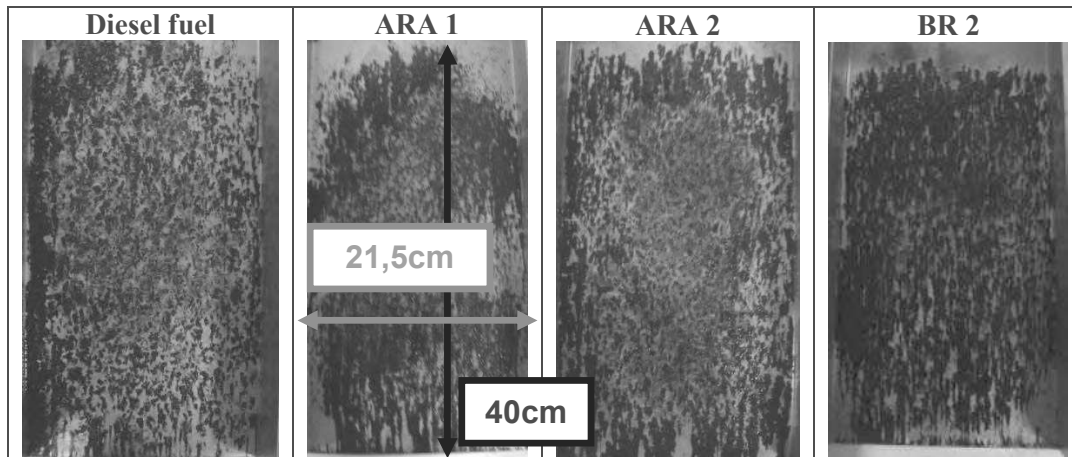


Table 3-11 Results for Asphalt Slide Test no. 4

Product	Residual mass (g/m <sup>2</sup> )	Time to beginning of slide (s)
<b>Control</b>	1200.48	-
<b>Diesel fuel</b>	2.59	1
<i>STDDEV <math>\sigma</math></i>	0.87	0
<b>ARA 1</b>	3.25	100
<i>STDDEV <math>\sigma</math></i>	0.35	60
<b>ARA 2</b>	1.48	92
<i>STDDEV <math>\sigma</math></i>	0.11	25

Table 3-12 Images of plates after Asphalt Slide Test final (asphalt mass: 1200±10 g, ARA: 65 mL/m<sup>2</sup>, cooling time: 30min, heating of plate: 60°C, inclination angle of plate: 45°)



For the final test, performed with three trials for each sample, it was decided to increase the quantity of the asphalt mix to  $1200 \pm 10$  g and the quantity of the ARA to  $65 \text{ mL/m}^2$  in order to reduce the variability from lack of coverage of the plate. The test was conducted with diesel, ARA 1, ARA 2 and BR 2 (BR 2 had obtained a result in the BDT that suggested that it was safe enough to use as an ARA as described in Section 3.4.2). The photos of the plates after the test are shown in Table 3-12 and the results of the test in terms of residual mass and time to beginning of slide are shown in Table 3-13. The variation in residual mass was about the same ( $\sigma$  of  $0.11$ - $0.87 \text{ g/m}^2$ ), despite an increase in residual mass in general due to the higher dosage of ARA and asphalt. The variation in time to beginning of slide was reduced as well ( $\sigma$  of  $4$ - $13$ s), as it would with the reduction of retention time, but remains significantly higher than the variation in residual mass.

Table 3-13 Results for Asphalt Slide Test final (asphalt mass:  $1200 \pm 10$  g, ARA:  $65 \text{ mL/m}^2$ , cooling time: 30 min, heating of plate:  $60^\circ\text{C}$ , inclination angle of plate:  $45^\circ$ )

Product	Residual mass ( $\text{g/m}^2$ )	Time to beginning of slide (s)
<b>Diesel fuel</b>	8.92	8
<i>STDDEV <math>\sigma</math></i>	0.21	4
<b>ARA 1</b>	7.12	5
<i>STDDEV <math>\sigma</math></i>	0.55	5
<b>ARA 2</b>	8.20	10
<i>STDDEV <math>\sigma</math></i>	0.82	13
<b>BR 2</b>	8.92	13
<i>STDDEV <math>\sigma</math></i>	0.63	10

### 3.3.4 Discussion on the development of test methods for ARA performance

The Asphalt Slide Test was developed with the optimization of five different parameters including the quantity of ARA, the mass of asphalt, the cooling time, the under-plate heating and the angle of inclination for the final slide (Table 3-6). The ARA-PEA (ARA Performance Evaluation Apparatus)

provides an adequate platform for this test. While the pre-heating of the plate is not necessary, the heating of the plate during inclination is for the asphalt to slide down by itself. A cooling time of 30 min appears to be adequate to allow for the mixture – subject to a 2.5 kPa load simulating the mixture mass in the truck – to adhere to the plate. Practical situations would vary significantly from load to load depending on the transportation distance and outdoor temperature. The 30 min is applied as being both i) within range of a normal transportation times for hot mix asphalt (*The Asphalt Paving Industry*, 2011) and ii) is not excessively long so as to be able to conduct the testing in a timely fashion. A mixture quantity of 1.2 kg and an ARA quantity of 65 mL/m<sup>2</sup> were found to be the optimum parameters. Our objective was to have a complete covering of the plate by the ARA, and a higher dosage was needed to ensure this.

There were two types of results observed during the testing:

- Time the asphalt was retained on the plate after inclination;
- Mass of residue retained on the plate after the asphalt slides down.

The parameters are quantitative results that can be used to compare the performance of various ARAs. For the residual mass, the variability is quite low; while it is quite significant for the retention time; even at higher dosages of ARA.

In terms of field applications, the residual mass would correspond either: i) to the mass of residual bitumen that would need to be cleaned off the surface of the truck bed, with higher mass increasing required workload or ii) a significant mass of ARA remains on the truck bed and can be left for the next asphalt mix load, increasing time between ARA application and reducing the required quantity of product. From the observation of residual bitumen on the plates after testing, we can hypothesize that it is the former and that less residual mass may be preferred. However, it should be noted that in this part of our study – of the mainly diesel fuel and C18 ester based formulations that were tested – all of them were found to have degraded the bitumen to a certain degree. There are however, ARAs that function as a substrate and that do not degrade the bitumen, such as those described in (Bymaster and Smith, 2009; Chesky, 2003; Davies, 2005; Dituro et al., 2002; Kinnaird, 2000; Kodali et al., 1997; Kultala, 2000, 2000; Lockwood et al., 1999; Mahr et al., 2003; Martin and Coffey, 2000; Olson et al., 1999; Salmonsens et al., 1999; Zaki and Troxler, 2013), which will be further studied in Section 3.5

If there was only ARA left on the plate, it would be to an advantage to have a higher residual mass so as to have multiple asphalt mix loads without having to re-apply the agent, resulting in reduced cost. The retention time for the asphalt mix has a high variability, and taking into account all of the variables that could involve themselves in the process, it is reasonable to expect this. For one, it can

be difficult to ensure that the agent is applied evenly over the surface of the plate. While we can apply the agent at a controlled mass, this does not ensure equal distribution of the agent all along the surface of the plate. While care was taken to distribute the agent as evenly as possible, this was limited by the scope of the vision of the user and the capability of the sprayers. The ARAs also have varied viscosities, with the agents with lower viscosity – such as diesel – spreading more easily on the plate. As another parameter of performance, it may be useful to measure how easily the mixture spreads on the plate by using a camera that can measure the contact angle between the ARA and the plate. Other factors of variability include the way the mixture is applied, mixture temperature at contact with plate and ambient temperature.

### **3.4 Development of test methods for the determination of asphalt release agent damage to asphalt and bitumen remover performance**

The principle of determining ARA damage to asphalt is to quantify the damage that ARAs could cause to pavement through observing its interaction with asphalt and bitumen. This is done with:

- the indirect tensile test to measure the effect on asphalt,
- the bitumen degradation test to measure the effects on the bitumen,
- FTIR analysis in order to observe the chemical interaction of the agent and bitumen.

The bitumen degradation test is used to determine the performance of the BRs, while the BRs also serve as reference to determine relative ARA damage to asphalt as BRs are intended to degrade the asphalt.

#### **3.4.1 ARA degradation of asphalt**

The propensity of the ARA to degrade the asphalt needs to be evaluated before it can be determined to be suitable for road construction.

##### **3.4.1.1 Asphalt Compaction**

The type of compaction method significantly influences the mechanical properties of asphalt, especially the granular skeleton (Bahia et al., 2013). Two types of asphalt compaction methods were considered in this study: by proctor and by compression.

###### **3.4.1.1.1 Compaction by Proctor**

The first method is similar to the French NF P 18-127 standard for compacting asphalt, as well as the method used in (Nivet and Alliot, 2011; Randrianarimanana, 2010). The mixture (1000±10g) was heated to 160±10°C and placed in a Ø100mm mould (NF EN 13297-30). The asphalt was then proctor compacted by 2 series of 25 drops, cleaning the proctor head of bitumen and turning the mould 45° horizontally between the series, as one series of compacting did make the asphalt rigid enough to have a clear rupture point (Figure 3-9). Additionally, the two series of compaction resulted in a void

content of around 9% for the asphalt (as tested by NF EN 12697-6), compared to 13% by single compaction, in accordance with the allowed content of 10% for road asphalt.

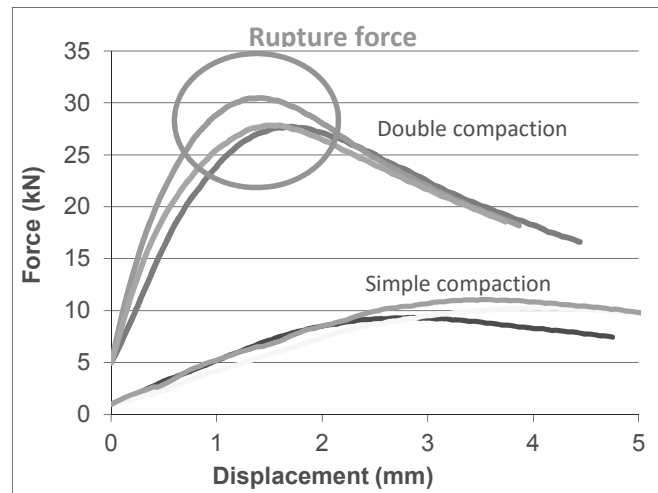


Figure 3-9 Influence du compaction on the resistance of control samples with CBR loading

The mould is placed to cool to less than 40°C so as to allow the compacted asphalt to harden, after which the sample is demoulded (Figure 3-10). The samples produced were short cylindrical samples (pills) Ø100 mm with a height of 62±2 mm, always higher on the outer perimeter (by about 3mm) than at the center of the specimen because of a non-uniform compaction (edge effect of the mould wall) of the sample.



Figure 3-10 Demolding asphalt sample

#### 3.4.1.1.2 Compaction by Compression

The second method of compaction is by compression and is based on the compaction method from the French NF P 98 251-1 standard, adapted for use with Ø100 mm molds (NF EN 13297-30). The asphalt was heated or fabricated so that it was at 150±10°C before compaction and placed in the mold (Figure 3-11). The asphalt (1000±10 g) was compacted by a piston pressed (pre-heated to 100±10°C, due to the issues when using a cold piston as shown in Figure 3-11) on the asphalt



through a compressor and maintained for a certain period of time at a constant pressure. While the standard provides a pressure of 11.94 MPa for 5min as the time for the piston to stay in contact with the asphalt sample, it was found that these specifications were not necessary or practical for this test, the pressure appearing to cause a debitumenization of the asphalt on the surface of the cylinder (T6 in Figure 3-12). Following a series of preliminary testing (Table 3-14), a pressure of 2.5MPa for 3 min was found to be adequate to attain a 4-8% voids content (6.9% as determined by NF EN 12697-6) and thereby, be in accordance with NF P 98-150-1 norm for this mixture. The time of compaction (cooling time) was found to be adequate as well so as to not have the piston stick to the cylinder and have it damage the sample when it is removed from its surface (Figure 3-12). The samples produced were Ø100 mm cylinders with a height of 62±2 mm, with a plain surface on either side.

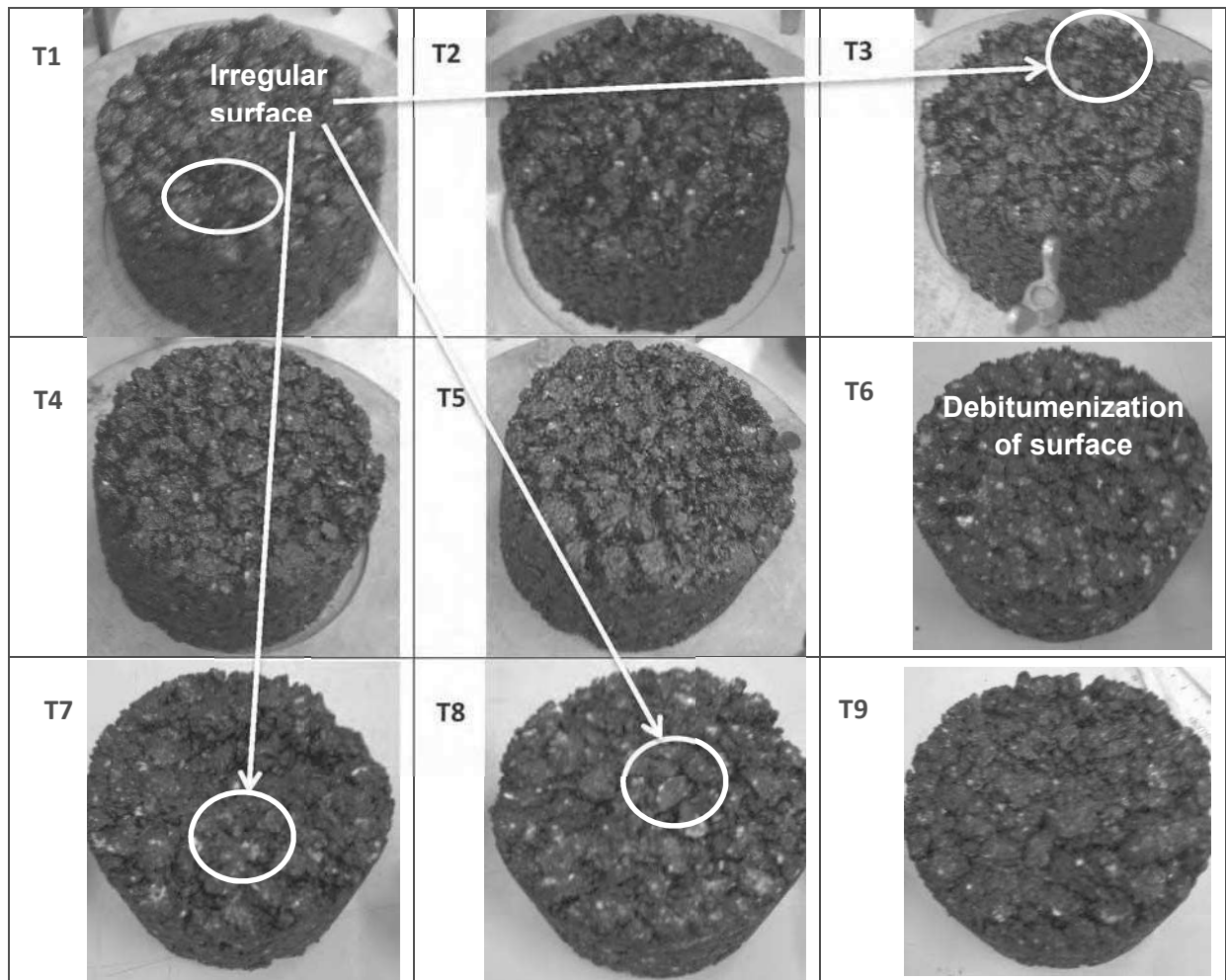


Figure 3-11 Compaction of asphalt sample by hydraulic compressor (left) and damaged surface of sample from the use of a cold piston (right)

Table 3-14 Asphalt samples compacted by compression

Sample	Time of compaction (min)	Compaction		Temperature (°C) after compaction	Height (mm)	State of surface
		Force (kN)	Pressure (MPa)			
T1	5	9.18	1.17	92	64	irregular
T2	3	16.33	2.08	105	65	flat
T3	1.5	20.41	2.60	123	63	irregular
T4	2	20.41	2.60	112	61	flat
T5	2	20.41	2.60	112	61	flat
T6	2	94	11.97	84	53	debituminized
T7	10s	40	5.09	130	60	irregular
T8	20s	40	5.09	110	62	irregular
T9	2	20	2.55	96	59	plane

Figure 3-12 State of surfaces for asphalt samples compacted by compression corresponding to Table 3-14



### 3.4.1.2 Asphalt degradation by ARAs

The degradation of the asphalt mix by the ARA from CBR or indirect tensile loading is taken as the reduction in resistance (RR%). The reduction of resistance represents the difference between the maximum resistance in tensile strength ( $S_{ARA}$ ) of the samples treated with an ARA and the control ( $S_C$ ) samples as described in Equation 3-1.

Equation 3-1

$$RR\% = 100\% \times (S_C - S_{ARA}) / S_C$$

#### 3.4.1.2.1 ARA Application

The ARA is applied to the center of the flat surface on top of the sample by a graduated burette (Figure 3-13). This is done either just before compaction or after compaction of the asphalt mix,

representing in the field contact during production on pre-compacted mixture or accidental spills on compacted mixture, respectively.

It was determined from preliminary testing that a dosage of above 5 mL was too damaging to the samples for the purposes of our testing. Dosages of 5, 2 and  $1\pm 0.2$  mL were tested in order to determine the optimum. The samples were allowed to rest for 7 days before they were subjected to testing in order for the ARA to have time to interact with the asphalt mix. Continued effects of the ARA from 0-7 days were observed in a previous study (Randrianarimanana, 2010).



Figure 3-13 Application of ARA in the center of the sample

#### 3.4.1.2.2 Resistance of Asphalt by Vertical CBR Loading

To test the degradation of the sample by the ARA, the samples were subjected to loading by California Bearing Ration (CBR) piston as attempted in (Nivet and Alliot, 2011; Randrianarimanana, 2010) at 1.27 mm/min (Figure 3-14 and Figure 3-15).

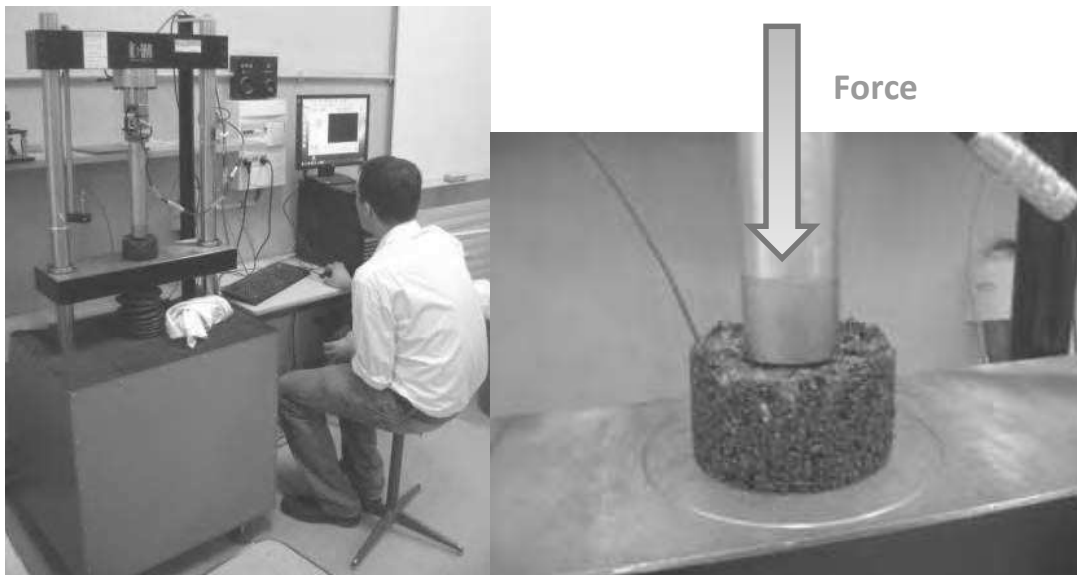


Figure 3-14 CBR loading press and a sample being loaded in CBR



Figure 3-15 Asphalt samples after CBR loading

#### 3.4.1.2.3 Resistance of Asphalt by Indirect Tensile Loading

An alternative to CBR loading was investigated in resistance by indirect tensile strength (ITS), which places the cylindrical sample on its tangential side and proceeds to load it from the top uniaxially creating tension forces in the middle of the sample (Figure 3-16). ITS is preferred to direct tension as the latter is very time consuming to implement (Huber and Decker, 1995; Partl, 2003; Silva, 2003). This method has been developed with cyclic loading at different temperatures to determine an indirect tensile stiffness modulus (ITSM) (Benedetto et al., 2013; Carbonneau, 2003; Chen and Huang, 2008; Grant, 2001; Neves and Correia, 2005; Nguyen et al., 2013; Partl, 2003; Partl et al., 2013), although this may not be necessary for our purposes.

Simple ITS testing have been looked at by (Anagnos and Kennedy, 1972; Dave et al., 2011; Katman et al., 2013; Tran and Van Loon, 2009), which will be the kind used in this case.

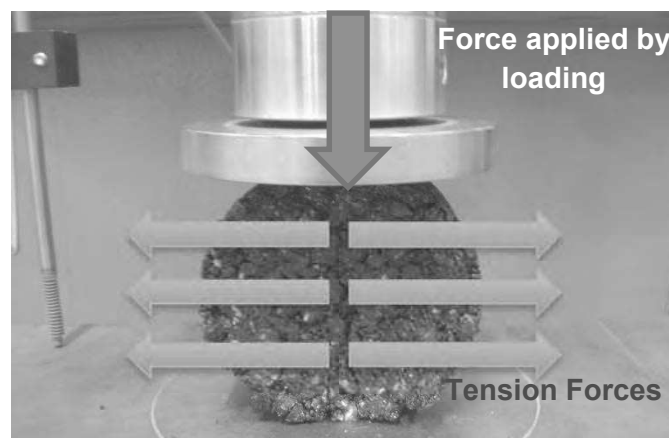


Figure 3-16 ITS loading

Standards for ITS on asphalt include NF EN 12697-34, AASHTO T322 and ASTM D 4867. In the latter, the samples are submerged in water to test the effects of moisture on the asphalt. The aforementioned testing has used a defined loading strip (contact area between testing apparatus and sample), and in (Dave et al., 2011), it was determined that maximum ratio of tension to compression strength is attained with a flat loading surface.

The loading rate was set at 1.27 mm/min.

The tensile strength  $S_t$  (Katman et al., 2013) can be derived from the maximum rupture force  $P$ , the thickness of the sample  $t$ , and the diameter of the sample  $d$ , as shown in Equation 3-2.

Equation 3-2

$$S_t = \frac{2P}{\pi dt}$$

### 3.4.1.3 Determining asphalt degradation test validity and parameter optimization

In evaluating the tests for the degradation of asphalt by ARAs, there were several considerations. These included the state of the moulds, the resistance of the asphalt to CBR/Indirect Tensile loading and the distribution of the ARA inside the sample itself. The most important trials in finding the optimum parameters are summarized in Table 3-15. Five series of tests were performed, which served to determine four of the parameters including method of loading, compaction, ARA application and the quantity of the ARA applied.

Table 3-15 Parameters for Asphalt Degradation Testing

Test No	Method of Loading	Compaction Method	Method of ARA Application	Quantity of ARA (mL)
1&2	CBR	Proctor	After compaction	5
3	ITS	Compression	After compaction	5
4	ITS	Compression	Before compaction	2
5-Final	ITS	Compression	Before compaction	1

#### 3.4.1.3.1 Resistance of Asphalt by Vertical CBR Loading

All of the samples for CBR loading were made with proctor compaction and had a 5 mL dosage of ARA, determined by a series of preliminary testing. The resistance to CBR loading of the control samples manufactured 10 days apart, shows a significant difference in both the shape of the resistance (kN) vs. displacement (mm) curve and the maximum resistance with a coefficient of variability (CVAR%, Equation 3-3) of 22% for the 6 samples (Figure 3-17).

Equation 3-3

$$CVAR\% = \frac{\sigma_{std}}{avg} \times 100\%$$

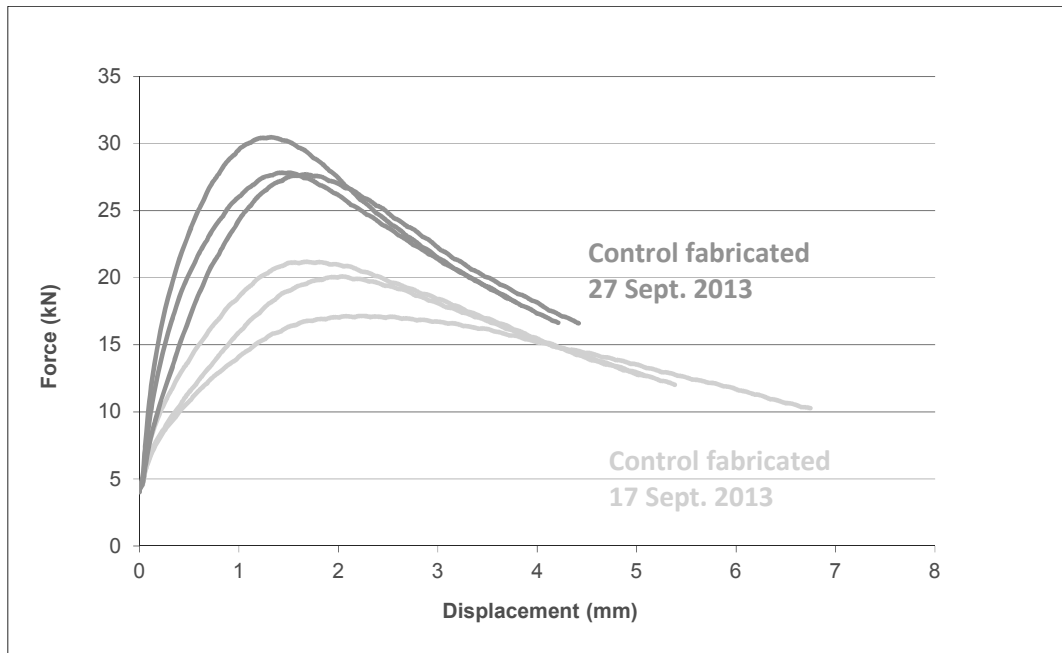


Figure 3-17 CBR Loading Test No. 1 Resistance Curves for Control Samples

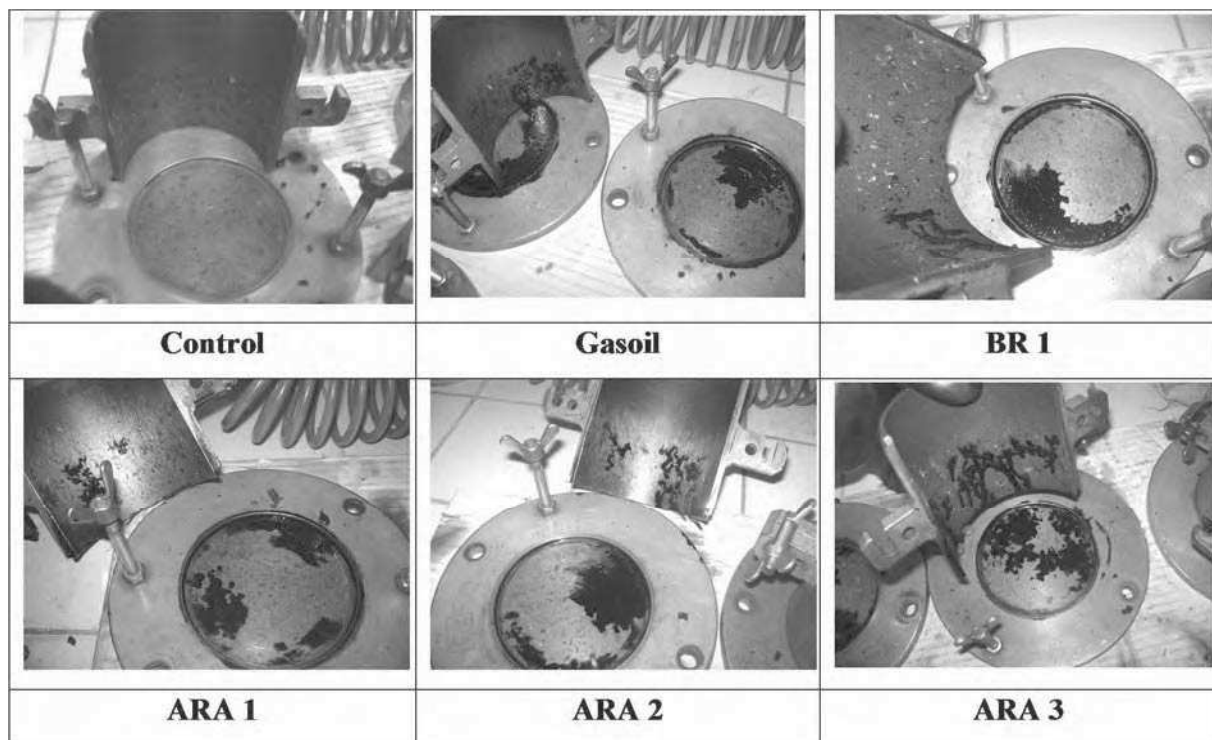
Another set of tests (Test No. 2) was completed to see if the source of the error was the asphalt. Extra precautions were taken to keep the asphalt homogenous.

A comparison of the maximum CBR resistance for the first and second trials is shown in Table 3-16. The second set of control samples also has a high CVAR% of 13.3%. In addition to this, some ARAs appear to actually increase the resistance of the asphalt as such is the case for ARA 1 and 3 in Test No. 1. In addition, the maximum resistance of ARA 1 for Tests 1 and 2 have a difference of more than 30%.

Table 3-16 Comparison of CBR Loading Trial No. 1&2

Product	Test No. 1		Test No. 2	
	Maximum Resistance (kN)			
	AVG	CVAR%	AVG	CVAR%
Control	24,08	22.0	19,52	13.3
Gasoil	18,65	12.2	19,81	10.6
BR 1	-	-	20,43	0.5
ARA 1	25,94	3.0	18,09	6.5
ARA 2	21,51	10.1	21,12	6.4
ARA 3	23,4	4.4	20,26	4.9

Table 3-17 Proctor-CBR loading Test No. 1 samples showing leaching of bitumen onto moulds

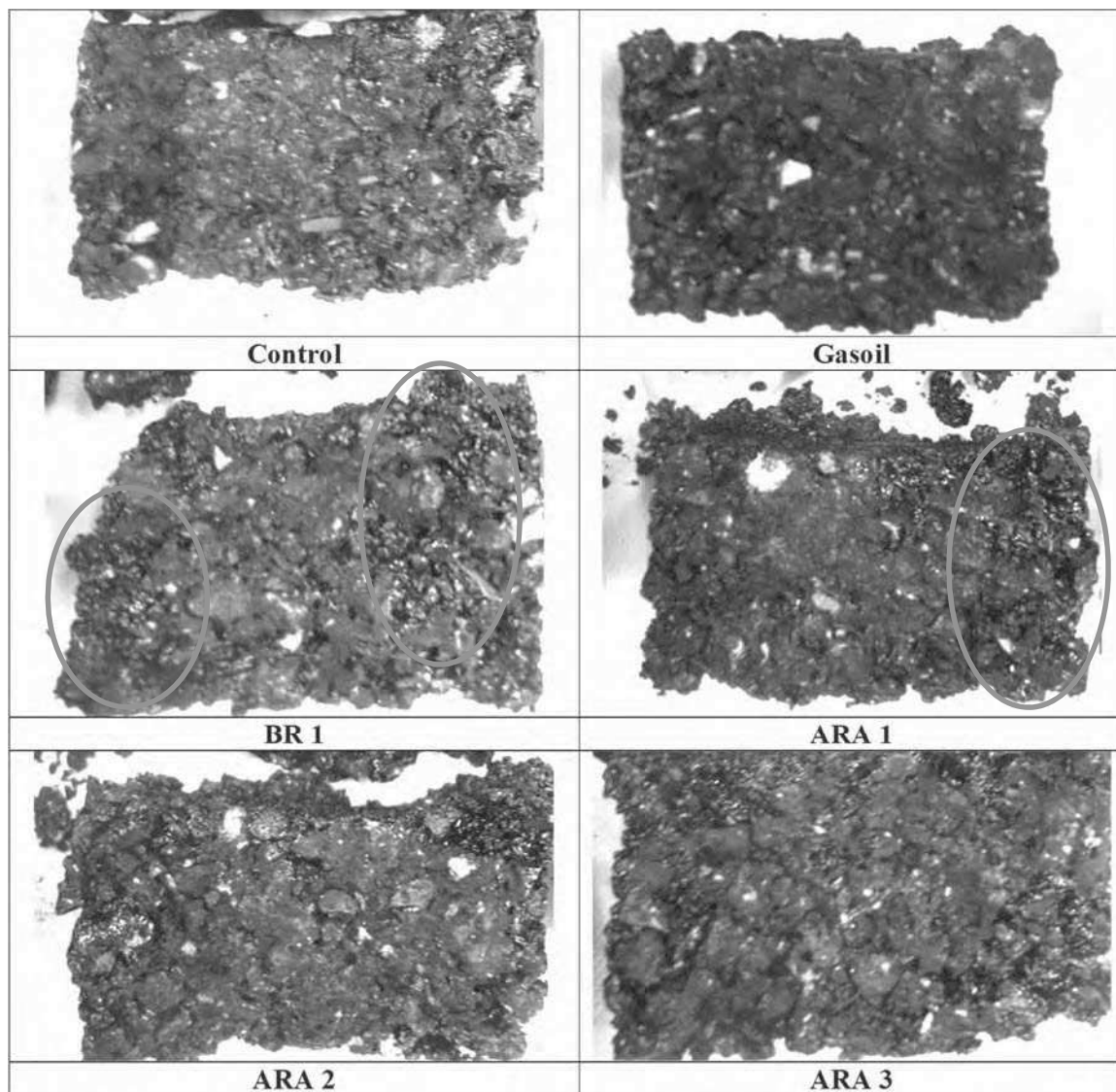


The observation of the moulds after production of CBR Loading Test No. 2 is shown in Table 3-17. The images show that Gasoil, the ARAs and the BR cause leaching of the bitumen onto the moulds.

Table 3-18 shows the observation of the interior of the samples after Test No. 2. The pictures clearly shows the tendency of the ARAs to move to the sides of the samples due to the center of the samples having a higher density from the proctor compaction process, that is, away from the part of the sample tested by CBR.

All of these observations indicated that the test method: proctor for the compaction of the asphalt and CBR for evaluating the damage to asphalt by the ARA, were not suitable for our purposes and needed to be changed.

Table 3-18 Proctor-CBR loading Test No. 1 samples showing flow of ARA towards the side of the sample



#### 3.4.1.3.2 Resistance of Asphalt by Indirect Tensile Loading (ITS)

The CVAR% for the ITS control samples (all made on different days) was 5%, lower than for the CBR samples.

For Test No. 3 with ITS, samples were compacted by compression and the ARA quantity was  $5 \pm 0.2$  mL applied immediately after compaction at an asphalt temperature of around 130°C. It was found (Table 3-19) that all of the RR% values are above 50%, indicating that the quantity of ARA could be reduced. The images in Figure 3-18 show that there was significant leaching on the molds, which would reduce the repeatability of the test. The evaporation of the samples was determined by closely observing the sample after ARA application. Only the diesel appeared to vaporize on contact with the hot asphalt (150°C), which is logical since diesel has a much lower evaporation point (around 60°C) than the ester-based agents (250°C and higher).

**Table 3-19 Resistance reduction % for ITS Trial No. 3 ITS (5mL ARA applied after compaction), ITS Trial No. 4 (2mL ARA applied before compaction) and ITS Final Test (1mL ARA applied before compaction)**



Product	Evaporation on surface	Resistance reduction %		
		5mL after compaction	2mL before compaction	1mL before compaction
<b>Diesel</b>	Some	71.4	-	43.2
<i>CVAR%</i>		2		7
<b>ARA 1</b>	Negligible	65.8	55.2	32.2
<i>CVAR%</i>		5	1	20
<b>ARA 2</b>	Negligible	58.3	54.7	21.8
<i>CVAR%</i>		8	3	7
<b>BR 1</b>	Negligible	-	66.9	43.1
<i>CVAR%</i>			1	6

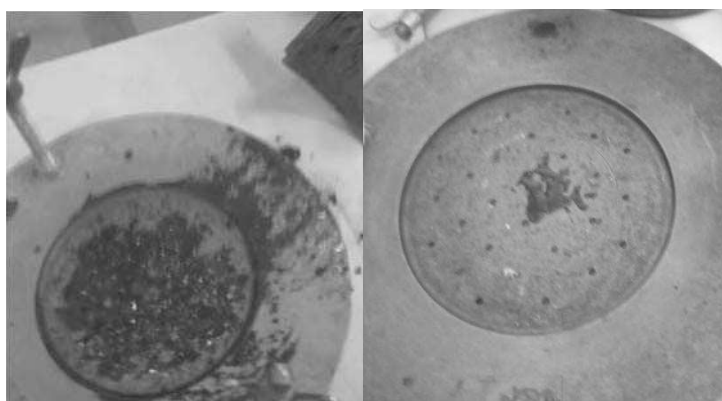


Figure 3-18 Compressor compacted ITS samples showing leaching of bitumen with 5mL ARA applied after compaction (left) and 2mL ARA applied before compaction (right)

For Trial No. 4 with ITS, the samples were compacted by compression and the ARA quantity was  $2 \pm 0.2$  mL applied immediately before compaction at around  $150 \pm 10^\circ\text{C}$ . The application of the ARA after compaction represented an ARA accidentally spilled on the compacted asphalt, or from a roller. While this is a potential source of degradation by ARAs; it may not represent the most severe case, which is more likely be the interaction of the asphalt and the ARA applied to the truck bed, an interaction that occurs before compaction.

Table 3-19 shows that all of the RR% values are above 50%, indicating that the ARA quantity is rather elevated. However, there is a clear difference between the ARA resistance values and that for the BR. Additionally, the leaching of bitumen on the moulds (Figure 3-18) is almost negligible, indicating that nearly the entire quantity of the ARA stays in the sample. The variability in the results was lower as well with CVAR% of 1-3%.

For the final test, with three trials for each agent, it was decided to lower the ARA quantity to  $1 \pm 0.2$  mL while keeping the rest of the parameters from Trial No. 4 the same. The loading curves for the final test are shown in Figure 3-19, Figure 3-20 and Figure 3-21.

It was found that the RR% values were less than 50% for all of the three products tested, while there is an even larger discrimination between the ARA RR% values (21.81-32.18%) and those for the BR (43.11%).

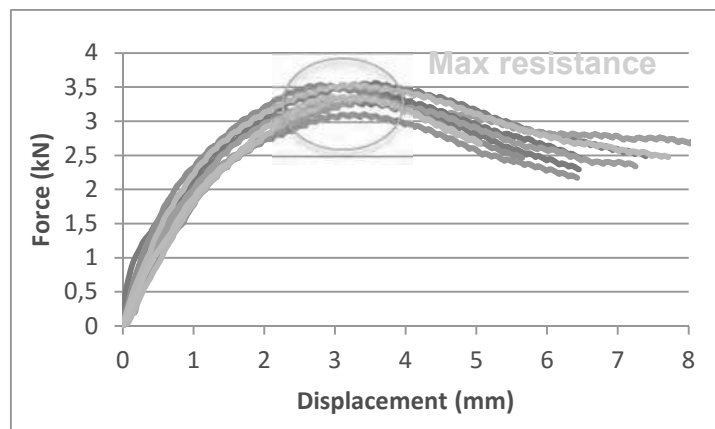


Figure 3-19 Loading curves for ITS Final Test control sample

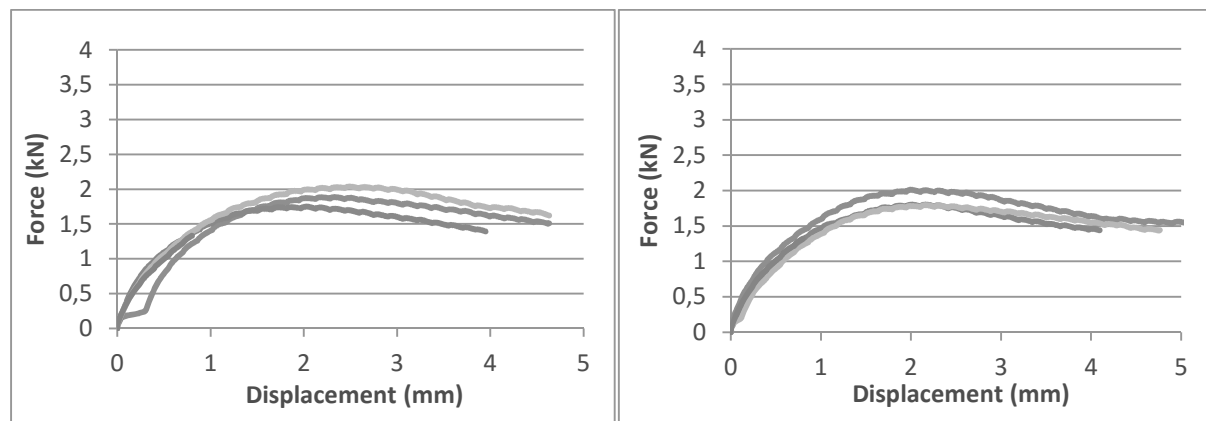


Figure 3-20 Loading curves for ITS Final Test Diesel (left) and BR 1 (right)

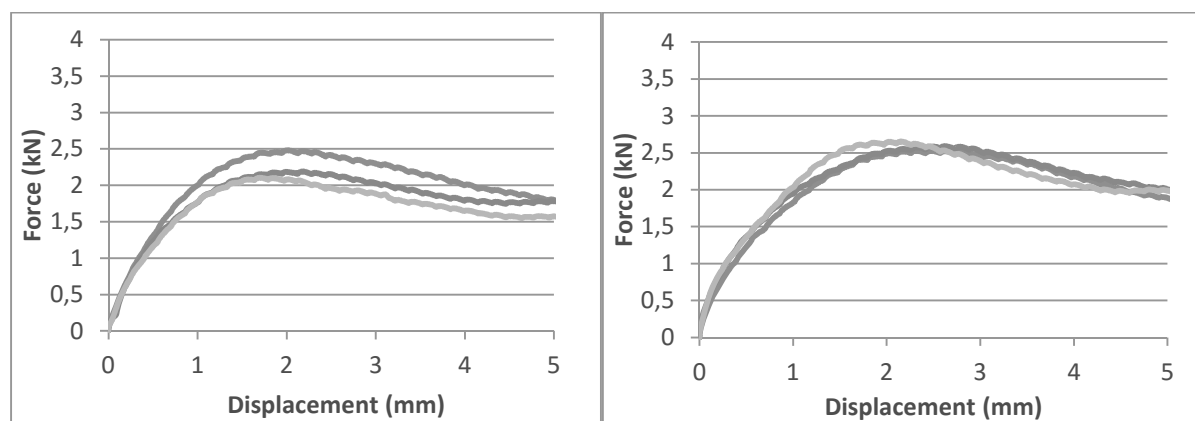


Figure 3-21 Loading curves for ITS Final Test ARA 1(left) and ARA 2 (right)

### 3.4.2 Degradation by asphalt release agents and bitumen removers of bitumen and construction materials

The degradation of bitumen by ARAs and BRs can be measured through the bitumen degradation test. While for ARAs it is an indication of safety - that is, how much they can damage the bitumen, for BRs it is an indicator of performance in how efficiently they can degrade and thereby clean bitumen residue.

Furthermore, the effects of the formulations on PVC (a common construction material) and tire rubber were tested, in order to determine the degradation by the prospective BRs of other materials on the construction site.

#### 3.4.2.1 Bitumen degradation test

A test for the degradation of asphalt by ARAs exists in (NTPEP, 2014), although it is rather subjective. The degradation of bitumen directly by the ARA was determined in the present study by the Bitumen Degradation Test (BDT). The samples were prepared by pouring  $10 \pm 1$ g of hot bitumen, heated at  $160 \pm 5^\circ\text{C}$  for 2h, into circular silicon moulds. This produces “cone with flat top” shaped samples with the dimensions:  $\varnothing 37 \pm 0.5$ mm top,  $\varnothing 31 \pm 0.5$ mm bottom,  $h = 10 \pm 0.5$ mm (Figure 3-22).

The samples were left to cool for  $8 \pm 4$ h after which they are demolded, and weighed to the nearest 0.01g. The samples were placed into 150mL graduated glass beakers of known mass, and the product was poured in so that the bitumen sample was submerged in it completely (approximately 18g of product, depending on its density). The sample was left for 24h at a temperature of  $20 \pm 1^\circ\text{C}$ , after which, the product was drained out, with the bitumen sample now sticking to the bottom of the beaker. The sides of the beaker above the bitumen sample were wiped with a cloth and the remains of the samples were weighed to the nearest 0.01g. The bitumen degradation (BD%) was taken as the difference between the mass of the bitumen sample before ( $B_B$ ) and after ( $B_A$ ) the test as shown in Equation 3-4.

Equation 3-4

$$\text{BD}\% = 100\% \times (B_B - B_A)/B_B$$



Figure 3-22 BDT silicon sample moulds (top left), sample submerged in ARA product (top right and bottom left) and beakers after test (bottom right)

#### ***3.4.2.2 FTIR-ATR Analysis of bitumen-agent interaction***

The liquid collected from the beaker was subjected to Fourier Transformed Infrared Spectrometry (FTIR) - Attenuated Total Reflectance (ATR) with a PerkinElmer Spotlight 400 (Figure 3-23). The liquid left in the beaker was mixed and sampled with a pipette. Around 0.1-0.4 mL of the liquid was poured with the pipette on a Germanium crystal so that it was completely covered, and an analysis was effectuated 16 times with a  $4\text{ cm}^{-1}$  resolution in a range of  $4000\text{--}600\text{ cm}^{-1}$ . The objective of the test was to gain more information on the severity and the nature of the softening of the bitumen by ARA and BR agents. The spectra of the original ARA or BR agents were compared with the spectra for the solution after the BDT test. This in turn was compared with the spectrum for bitumen.



Figure 3-23 FTIR-ATR analysis of the residual liquid from the BDT

### 3.4.2.3 Determining bitumen degradation test validity

The BDT was performed at 24h (contact time between product and bitumen) for diesel fuel, ARA 1, ARA 2, ARA 3, BR 1, BR 2 and BR 3 (3 trials for each), then at 7 days (single trial) for ARA 1, ARA 2 and BR 1. As shown in Table 3-20, the mass of all of the bitumen samples were reduced in this test, with the reduction being increased further for the samples submerged for 7 days.

In general, the BD% for the ARA samples was far lower than for the BR, with the exception of ARA 3, which appeared to cause high degradation (54%) while BR 2 had a relatively low degradation (33%) compared to the other BRs.

Table 3-20 Bitumen Degradation Test results

Product	% Bitumen degradation	
	after 1 day	after 7 days
<b>Diesel fuel</b>	67.1	-
<i>CVAR%</i>	6.4	
<b>ARA 1</b>	29.0	69.4
<i>CVAR%</i>	4.4	-
<b>ARA 2</b>	21.4	75.8
<i>CVAR%</i>	5.0	-
<b>ARA 3</b>	53.6	-
<i>CVAR%</i>	0.6	
<b>BR 1</b>	53.7	95.3
<i>CVAR%</i>	2.2	-
<b>BR 2</b>	32.7	-
<i>CVAR%</i>	-	
<b>BR 3</b>	51.9	-
<i>CVAR%</i>	10.7	

### 3.4.2.4 Degradation of PVC and tire rubber by BRs

The testing of the effects of the agents on PVC and rubber was conducted on the same principle as for the BDT. The test consisted of submerging PVC or rubber in the agent. For the sample, 10±1g of PVC or 2±0.1g of crumb rubber are placed in a 150mL glass beaker. The agent (18±2g) was poured into the beaker, and it was left for 1d at 20°C. The solution in the beaker was then analyzed by FTIR-

ATR and compared to the spectra of the agent by itself in order to see if there is a difference and whether the bitumen has been degraded by the agent. The test was conducted on the best performing BRs and BR candidate formulations, in order to determine their adequacy for construction sites in terms of not damaging PVC pipes or rubber tires.



Figure 3-24 PVC and crumb rubber samples for testing BR degradation of construction materials

### 3.4.3 Discussion on the development of test methods to determining the degradation of asphalt by ARAs and BRs

The evaluation of asphalt degradation by ARAs involved testing two different methods of loading resistance with two different methods of compaction (Table 3-15). The samples tested with CBR loading and proctor compaction did not provide results that were repeatable. Even though samples manufactured at the same time had similar resistance values, both control samples and samples with ARA addition did not correlate if they were made on different days. Additionally, many of the samples where ARAs were used, showed similar or higher resistance to CBR loading than the control samples.

It was clear that the ARAs had caused the leaching of bitumen from the observation of moulds after the samples were demoulded. However, this effect was not understood from the results of CBR loading. It was interesting to note that from the photos of the insides of the asphalt mix samples after testing; the ARAs appeared to move towards the sides the samples. On the other hand, the CBR loading tested the middle 50mm diameter of the sample, which would mean less of the ARA-asphalt mix interaction areas in the asphalt mix, would be subject to the test.

ITS was evaluated as an alternative to the CBR. As opposed to solely loading the inner zone of the sample, ITS subjects the entire mid-section to loading. The maximum resistance from the ITS corresponded to a vertical crack formed in the middle of samples. The tensile resistance is observed at the beginning of the loading, before the formation of the crack corresponding to the maximum resistance of the sample.

After the formation of the crack, the resistance to loading is essentially the resistance in compression of the two halves of the original sample. While both the tensile and compression properties are observed before the formation of the crack, the tensile resistance of the samples depends more on the properties of the bitumen (the part of the asphalt mix affected by ARA degradation, as the aggregates are inert to degradation by hydrocarbons such as ARAs), which are found in the sample loading before maximum resistance is reached. By comparison, the resistance to CBR loading depends more on the arrangement and the mechanical properties of the aggregate skeleton than for ITS. This is also why ITS is far more common in testing asphalt mix resistance than compression or CBR (Benedetto et al., 2013; Partl et al., 2013).

Compaction by compressor was used as an alternative to proctor compaction in order to obtain a more evenly distributed density in the sample. The voids content, for a compression pressure of 2.5MPa for 3min, was determined to be 6.9% in accordance with NF P 98-150-1 for this mixture. With this method, the CVAR% for resistance to loading for the control samples was much smaller than with the CBR-proctor samples.

For an ARA quantity of 5mL applied after compaction, the results in loss of resistance for diesel, the ARAs and the BRs were all over 50%. Additionally, there was significant leaching of the asphalt mix by the ARA onto the moulds, indicating that the dosage had to be lowered. There was however, a significant difference in loss of resistance for ITS between the ARA 2 and BR 1 (Table 3-19), indicating that the test was able to distinguish between products that are meant to degrade bitumen and those that are not.

The application of the ARA after compaction was generally performed at around 130°C. This situation represented an ARA accidentally spilled on the compacted asphalt mix, or from a roller. While this is a potential source of degradation by ARAs; it may not represent the most severe case, which could be the interaction of the asphalt mix and the ARA applied to the truck bed, an interaction that occurs before compaction.

For the second ITS test, the ARA was applied at 2mL before compaction of the sample, allowing it to be applied at around 160°C, which is generally the peak temperature in mixture fabrication, and can be assumed to increase the dynamics of the ARA-bitumen interaction as well. After the fabrication, the moulds did not show much bitumen leaching by the ARA, indicating that almost all of the ARA stayed in the sample. This is important because too much bitumen leaching could vary the quantities of ARA that act on the mixture, sample to sample. The loss of resistance was still over 50% for all of the applied products.

For the finalized ITS test, the ARA was applied at 1mL before compaction and showed RR% values below 50%. Additionally, there was higher distinction between the values for the two ARAs and BR 1,

indicating a test that can differentiate ARA products in terms of their tendency to degrade asphalt mix.

For further development of the test, the difference of adding the ARA before and after compaction should be considered as two relevant tests with this method, although before compaction seems like a more relevant condition of application in the development of ARAs. Furthermore, a higher loading rate as used in AASHTO T322, which is more common for softer materials such as asphalt mix. The temperature control of the test should also be considered as asphalt mix performance is very dependent on temperature change (Hihara et al., 2014; Lesueur and Youtcheff, 2014), as was also observed in this study. The defining of a loading strip width could also help to reduce variability. Preparation of the cylindrical sample such as flattening the rounded contact surface (Dave et al., 2011), pre-cutting a fracture plane or setting up a semicircular bend test, where a fracture plane is cut into a semicircular specimen (Wagnoner et al., 2005), could help the tensile forces to be more pronounced in the results.

The bitumen degradation test – based on mass loss of bitumen samples immersed in the tested agent – is able to differentiate the degradation from ARAs and BRs on bitumen and is a repeatable test that is relatively simple to implement. Samples were submerged for both 1 and 7 days, and the 7 day samples showed that the bitumen continued to degrade after 24 h from exposure to the product. Despite this, due to the severity of the conditions of the BDT, a 1 day test is more just for evaluating the performance of BRs because faster degradation is required.

### **3.5 Performance and degradation of asphalt by commercial asphalt release agents and bitumen removers**

In order to be able to formulate well performing and safe bio-based ARAs and BRs, the performance, safety and chemistry of the currently available bio-degradable ARAs and BRs from both French and American construction industry were analysed. This provided insight into how ARAs and BRs functioned, insight that is as of now, not available. The products tested included diesel oil, 3 bio-sourced ester based ARAs, 1 synthetic biodegradable ARA, 4 bio-sourced ester based BRs, 1 synthetic biodegradable BR and 6 formulations of varying chemistries in order to the role of chemical composition in the ARA and BR functioning mechanisms.

General information and physical properties for commercial ARAs and BRs are shown in Table 3-1, followed by chemical properties in Table 3-2.

Diesel fuel is petroleum based, consisting of 30% aromatics, 46% cycloalkanes and 24% n-alkanes. The other 8 agents analyzed were organic ester based agents, consisting primarily of C18:1 (33-59%)



and C18:2 (22-36%), with notable quantities of C16:0, C18:0 and C18:3. BR 1 contained significant quantities of short chain esters C10 and C12.

### 3.5.1 Test results

The testing of ARA performance was done by the asphalt slide test. The testing of the damage to asphalt of the ARAs consisted of the indirect-tensile strength and bitumen degradation testing. The bitumen degradation test also served as a test to find the most effective bitumen remover.

#### 3.5.1.1 Bitumen degradation by ARAs and BRs

The results of BDT at 24h for all of the commercial agents tested in this project are shown in Table 3-21. The BDT measures the % of the bitumen immersed in an agent, that has degraded during the test time of 1 d.

In terms of the bio-sourced ARAs, ARA 1, ARA 2 and ARA 4 were found to be least damaging to the bitumen by the BDT. ARA 1 and ARA 2 had degradations of 21-29%, significantly less than for the BRs (33-65%); a comparison of the samples is shown in Figure 3-25.

Not all of the samples lost mass, notably ARA 4. The negative value indicates that the weight of the bitumen samples increased to some extent, which would indicate that the bitumen sample adsorbed ARA 4. The liquid after the test stayed the same milky colour as at the beginning (Figure 3-26), indicating that instead of degrading the bitumen, a small part of the substance was actually adsorbed by the bitumen sample.

ARA 3 was found to be more damaging than the other ARAs after 24h at 54%, indicating that this may be a product that is risky to use as an ARA.

The bio-sourced ester based BRs BR 1, BR 3, BR 4 and BR 5 degraded the bitumen samples by 52-65% after 24h. The degradation for diesel fuel was at 67%.

BR 2 was the least effective BR at 33%.

Table 3-21 Bitumen Degradation Test results for commercial ARAs and BRs

ARA/ BR	% Bitumen degradation	CVAR%
Diesel fuel	67.1	6.4
ARA 1	29.0	4.4
ARA 2	21.4	5.0
ARA 3	53.6	0.6
ARA 4	-1.8**	6.6
BR 1	53.7	2.2
BR 2	32.7	- *
BR 3	51.9	10.7
BR 4	55.8	3.7
BR 5	64.9	2.3

\*Only single test conducted; \*\*Bitumen sample gained mass

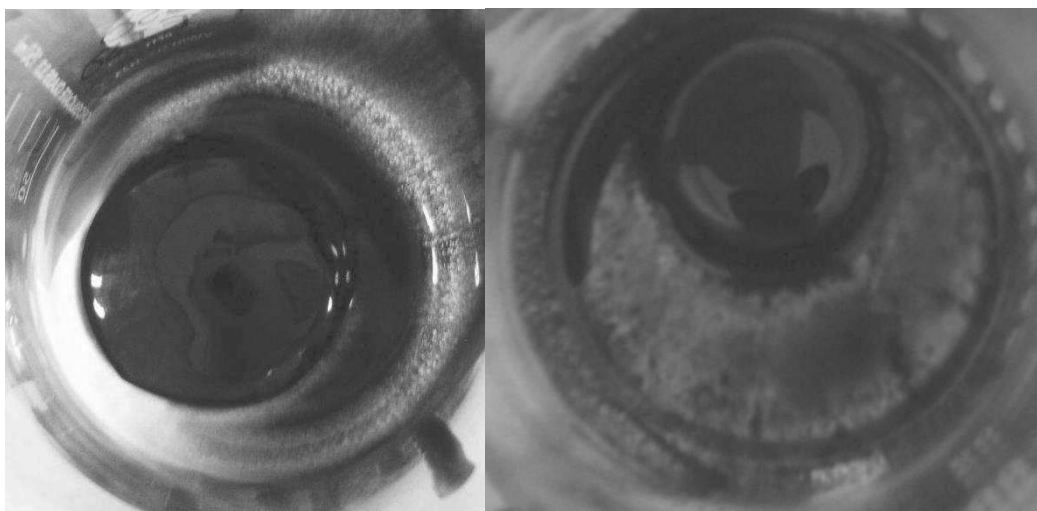


Figure 3-25 BDT sample showing i) light degradation of bitumen after 1d exposure to ARA 2 (left) and ii) heavy degradation after 1d exposure to BR 5 (right)



Figure 3-26 ARA 4 in glass beaker (left), with bitumen sample after 1 d contact with ARA 4 in BDT (right)

### 3.5.1.2 ARA and BR interaction with bitumen by FTIR-ATR

FTIR-ATR analysis was performed for all of the ARA or BR agents shown in Table 3-1, including the (i) samples themselves, (ii) the samples after the BDT described previously and (iii) 35/50 grade bitumen used in the BDT. The complete set of FTIR spectra can be found in Appendix D.

ARA 1, ARA 2, ARA 3, BR 1, BR 2, BR 3 and BR 4 are all ester-based formulations that had similar spectrum signatures. They can be identified as esters due to a large peak at around  $1740\text{ cm}^{-1}$  corresponding to C=O stretching at an intensity of around 0.04 as well as 3-4 strong peaks at  $1100\text{--}1285\text{ cm}^{-1}$  corresponding to C-O stretching (Nakanishi, 1962), with the highest being 0.02 at around  $1160\text{ cm}^{-1}$  (Figure 3-27). These peaks do not appear to change in the spectra for the BDT solutions relative to the spectra for the agents by themselves. These esters also contain aliphatic signatures similar to those of bitumen. They are peaks corresponding to  $\text{CH}_3$  aliphatic stretches at  $2950$  and  $2850\text{ cm}^{-1}$ ;  $\text{CH}_2$  aliphatic stretch at  $2920\text{ cm}^{-1}$ ; C- $\text{CH}_2$  carbonyl stretch  $1460\text{ cm}^{-1}$  and C- $\text{CH}_3$  carbonyl

stretch at  $1376\text{ cm}^{-1}$  (Woods et al., 2004; Yao et al., 2013) (Figure 3-27 and Figure 3-28). These signatures appear even stronger in the agents than in the bitumen and therefore, are not good indicators of degradation (Figure 3-28).

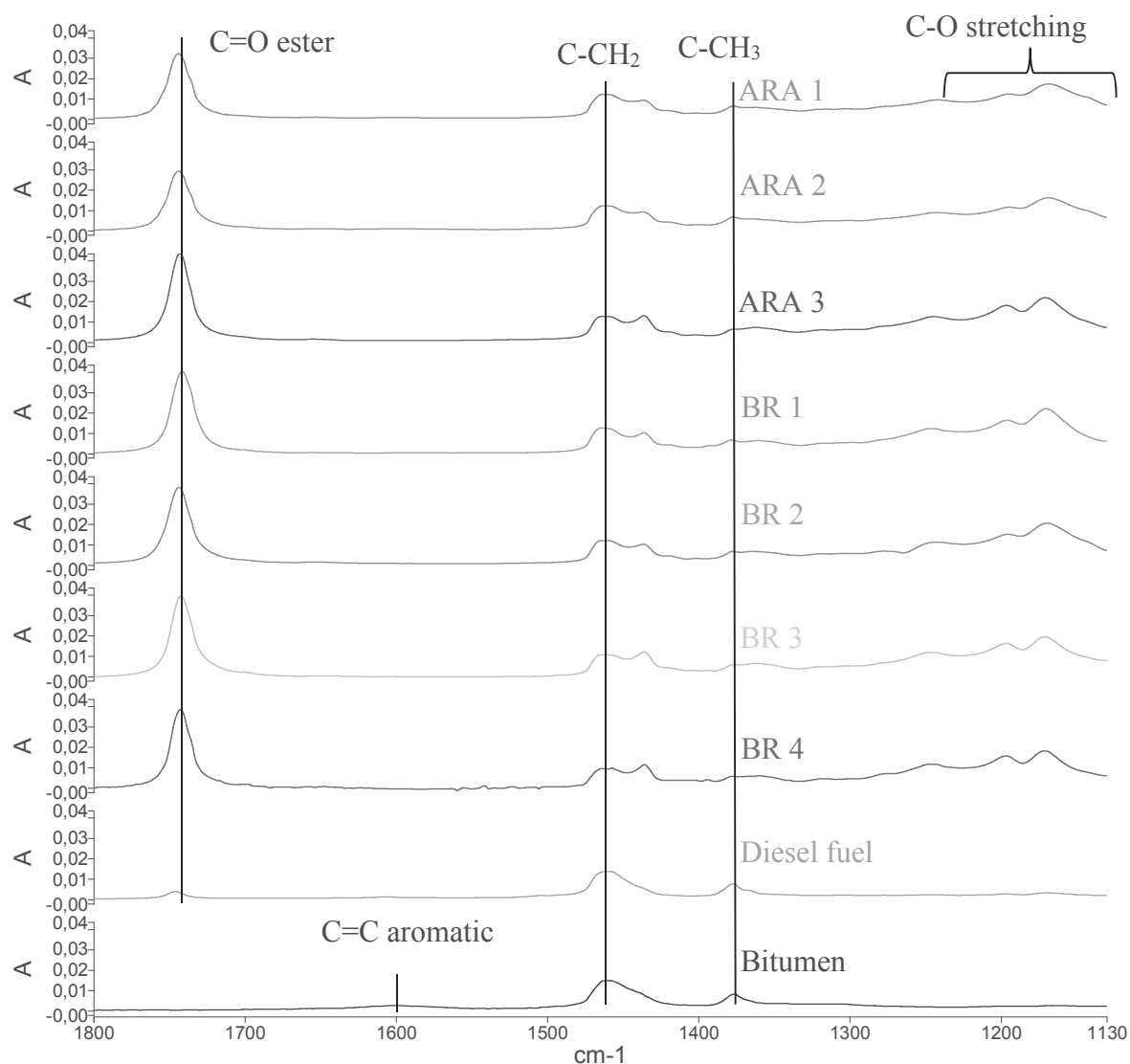


Figure 3-27 FTIR-ATR spectra (1800-1130  $\text{cm}^{-1}$ ) for ester-based commercial ARAs and BRs: ARA 1, ARA 2, ARA 3, BR 1, BR 2, BR 3 and BR 4 along with diesel and 35/50 bitumen

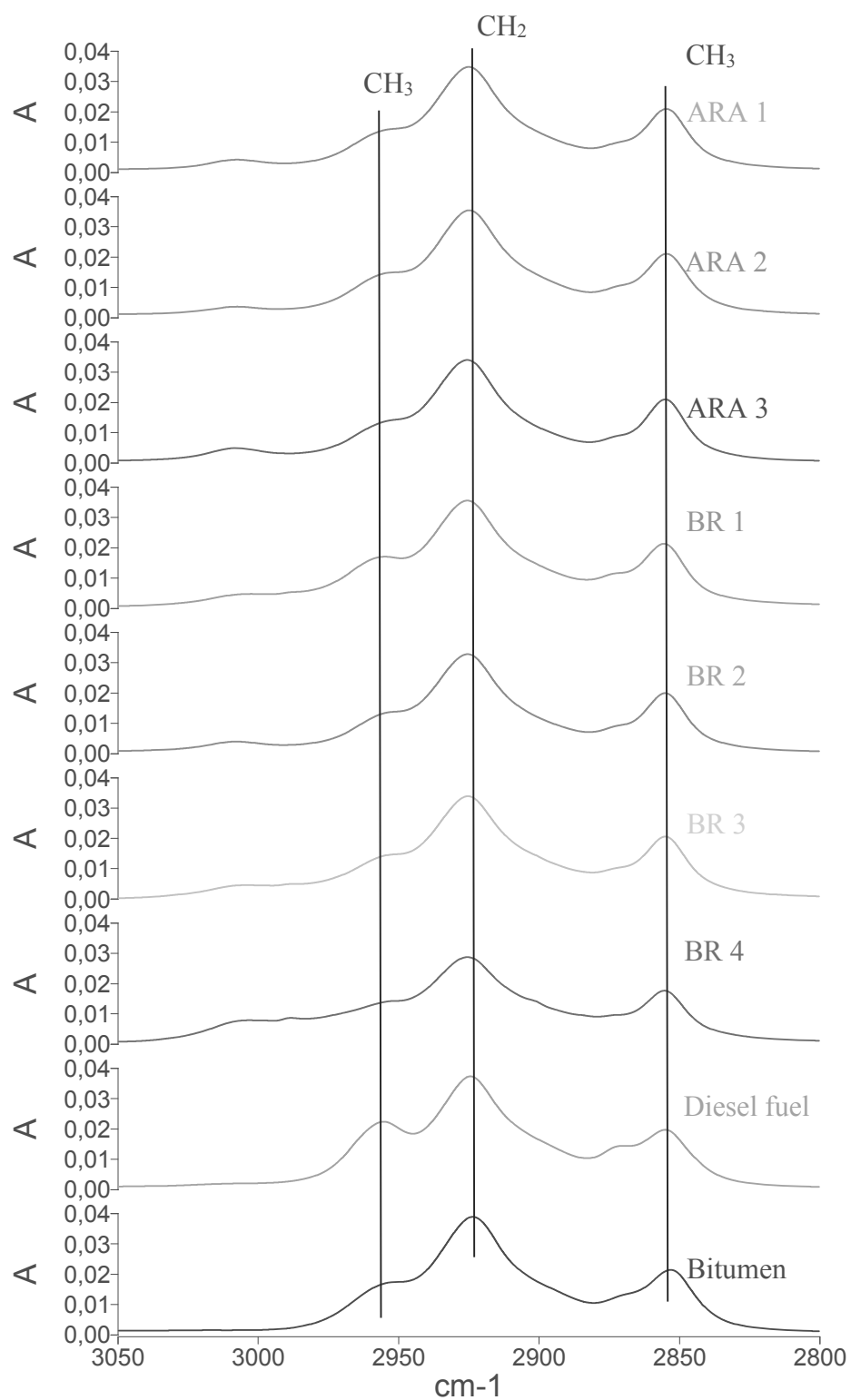


Figure 3-28 FTIR-ATR spectra (3050-2800  $\text{cm}^{-1}$ ) for ester-based commercial ARAs and BRs: ARA 1, ARA 2, ARA 3, BR 1, BR 2, BR 3 and BR 4 along with diesel and bitumen

Like for the esters, diesel contains aliphatic signatures that correspond to those of bitumen, which would be understandable since they both originate from crude oil and the results are in agreement with those of (Higgins, 2012; Santos Jr. et al., 2005).

The peak at  $1600\text{ cm}^{-1}$ , corresponding to C=C aromatic stretches (Lamontagne et al., 2001a; Mouillet et al., 2008; Nakanishi, 1962; Tachon, 2008; Woods et al., 2004; Yao et al., 2013) is present in the bitumen, as well as in the BDT solutions for ARA 3, BR 1, BR 2, BR 3 and BR 4 (Figure 3-29), but not in the agents themselves. This band is not present, or appears far weaker for the BDT solutions for ARA 1 and 2 along with BR 2.

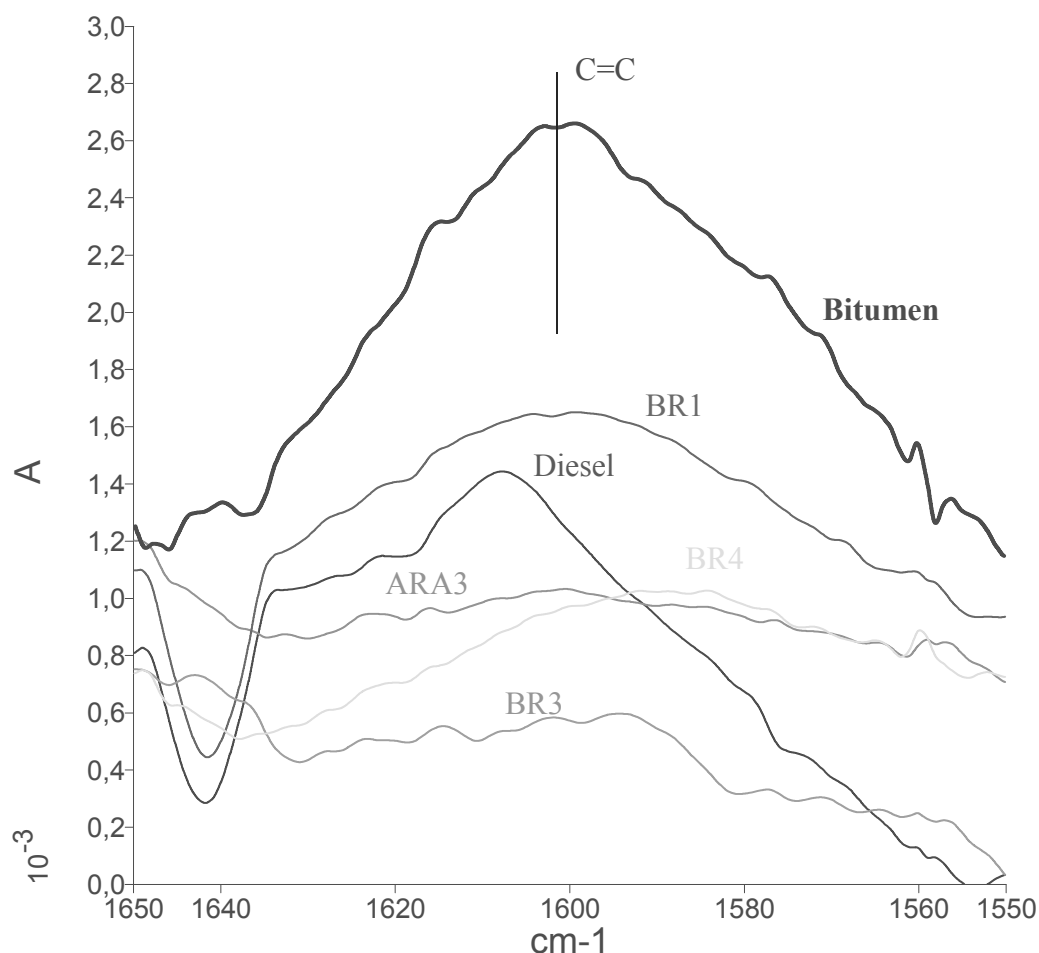


Figure 3-29 FTIR-ATR spectra ( $1650\text{--}1550\text{ cm}^{-1}$ ) of BDT solution for ester-based commercial ARAs: ARA 3, BR 1, BR 2, BR 3, BR 4, bitumen, and diesel fuel

For ARA 4, a high proportion of water (found to be at 90%) is observed with a strong and broad peak around  $3400\text{ cm}^{-1}$  (Eisenberg and Kauzmann, 1969). As to the composition, the peak at  $1640\text{ cm}^{-1}$  may indicate a C=C alkyl signature, while the peak at  $1080\text{ cm}^{-1}$  may indicate C-O ether, methoxy or alcohol aliphatic bonds (Delmas, 2011). The liquid before and after the BDT remained almost the same (red and blue spectra in Figure 3-30), indicating that there was no degradation of the bitumen, as also indicated by the negative change in mass. The small difference in peaks at  $1260$ ,  $1090$  and  $800\text{ cm}^{-1}$ , that are present in ARA 4 by itself but not the BDT solution (green spectra in Figure 3-30) - can be attributed to the agent being adsorbed by the bitumen sample. This is confirmed by the fact that it is indeed these peaks that are present for the bitumen sample after the test.

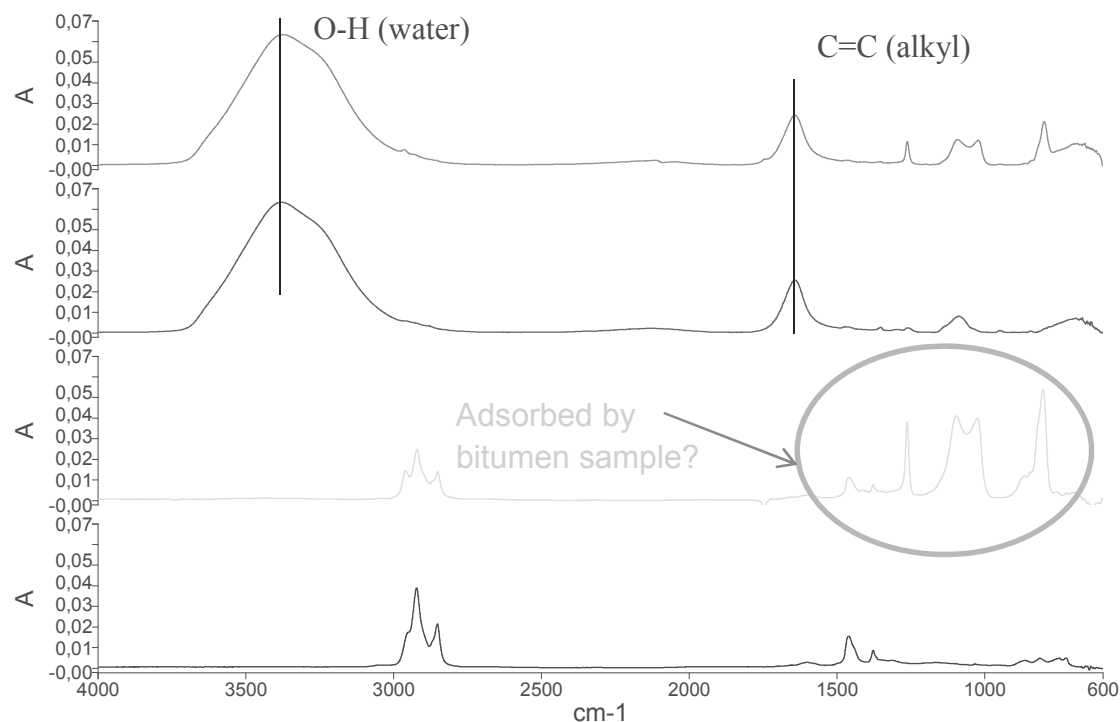


Figure 3-30 FTIR-ATR Spectra ARA 4 for BDT solution (blue), agent (red), bitumen sample after test (green) and 35/50 bitumen (black)

BR 5 contains a water signature at  $3400\text{ cm}^{-1}$ , that is much weaker than for ARA 4, indicating some presence of water (Figure 3-31). A strong ester peak is present at  $1740\text{ cm}^{-1}$  for the ARA, which is somewhat diluted in the BDT solution. In terms of aliphatics, BR 5 shows a somewhat stronger  $\text{C-CH}_3$  peak at  $1376\text{ cm}^{-1}$  than for bitumen but much stronger stretches at  $2920\text{ cm}^{-1}$  and  $2850\text{ cm}^{-1}$ , which are present in the spectrum of the BDT solution, making them indicators of bitumen degradation in this case, as they are diluted in the BDT. BR 5 also contains strong peaks around  $1270$  and  $1100\text{ cm}^{-1}$ , possibly corresponding to  $\text{C-O}$  acid ester stretches (Nakanishi, 1962). There is also a strong peak at  $710\text{ cm}^{-1}$  possibly corresponding to some lighter aromatics (Higgins, 2012) and indicating a substance containing or being similar to benzyl benzoate.

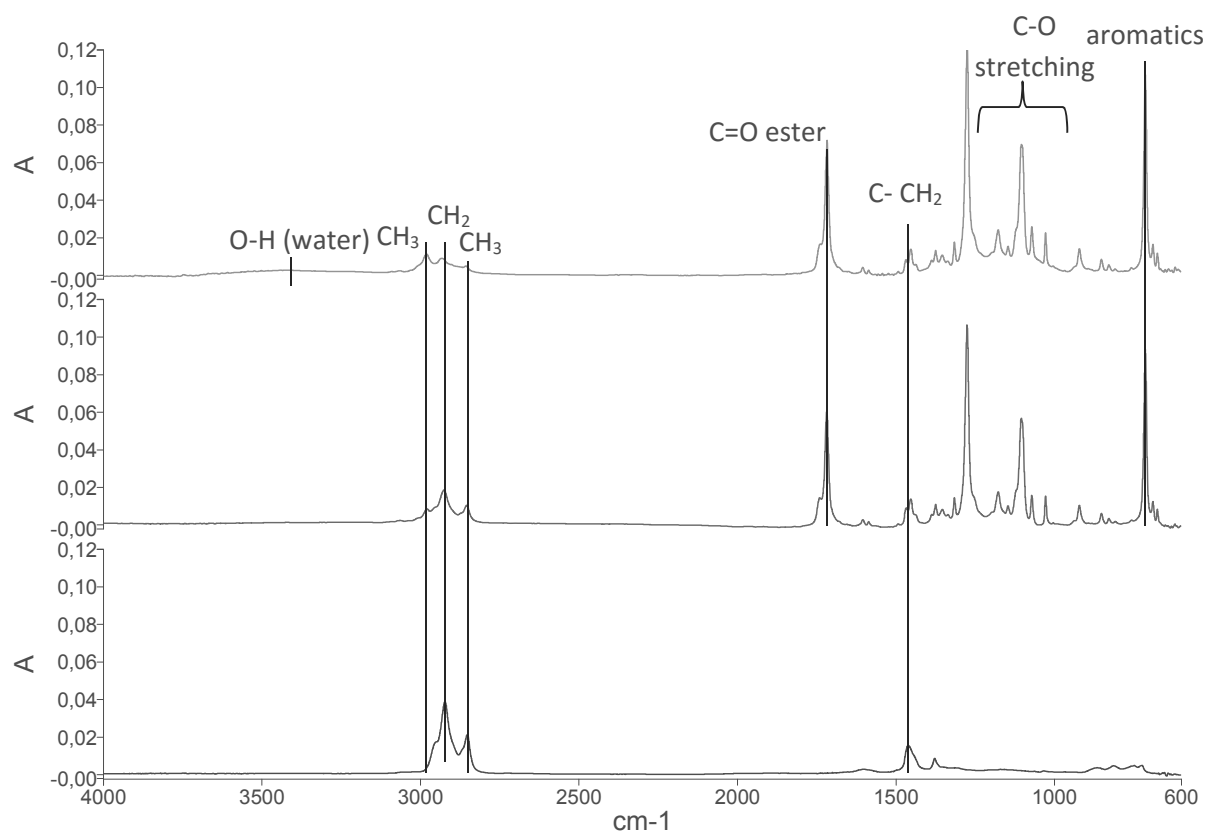


Figure 3-31 FTIR-ATR Spectra BR 5 for BDT solution (blue), agent (red) and 35/50 bitumen (black)

### 3.5.1.3 ARA performance by Asphalt Slide Test

For the Asphalt Slide Test, the results for diesel fuel, ARA 1 and ARA 2 (bio-sourced ARAs, available on the French market), BR 2 (found to be a low-degrading BR for BDT in Section 3.5.1.1) and ARA 4 (synthetic biodegradable from the USA market) are presented in this section. A photo of each plate was taken immediately after the test and representative photos for each product tested are shown in Table 3-22. The results of the test in terms of residual mass and time to beginning of slide are shown in Table 3-23.

Table 3-22 Images of plates after Asphalt Slide Test

Diesel fuel	ARA 1	ARA 2	ARA 4	BR 2

In terms of residual mass, diesel fuel, ARA 1, ARA 2 and BR 2 were all very close at 7-9 g/m<sup>2</sup>. The residual mass for these samples consisted of some similar combination of lixiviated bitumen and the substance that lixiviated it. In terms of the time to beginning of slide, it was ARA 1 and ARA 2 performing the best at 5-6s. Diesel fuel was somewhat higher at 8s with BR 2 at 13s. ARA 4 functioned in a substantially different way than the other agents. The residual mass was almost negligible at 0.37 g/m<sup>2</sup>. Furthermore, as shown in Table 3-22, the residual mass contains only the ARA and no bitumen. ARA 4 also had a much higher time to beginning of slide at 85s, with a higher variability relative to the other samples.

Table 3-23 Results for Asphalt Slide Test

Product	Residual mass (g/m <sup>2</sup> )	<i>STDDEV</i> $\sigma$	Time to beginning of slide (s)	<i>STDDEV</i> $\sigma$
<b>Diesel fuel</b>	8.92	0.21	8	4
<b>ARA 1</b>	7.12	0.29	6	4
<b>ARA 2</b>	8.20	0.82	5	4
<b>ARA 4</b>	0.37	0.27	85	48
<b>BR 2</b>	8.92	0.63	13	10

#### 3.5.1.4 Reduction in resistance in ITS of Asphalt in contact with ARAs

The ITS results for the two ARAs with the lowest degradation (ARA 1 and 2) are shown from the final test in the previous section (Table 3-24). The C18 based ARA 1 and ARA 2 degraded (in terms of reducing the resistance of asphalt in ITS) the asphalt at 32 and 22%, respectively. ARA 4 had a significantly lower reduction in resistance at 11.28%.

Table 3-24 Resistance Reduction for ITS Testing

Product	% Resistance reduction	<i>STDDEV</i> $\sigma$
<b>Diesel fuel</b>	43.16	6.54
<b>ARA 1</b>	32.18	6.47
<b>ARA 2</b>	21.81	1.62
<b>ARA 4</b>	11.28	1.47

### 3.5.2 Discussion

#### 3.5.2.1 Evaluation of commercially available BRs

The higher degradation value for bitumen would indicate a better performing BR, as high degradation of bitumen at 24h is the measure of performance for the product. Diesel fuel was found to have a relatively high bitumen degradation of 67.1% which is not surprising since diesel fuel has been used for a long time in the field as a reliable BR considering this efficiency. Diesel was also



found to have a significant degrading effect on asphalt mix at 43%, similar to that for BR 1, even when applied to the mixture at high temperatures ( $150\pm 10^{\circ}\text{C}$ ). Despite the fact that diesel fuel is much more volatile (evaporation at around  $60^{\circ}\text{C}$ ) compared to the bio-sourced ARAs (evaporation at  $250^{\circ}\text{C}+$ ), there is always a significant part of diesel fuel that stays in the sample and degrades the asphalt. The deterioration of asphalt by diesel fuel has also been described in (Lavin, 2003; Martin, 1978). It should also be added, that under laboratory conditions, many effects that would increase evaporation, and decrease the degradation of asphalt by diesel fuel, such as wind and UV-rays are not possible to replicate. However, in any case, diesel is banned on many construction sites as ARAs or BRs (Acton, 2013), and so, the development of biodegradable and safe ARA remains indispensable for the reasons mentioned.

BR 5 (at 65% in BDT, Table 3-21) was the most effective commercially available BR in this study, while having both the highest ester content at 86% and the highest proportion of the short chained ester C10 (74%). The most effectively degrading C18-based agents had the highest ester contents (69-82%) as shown in Figure 3-32.

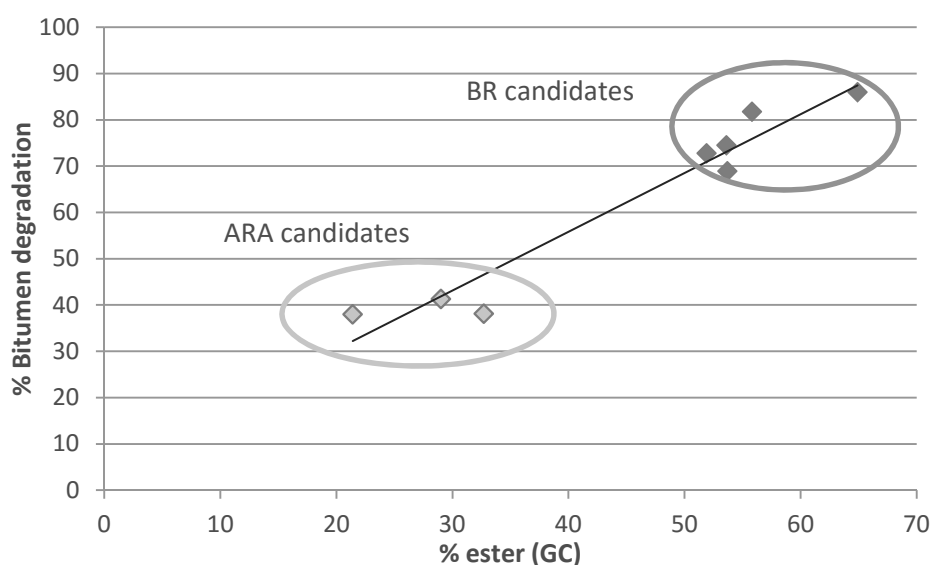


Figure 3-32 Ester content of commercial ARAs and BRs compared to their mass loss in BDT

The most significant example of bitumen degradation in the FTIR-ATR analysis could be found with the peak at  $1600\text{ cm}^{-1}$ , corresponding to C=C aromatic stretches (Lamontagne et al., 2001a; Mouillet et al., 2008; Nakanishi, 1962; Tachon, 2008; Woods et al., 2004; Yao et al., 2013). While this band does not appear for the BDT solutions after ARA 1 and 2, corresponding to relatively light degradation, it is significant in the solutions after ARA 3, BR 1, BR 3 and BR 4, which all caused significant degradation in BDT. There are a combination of heavier (asphaltenes and resins) and lighter aromatics in bitumen, so this cannot be determined with certainty. However, there are

indications (Lamontagne et al., 2001a; Mouillet et al., 2008) that the  $1600\text{ cm}^{-1}$  peak increases with aging, and would therefore be more likely to correspond to heavier aromatics. The analysis by Tachon (2008) endorses this hypothesis, with asphaltenes having been shown to have a strong aromatics peak. It is the asphaltenes that are known to have the highest importance in the structure and rigidity of the bitumen (El Béze, 2008; Olard, 2003; Peralta, 2009; M.N. Siddiqui and Ali, 1999; Tachon, 2008), so this would correlate with real lixiviation of the bitumen observed in BDT. This signature is also present in the BDT solutions for the short chained esters, which had the highest degradation in BDT. Unlike the esters, diesel by itself appears to have a signature at  $1600\text{cm}^{-1}$ , although this it is smaller than for the BDT solution, this remains an indication of lixiviated bitumen, although a weaker one.

### *3.5.2.2 Evaluation and development of ARAs*

It is significant that diesel fuel appeared to have a lower time to beginning of slide while (i) being reputed as a powerful ARA and BR in the field and (ii) having the highest value for degradation in both ITS and BDT testing (Mikhailenko et al., 2015b). This indicates that diesel functions (as an ARA) by “dissolving” the bitumen in contact with the plate in the process of inducing the mixture to slide, a hypothesis which is supported by the images of the residue on the plates.

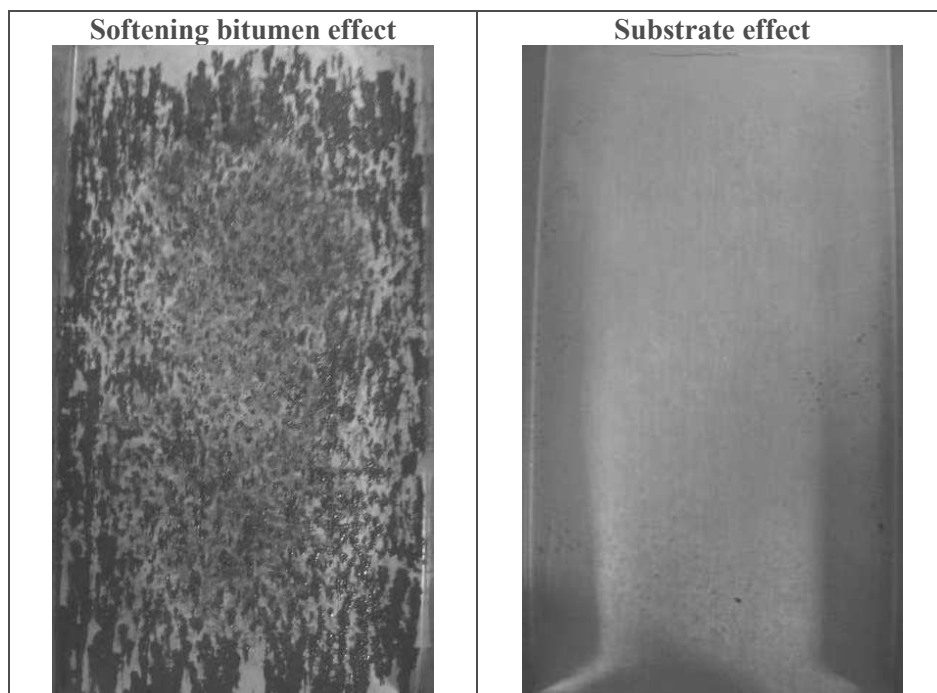
The ester C18 based agents ARA 1, ARA 2 and BR 2 functioned in a similar way to diesel, only they degraded the bitumen at a lower intensity than ARA 3, BR 1, BR3 and BR 4, which were also ester C18 based. This was a function of the ester content of the agents that degraded less, and had an ester content of 38-41%, compared to the ester content of the agents that degraded more, which was significantly higher at 69-82%.

Essentially, we have two different modes of functioning for biodegradable ARAs (Figure 3-33). The first (for diesel fuel, ARA 1, ARA 2 and BR 2), is the softening of the bitumen between the mixture and metal, causing the bitumen to slide. The second mechanism (for ARA 4) is to form a substrate layer between the bitumen and metal as described in (Ballenger and Light, 1993; Bymaster and Smith, 2009; Chesky, 2001; Davies, 2005; DeLong, 1996; Dituro et al., 2002; Kinnaird, 2000; Kodali et al., 1997; Kultala, 2000; Lockwood et al., 1999; Mahr et al., 2003; Martin and Coffey, 2000; Olson et al., 1999; Salmonsens et al., 1999; Zaki and Troxler, 2013). The fact that ARA 1 and ARA 2 have significantly lower time to beginning of slide, while having slightly lower residual mass values than diesel and BR 2 indicates that they have been designed with similar performance characteristics and thus, may contain some surfactants that contribute a combination of both effects. More precisely, they could have been formulated with some combination of esters and surfactants with the objective of the resulting ARA demonstrating both effects. The BRs on the other hand, were

formulated with mostly esters, taking the esters ability to break down the bitumen as the primary criterion.

In the practical sense, retention time would correspond to discharging the mixture from the truck, while the residual mass would correspond to the amount of residual asphalt left on the truck bed after discharging, and thereby, the frequency of cleaning the surface required. It remains to be determined which performance characteristic is more important, although if we assume that ARA 1, ARA 2 and ARA 4, are all reasonably well performing products in the field, it would be the residual mass that is the most important.

Figure 3-33 Characteristic mechanisms of ARA performance



More precisely, it is not so much the quantity of the mass, but rather the nature of the residual mass which is the key to understanding its performance. In the case where the bitumen is softened, the residual mass represents something that may need to be cleaned off the truck bed before the next mixture load. On the other hand, in the case where the ARA acts as a substrate, the residual mass represents the ARA left on the truck bed, and thereby a quantity of ARA that would not need to be reapplied before the next load.

In fact, the BDT results indicate that ARA 4 is adsorbed by the bitumen to a small degree. From the reduction in ITS of the asphalt mix by ARA 4, it is shown that this degradation does have a negative effect on the asphalt mix, although much less than the ester-based ARAs. Hypothetically, this

product could handle many more asphalt mix loads before it would need to be cleaned off and reapplied, making it more economical and efficient.

This hypothesis of course, would need to be tested in the field, however, it appears that ARA 4 represents a more advanced generation of ARAs that functions significantly differently from both diesel fuel and ester based formulations.

### **3.6 Bio-sourced formulations as asphalt release agents and bitumen removers asphalt release agents**

With the development of the methods for analysing ARA and BR performance and safety, the objective of developing new bio-sourced formulations can be attained. Due to the complexity of organic chemistry, there is admittedly a significant number of ways of going about this. Therefore, the choice of chemical formulations used in the trial processes were based on i) the results of the testing on the commercial agents and ii) the materials accessible for this project.

The candidate formulations fall into 6 main categories:

- i) C7 and RD 6 are highly concentrated short chain esters with hydrocarbon lengths ranging from 7-10;
- ii) RD 1 and RD 2 are colza oil with unsaturated fatty-acid content at 39% and 3%, respectively;
- iii) RD 4 is a commercially available oil, it is highly saturated with a high degree of iso-paraffinic structures;
- iv) RD 5 is a highly concentrated ester with a similar chemical composition to the commercial BRs shown previously, composed primarily of C18:1 (39%) and C18:2 (32%);
- v) RD 7 is a mixture of RD 2 and RD 5 at 50:50 in order to observe the combined effects;
- vi) MUG and MUDG are glycerol based formulations sourced from agricultural waste and are the primary ARA candidates for this study. A priority was given to these agents in the development of these chemicals as ARAs due to the fact that they are from agricultural waste and the fact that they can be produced from local sources, adding significantly to their environmental performance.

General information and physical properties for commercial ARAs and BRs were shown in Table 3-3, followed by selected chemical properties in Table 3-4.

#### **3.6.1 Glycerol-based formulations**

Glycerol as a bio-sourced compound has shown its versatility in several industrial applications including in textiles and pharmaceuticals (Leoneti et al., 2012) as well as in ARAs (Artamendi et al., 2012; Dituro et al., 2002; Lockwood et al., 1999; Zanzotto, 2003). The advantages of glycerol-based

agents is their biodegradability, water retention, and surfactant properties (Leoneti et al., 2012). Additionally, glycerol often is a secondary waste product of industrial processes such as biofuel production (Ma and Hanna, 1999). Therefore, the used of glycerol goes towards bio-waste reduction as well.

As explained in Section 3.2.1, the glycerol based formulations were developed by the partner laboratory LCA<sup>1</sup> of Toulouse with the work of Boussambe (2015). The glycerol is extracted from biological waste sources, which can include biological waste from the production of corn, rapeseed and duck fat. Glycerol is derived from the agricultural waste in the process of biodiesel production (transesterification), which produces biodiesel and glycerol as a waste product. Diglycerol is then produced from the etherification of glycerol using a catalyst. An overview of the development of these chemicals is shown in Figure 3-34.

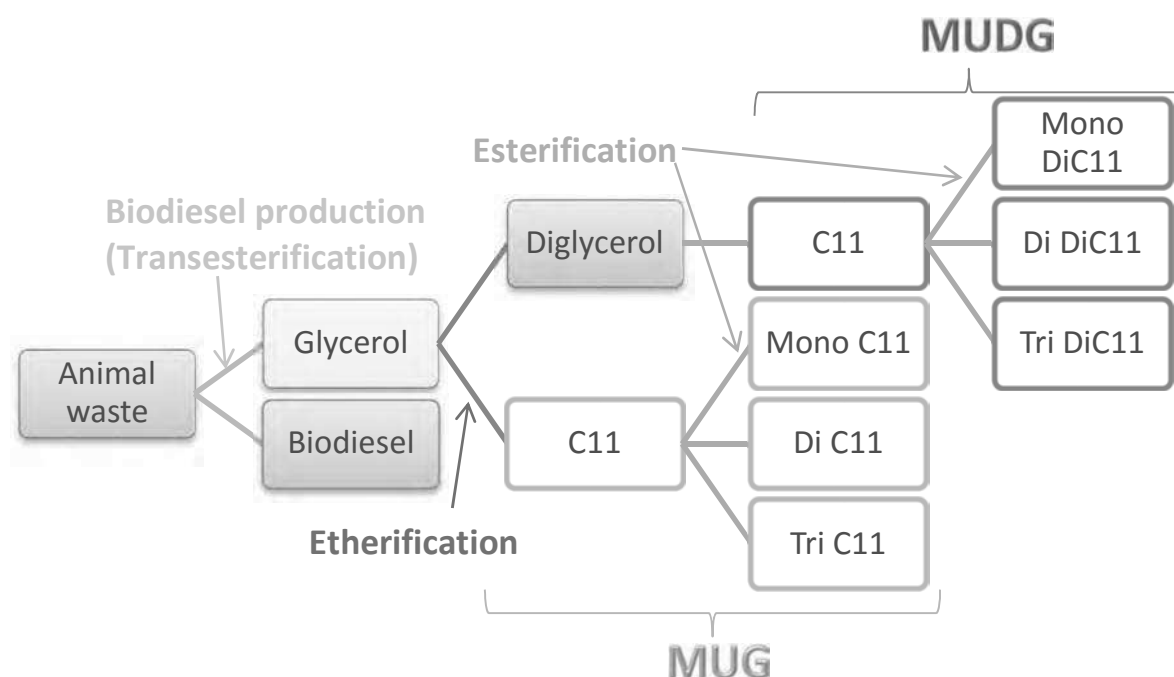


Figure 3-34 Chemical transformations involved in the production of MUG and MUDG

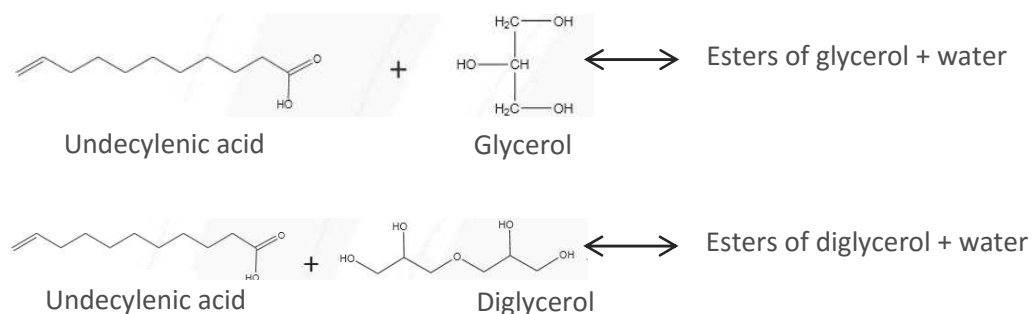


Figure 3-35 Esterification reactions of glycerol and diglycerol with undecylenic acid (Boussambe, 2015)

<sup>1</sup> Laboratoire de Chimie Agro Industrielle (INRA-INPT/ ENSIACET)

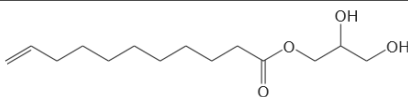
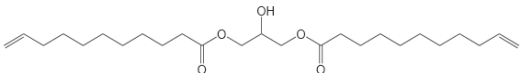
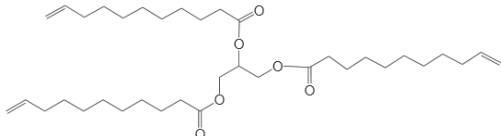
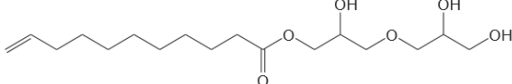
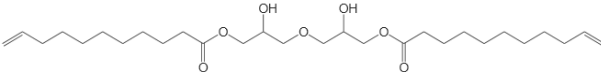
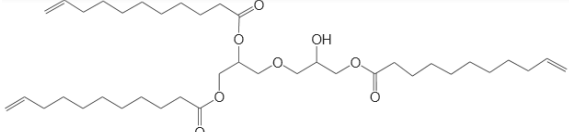
Glycerol undecenoates (MUG) and diglycerol undecenoates (MUDG) are glycerol based and diglycerol based compounds, respectively prepared by reacting them with undecylenic acid that transforms glycerol (C11) and diglycerol (DiC11) into three by-products with surfactant properties (Figure 3-35).

The byproducts for the transformation of glycerol are glycerol monoundecenoate (G MonoC11), glycerol diundecenoate (G DiC11), glycerol triundecenoate (G TriC11) and residual undecylenic acid (C11). For the transformation of diglycerol, the by-products consisted of diglycerol monoundecenoate (DiG MonoC11), diglycerol diundecenoate (DiG DiC11) and triundecenoate (DiG TriC11) along with residual undecylenic acid (Table 3-25). The structure of the composants is described in Table 3-26.

Table 3-25 Composition of glycerol-based formulations (Boussambe, 2015)

Compound	MUG (Glycerol undecenoates)	Compound	MUDG (Diglycerol undecenoates)
C11	6.9%	C11	6.4%
G MonoC11	66.0%	DiG MonoC11	64.2%
G DiC11	26.0%	DiG DiC11	24.9%
G TriC11	0.9%	DiG TriC11	4.4%

Table 3-26 Chemical structure for MUG and MUDG components (Boussambe, 2015)

Compound	Branch	Chemical structure
MUG	Glycerol MonoC11	
	Glycerol DiC11	
	Glycerol TriC11	
MUDG	Diglycerol MonoC11	
	Diglycerol DiC11	
	Diglycerol TriC11	

MUG is a white semisolid at room temperature while MUDG is a yellow liquid (Figure 3-36). The melting point for MUG is 40-45°C. Based on the functioning of ARAs as surface-acting agents, the

products were formulated with particular attention to the surface tension of the agents and can be considered to be functioning as surfactants. In addition to the base compounds, MUG and MUDG contained approximately 20 and 25%w water, respectively at delivery.

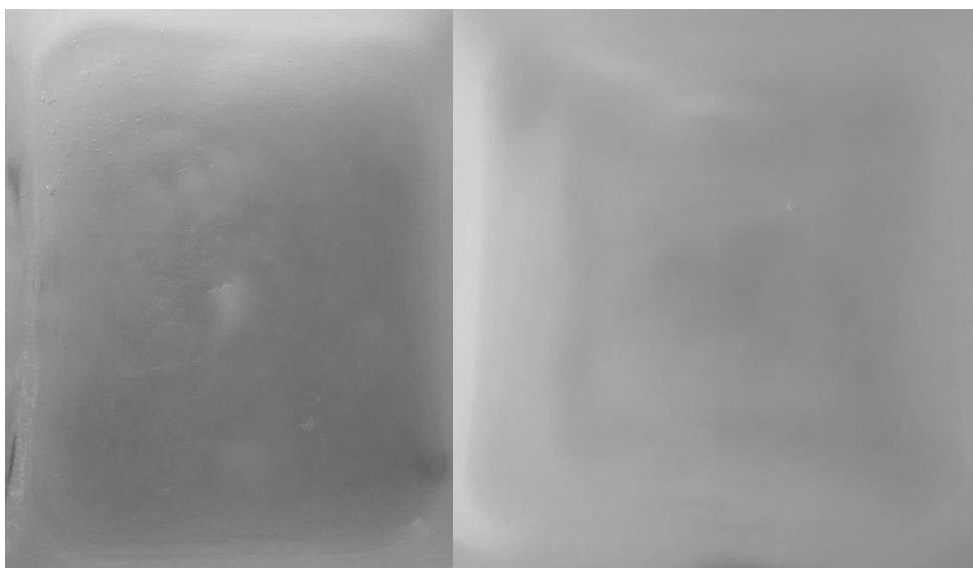


Figure 3-36 MUG (left) and MUDG (right) compounds at room temperature

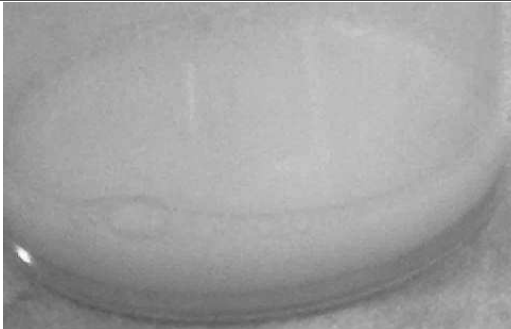





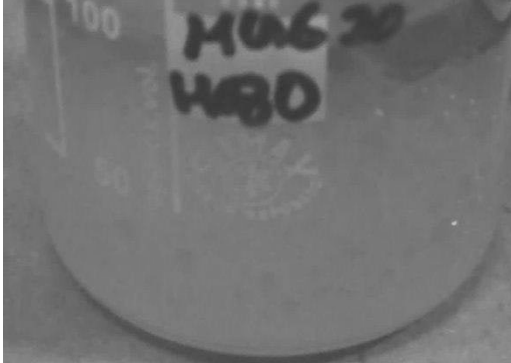
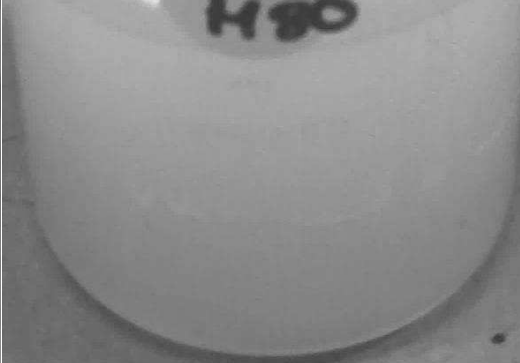

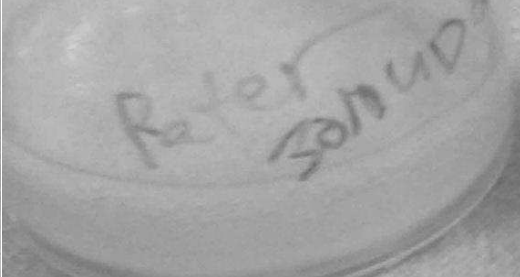
MUG and MUDG are amphiphilic compounds, meaning they have a hydrophilic head and hydrophobic tail (thus attracted to bitumen), and that they can in theory, form a barrier between the asphalt and the surface that the agent is protecting. Based on the testing of MUG and MUDG by the providers, this barrier would have good water retention properties.

The base formulations were mixed with water at different proportions due to i) the water retaining ability of the formulations and ii) economic considerations as water is far less expensive than the formulations. In theory, they would form the surfactant barrier shown in Figure 3-33.

The MUG compound was far more viscous than MUDG and could not be applied from a spray-bottle without being mixed with water, whereas MUDG could. The compounds were mixed with water in a beaker with a magnetic stirrer for 6 h at 600 rpm while covered airtight. The MUG and MUDG were mixed with at 5, 10, 15, 30, 50%w. MUDG was tested by itself as well. While the mixes of MUDG and water appeared to be stable, the mixes with MUG and water tended to separate (Table 3-27) and needed agitation before use as ARAs, which consisted of agitating the container for 30s.

Besides water (H), acetone, ARA 1 and ARA 2 were also mixed with the compounds. They were mixed with MUG or MUDG using a magnetic stirrer for 6 h at 600 rpm. Acetone was used due to its high volatility while ARA 1 and ARA 2, being the best performing commercial ester-based ARA 1, was used to observe the combination of fluxing and surfactant properties of mixing the most potent surfactant (MUG) with a commercial ester C18 based ARA.

Table 3-27 ARA formulations featuring glycerol-based formulations mixed with water

%w of compound in H <sub>2</sub> O	MUG	MUDG
5		
10		
15		
20		
50		



### 3.6.2 Test results

The testing of ARA performance was done by the asphalt slide test. The testing of the damage to asphalt of the ARAs consisted of the indirect-tensile strength and bitumen degradation testing of bitumen as well as PVC and rubber, two common materials in asphalt construction. The bitumen degradation test also served as a test to find the most effective bitumen remover. The effects of the best performing BRs on PVC and rubber were also tested.

#### 3.6.2.1 Degradation by bio-sourced formulations

##### 3.6.2.1.1 Degradation of bitumen by bio-sourced formulations

The bitumen degradation test was performed on all of the compounds described in Table 3-3 with four tests per formulation. Additionally, the MUG compound was tested after being mixed at concentrations of:

- 20% and 50% with water marked MUG 20 H 80 and MUG 50 H 50 respectively;
- 50% with acetone (MUG 50 A 50),
- 50% with ARA1 (MUG 50 ARA1 50),
- 50% with ARA2 (MUG 50 ARA2 50).

The MUDG compound was tested after being mixed at 20% (MUDG 20 H 80), 50% (MUDG 50 H 50) with water, with one or two tests per formulation.

The results of the testing on the bio-based formulation can be found in Table 3-28. The results show that the short chain esters C7 and RD6 degrade the bitumen the most effectively at 90-95%. The C18 ester based RD5 also shows a high degradation at around 50%. The other formulations show relatively low degradations of 8, 4 and 21% for RD1, RD2 and RD7, respectively. The petroleum-based lubricant RD4 appears to be adsorbed into the bitumen sample significantly, increasing the weight of the sample by 13% on average.

Table 3-28 Bitumen Degradation Test results for bio-sourced candidate formulations

Formulation	% Bitumen degradation	CVAR%	Formulation	% Bitumen degradation	CVAR%
C7	94.4	4.1	MUG 20 H 80	-3.2**	-
RD1	7.8	7.5	MUG 50 H 50	-4.3**	7.2
RD2	4.1	12.4	MUDG 20 H 80	-4.1**	-
RD4	-12.6**	12.5	MUDG 50 H 50	-3.6**	-
RD5	49.2	0.9	MUG 50 A 50	-2.8**	0.9
RD6	89.3	4.6	MUG 50 ARA1 50	3.5	-
RD7	20.8	8.3	MUG 50 ARA2 50	-21.7***	6.0
H <sub>2</sub> O	-1.1**	-	Acetone	-0.7**	-

\*Only single test conducted; \*\*Bitumen sample gained mass; \*\*\*Liquid appears coagulated as shown in Figure 3-38; H=water; A=acetone

The formulations of MUG and MUDG with water do not degrade the bitumen and even appear to be somewhat adsorbed into the bitumen judging from that their BD% values are lower than for water. This is also the case with the mixture of MUG and acetone, their BD% being slightly lower than for acetone at -2.79%.

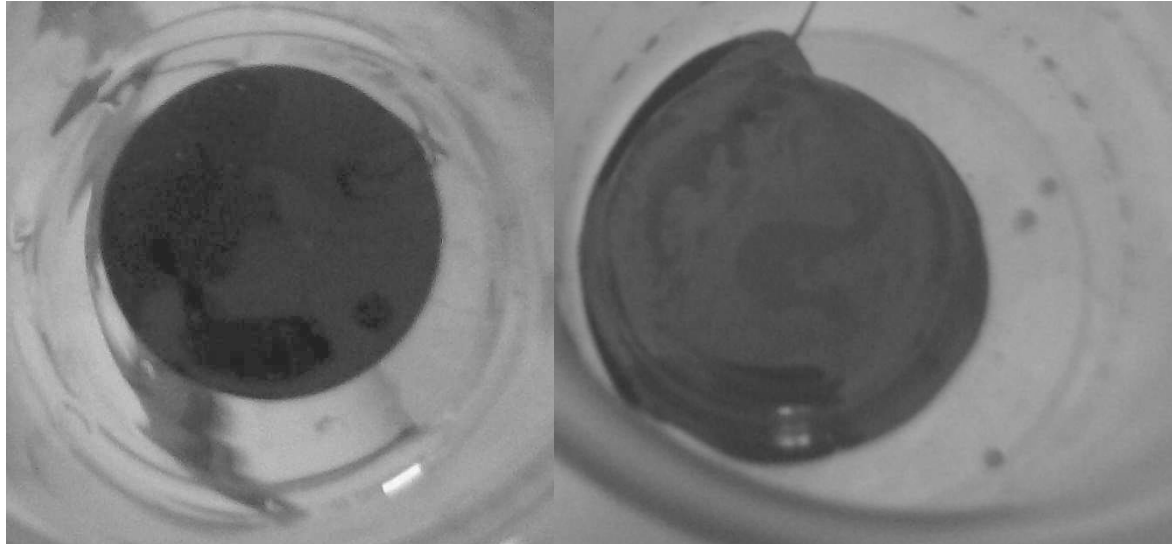


Figure 3-37 BDT sample showing i) no degradation of bitumen after 1d exposure to water (left) and ii) sample deformation after 1d exposure to acetone (right)

As for the mixtures with MUG and commercial ARAs, the mixture with MUG and ARA1 degrades the bitumen slightly (3.5%), but much less significantly than for ARA 1 by itself (29%). The mixture of MUG and ARA2 appeared to degrade the bitumen and then coagulate at the bottom of the sample. This coagulation led to the increase of the mass of the sample and the final result was not indicative of the test (Figure 3-38).



Figure 3-38 BDT sample showing bitumen after 1d exposure to MUG 50 ARA2 50; the bitumen has been degraded by the solution and the solution has coagulated

The RD samples were also tested up to 7 days as shown in Figure 3-39. The results showed continued degradation after one day, particularly for RD5. RD4 sample continued to be adsorbed into the bitumen sample after 1 day.

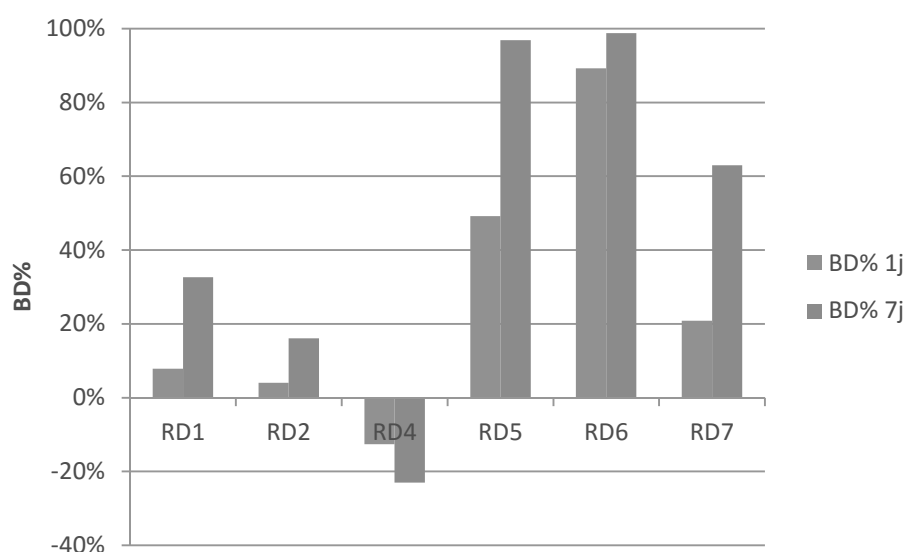


Figure 3-39 Bitumen degradation test results of RD formulations at 1 and 7 days

#### 3.6.2.1.2 Degradation of PVC and tire rubber by bio-sourced formulations

For this test, the two most promising BR candidate formulations (C7 and RD 6 as found by the BDT) were tested, along with the two most effective commercial BRs per BDT (BR 4 and BR 5). The analysis of the agents by FTIR-ATR after the test found that neither the commercial BRs nor the short-chained esters degraded the PVC or rubber, as the FTIR-ATR formulations were the same for both the agents by themselves and the solutions after the test.

#### 3.6.2.2 Bio-sourced formulations performance as ARAs by Asphalt Slide Test

The asphalt slide test was performed on RD 1, RD 2, RD 4, RD 7, along with formulations of MUG (at concentrations of 5-50%w in water) and MUG (at concentrations of 5-100% in water). RD 1, RD 2, RD 4, RD 7 were for AST particularly due to their relatively low degradation of bitumen in BDT, qualifying them as potential ARAs based on damage to asphalt, as it was assumed that the products that degrade significantly in BDT would not be appropriate as ARAs.

The plates after the AST are shown in Table 3-29 while the results are shown in Table 3-32.

From the images of the plates after the test, it is visible that the formulations RD 1, RD 2 and RD 7 function in a similar way to the ester-based agents discussed in Section 3.5, notably ARA 1 and ARA 2. The performance of the RD 1 and RD 2 agents can be characterized by a lower residual mass than ARA 1 and ARA 2 at around 5 g/m<sup>2</sup>. RD 1 had a comparable time to beginning of slide to the ester based ARAs at 9s while RD 2 was much higher at 50s. RD 7 had somewhat higher residual mass of

7.43 g/m<sup>2</sup>, corresponding to a higher bitumen degradation ratio (Table 3-28) while having a time to beginning of slide similar to RD 1 at 12s.

RD 4 was a particular case as it did not degrade the bitumen in BDT. However, it appears the plate is covered with bitumen residue (4.39 g/m<sup>2</sup>), which shows that: i) RD 4 despite being adsorbed by the bitumen sample, does somewhat degrade the bitumen and ii) unlike ARA 4, RD 4 does not create a barrier between the asphalt and the plate.

Table 3-29 Images of plates after Asphalt Slide Test for RD 1, RD 2, RD 4 and RD 7

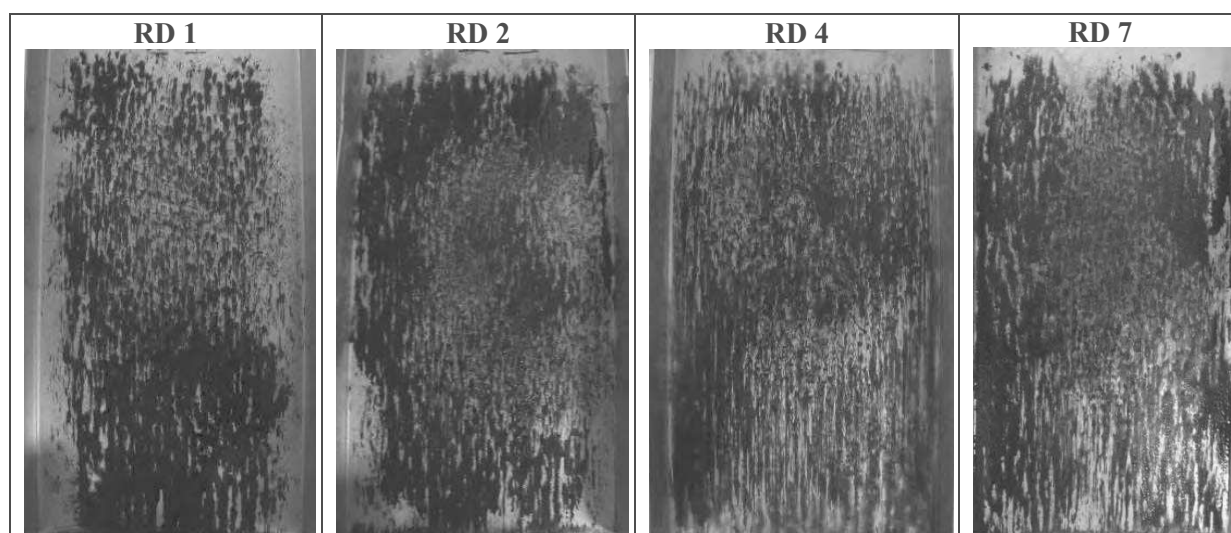


Table 3-30 Results of Asphalt Slide Test for RD 1, RD 2, RD 4 and RD 7

Candidate formulation	Residual mass (g/m <sup>2</sup> )	<i>STDDEV</i> $\sigma$	Time to beginning of slide (s)	<i>STDDEV</i> $\sigma$
RD 1	5.25	—*	9	—*
RD 2	5.50	0.13	51	25
RD 4	4.39	0.81	18	10
RD 7	7.43	0.95	12	13

\*Only single test conducted

The MUG compound was mixed with water at additions of 5, 10, 15, 20, 30 and 50% to be tested in AST. The MUG was also mixed with acetone at 10% in order to observe the effects of MUG mixed with a highly volatile compound. Additionally, it was mixed with ARA 1 in order to observe the effects of MUG, mixed with an organic C18 ester, in terms of whether there would be combined effects as with the BDT. ARA 2 was not used in this capacity due to its coagulation effects when mixed with MUG (Figure 3-38).

The images of the plate for the MUG compound are shown in Table 3-31 while the results are presented in Table 3-32. For the formulations with water, the MUG was able to create a barrier

between the plate and the asphalt – as with the barrier forming ARA 4 and like-products described in Section 3.5 – except for in the case of MUG 5 H 95, where the MUG was too diluted, and so was not able to form a barrier between the bitumen and the plate. While having longer times to beginning of slide (15-325s) than the C18 ester based ARAs, the MUG compositions had much lower residual masses (0.08-1.41 g/m<sup>2</sup>).

It should be noted that the residual mass increased as the proportion of MUG increased, while the time to beginning of slide decreased. As discussed in the previous section, the residual mass of surfactant ARAs is actually a useful property as it allows longer times before an ARA would need to be re-applied to a surface. In terms of optimization of the formulations, MUG 20 H 80 had the lowest time to beginning of slide while having the 2<sup>nd</sup> highest time to beginning of slide (15.7s) among the MUG formulations.

For MUG 10 A 90, the formulation evaporated too quickly for the agent to act as a barrier, functioning similarly to RD 4 and lightly degrading the bitumen it was in contact with. The residual mass was lower than for RD 4 however (2.22 g/m<sup>2</sup>) and the time to beginning of slide was 16.5s, similar to RD 4.

MUG 50 ARA1 50 showed performance characteristic of both agents in the mixture. The residual mass was lower than for ARA 1 (4.83 g/m<sup>2</sup>), while the time to beginning of slide was lower than for MUG 50 H 50 (11.3s).

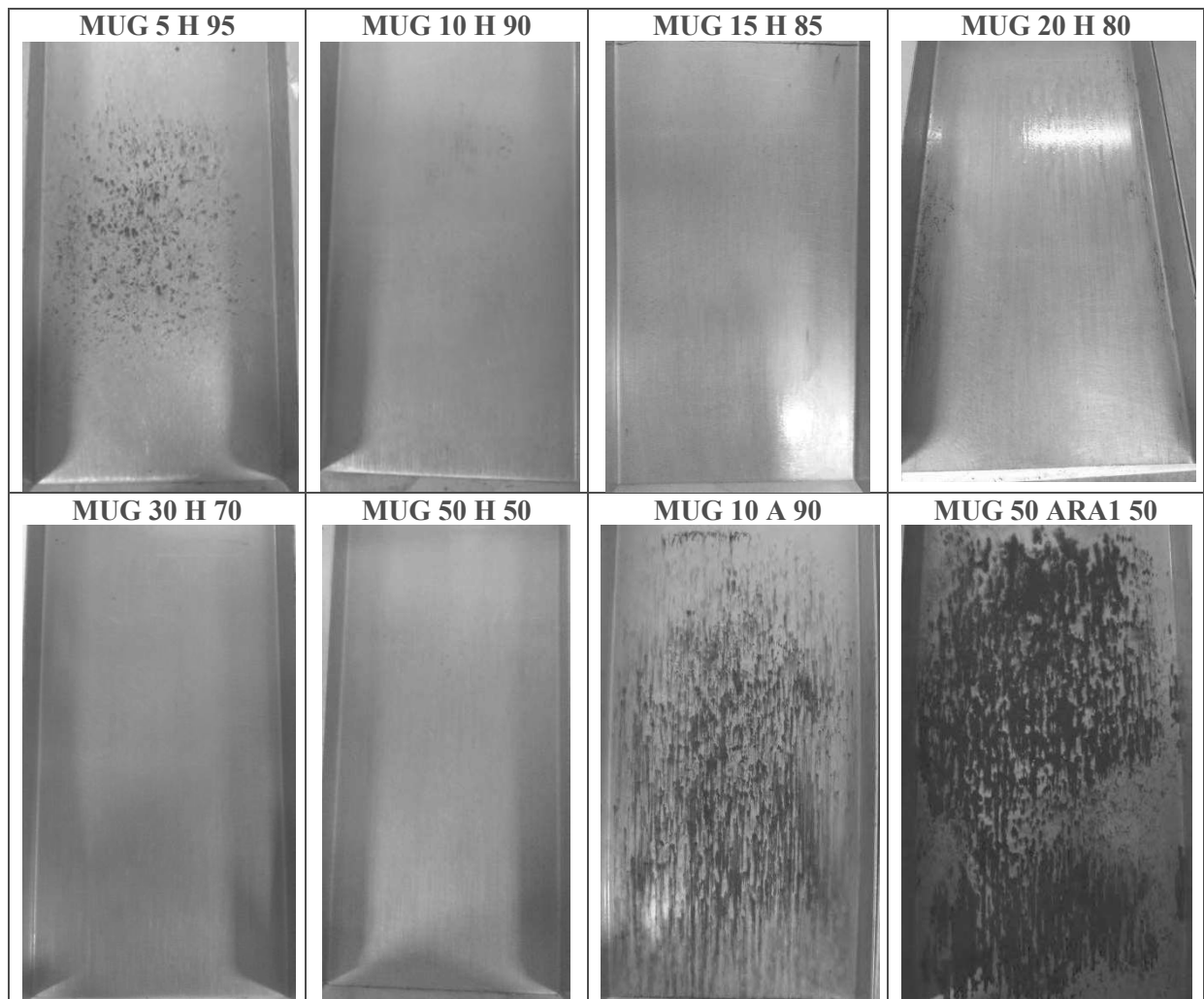
The MUDG compound was more liquid than MUG, and there by produced more liquid formulations. While this produced formulations that spread on the plate more easily, they were also more likely to evaporate. As with the MUG formulations, MUDG functioned as a surfactant, with the residual mass increasing as the proportion of MUG increased, while the time to beginning of slide decreasing.

For MUDG 5 H 95, the formulation mostly evaporated from the hot asphalt, and the asphalt stuck to the plate after inclination, as for a test without any agent.

This was also an issue with MUDG 10 H 90 agent MUDG 15 H 85 where part of the bitumen penetrated the agent to leave some residue on the plate, as with MUG 5 H 95. This small amount of bitumen residue was also associated with high time to beginning of slide.

In general, the MUDG molecule with the same proportion of water, functioned as a diluted MUG formulation with a lower residual mass (0.07-0.61 g/m<sup>2</sup>) and a higher time to beginning of slide (24-535s). The MUDG 50 H 50 had the lowest time to beginning of slide at 24s.

Table 3-31 Images of plates after Asphalt Slide Test for MUG-based formulations



H=water; A=acetone

Table 3-32 Results of Asphalt Slide Test for MUG-based formulations

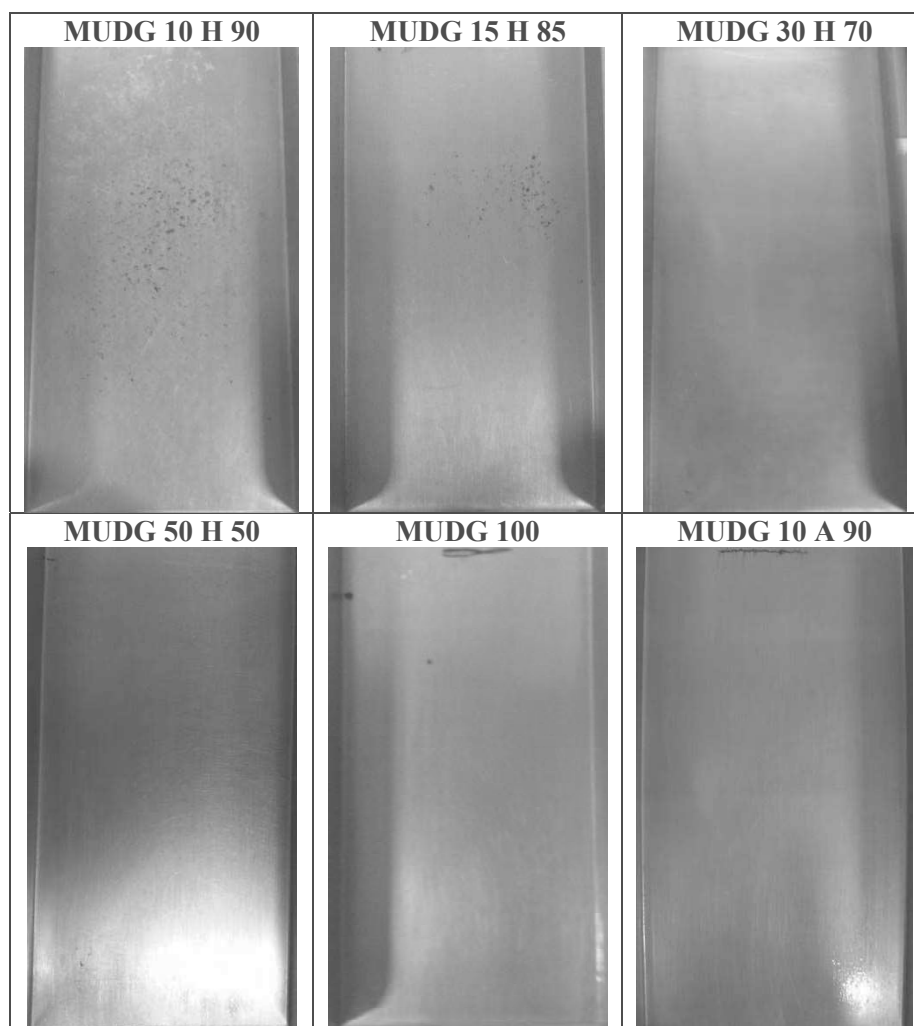
Candidate formulation	Residual mass (g/m <sup>2</sup> )	<i>STDDEV</i> $\sigma$	Time to beginning of slide (s)	<i>STDDEV</i> $\sigma$
<b>MUG 5 H 95</b>	0.08	0.07	325	64
<b>MUG 10 H 90</b>	0.12	0.07	73	23
<b>MUG 15 H 85</b>	0.57	0.26	30	31
<b>MUG 20 H 80</b>	0.86	0.15	16	4
<b>MUG 30 H 70</b>	0.86	0.24	51	26
<b>MUG 50 H 50</b>	1.41	0.15	25	2
<b>MUG 10 A 90</b>	2.22	0.19	17	18
<b>MUG 50 ARA1 50</b>	4.83	0.17	11	9

H=water; A=acetone

MUDG 10 H 90 gave an interesting performance result as it was able to perform better in time to beginning of slide than any of the MUDG-water formulations (11s). Unlike MUG 10 H 90, the

formulation was able to create a barrier between the plate and the asphalt that did not degrade the bitumen, qualifying it as a surfactant.

Table 3-33 Images of plates after Asphalt Slide Test for MUDG-based formulations



H=water; A=acetone

Table 3-34 Results of Asphalt Slide Test for MUDG-based formulations

Candidate formulation	Residual mass (g/m <sup>2</sup> )	<i>STDDEV</i> $\sigma$	Time to beginning of slide (s)	<i>STDDEV</i> $\sigma$
<b>MUDG 5 H 95</b>	DID NOT MOVE			
<b>MUDG 10 H 90</b>	0.07	0.05	535	162
<b>MUDG 15 H 85</b>	0.08	0.03	458	380
<b>MUDG 20 H 80</b>	0.10	0.10	260	184
<b>MUDG 30 H 70</b>	0.17	0.06	240	16
<b>MUDG 50 H 50</b>	0.61	0.09	24	16
<b>MUDG 100</b>	1.78	0.08	59	7
<b>MUDG 10 A 90</b>	0.64	0.00	11	1

H=water; A=acetone

Despite acetone being more volatile than water, the residual mass on the plate for MUDG 10 A 90 was higher (0.61 g/m<sup>2</sup>) than for the same content of MUDG with water. These are indications that there is a particular interaction between MUDG and acetone that does not occur with MUDG and water.

### 3.6.2.3 Bio-sourced formulation interaction with bitumen by FTIR-ATR

The FTIR-ATR analysis was conducted on all of the formulations described in Table 3-3 as well as their BDT solutions. Similar to the C18 ester peaks the candidate formulations C7, RD 1, RD 2, RD 5, RD 6, RD 7 large peak at around 1740 cm<sup>-1</sup> corresponding to C=O stretching as well as 3-4 strong peaks at 1100-1285 cm<sup>-1</sup> possibly corresponding to C-O stretching (Nakanishi, 1962) (Figure 3-40). RD 4 – being a petroleum-sourced lubricant – did not show the previously mentioned signatures in its spectra.

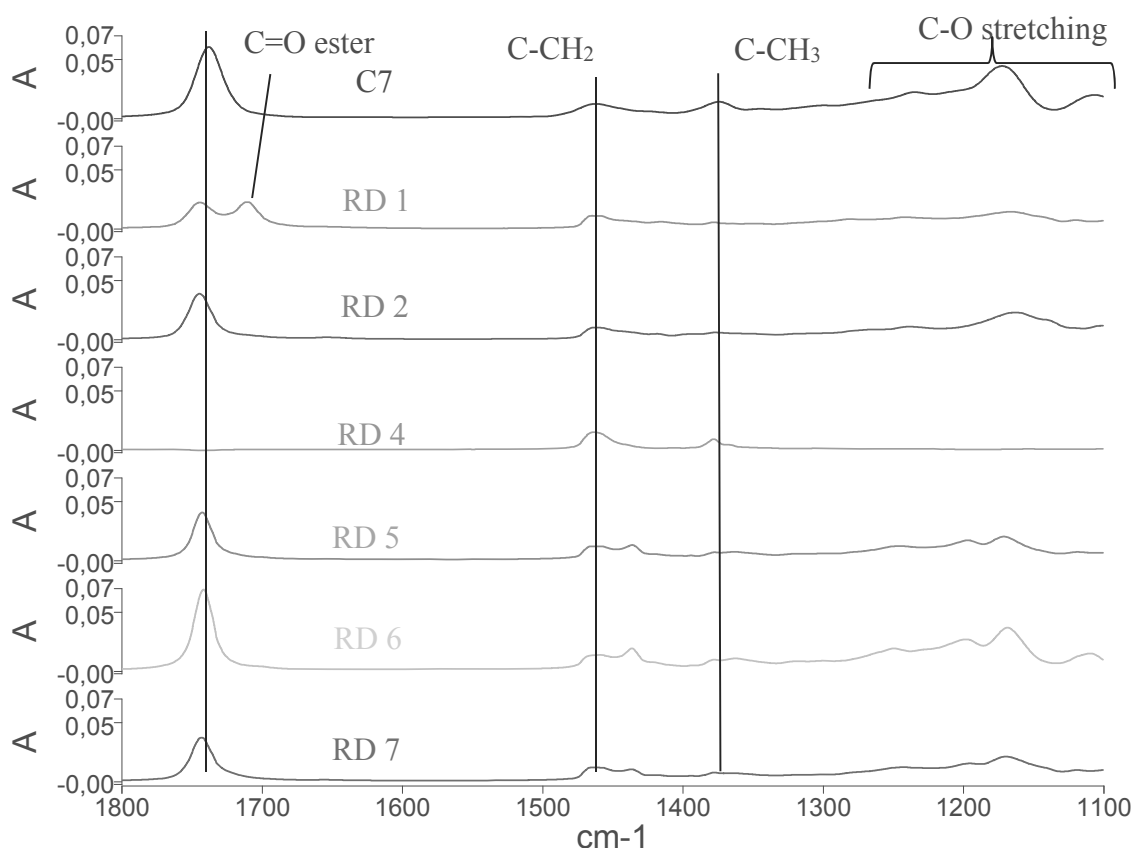


Figure 3-40 FTIR-ATR spectra (1800-1100 cm<sup>-1</sup>) for candidate ARA and BR formulations: C7, RD 1, RD 2, RD 4, RD 5, RD 6, RD 7

The spectra for the formulations C7, RD 1, RD 2, RD 4, RD 5, RD 6, RD 7 showed peaks corresponding to CH<sub>3</sub> aliphatic stretches at 2950 and 2850 cm<sup>-1</sup>; CH<sub>2</sub> aliphatic stretch at 2920 cm<sup>-1</sup>; C-CH<sub>2</sub> carbonyl stretch 1460 cm<sup>-1</sup> and C-CH<sub>3</sub> carbonyl stretch at 1376 cm<sup>-1</sup> (Woods et al., 2004; Yao et al., 2013) (Figure 3-40 and Figure 3-41), something that was found for both the C18 ester base commercial agents as well as the commercial diesel in Section 3.5.1.2.



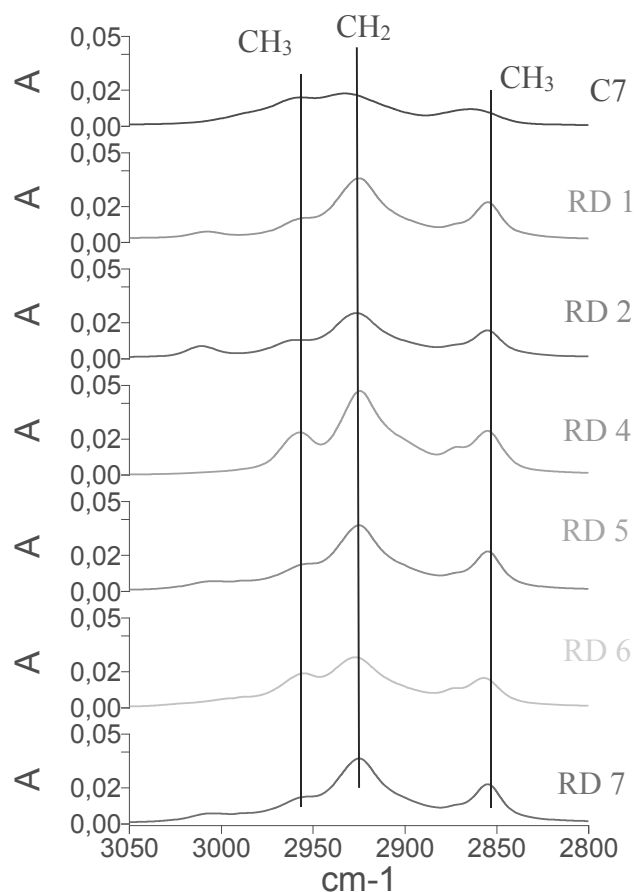


Figure 3-41 FTIR-ATR spectra (3050-2800  $\text{cm}^{-1}$ ) for candidate ARA and BR formulations: C7, RD 1, RD 2, RD 4, RD 5, RD 6, RD 7

In terms of signatures of bitumen degradation, the aromatic C=C peak around  $1600\text{ cm}^{-1}$  was again (as in Section 3.5.1.2) found for agents C7, RD 5, RD 6 and RD 7, which degraded the bitumen at elevated levels (21-94% for BDT, Figure 3-42). The BDT solutions for the agents RD 1 and RD 2, which degraded the bitumen less (4-8% for BDT), did not have the  $1600\text{ cm}^{-1}$  signature.

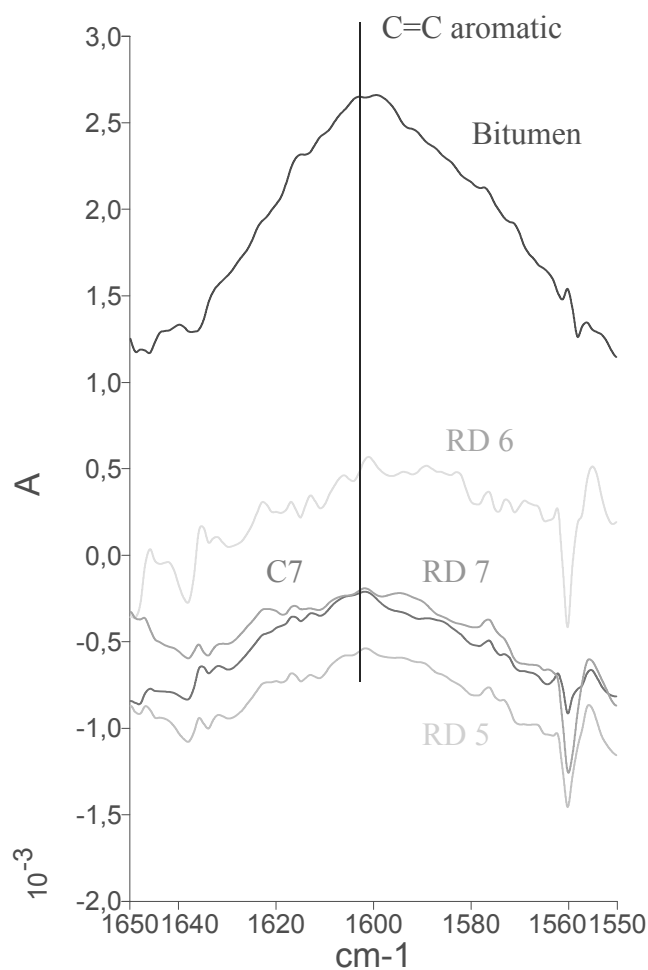


Figure 3-42 FTIR-ATR spectra around the peak at  $1600\text{ cm}^{-1}$  for candidate ARA and BR (C7, RD 5, RD 6, RD 7) BDT solutions compared to bitumen

The spectra for RD 4 found that its composition is similar to bitumen with corresponding aliphatic peaks (Figure 3-43). The spectra of the RD 4 BDT solution confirmed as with the BDT result that RD 4 does not degrade bitumen, but is on the contrary, adsorbed by it.

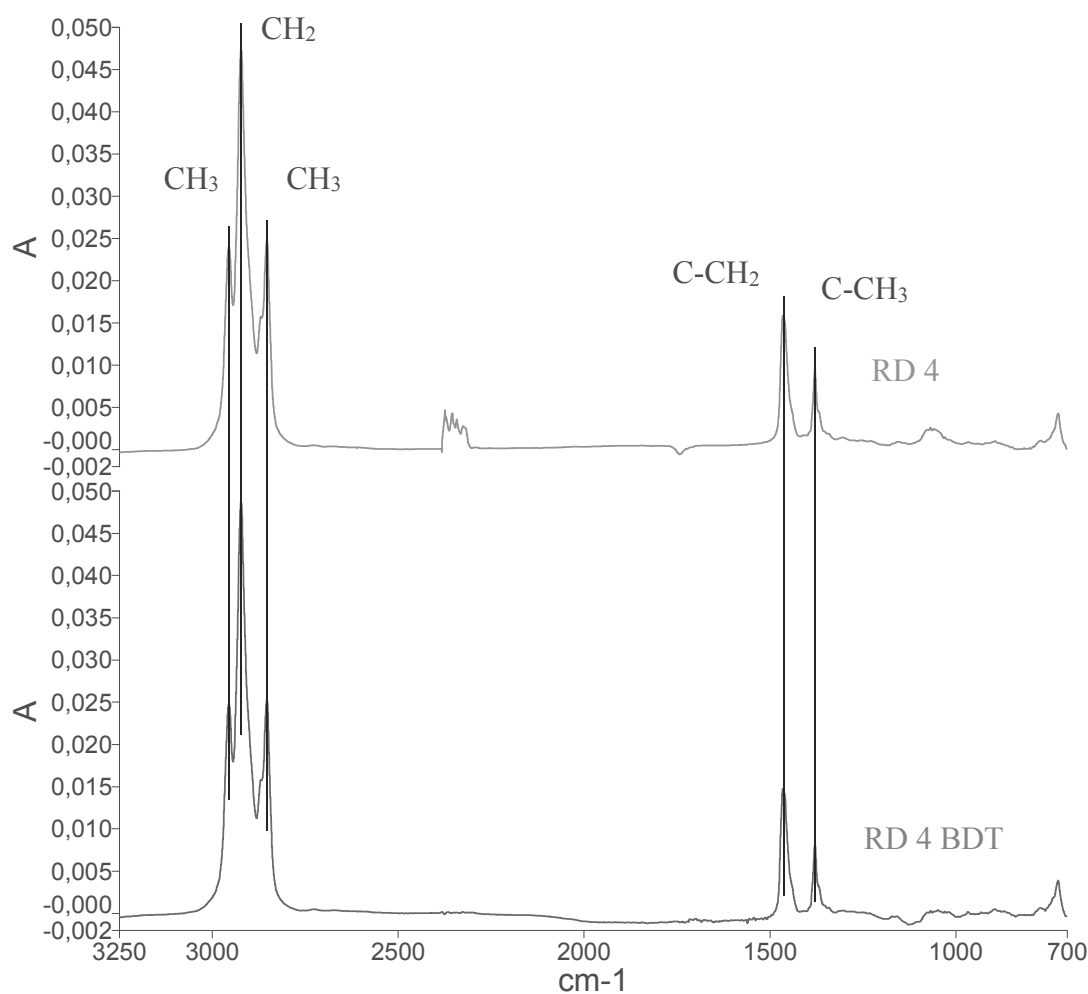


Figure 3-43 FTIR-ATR spectra (3250-700  $\text{cm}^{-1}$ ) for RD 4 (red) and RD 4 BDT solution (blue); the small peak around 2350  $\text{cm}^{-1}$  is carbon dioxide from the air and is not part of the sample

The MUG and MUDG compounds were tested in FTIR-ATR analysis as pure, and after being mixed at 20% in water (MUG 20 H 80 due to promising performance in AST of this formulation and MUDG 20 H 80 for comparison). The MUG 20 H 80 and MUDG 20 H 80 BDT solutions were analyzed in FTIR-ATR as well, the full results can be found in Appendix D.

The FTIR-ATR analysis of the MUG 20 H 80 and MUDG 20 H 80 formulations (Figure 3-44) found heavy indications of water as can be expected (due to both formulations being over 80% water) with a broad peak around 3450  $\text{cm}^{-1}$  corresponding to O-H stretching and a peak around 1640  $\text{cm}^{-1}$  corresponding to the H-O-H scissors (Mojet et al., 2010). The FTIR signatures of the two formulations were identical, likely due to the overwhelming presence of water. The BDT solution confirms the BDT result that the MUG and MUDG formulations did not degrade the bitumen but were adsorbed by it, with the formulations and their BDT solutions showing no difference except for a peak around 1060  $\text{cm}^{-1}$  that is present in the MUG 20 H 80 and MUDG 20 H 80 formulations, but not the BDT solution.

This peak possible corresponds to C-O stretching (Nakanishi, 1962) and could be an indication of some part of the formulations being adsorbed by the bitumen as with ARA 4 (Figure 3-30).

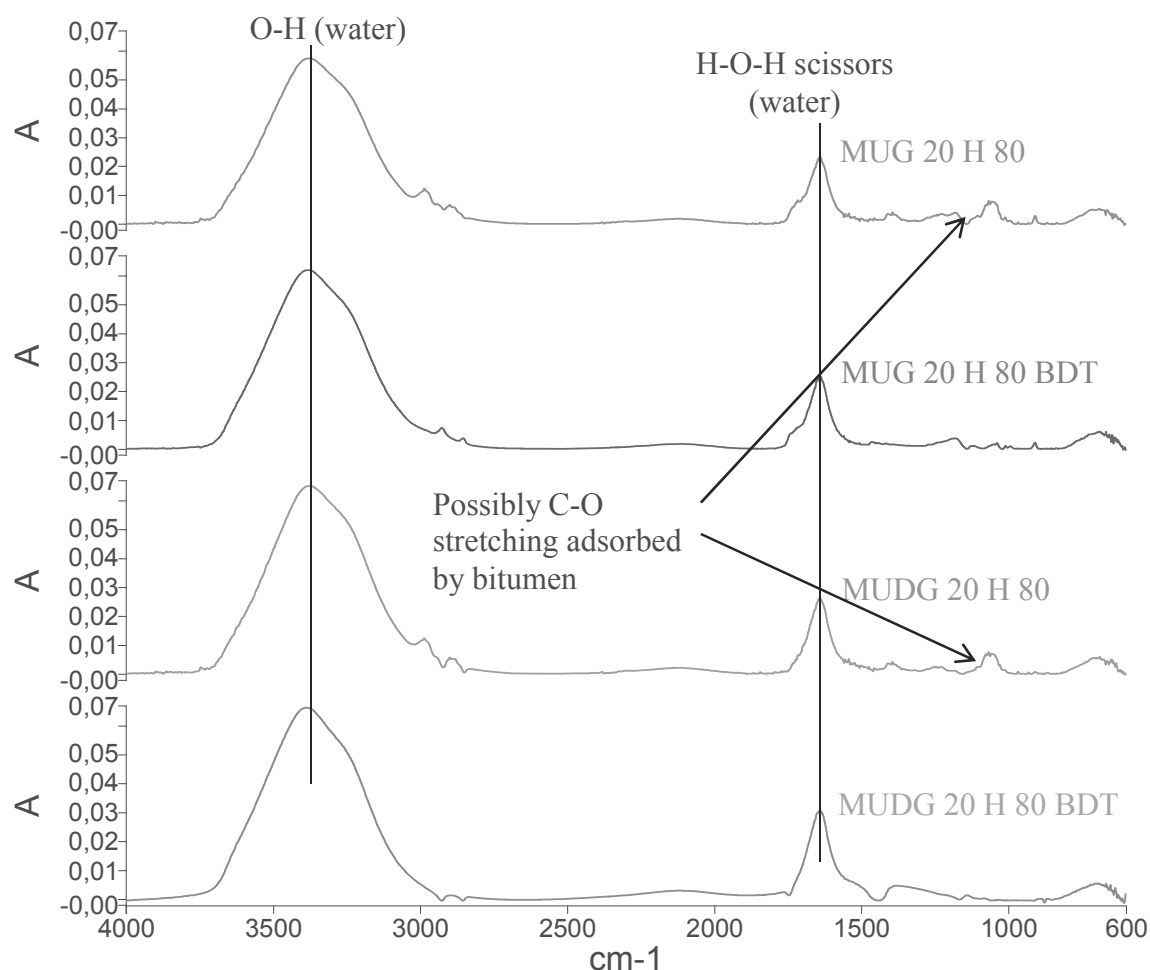


Figure 3-44 FTIR-ATR spectra MUG 20 H 80 (red), MUG 20 H 80 BDT solution (blue), MUDG 20 H 80 (pink) and MUDG 20 H 80 BDT solution (green)

In order to determine if the bitumen was modified, an FTIR-ATR analysis was conducted on the samples after the BDT test of MUG 20 H 80 and MUDG 20 H 80 (Figure 3-45). The spectra for the BDT bitumen samples were modified relative to the bitumen by itself. The presence of water and possible C-O stretching around  $1060\text{ cm}^{-1}$  described previously are present in the bitumen samples. The peaks are more significant for MUDG 20 H 80 BDT bitumen sample, likely due to the fact that MUDG is less viscous than MUG, and is thereby more easily adsorbed by the bitumen.

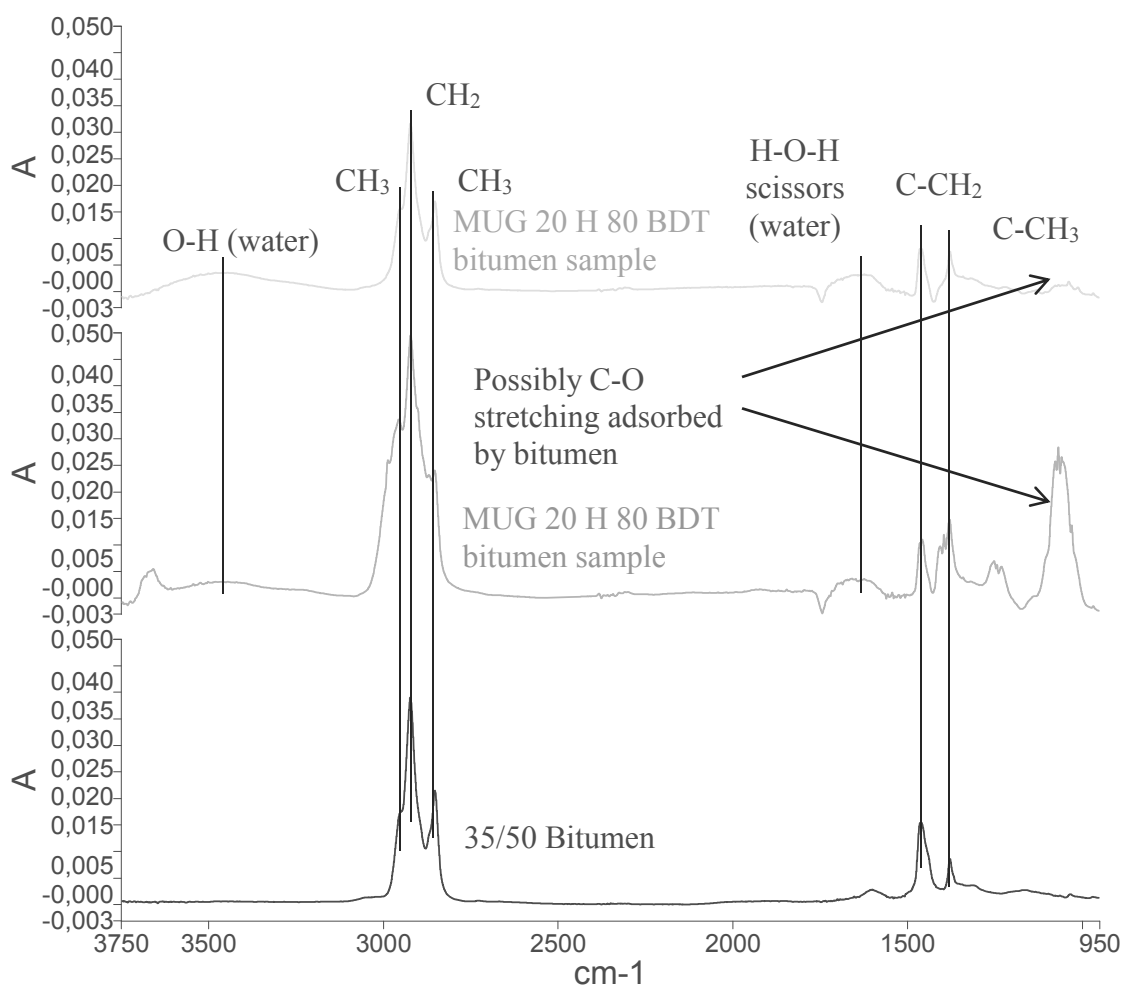


Figure 3-45 FTIR-ATR spectra (3750-950  $\text{cm}^{-1}$ ) MUG 20 H 80 BDT bitumen sample (green), MUDG 20 H 80 BDT bitumen sample (pink) and 35/50 bitumen (black)

### 3.6.2.4 Reduction in resistance in ITS of Asphalt in contact with ARAs

ITS testing was conducted on the MUG 20 H 80 formulation, due to its superior performance in the AST compared to the other MUG and MUDG based formulations. The RR% was found to be 21.2% for the two samples tested with a standard deviation of 3.16%, making it more damaging to asphalt than ARA 4, the same as ARA 2 (Table 3-35).

Table 3-35 Resistance Reduction for ITS Testing (MUG 20 H 80)

Product	% Resistance reduction	STDDEV $\sigma$
ARA 2	21.81	1.62
ARA 4	11.28	1.47
MUG 20 H 80	21.2	3.16

### 3.6.3 Discussion on the development of bio-sourced formulations

#### 3.6.3.1 Evaluation and development of bio-sourced formulations as ARAs

As with the commercial C18 based ARAs, the C18 based formulation RD 1, RD 2 and RD 7 functioned by softening the bitumen in contact with the steel plate in AST. Out of the RD formulations determined by BDT to be suitable for use as ARAs, RD 1 appeared to be the most promising. This could be related to RD 1 having a higher proportion of C18 molecules (Table 3-4).

For RD 4, despite the mineral oil not degrading the bitumen sample in BDT, it is clear that the oil is adsorbed by the bitumen. From the performance on the plate, it is clear that the agent softens the bitumen to a certain degree (Table 3-29). Due to the fact that the time to beginning of slide is significantly higher than for the C18 based agents, RD 4 is not a candidate as an ARA.

Formulations based on MUG and MUDG were found to function as substrate surfactants in their performance as ARAs. The residual mass from the asphalt slide testing for the MUG and MUDG formulations with water did not contain bitumen residue, with the exception of MUG 5 H 95, MUDG 5 H 95 MUDG 10 H 90 and MUDG 15 H 85, which had a content of active product too low to create barrier between the asphalt and the plate.

The MUG was a more viscous (dynamic viscosity of 1 Pa\*s for MUG compared to 13 Pa\*s for MUDG), and so was more effective at lower concentrations. Additionally, MUG had a higher evaporation temperature before being mixed with water, indicating that the MUDG could have had a tendency to evaporate from the contact with the hot asphalt, especially with high proportions of water. The fact that MUG-water formulations functioned as surfactants had higher residual mass and lower time to beginning of slide durations made them superior performing ARAs to MUDG-water formulations.

Theoretically, the surfactant containing formulations would create the barrier, where the hydrophilic heads of the formulations retaining the water in the middle, while the hydrophobic tails are partially adsorbed by the lipophilic bitumen. Nevertheless, this hypothesis is limited in its representation of the complexity and water retention mechanisms of the MUG formulations. The work of Boussambe (2015) found that the water retention by the MUG compound is actually much more complex and involves a series of vesicles aggregates or gels, which can carry high amount of water molecules. The MUG-water formulations were also found to have a low contact angle with the steel at  $<140^\circ$ , indicating good wettability, while also having superhydrophilic characteristics (Valentin and Mouloungui, 2013).

Additionally, MUDG was more adsorbed by the bitumen as shown by the BDT with -4% for MUDG 20 H 80 compared to -3% for MUG 20 H 80 test and the FTIR-ATR analysis of the bitumen samples after the BDT test. This resulted in less MUDG being available to form a barrier relative to MUG.

In terms of comparing the MUG and MUDG formulations with commercial agents, the only comparison from this study is ARA 4 (the commercial substrate agent), which functions in the same way as MUG and MUDG, that is, as a barrier. A comparison of AST performance characteristics of MUG and MUDG formulations with water relative to the commercial substrate is shown in Figure 3-46 and Figure 3-47. A higher residual mass for substrate ARAs are preferable, due to the economic advantage of being able to go a longer time before having to re-apply the agent. The residual mass for ARA 4 of 0.44 g/m<sup>2</sup> corresponds to a similar residual mass for MUG concentrated at 10-15% in water and MUDG concentrated at 30-50% in water. For time to beginning of slide, ARA 4 is comparable to MUG at 5% in water and MUDG at 30-50% in water. It should be noted as well that the results for the time to beginning of slide have higher standard deviations than residual mass and that the residual mass is the more important and consistent indicator of ARA performance.

When looking at the performance characteristics of MUG 20 H 80, it performs better than the commercial substrate in AST with a residual mass and lower time to beginning of slide, as is the case for all MUG-water formulations where MUG is dosed above 15%. However, the commercial substrate ARA is less degrading in AST than MUG 20 H 80, which corresponds to MUG 20 H 80 being more adsorbed by the bitumen in BDT compared to ARA 4.

MUG and MUDG were mixed with acetone at 10%. While the MUG-acetone formulation lixiviated the bitumen on the plate, the MUDG-acetone formulation performed as a substrate. Additionally, the time of beginning of slide was lower for the MUDG 10 A 90 than for the MUG-acetone formulation or any formulation of MUDG and water. These results suggest an interaction between MUDG and acetone that is markedly different from the one between MUG and acetone. Nevertheless, it should be kept in mind that acetone is far more expensive than water, and so a water based solution is still preferable.

Based on this analysis, MUG 20 H 80 was selected as the optimum formulation for an ARA from this study. The ITS sample with MUG 20 H 80 was found to be 21% less resistant than the control, a result comparable to the least damaging C18 based ARA 2, but more than for ARA 4 (11%). This difference can be explained by the BDT result and FTIR-ATR analysis, as MUG 20 H 80 (-3.2%) was more adsorbed by the bitumen than ARA 4 (-1.8%). As it is shown that ARAs adsorbed into the bitumen reduce its resistance and therefore, it is in the interests of ARA development to reduce the adsorption of the agent by bitumen. Nevertheless, MUG 20 H 80 remains a strong ARA candidate.

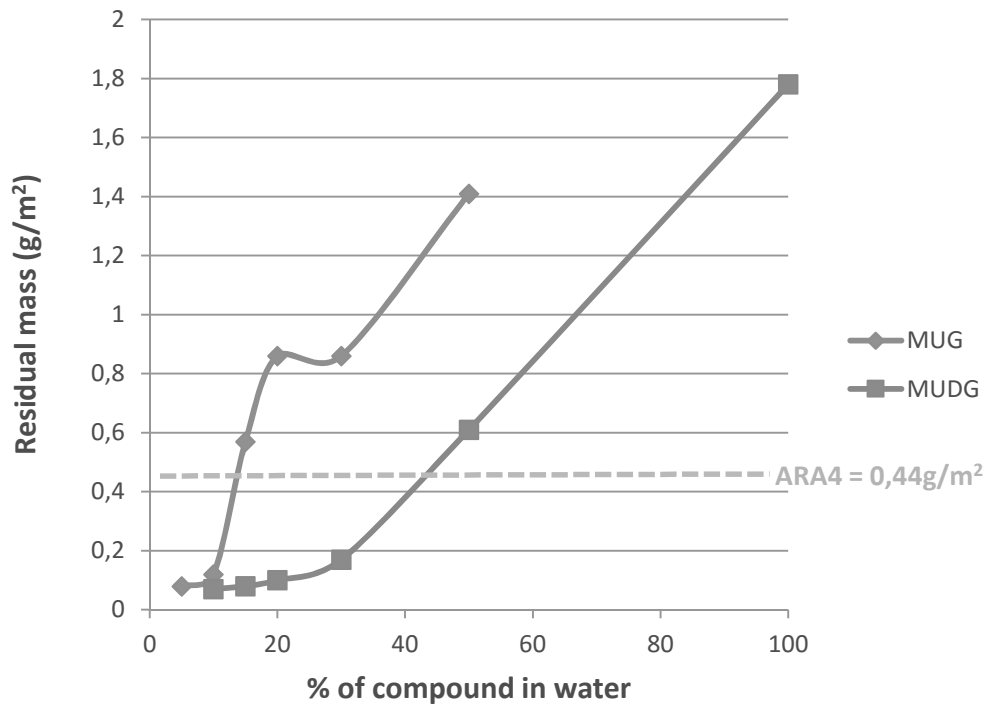


Figure 3-46 AST Performance of MUG and MUDG formulations with water in terms of residual mass compared to ARA 4

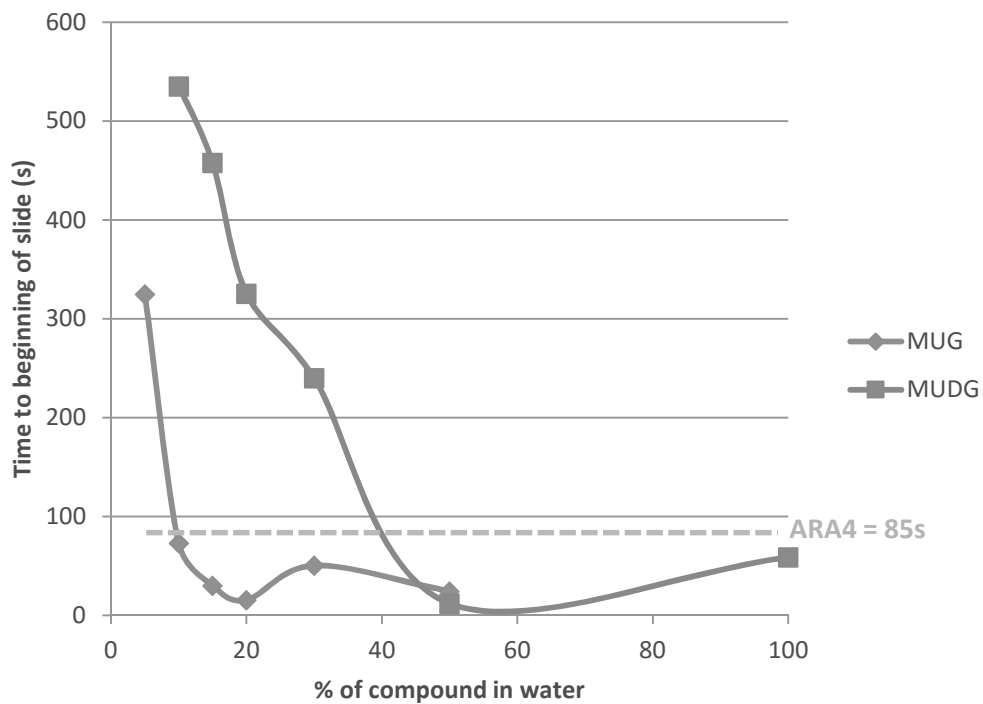


Figure 3-47 AST Performance of MUG and MUDG formulations with water in terms of time to beginning of slide compared to ARA 4



### ***3.6.3.2 Evaluation and development of bio-sourced formulations as BRs***

The BDT was used to determine the formulations that were good candidates for bitumen removers. RD 4, along with the MUG and MUDG formulation were disqualified from being BR candidates due to the agents being adsorbed by the bitumen in place of degrading it. Among the C18-based formulations tested in BDT, only RD 5, had a degradation comparable to commercial BRs at around 50%. This was due to the fact that RD 5 had the highest proportion of esters.

The highly concentrated short chained esters C7 and C8-10 degraded the bitumen far more effectively than the commercial products or diesel, both being more than 90% for the BDT, significantly more than diesel or the ester C18 based BRs. This and the result for BR 5 are strong indicators that these esters, or formulations composed around them, would serve very well as bitumen removers. C7 corresponds to a slightly higher degradation than C8-10, indicating shorter ester chains, could be even more effective, although they would likely be more volatile (Knapp, 1979).

The 1600 cm<sup>-1</sup> peak was once again found to be an indicator of bitumen degradation, as it was present in the BDT solutions of the agents that had the highest BDT loss of mass. Nevertheless, it was not proportional as the peak was not significantly larger for the very potent bitumen dissolvers C7 (94% in BDT) and RD 6 (89%) than for the agents that degraded the bitumen by a significant less amount in BDT, RD 5 (49%) and RD 7 (21%).

## **3.7 Conclusion for the determination of the performance and damage to asphalt of bio-sourced asphalt release agents and bitumen removers**

The conclusions in developing test methods for the determination of the performance and damage to asphalt of bio-sourced ARAs are as follows:

- ARA Performance
  - The asphalt slide test provides two indicators of ARA performance including mass of asphalt residue (residual mass of ARA for the barrier agents), and time for mixture to begin sliding after inclination (retention time). The residual mass for the AST has less variability and likely a more significant indicator of performance than the retention time;
  - For the AST, heating under the plate is needed for the mixture to begin sliding on the ARA-PEA;
- ARA damage to asphalt
  - The testing of asphalt mix degradation by ARAs with the CBR-loading does not produce reproducible or coherent results;

- The testing of asphalt mix degradation by ARAs with ITS produces reproducible results and is able to differentiate the damage from ARAs and BRs;
- A dosage of 1mL for the asphalt mix degradation by ARAs with ITS produced results that enabled the discrimination of agents that are intended to degrade asphalt mix and those that are not;
- Compaction of the asphalt mix by compression as opposed to proctor produces a more consistent sample in terms of density distribution for the testing of damage to asphalt;
- The reduction in resistance for asphalt mix by ITS shows a strong correlation with BDT, with the C18 based ARAs degrading the asphalt more in ITS than ARA 4, the commercial substrate agent. ARA 4 was adsorbed by the bitumen to a small degree, and the ITS indicated that it weaken the bitumen to an extent, though to a lower degree than the other ARAs;
- BR performance
  - The bitumen degradation test at 1 day is able to differentiate the damage from ARAs and BRs on bitumen with low variability, proving this to be a simple and efficient test for bitumen degradation from ARAs and BRs;
  - The most effective BRs among the C18 based agents corresponded to those that had the highest ester concentrations;
  - Short chained esters are strong candidates for use as BRs due to their high degradation performance in BDT, significantly higher than the best performing commercial BRs in this study, as well as diesel fuel;
- Chemical interactions between ARA and bitumen
  - In terms of FTIR-ATR analysis for the interaction between bitumen and C18 ester based ARAs and BRs (as found by GC analysis), the presence of a  $1600\text{cm}^{-1}$  aromatics peak in the BDT solution correlates with bitumen degradation;
  - There were two ARA modes of functioning, as a bitumen softener (diesel C18 ester based agents) and as a substrate (ARA 4);
  - Although the C18 based ARAs are the best performing ARAs in AST in terms of time to beginning of slide, the results of the AST with the agents that act as a substrate indicated that the most important criteria for this test is the nature of the residual mass. Since the use of substrate agents leaves a plate that does not contain any bitumen residue, it is hypothesized that it is a superior performing ARA.

Furthermore, since the residual mass is the agent itself, it does not need to be cleaned off, adding an economic benefit;

- The substrate agents, particularly ARA 4, are significantly less damaging to asphalt. In-field testing is needed to confirm this hypothesis;
- MUG appeared to be a more effective substrate than MUDG when the agents were used mixed with water. MUDG is more adsorbed in the bitumen than MUG when both were mixed with water. However MUDG mixed with acetone was a more effective substrate than the latter mixed with MUG.

## **4 Physico-chemical characterization of bitumen aging, rejuvenation and remobilization by rejuvenating agent**

Rejuvenating agents for asphalt are used to restore the asphalt performance properties lost during the aging of the bitumen surrounding RAP aggregates. These include viscosity, ductility and low-temperature cracking. The objective of this part of the study is to physico-chemically characterize bitumen aging and the effects of rejuvenating agents in modifying the aged bitumen. With this, three primary aspects will be studied:

- Bitumen aging – the laboratory aging of bitumen will be studied. The oxidation of the bitumen was observed by FTIR analysis. TGA was evaluated for its ability to describe bitumen aging;
- Remobilization of aged bitumen – this part of the study was focused on the identification of bitumen remobilization with respect to how far the rejuvenating agent can penetrate the aged bitumen surrounding the RAP. This method was implemented with the aid of tracers ( $\text{TiO}_2$ ) combined with SEM observations and analyses. Additionally, FTIR imaging also served this purpose;
- Rejuvenation of aged bitumen – the objective of this part is to study the chemical transformations that may take place when a rejuvenating agent is incorporated in with the RAP. This was conducted with the aid of FTIR-ATR and FTIR imaging analysis, along with TGA analysis.

The testing was conducted on both bitumen and mastic (bitumen + sand) samples, where the mastic served as a model asphalt. The rejuvenating agents tested included commercial agents and a bio-sourced agent developed specifically for this project. They were added to the bitumen and asphalt during mixing at high temperatures.

This work was completed in the context of developing a bio-sourced rejuvenating agent. First presented, will be the study of the remobilization of the bitumen using SEM-EDS – was begun but not fully realized – and is therefore in need of further development.

This will be followed by the study of the chemical mechanisms of bitumen aging and rejuvenation with FTIR spectrometry techniques. The principal tasks were to (i) adapt a method for aging bitumen and mastic in a ventilated oven, (ii) analyse the nature of bitumen oxidation globally using FTIR-ATR along with rheology and penetration results from a parallel study, and microscopically (locally) using FTIR imaging while determining the most reliable aging indicators (peaks), (iii) analyse the nature of

the rejuvenating agents and their effect on bitumen by FTIR-ATR microscopy, (iv) determine the merits of TGA in identifying bitumen aging.

#### **4.1 Bitumen remobilization by SEM-EDS analysis**

The scanning electron microscope (SEM) allows for the observations of samples using high magnification. Furthermore, the energy-dispersive X-ray spectrometry (EDS) attachment, allows for the analysis of the elemental composition of the sample.

To begin, the objectives of the testing were:

- To determine the bitumen sample preparation that is appropriate for SEM observation;
- To incorporate tracer ( $\text{TiO}_2$ ) into the bitumen at varied quantities;
- To attempt to quantify the tracer in the bitumen by image analysis and EDS;
- To observe the nature of mastic (model asphalt) with SEM and EDS.

With this, the overall objective of this part of the study is to observe the remobilization of bitumen by rejuvenating agents with SEM-EDS analysis and inert tracers. The study of the remobilization of the bitumen was begun but not fully realized. Nevertheless, some of the findings in terms of the analysis methods will be presented. This includes the analysis of bitumen with SEM/EDS in terms of the structures found in the bibliography (see Section 2.1.3.5). The analysis of tracers and sand incorporated into the bitumen will also be presented, along with some selected analysis techniques.

##### **4.1.1 Materials and methods**

###### **4.1.1.1 Materials**

Two different types of materials were fabricated, including bitumen samples: mastic (bitumen + silicious or limestone sand). The materials used are as follows:

- Bitumen 35/50;  $\rho_v = 1.03 \text{ g/cm}^3$
- Sand (for the fabrication of mastic)
  - o Silica sand 0/0.315 mm (Source: Palvadeau);  $\rho_v = 2.75 \text{ g/cm}^3$
  - o Limestone sand 0/1 mm (Source: Durruty Larronde-Ainhoa);  $\rho_v = 2.82 \text{ g/cm}^3$
- Titanium dioxide tracers ( $\text{TiO}_2$ , source: Samefor)
  - o Rutile
  - o Anatase

###### **4.1.1.1.1 Sand**

Two types of sands were used in the fabrication of bitumen mastic, silica sand and limestone sand. As for FTIR imaging, it was found preferable to sieve and wash the sand before mixing them with

bitumen. Two types of sand were used with the idea that one of the sand types would serve as the model RAP mastic (limestone), while the other would be integrated with the rejuvenating agent and new bitumen (silica), thereby serving as a type of tracer as in (El Béze, 2008).

#### 4.1.1.1.2 Tracers

The tracers were added to the bitumen as a way of tracking the rejuvenating agent as it comes into contact with the RAP binder as in (Navaro, 2011). Since the rejuvenating agents are carbon-based organics, they are difficult to distinguish from bitumen in elemental analysis (EDS), as they are also composed primarily of C. As such, tracers were added to the bitumen in order to see which ones were the most compatible and the most visible in the bitumen by EDS. Two types of traces were tested, including  $\text{TiO}_2$  in rutile and anatase form. The tracers were in the form of a white power, the properties in density and purity of the tracers are shown in Table 4-1.

Table 4-1 Properties of tracers for bitumen

Tracer	Density (g/cm <sup>3</sup> )	Purity %
<b>TiO<sub>2</sub> rutile</b>	4.23	93
<b>TiO<sub>2</sub> anatase</b>	3.97-4.79	98

#### 4.1.1.2 Fabrication of bitumen and mastic samples

The bitumen and mastic samples were prepared in the manner described in Section 4.2.1.1. When a tracer was due to be incorporated, it was heated at 160°C for at least 6 h and mixed in a 1 L pot with the aid of a Heidolph RZR mixer for 10 min on a heated plate (which maintained the temperature of the pot at 160°C).



Figure 4-1 : Préparation the samples for SEM analysis including the addition of  $\text{TiO}_2$  tracer (left) and the mixing with a Heidolph RZR mixer (right)

At the end of mixing, the bitumen was poured into trap silicone moulds having the dimensions 65-77 mm x 21-29 mm x 30 mm (Figure 4-2), and stored at ambient temperature for at least 6 h before testing. They were further demoulded and stored in a freezer at -18°C. Following storage, the samples were cut with a diamond saw and stored again at -18°C in order to minimize melting (Figure 4-3).

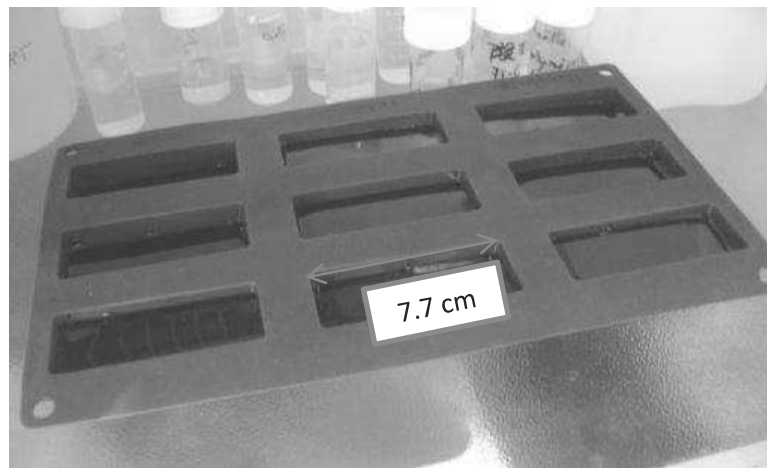


Figure 4-2 Bitumen samples stored in silicone moulds



Figure 4-3 Bitumen sample for SEM being cut with a diamond saw

#### **4.1.1.3 Bitumen observation with SEM**

The observations were performed using a Jeol JSM-6380LV SEM with an EDS attachment. The conditions of the observation were: 15 kV acceleration voltage, pressure of 60 Pa (partial vacuum), filament intensity of 78-89  $\mu$ A, size of beam at 59  $\mu$ m and a 25 mm distance from the sample. These were the normal observation conditions for the given SEM when observing cementitious materials.

In these conditions, the bitumen began to melt during the analysis, causing discrepancies in the tracer identification. In order to reduce the melting (Figure 4-4), the intensity of the filament was

lowered to 60-62  $\mu\text{A}$ , although this only had a partial effect. The images were taken in backscatter electron mode (BSE), which allowed us to visualize the contrast between elements with different atomic numbers and differentiate the densities between the phases of the sample.

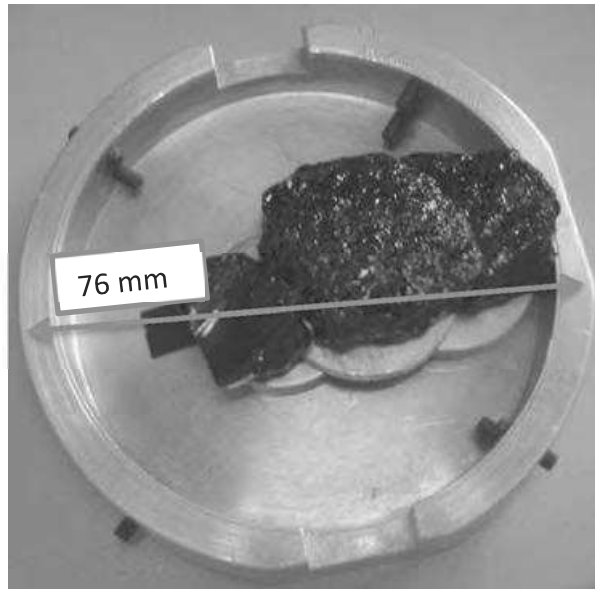


Figure 4-4 Bitumen and Ti rutile tracer sample melted by the electron beam

The elemental analysis was performed by the EDS (RONTEC XFLASH 3001), with the aid of Bruker Quantax 1.8.1 acquisition and data processing software. The electron beam of the SEM caused the fluorescence in the bitumen, resulting in the dislodging of relatively light carbon atoms and their propagation in the observation chamber. The presence of carbon in turn, has a great effect of the EDS analysis. This meant that any EDS analysis would be a comparative one, due to the interference by the carbon accumulating in the space between the EDS signal and the sample. Three EDS analysis techniques were explored including point analysis, area cartography and line scanning.

#### ***4.1.1.4 Platine Peltier effect for SEM***

The Peltier effect device for the SEM allows for the cooling of the sample inside of the SEM chamber through electrical currents and water (Figure 4-5). It has been utilized by (Durand et al., 2010b; Loeber et al., 1998; Naskar et al., 2013) in order to reduce the melting of bitumen samples. This device allowed for the cooling of the sample inside the chamber to as low as  $-20^{\circ}\text{C}$ .



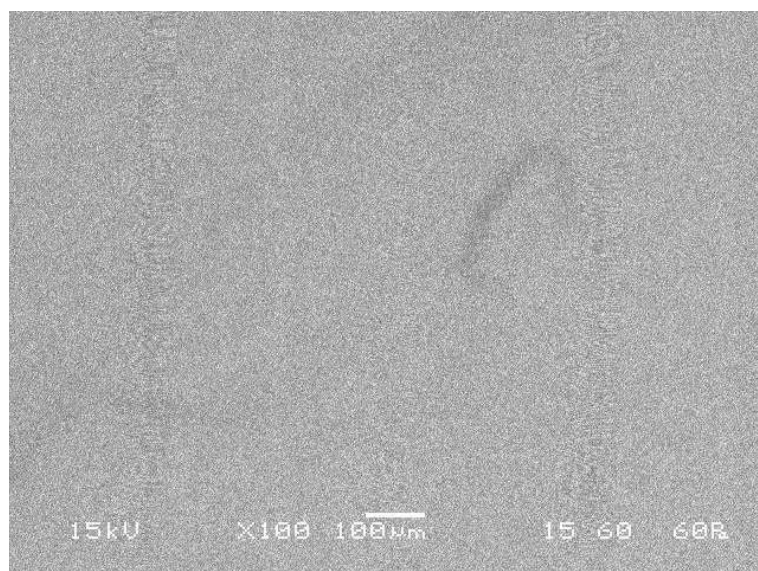


Figure 4-5 Peltier effect device with mastic sample inside the chamber and on the device (left) and the device coming out of the SEM chamber to the water source cooling the device (right)

## 4.1.2 Results and discussion

### 4.1.2.1 Bitumen

The observation of bitumen by itself is shown in Figure 4-6. An EDS analysis was conducted for its two of the three main components: carbon and sulfur. The percentages (given as oxides of the elements by weight) are based on the relative presence (among the elements searched for) of element analyzed in the particular area. It should be noted that hydrogen (around 10.8% according to *The Bitumen Industry*, 2011) cannot be detected by EDS. The carbon was found to be at 97% and the sulfur at around 3% (within the 0.9-6.6% range described by *The Bitumen Industry*, 2011).



Element	% atom weight
CO <sub>2</sub>	96.83
SO <sub>3</sub>	3.17

Figure 4-6 SEM observation of bitumen 35/50 sample with Peltier device cooling at -10°C. The EDS chemical analysis (in %w of oxide) for the area of the image is shown in the table on the right

As mentioned before, the bitumen samples observed without a Peltier effect cooling tended to melt relatively quickly. If the electron beam of the SEM was targeted over the same place for several minutes, this produced a structural effect on the bitumen image (Figure 4-7, Figure 4-8) similar to the one described in the literature by Loeber et al. (1996), Rozeveld et al. (1997), Stangle et al. (2006) with the ESEM and Golubev et al. (2008) with the SEM.

The hypothesis proposed by Rozeveld et al. (1997) and Stangle et al. (2006) was that the structures – although created by the electron beam – represented the asphaltene structure in which the lighter bitumen hydrocarbons (maltenes) were directed away by the beam. The change in the structure was also correlated to bitumen aging.

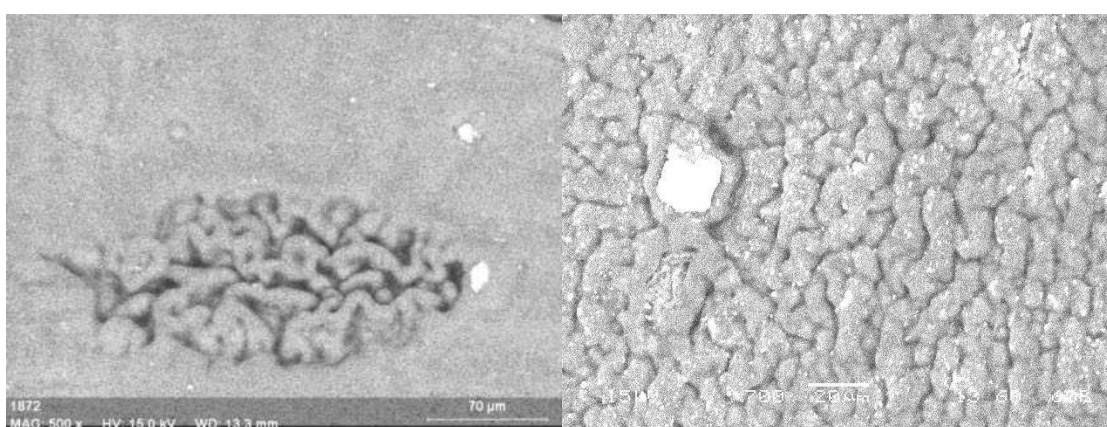


Figure 4-7 SEM observation of bitumen with structures caused by the beam at x500 (left) and x700 (right)

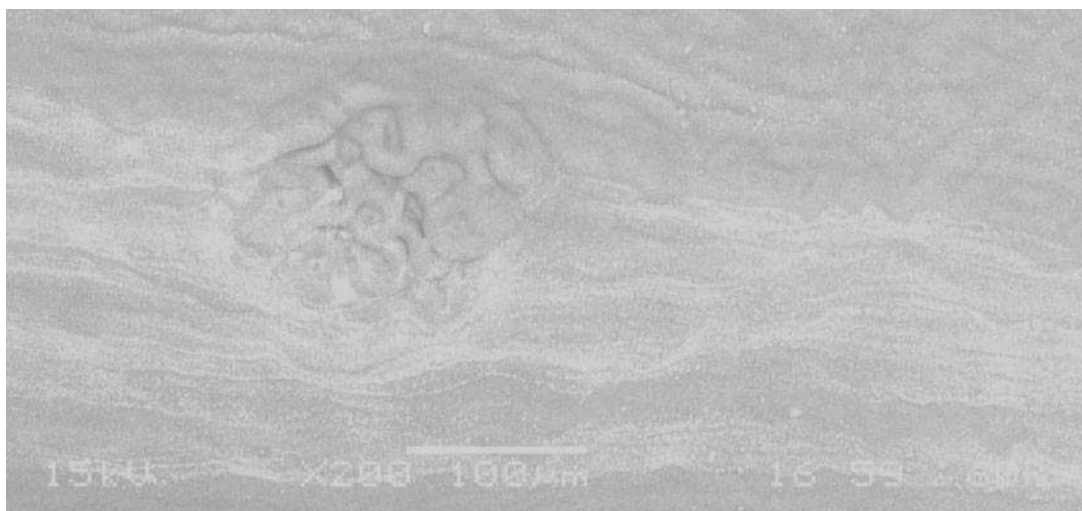


Figure 4-8 SEM observation of bitumen with structures caused by the electron beam at x200 (HD image with special acquisition mode)

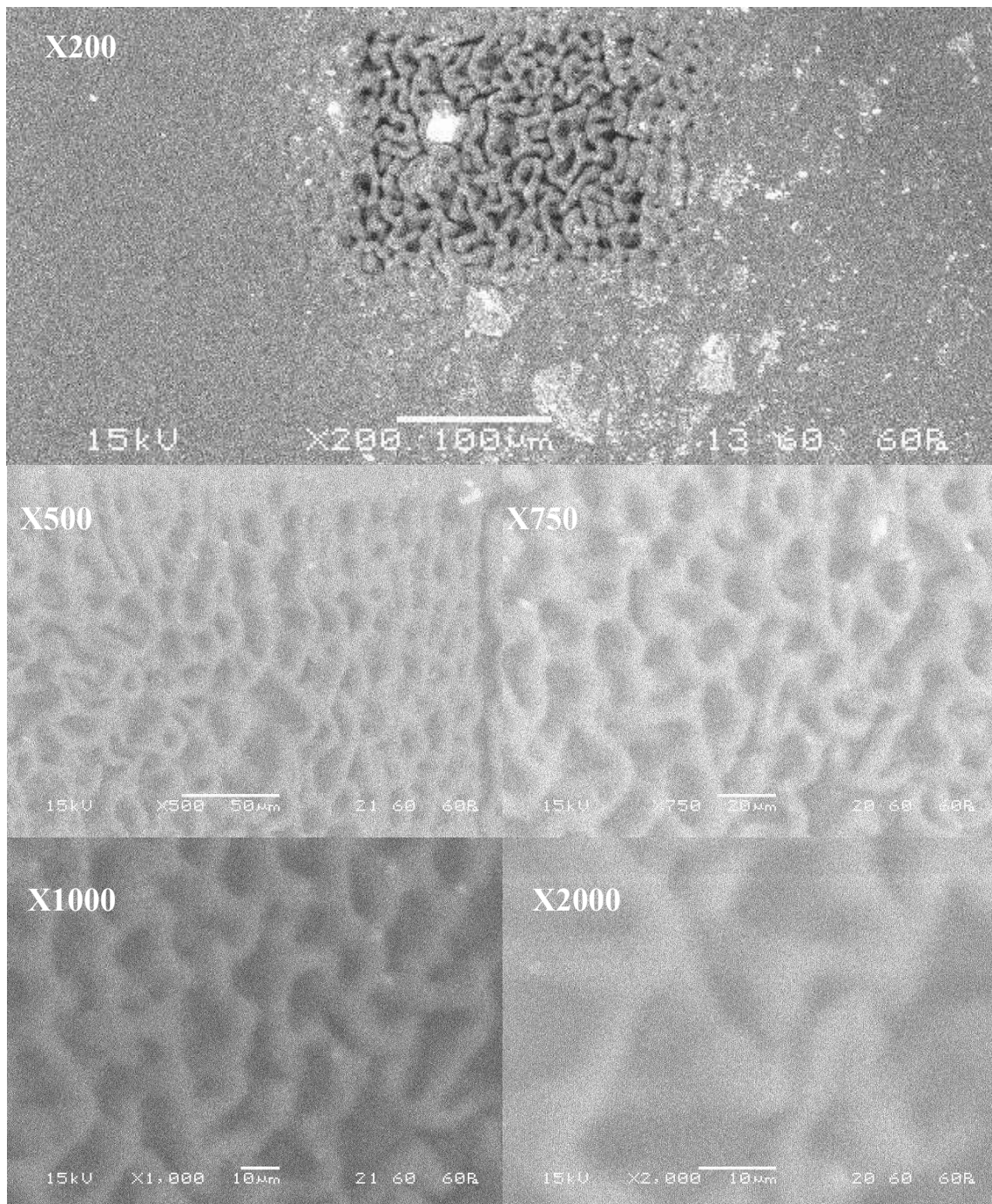


Figure 4-9 SEM observation of bitumen with structures caused by the electron beam at magnifications of x200, x500 x750, x1000 and x2000

The structure was observed under SEM and ambient temperature at magnifications from x200 to x2000 (Figure 4-9). The structure shown in the x200 images comes just after a “zoom out” from x500, demonstrating the rectangular electron beam from the SEM. Nevertheless, as the microscope

zooms in, the thickness of the micelle-like structure remains the same at around 5  $\mu\text{m}$ , indicating that the structure is strongly related to the nature of the bitumen itself. This was similar to the size found by Rozeveld et al. (1997) at around 3  $\mu\text{m}$  for virgin binder.

#### 4.1.2.2 SEM-EDS observation of bitumen with $\text{TiO}_2$ tracers

Two types of  $\text{TiO}_2$  tracers were analyzed: anatase and rutile. Seven types of samples were observed:

- i. Bitumen by itself;
- ii. Bitumen with 0.5, 1 and 2%w of  $\text{TiO}_2$  rutile;
- iii. Bitumen with 0.5, 1 and 2%w of  $\text{TiO}_2$  anatase.

From the EDS analysis of the samples, a tracer quantity of 2%w was found to be sufficient for the sample to be well distributed – that is – so that it can be identified anywhere in the samples at a magnification of x50. The distribution of the rutile particles was found to be better than for the anatase as shown in Figure 4-10, possibly due to a problem in more coagulation among the anatase particles. The tracer particles are visible in white on the BSE images due to their higher density relative to the bitumen. Nevertheless, the particle size was quite variable, often with particles of >40  $\mu\text{m}$  due to particle aggregation.

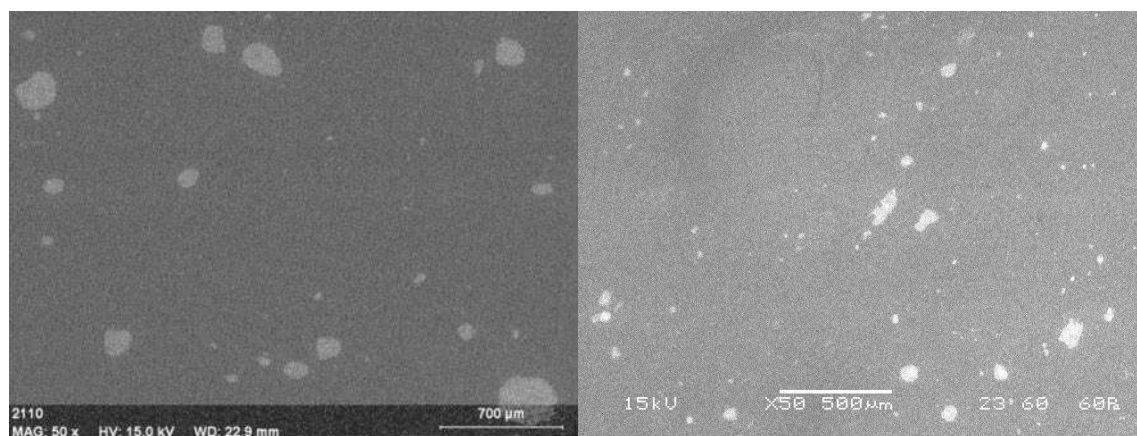


Figure 4-10 : Particles of  $\text{TiO}_2$  rutile (2%w of bitumen, left) and  $\text{TiO}_2$  anatase (2%w of bitumen, right) observed by SEM in ambient temperature

The cartographic analysis of the samples at ambient temperatures was found to be altered by fluorescence of the bitumen by the electron beam and the lighter carbon particles flooding the SEM chamber. Even chemical analysis targeted at only the tracer showed high traces of carbon (81%) and only 14% Ti, despite the limitation of the observation time to 10 min. The small quantity Al is from the rutile.

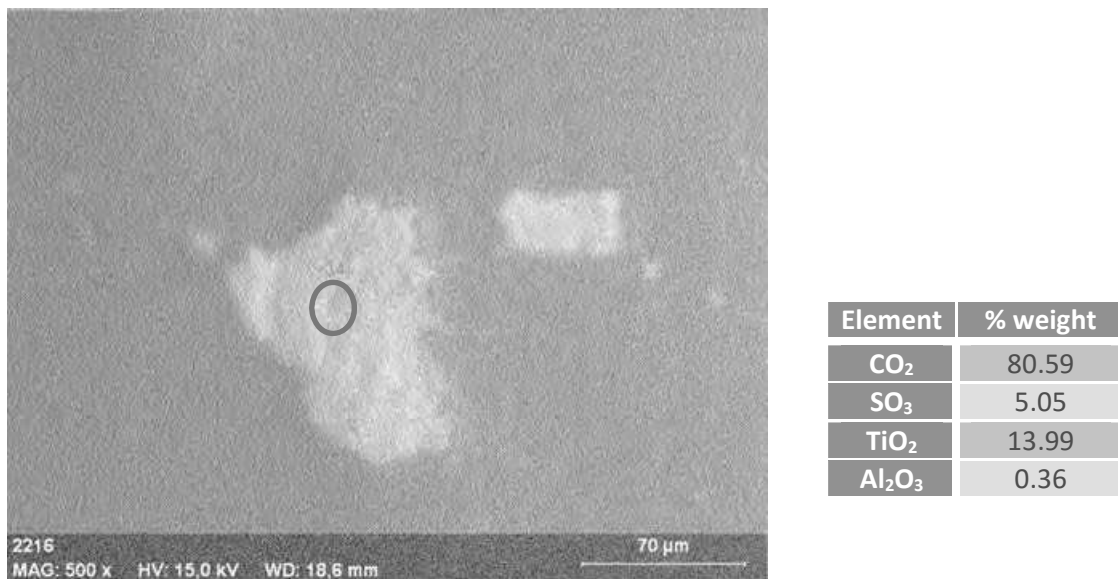
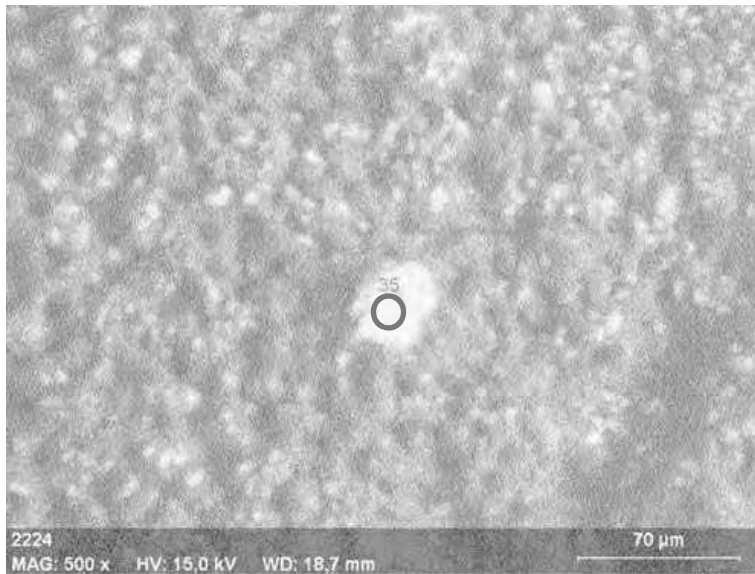


Figure 4-11 : Observation of a rutile particle in bitumen by SEM at ambient temperature with EDS analysis of the area inside the blue circle

#### 4.1.2.3 Bitumen with limestone and silica sand

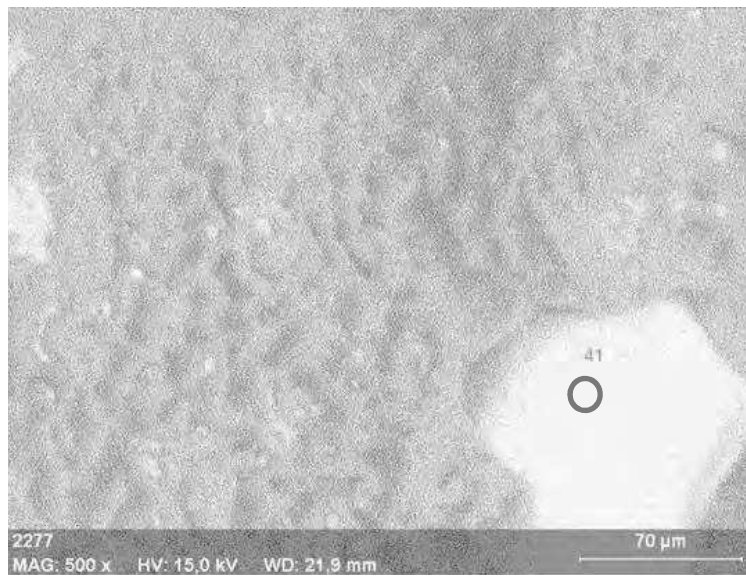
Limestone and silica sand were mixed with bitumen initially at quantities of 20%w with the intention of observing the sand particles in SEM. For the first series of observation, particles sized 0-0.315 mm were used, and the samples were observed at ambient temperature, resulting in problems with samples melting during observation. As with the previous analysis, the fluorescence of the carbon in the bitumen by the electron beam results in the interference in the EDS analysis by the carbon particles flooding the chamber. This is present even for focalized analysis on limestone and silica particles (Figure 4-12, Figure 4-13). The particles are visible while in the BSE images dues to their higher density.

In order to reduce bitumen melting, mastic (with 70% limestone sand, 30% bitumen) samples were fabricated. The limestone sand was graded to 0.315/1 mm in order to reduce the fines that may interfere with the analysis. The analysis of this sample was conducted with the aid of the Peltier effect device, reducing the temperature in the SEM analysis chamber to -10°C. As shown in Figure 4-14, the freezing of the bitumen sample inside the SEM chamber stops the melting of the bitumen and results in the crystalizing of water on the sample.



Element	% weight
CO <sub>2</sub>	83.79
SO <sub>3</sub>	3.81
CaO	12.13

Figure 4-12 Limestone sand particle (0-0.315 mm) SEM image x500 with EDS analysis (in blue circle) observed at ambient temperature



Element	% weight
CO <sub>2</sub>	71.64
SO <sub>3</sub>	3.73
SiO <sub>2</sub>	24.62

Figure 4-13 Silica sand particle (0-0.315 mm) SEM image x500 with EDS analysis (in blue circle) observed at ambient temperature



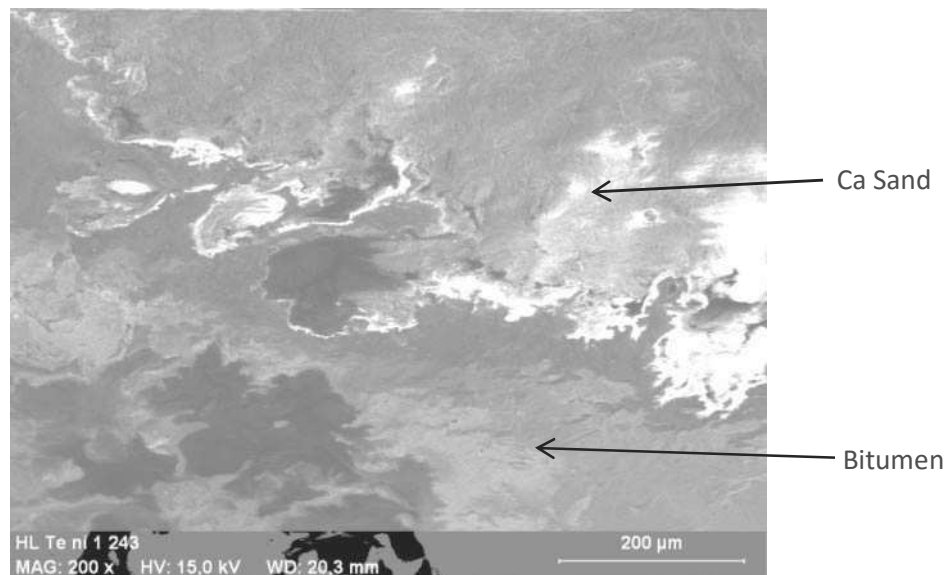


Figure 4-14 Limestone sand particle (0.315-1 mm) in bitumen SEM image x200 observed with the aid of a Peltier effect device at -10°C

The EDS cartography of the sample shows clearly the relative presence of Ca in the sample (Figure 4-15), corresponding to the limestone sand particle. The grading of the fines from the sand reduced the pollution in the cartographic analysis, while the sample cooling limited the melting.

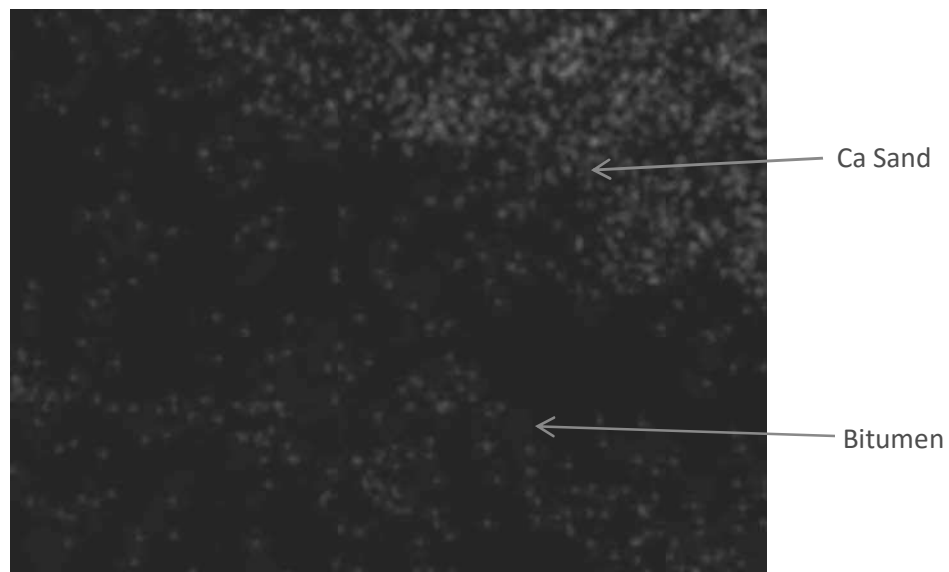


Figure 4-15 EDS analysis cartography for calcium (blue dots) of limestone sand (0.315-1 mm) mastic observed with the aid of a Peltier effect device at -10°C, corresponding to the SEM image in Figure 4-14

In addition to EDS cartography, EDS line scans were performed on the previously describe mastic samples in order to explore this analysis technique. The linescan was performed between two sand particles for C, S, Si and Ca. The linescan shows (Figure 4-16) elevated Ca (50%) and Si (5%) quantities

on the limestone part of the image, while elevated C (50%) and S (5%) quantities are present on the bitumen part. The limestone particles still show a significant presence of C (20%) on the limestone part of the linescan, likely due to fluorescence, although this is greatly reduced with the cooling of the Peltier effect.

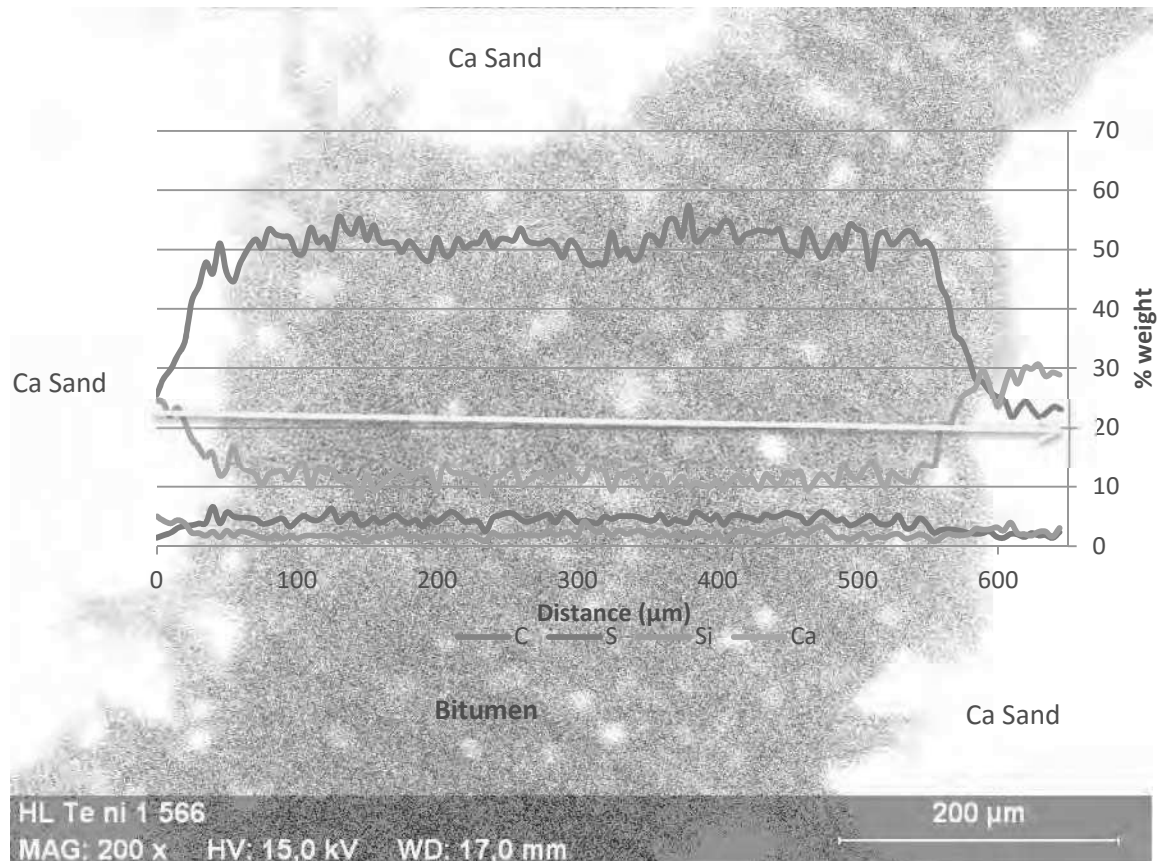


Figure 4-16 EDS analysis line scan for C, S, Si and Ca of limestone sand (0.315-1 mm) mastic observed with the aid of a Peltier effect device at -10°C

#### 4.1.3 Conclusions of the characterization of bitumen remobilization by SEM-EDS

The conclusions for the characterization of bitumen remobilization with SEM-EDS are as follows:

- The analysis of bitumen by SEM and EDS results in the melting of the bitumen samples, which affects the EDS analysis. This can be mitigated to a certain degree by using a Peltier effect device to cool the chamber;
- The structure of the bitumen from the SEM beam is a result of the electron beam, but is at the same time an indication of the structure of the bitumen;
- The EDS is able to identify Si and Ca sand, along with TiO<sub>2</sub> tracers in the bitumen, but not in exact quantities.



The work for asphalt remobilization was not carried through all the way due to the damage to the SEM apparatus itself is the limiting factor. An ESEM would have been more appropriate in this type of analysis. The structures formed by the electron beam are of interest in this case, as they have been found to change with aging in the literature (Stangle et al., 2006), but have not been analyzed with rejuvenating agents.

Alternative methods for observing bitumen with tracers could have included visual microscopy, however, this may not be necessary if trace signatures (such as with FTIR) can be found in the rejuvenating agent itself, which is the case for bio-sourced agents, but not petroleum based ones.

## 4.2 Physico-chemical characterization of bitumen aging and rejuvenation

The purpose of this part of the study is the characterization of bitumen aging and rejuvenation. For bitumen aging in a ventilated oven, an appropriate bitumen aging duration was determined that was comparable in its effect to conventionally used aging such as RTFOT+PAV (Section 2.3.1.1.1). FTIR-ATR analysis is a renowned method for the analysis of bitumen oxidation. FTIR-ATR imaging can further aid in this characterization in allowing for the characterization of the bitumen oxidation relative to the aggregates. Additionally, TGA was examined in terms of its ability to characterize bitumen aging.

### 4.2.1 Materials and methods

#### 4.2.1.1 Materials

Several types of samples were prepared for this part of the study, including bitumen and mastic with and without rejuvenating agents as outlined in Table 4-2.

Table 4-2 Summary of samples prepared for this study of bitumen aging and rejuvenation

Composition	Aging	Analysis techniques
Bitumen 35/50	Unaged, aged 1-42 days	FTIR-ATR, TGA, rheology**, penetration**
Bitumen 35/50 (80%) aged 14 days + rejuvenating agent* (20%)	Unaged, aged 14 days, RTFOT+PAV**	FTIR-ATR, TGA, rheology**
Mastic: Ca sand (70%) + bitumen 35/50 (30%)	Unaged, aged 14 days	FTIR-ATR Microscopy
Mastic: [Ca Sand (70%) + bitumen 35/50 (30%)] aged 14 days (92.5%) + rejuvenating agent* (7.5%)	Unaged	FTIR-ATR Microscopy

\*Agents B1, P1 and P2 described in Section 4.2.1.1.4

\*\*The results from of rheology and penetration for bitumen are from a parallel study. The quantity of rejuvenating agent used in this study was the %w of rejuvenating agent needed to have a 35/50 bitumen aged by RTFOT+PAV to return to a penetration value of a 35/50 virgin bitumen

#### 4.2.1.1.1 Bitumen

The bitumen used for testing and in the asphalt was Total 35/50 as classified by NF EN 12591, indicating a penetration (ASTM D5-NF EN 1426) value of between 3.5 and 5.0 mm.

#### 4.2.1.1.2 Sand

The limestone sand was 0-1mm Larronde – Ainhoa ( $\rho_v = 2.85\text{g/cm}^3$ ) limestone (Figure 4-17). The sand was graded and washed in order to remove fines ( $< 0.315\text{ mm}$ ) that may interfere with the FTIR-ATR imaging analysis as in the work by El Béze et al. (2012), which also used mastic and FTIR imaging in order to study the mastic aging.



Figure 4-17 Larronde – Ainhoa limestone sand graded to 0.315/1 mm

#### 4.2.1.1.3 Mastic

While the grain size of the RAP can be controlled through the crushing process – due to the diverse conditions of fabrication and service life for the RAP pavement – its properties often have a high variability potential from one source to the next. In addition to this, one source of RAP may have a high variability within it depending on where the aggregates were positioned in the road (depth, near water sources, amount of sun exposure). The RAP bitumen in the top few millimeters of the surface of the pavement tends to have a higher viscosity compare to the rest (Smith and Edwards, 2001). Thus, there exists a need for lab-manufactured RAP in order to provide a homogeneous material for testing. El Béze et al. (2012), Navaro et al. (2012), and Van den bergh and Van de Ven (2012) have fabricated RAP mastic (bitumen + sand) in laboratory conditions with the purpose of conducting research related to RAP asphalt.

For the preparation of the mastic (Figure 4-18), the bitumen (30%) was pre-heated at 160°C for 2h±15min in a closed pot. The Ca sand (70%) was heated to 160°C for at least 6 hours before the

mixture. The sand was incorporated in the pot and mixed with a Heidolph RZR mixer (2-5min) disposed on a Fisher Scientific Isotemp hot plate (160°C, temperature control with thermocouple in the pot). The mastic was then poured into a trapezoidal of silicone mold with dimensions 65-77 mm x 21-29 mm x 30 mm and compacted with a spatula (Figure 4-19). The samples were cooled for 6 h at room temperature and were then stored at 4°C in a refrigerator, so as to reduce sample melting, but not so cold as to induce damage to the bitumen from crystallization of the saturates that occurs below -7°C (Fuentes-Audén et al., 2008; Garcia-Morales et al., 2006; McNally, 2011).

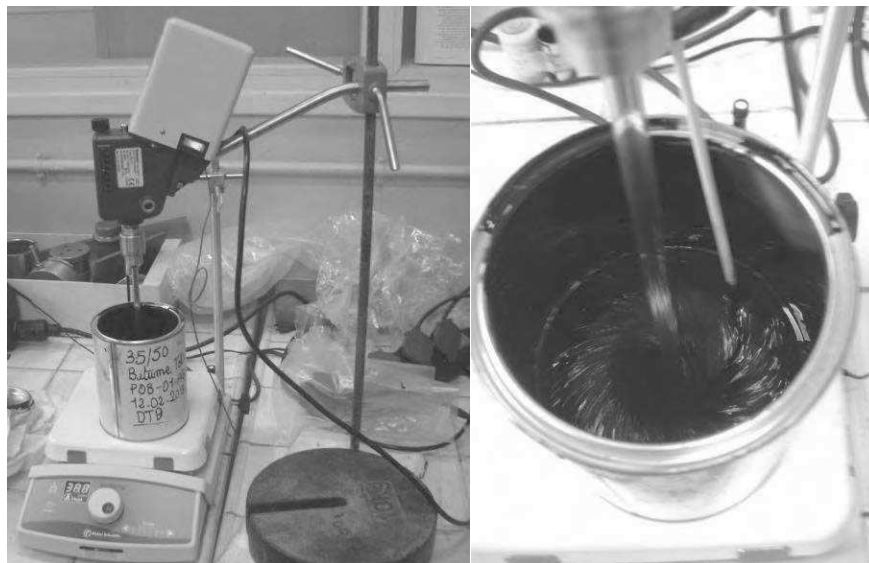


Figure 4-18 Preparation of mastic samples using Heidolph RZR mixer and Fisher Scientific Isotemp hot plate

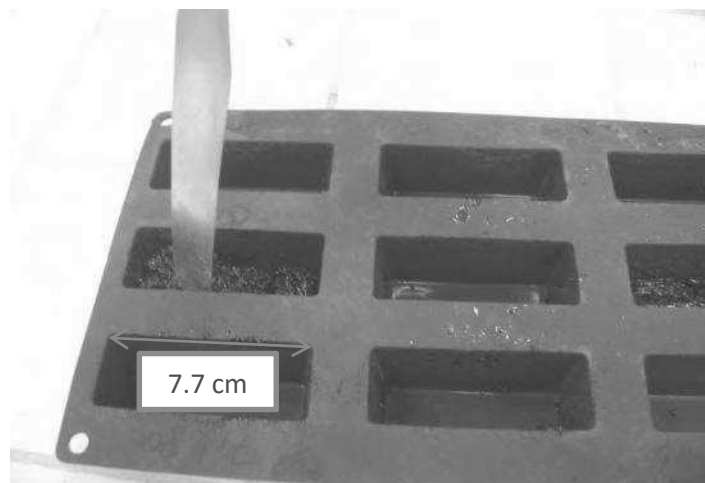


Figure 4-19 Compaction of mastic sample with spatula after mixing

#### 4.2.1.1.4 Rejuvenating agents

The development of bio-sourced agents is still relatively novel (Hajj et al., 2013; Kim, 2014; Reinke et al., 2014; Zargar et al., 2012). Part of this study was the development of a bio-sourced and biodegradable rejuvenating agent by our partner LCA, labelled B1. Additionally, two petroleum sourced rejuvenating agents were tested labelled P1 and P2. Some physical and chemical properties of these products are shown in Table 4-3.

B1 is a bio-sourced agent engineered with the idea of replicating the maltenes in the bitumen. Its formulation is subject to industrial property right and this cannot be discussed at the time that the current work is being submitted.

P1 and P2 are petroleum based hydrocarbons that are lighter than the ones in bitumen. P2 has a higher quantity of asphaltenes, which corresponds to a higher viscosity and specific gravity as well. All three agents have boiling points of well above 200°C, that is, above the temperature for the production of asphalt of 160°C.

Table 4-3 Properties of rejuvenating agents

Property	Function and Purpose	ASTM Test Method	B1	P1	P2
<b>Viscosity @60°C, cSt</b>	Asphalt viscosity adjustment in recycled mix	D-2170	-	200-500	100-200
<b>Saturates %w</b>	Compatibility with aged asphalt	D-2007	-	28 max	21-28
<b>Asphaltenes %w</b>	Compatibility with aged asphalt	D-2006-70	-	1.5 max	0.75 max
<b>Specific Gravity</b>		D-70	-	0.98-1.02	0.92
<b>Boiling Point °C</b>	Volatility	-	200	288	288

When incorporated with aged bitumen or mastic, the bitumen was heated for 2 h at 160°C in a closed pot, and the rejuvenating agent was incorporated into the pot at 20%w for the bitumen or 7.5%w of the mastic. This was performed with a spatula directly into the pot on a balance. It was mixed using a Heidolph RZR mixer (2-5 min) for homogenization. The sample was left to cool to room temperature for 6h before testing.

The results from of rheology and penetration for rejuvenated bitumen are from a parallel study. The quantity of rejuvenating agent used in this study was the %w of rejuvenating agent needed to have a 35/50 bitumen aged by RTFOT+PAV to return to a penetration value of a 35/50 virgin bitumen.

#### 4.2.1.2 Bitumen and mastic aging

Due to the fact that the life cycle of asphalt is many years, several accelerated laboratory aging methods have been developed in the literature in order to simulate the effects of aging on bitumen for a shorter period of time.

For this study, a ventilated oven was used for the long-term aging process of both bitumen and mastic. The oven needs to be well ventilated for the test to provide a consistent supply of oxygen to the sample, which should be made as thin as possible in order to provide more surface area for the oxidation. For asphalt aging, there are varied temperatures suggested as discussed in Section 2.3.1.1.3. De la Roche et al. (2013) – In the context of developing an asphalt oven aging method for the 237-SIB RILEM Technical Committee – conducted the aging of asphalt in two stages; the first at 135°C for 4 h and the second at 85°C for 9 days, finding that plant and laboratory manufactured asphalt aged differently in terms of the same indicators.

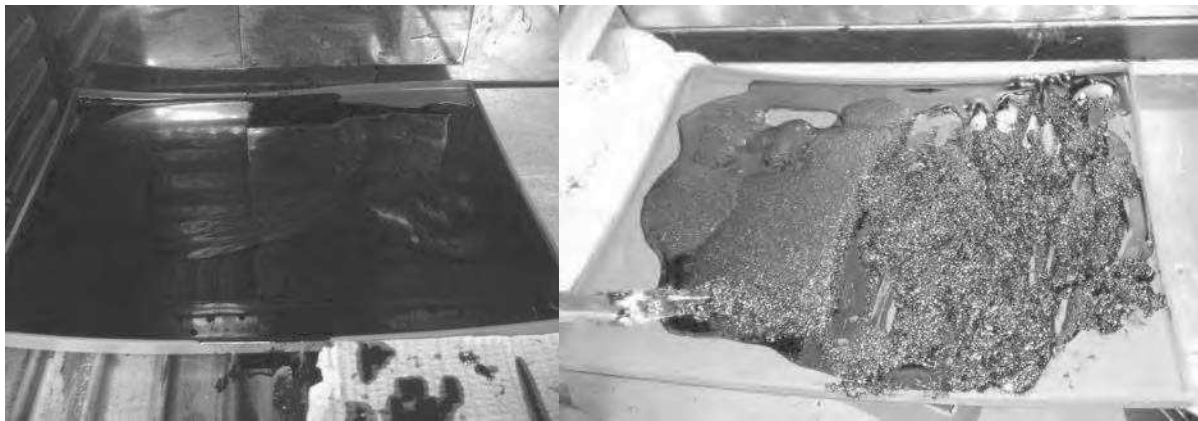


Figure 4-20 Oven aging of bitumen (left) and mastic (right)

The same aging time and temperature parameters were used in this study, only adapted for bitumen and mastic.

The bitumen was aged by pouring a  $2.5 \pm 0.2$  mm layer of bitumen (pre-heated in a closed pot at 160°C for 2 h) on a silicone plate, as silicone has a very low adhesion to bitumen.

The bitumen was placed in the oven at 135°C for 4 h and the second at 85°C for a period determined from correlating with the rheology of the aged bitumen.

The bitumen was allowed to cool for at least 6h before being tested. For mastic aging, the sample was preheated at 160°C for 2 h, placed on a silicone plate for a thickness of  $20 \pm 10$ mm. The mastic was agitated after 1 day and then every two days for the aging process, and the aging parameters were the same as for bitumen (Figure 4-20).

#### 4.2.1.3 FTIR-ATR spectrometry

The FTIR-ATR analysis was performed with a PerkinElmer Spotlight 400 (Figure 4-21) and an ATR crystal. The analysis was effectuated 16 times (per sample) with a  $4\text{ cm}^{-1}$  resolution and a band range of  $4000\text{-}600\text{ cm}^{-1}$  on a Germanium crystal, due to the compatibility of Ge with analyzing organic compounds.

For the bitumen, around 0.5 g was placed with a spatula (at ambient temperature) on the crystal with a vertical pressure of  $100\pm 10\text{ N}$  in order to reduce air between the sample and the crystal. The crystal is cleaned with ethanol before each test. The analysis of aging and oxidation was be conducted based on Table 4-4, with particular attention to the  $I_{\text{C=O}}$  and  $I_{\text{S=O}}$  indices as indicators of oxidation.



Figure 4-21 PerkinElmer Spotlight 400 FTIR-ATR

Table 4-4 FTIR bands with bitumen aging

Chemical Group	Bond	Approximate Wavenumber ( $\text{cm}^{-1}$ )	Change with aging	Intensity	Expression	References
Sulphoxide	S=O	1030	Increases in short-term	Weak	$\frac{A_{1030}}{A_{1460} + A_{1376}}$	Lamontagne et al. (2001a) Lu and
Carbonyl	C=O	1700	Increases in long-term	Weak to medium	$\frac{A_{1700}}{A_{1460} + A_{1376}}$	Isacson (2002) Chávez-Valencia et al.
Aliphatics (deform)	C-CH <sub>3</sub>	1460, 1376	Relatively constant	Medium	$\frac{A_{1460} + A_{1376}}{\Sigma A^1}$	(2007) Mouillet et al.

			to small decrease			(2008) El Béze et al. (2012) Yao et al. (2013)
<b>Aromatics</b>	C=C	1600	Relatively constant to increase	Medium	$\frac{A_{1600}}{\Sigma A^1}$	Lamontagne et al. (2001b) Mouillet et al. (2008) Tachon (2008) <sup>2</sup>
<b>Aliphatics (stretch)</b>	CH <sub>2</sub> , CH <sub>3</sub>	2923, 2853	Relatively constant to small decrease	Medium to strong	$\frac{A_{2923} + A_{2850}}{\Sigma A^1}$	Tachon (2008) <sup>2</sup> Lins et al. (2008) Yao et al. (2013) <sup>3</sup>
<b>Polarity</b>	O-H	3450	Increases	Strong	$\frac{A_{3450}}{\Sigma A^1}$	Tachon (2008) <sup>2</sup> Araújo et al. (2011)
<sup>1</sup> $\Sigma A = A_{1700} + A_{1600} + A_{1460} + A_{1376} + A_{1030} + A_{864} + A_{814} + A_{743} + A_{724} + A_{(2953, 2923, 2862)}$ (Lamontagne et al., 2001a) or $\Sigma A = A_{2000} + A_{600}$ (Yao et al., 2013) <sup>2</sup> Hypothesized from results of FTIR analysis of SARA fractions by Tachon (2008) <sup>3</sup> Observed from results of FTIR analysis of SARA fractions by Yao et al. (2013)						

#### 4.2.1.4 FTIR-ATR microscope imaging

FTIR-ATR imaging allows for imaging of the distribution of the spectra in the asphalt, that is, in relation to the position of the bitumen and aggregates.

The analysis was conducted on mastic samples of approximately 10x10 mm and 5 mm thickness. For preparation, the samples were stored at 4°C for a minimum of 6h and then cut by a saw to ensure that they were relatively flat on both sides.

The samples were then polished (procedure established with the GET<sup>2</sup>, Figure 4-22) using 3 polishing discs (Presi-Tissediam) at 250 µm (2-3 min), 75 µm (1 min) and 40µm (30s) at a rotational speed of around 180-200rpm. The samples were kept in a cooler between each step of this process in order to reduce melting.

The FTIR microscope analyses were performed with a PerkinElmer Spotlight 400 coupled with a PerkinElmer Frontier Imager and a ZnSe ATR crystal (Figure 4-23). The analyses were effectuated 8 times (per sample) with a 4 cm<sup>-1</sup> resolution, a band range of 4000-720 cm<sup>-1</sup> [mid infrared (MIR) analysis mode], and a pixel size of 1.56 or 6.25 µm, depending on the nature of the sample.

The mastic was analyzed by applying the crystal to the surface of the samples, taking FTIR cartographies of 150x150 µm (Figure 4-24).

<sup>2</sup> Laboratoire Géosciences Environnement, Toulouse

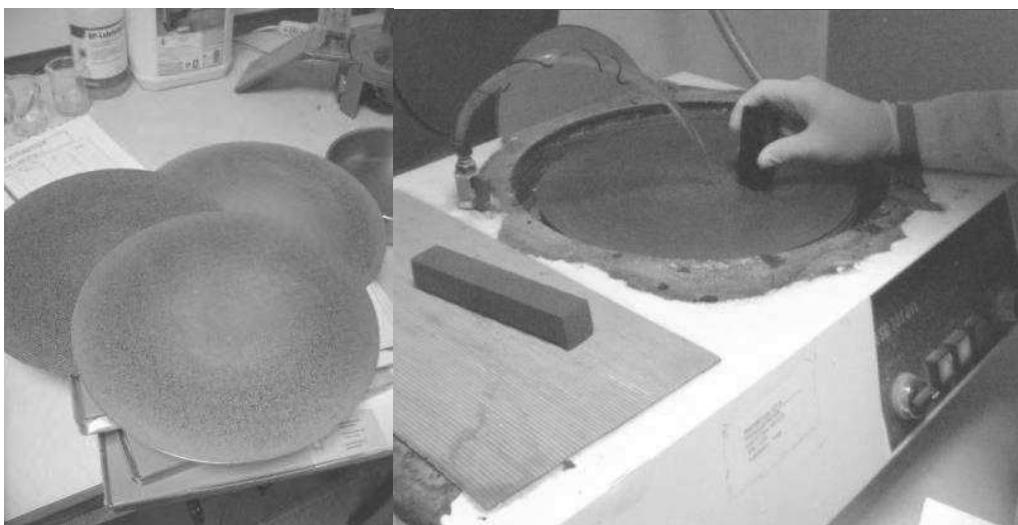


Figure 4-22 Polishing of mastic samples with discs (left) and polishing at 180-200rpm (right)



Figure 4-23 PerkinElmer Spotlight 400 coupled with a PerkinElmer Frontier Imager (left) and ZnSe ATR crystal (right)

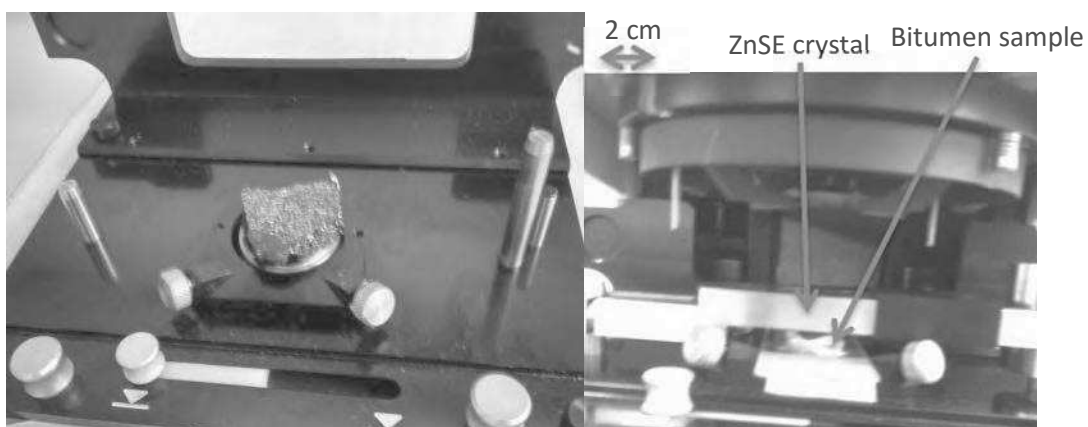


Figure 4-24 Mastic sample for FTIR imaging (left) and FTIR microscope analysis on mastic sample (right)



#### 4.2.1.5 Rheology of rejuvenated bitumen

In a parallel study conducted by Malet, bitumen aged 0-18 days was tested in penetration (EN 1426) and rheology in order to determine an appropriate duration of oven aging relative to these characteristics.

Additionally, bitumen aged with RTFOT + PAV aging was mixed with rejuvenating agents B1, P1 and P2 at a quantity of rejuvenating agent used in this study was the %w of rejuvenating agent needed to have a 35/50 bitumen aged by RTFOT+PAV to return to a penetration value of a 35/50 virgin bitumen.

The rheology (Section 2.1.4.3) of the aged and rejuvenated bitumens was determined by a DSR (EN 14770) at a temperature range of -5-55°C and an oscillation frequency of 0.01-100 Hz (Malet, 2015).

#### 4.2.1.6 TGA

The TGA allows for the characterization of bitumen by heating it to a high temperature and analyzing the change in mass. The volatilization of the sample at various temperatures can allow for the identification and quantification of certain compounds. As found in the literature (Section 2.3.1.3.4), in the research of TGA on bitumen, the identification of the volatilized bitumen compounds has yet to be more precise than the identification of heavy and light hydrocarbons, presenting a challenge in this study.



Figure 4-25 Netzsch thermogravimetric analyzer coupled with a mass spectrometry attachment (right, not used)

For this study, a Nietzsche thermogravimetric analyzer was used to analyze the bitumen by heating it from 20°C to 700°C and measuring the volatiles (Figure 4-25). Around 0.1 g of the bitumen sample was placed in the TGA and it was heated up to 700°C at a heating rate of 4K/min while the change in mass is measured. The samples were tested in both air and inert argon gas in order to observe the volatilization of the bitumen in both cases.

## 4.2.2 Results and discussion

### 4.2.2.1 Bitumen aging with FTIR-ATR analysis

The bitumen samples were subjected to oven aging in order to determine the most consistent aging indicators (peaks) and the appropriated aging duration. Two series of aging were conducted with FTIR-ATR analysis for oven aging of up to 17 d (3 samples) and 42 d (1 sample), with two spectra for each sample.

For the first series of aging, the change in mass of the 3 samples was measured with a balance precise to 0.01g.

An FTIR-ATR analysis was conducted after 1, 2, 3, 4, 7 and 17 days of aging. The results for the change in mass,  $I_{C=O}$  and  $I_{S=O}$  and  $A_{1600}$  (Table 4-4), are shown in Figure 4-26 to Figure 4-29, respectively.

During the oven aging, the bitumen loses the majority of the volatiles (3% of its total mass) during the first 24h. There is no further mass loss after 48h, while there is a very small gain after 7 days, which could be either an increase in oxidation products in the bitumen or an error with the balance.

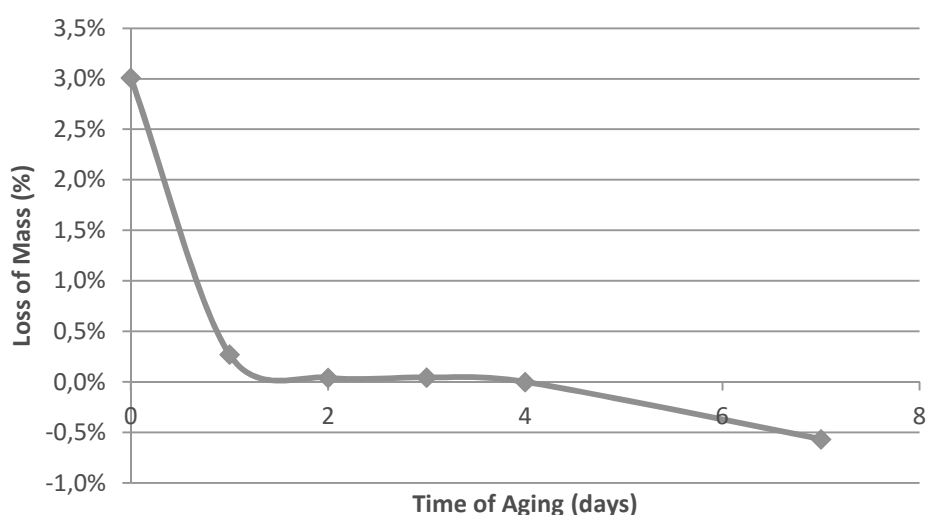


Figure 4-26 Mass loss % for 0-17 days of bitumen aging

For the first series of aging up to 17 d, the C=O index increased for the first 7 d of aging, after which, it plateaued. The S=O continued showed a small increase from 7-17 d, and so a second series of aging was conducted up to 42 d. The  $A_{1600}$  area appeared to decrease up to 7 d of aging, after which it stabilized.

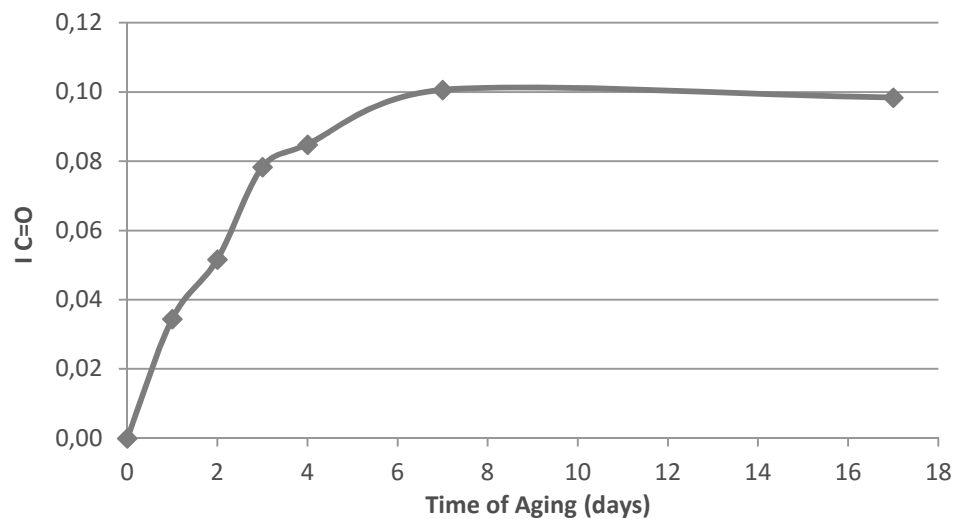


Figure 4-27 Change in  $I_{C=O}$  for 0-17 days of bitumen aging

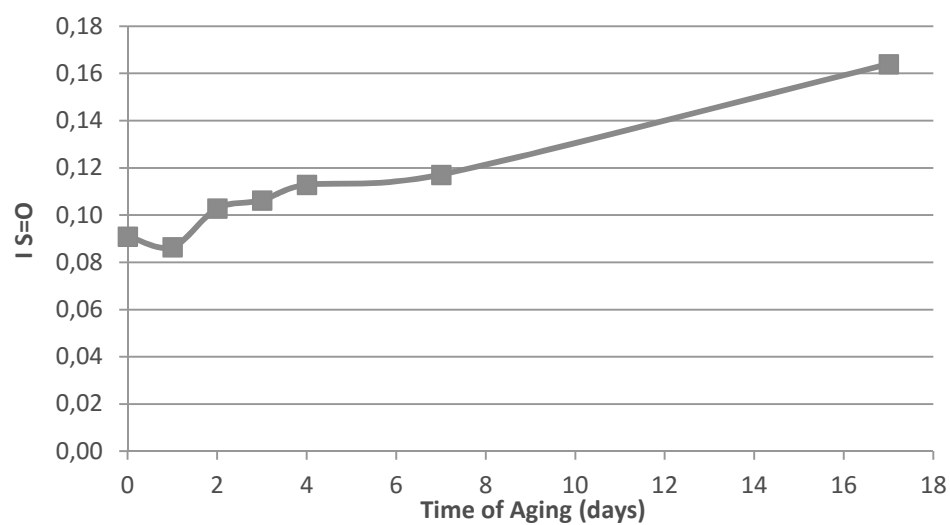


Figure 4-28 Change in  $I_{S=O}$  for 0-17 days of bitumen aging

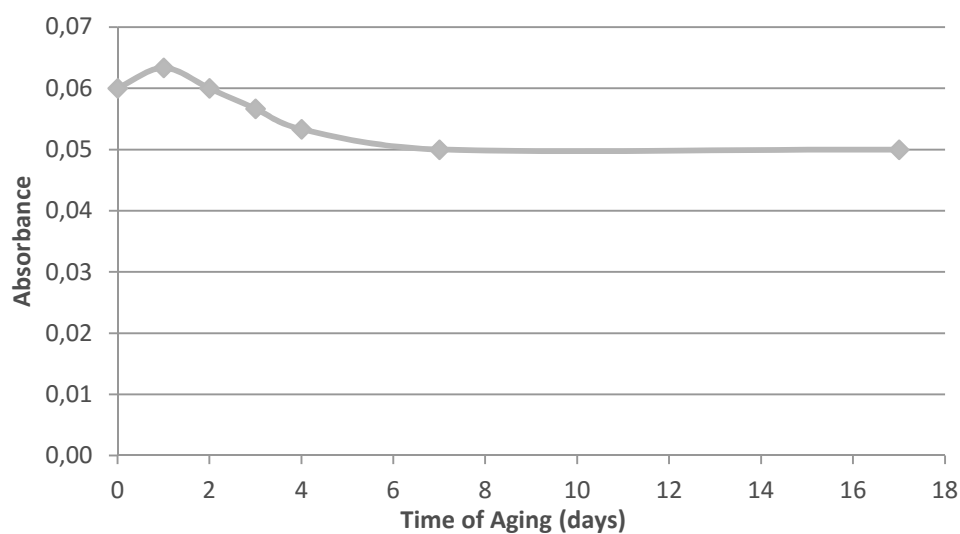


Figure 4-29 Change in  $A_{1600}$  for 0-17 days of bitumen aging

The second series was conducted for 1 sample (tested twice) at 1, 2, 7, 14, 21, 29 and 42 d of aging. The C=O index, after an initial plateau after 7 d, appeared to increase further after 21 d of aging, and continues up to 42 d (Figure 4-30), the increase in the peaks with aging shown in Figure 4-31. The S=O index plateaus after 7 d with some fluctuation (Figure 4-32), through 42 d as shown in the S=O peaks with aging in Figure 4-33.

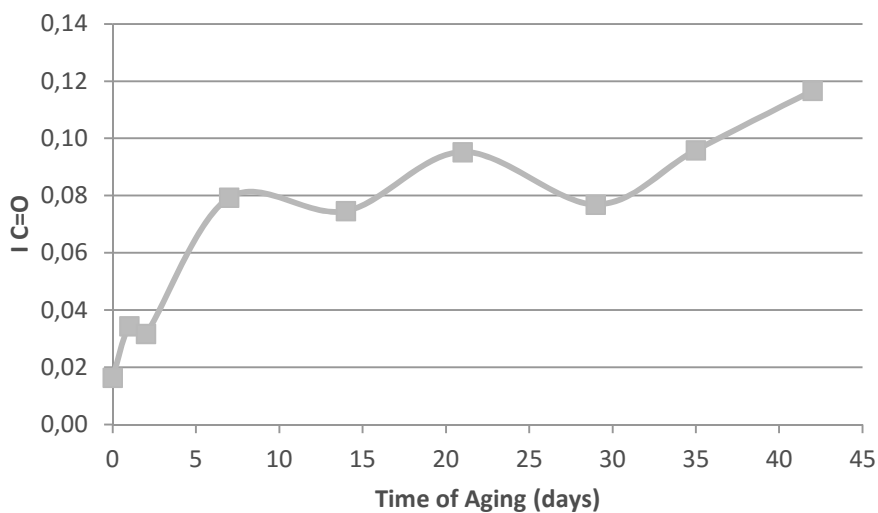


Figure 4-30 Change in  $I_{C=O}$  for 0-42 days of bitumen aging

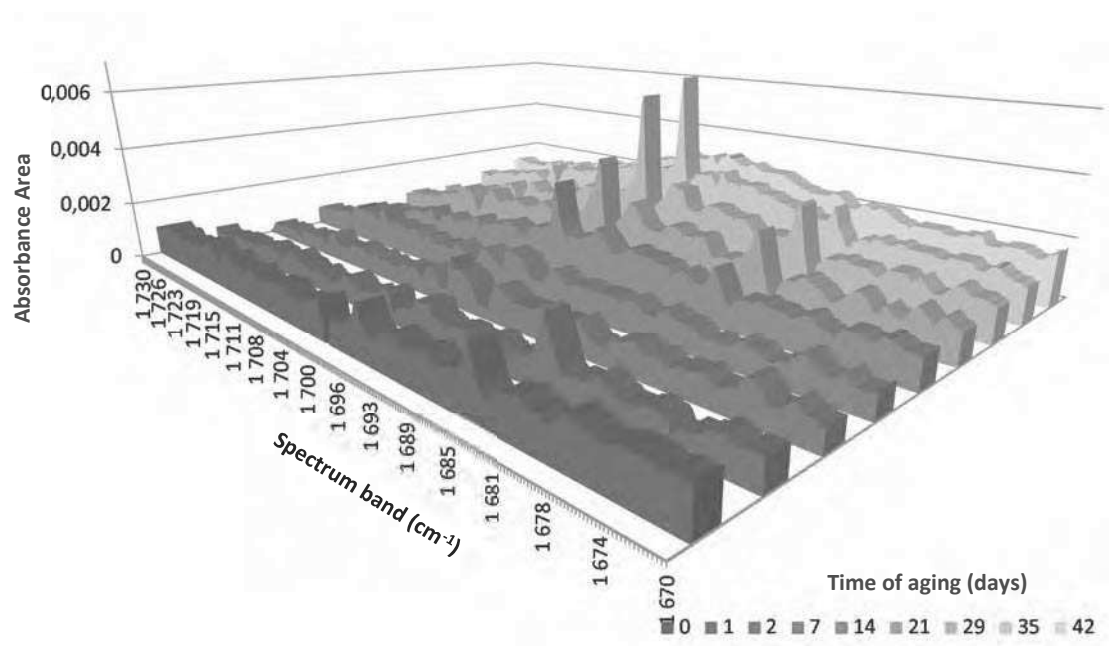


Figure 4-31 Spectra 1730-1670cm<sup>-1</sup> for 0-42 days of bitumen aging

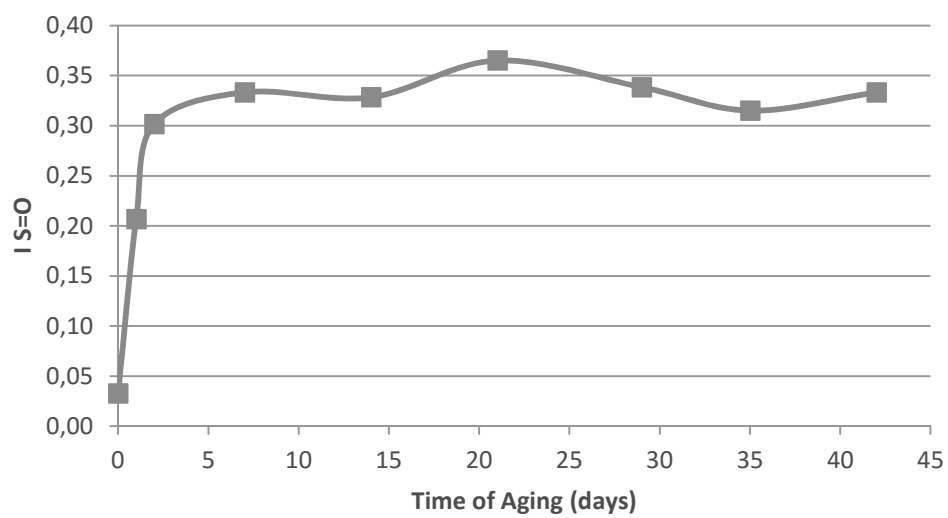


Figure 4-32 Change in  $I_{s=0}$  for 0-42 days of bitumen aging

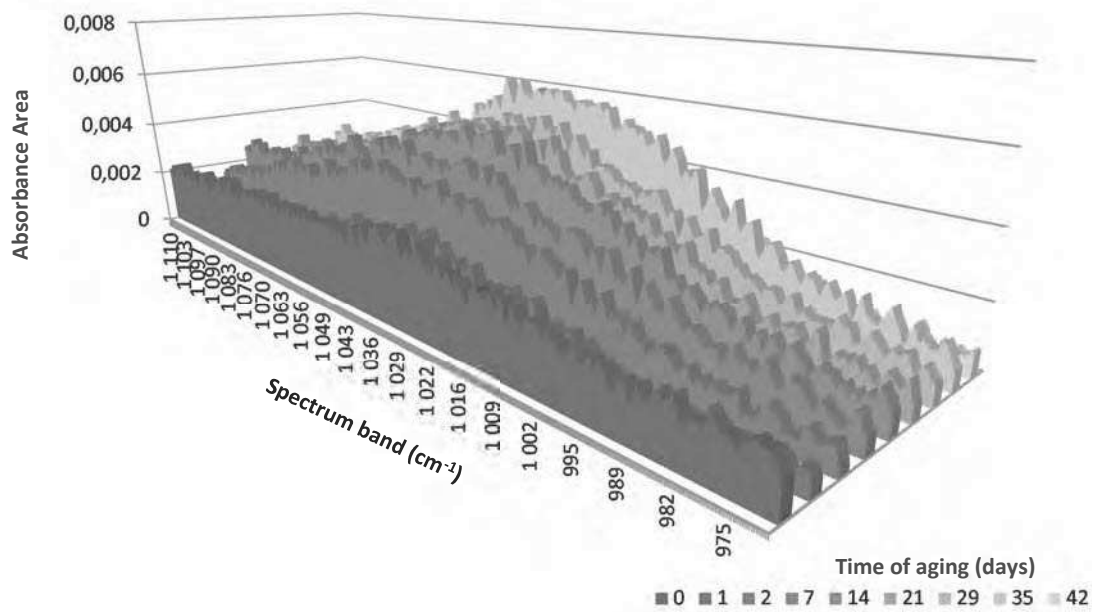


Figure 4-33 Spectra 1110-970cm<sup>-1</sup> for 0-42 days of bitumen aging

The nature of the A<sub>1600</sub> was inconclusive in the second series (Figure 4-34), increasing after 2d and further up to 29 d and descending thereafter to 42 d when the testing was terminated. An increase with aging in the A<sub>1600</sub> found with Lamontagne et al. (2001b) and Mouillet et al. (2008). The 1600cm<sup>-1</sup> can be an indicator with aging, but is much less reliable than the oxidation bands.

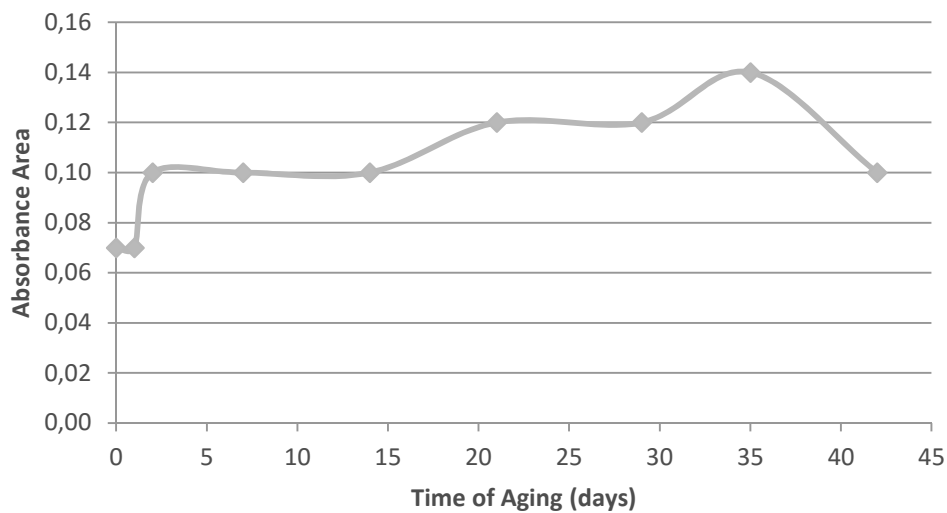


Figure 4-34 Change in A<sub>1600</sub> for 0-42 days of bitumen aging

The stretch aliphatic peaks at 2923 and 2853 $\text{cm}^{-1}$  appeared to show as small increase for the first series of aging, while being relatively stable for the second series (Figure 4-35). The deform aliphatic peaks at 1460 and 1376 $\text{cm}^{-1}$  were stable for both aging series (Figure 4-36).

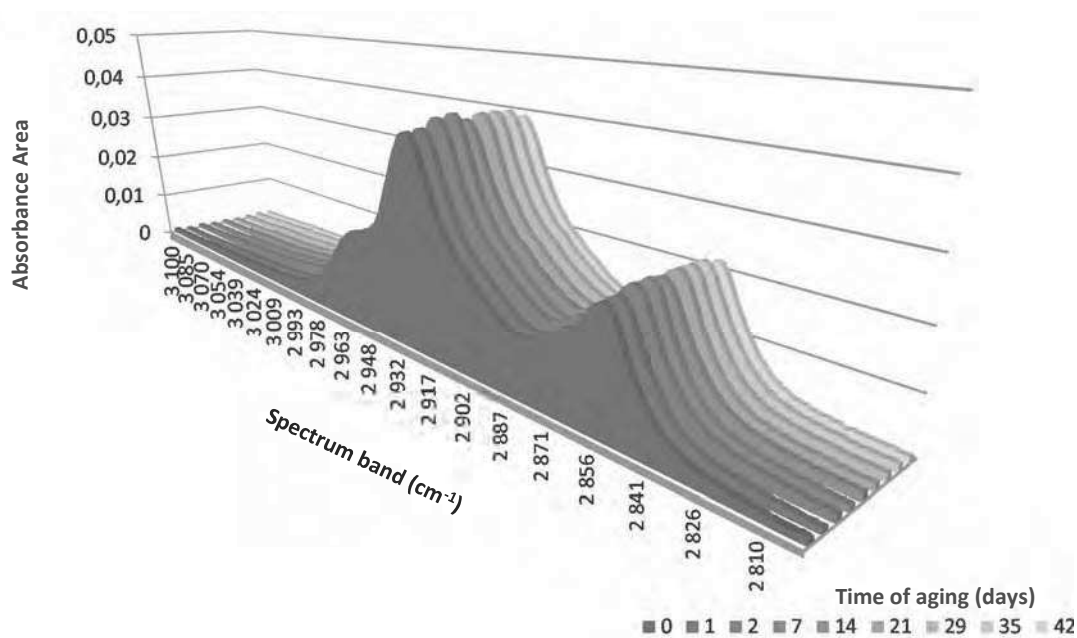


Figure 4-35 Spectra 3100-2800 $\text{cm}^{-1}$  for 0-42 days of bitumen aging

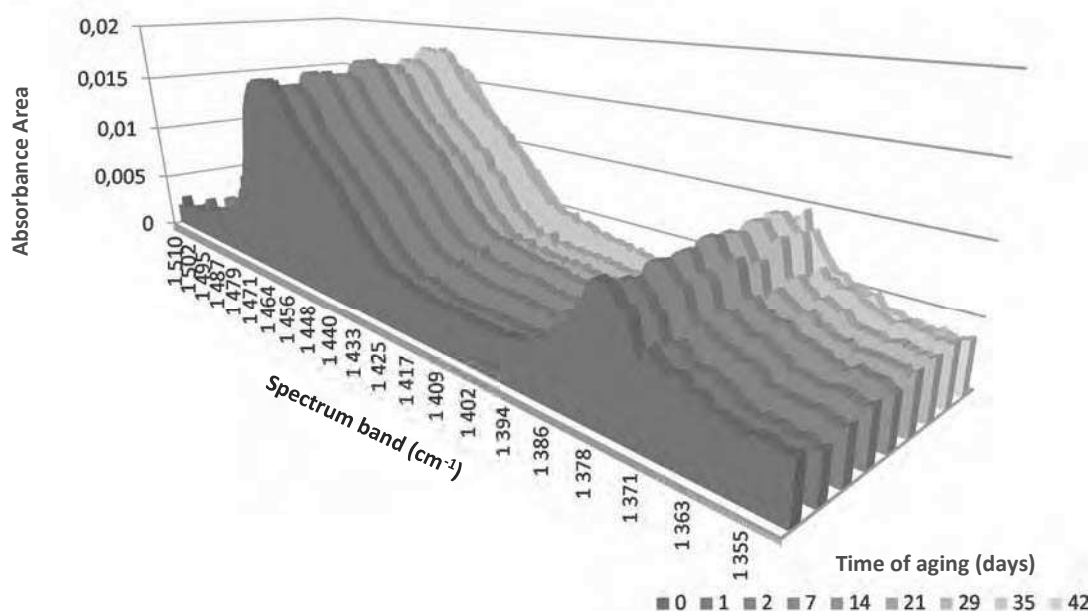


Figure 4-36 Spectra 1510-1350 $\text{cm}^{-1}$  for 0-42 days of bitumen aging

#### 4.2.2.2 Bitumen aging with TGA

The DTG analysis in air (20-800°C) of oven-aged bitumen was conducted one time respectively on a virgin sample as well as on samples aged 1, 2, 14, 29 and 42 days. From the DTG curves, there were 3 principal peaks detected: at 340, 390, 450 and 575°C (Figure 4-37).

The largest peaks occurred around 450°C, although there are actually several peaks around this area, which could correspond to different types of hydrocarbons. These peaks tended to be broader for the late aged samples (14-21 d), but higher in amplitude for the early aged samples (0-2 d).

The area for the peaks at 450°C was somewhat greater for the early aged samples (Figure 4-38). The peaks at 340 and 390°C were the smaller and occurred only for the virgin binder and the samples aged at 1 and 2 d. They correspond to the more volatile molecules in the bitumen. It is possible that the 390°C peak was also present in the later aged samples, but was not distinguishable due to the broadness of the peak.

The broad peak at 575°C occurred for all of the samples, and was somewhat greater in area for the late-aged samples (Figure 4-39). All of the samples stopped losing mass at around 700°C.

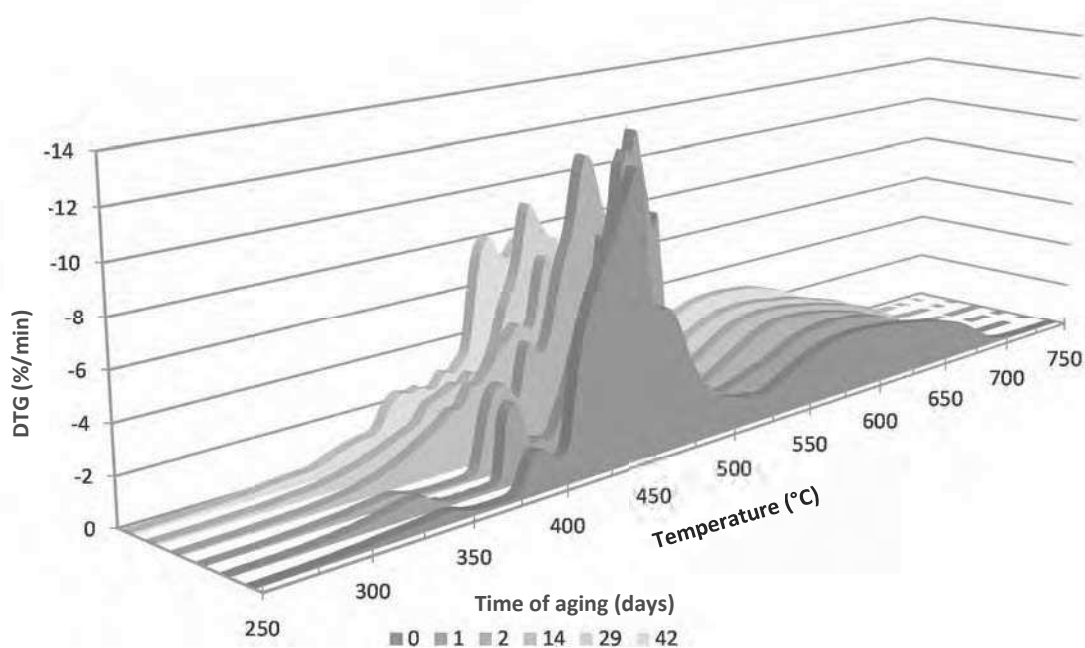


Figure 4-37 DTG in air curves for bitumen aged from 0-42 days



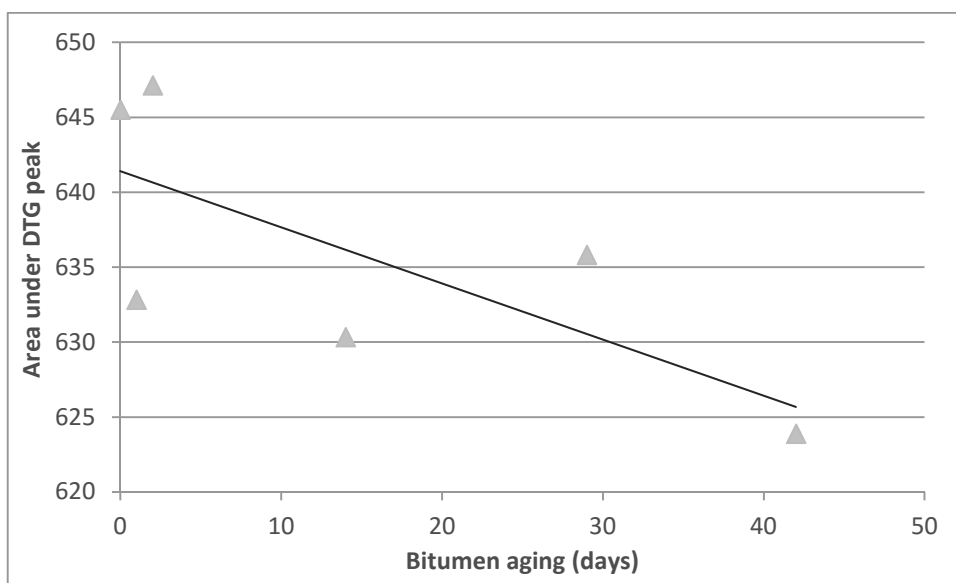


Figure 4-38 Evolution of DTG peak in air at 450°C for bitumen aging 0-42 days

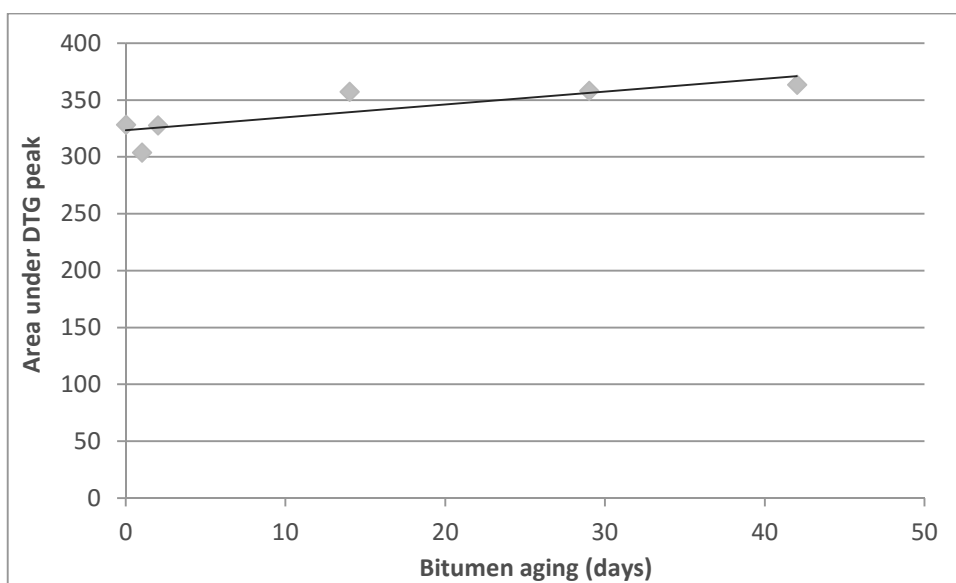


Figure 4-39 Evolution of DTG peak in air at 575°C for bitumen aged 0-42 days

Bitumen samples aged 0, 1 and 7 d were also tested by TGA in argon, which is an inert noble gas (Figure 4-40). In this case, all three samples produced one large peak at around 450°C, beginning at 350°C, with all of the samples incinerated at around 550°C. Pauli (2014) in testing SARA fractions with TGA in Ar (Figure 2-24) attributed this peak to pyrolysis of the bitumen

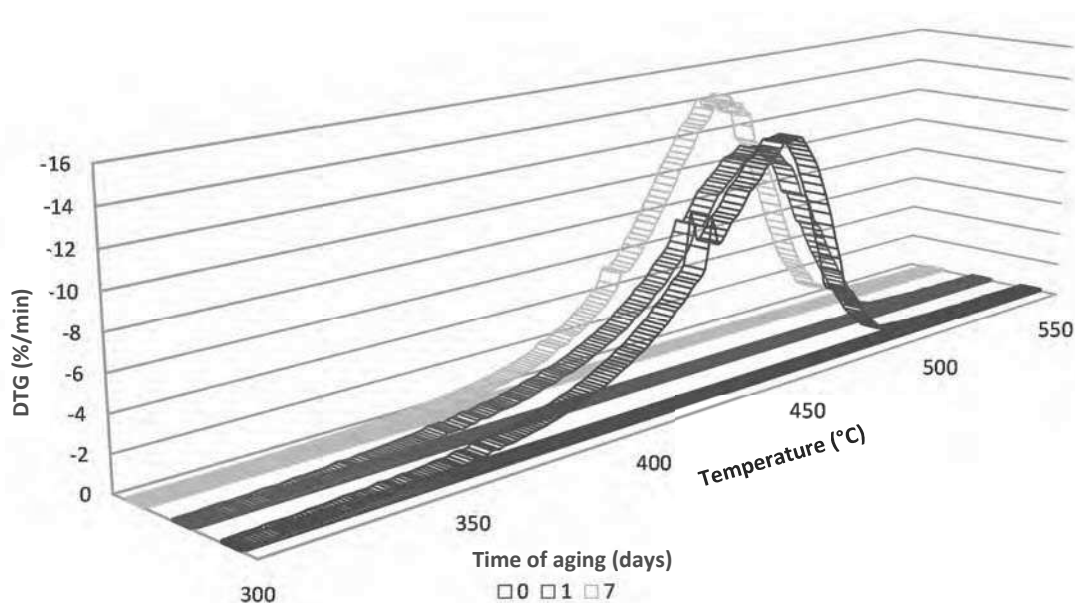


Figure 4-40 DTG in argon curves for bitumen aged from 0-7 days

There was a small peak at around 430°C (in the larger 450°C peak), that was more pronounced in the virgin binder and in the aged samples. It is possible that it corresponds to the decomposition of some lighter hydrocarbons.

The size of the peaks was similar for all of the samples, and this did not appear to be an effective method for observing bitumen aging.

The DTG analysis of bitumen confirmed that the presence of lighter hydrocarbons in bitumen decreases with bitumen aging. This was also found by Pauli (2014) in his analysis of SARA fractions in Ar, where a significant fraction of light aromatics and saturates were incinerated prior to the principal 450°C peak. The peaks around 340 and 390°C for the virgin binder and the bitumen aged 1 and 2 d should be distinguished from the tendency of the 450°C peak to begin at a lower temperature for the more aged samples. This tendency can be correlated to the results of the asphaltene fraction from Pauli (2014), where the peak around 450°C began came after a smaller peak centered around 300°C (Figure 2-24). The peak that occurred at 575°C – which has a tendency to increase with bitumen aging – was not found in other studies, although Sonibare et al. (2003) found peaks close to these temperatures in their analysis of oil sands.

#### 4.2.2.3 Evolution of rheology with bitumen aging

In a parallel study (Malet, 2015) 35/50 bitumen aged 6 h, 1, 3, 7, 11 and 18 d with the oven method was tested in penetration (EN 1426) and rheology (EN 14770); the results being compared with

those of virgin binder and binder from asphalt (recovered using ASTM D 5404) aged with the RILEM method (de la Roche et al., 2013), where the asphalt is oven aged at 135°C for 4 h and at 85°C for 9 days.

It was found that:

- the penetration result for bitumen oven aged for 11 d corresponded to the penetration bitumen aged with the RILEM method
- the rheology of the bitumen oven aged 18 d corresponded to the rheology of bitumen aged with the RILEM method, as shown in the Black curves in Figure 4-41.

In a compromise of the two bitumen characteristics, 14 d were chosen as the duration of the oven aging.

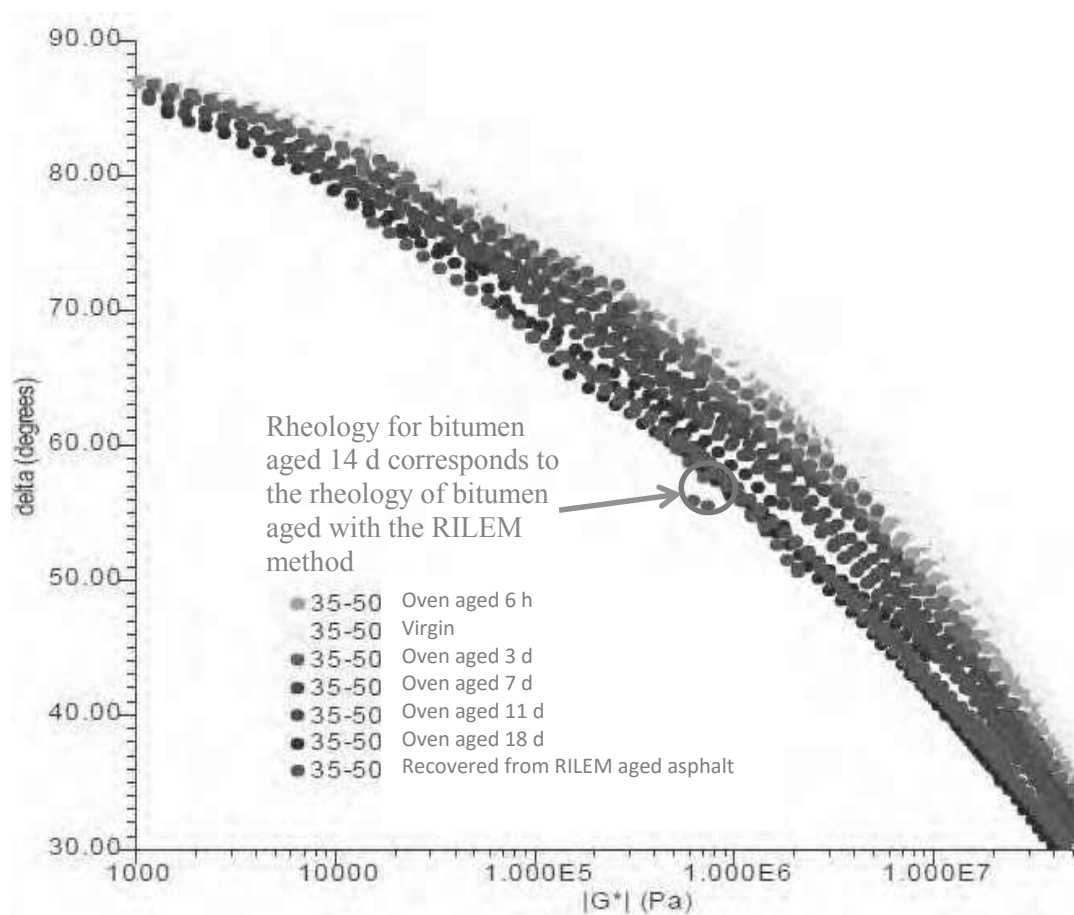


Figure 4-41 Black curved for virgin 35/50 bitumen, bitumen oven aged 0-18 d and bitumen recovered from asphalt aged with the RILEM method

#### 4.2.2.4 Bitumen rejuvenation with FTIR-ATR analysis

FTIR-ATR analysis was conducted on bitumen samples oven aged 14 d, mixed (in a metal pot at 160°C with mechanical mixer) with 20%w rejuvenating agents (B1, P1 and P2) in order to observe the effects of the rejuvenating agent on the aged bitumen. The rejuvenated samples were oven aged again for 14 d in order to observe the agents resistance to aging.

The FTIR spectra for bitumen oven aged 14 d (black), the aged bitumen rejuvenated (blue), the rejuvenated bitumen oven aged 14 d (green) and the rejuvenating agents by themselves (red) are shown in Figure 4-42, Figure 4-43 and Figure 4-44 for agents B1, P1 and P2, respectively.

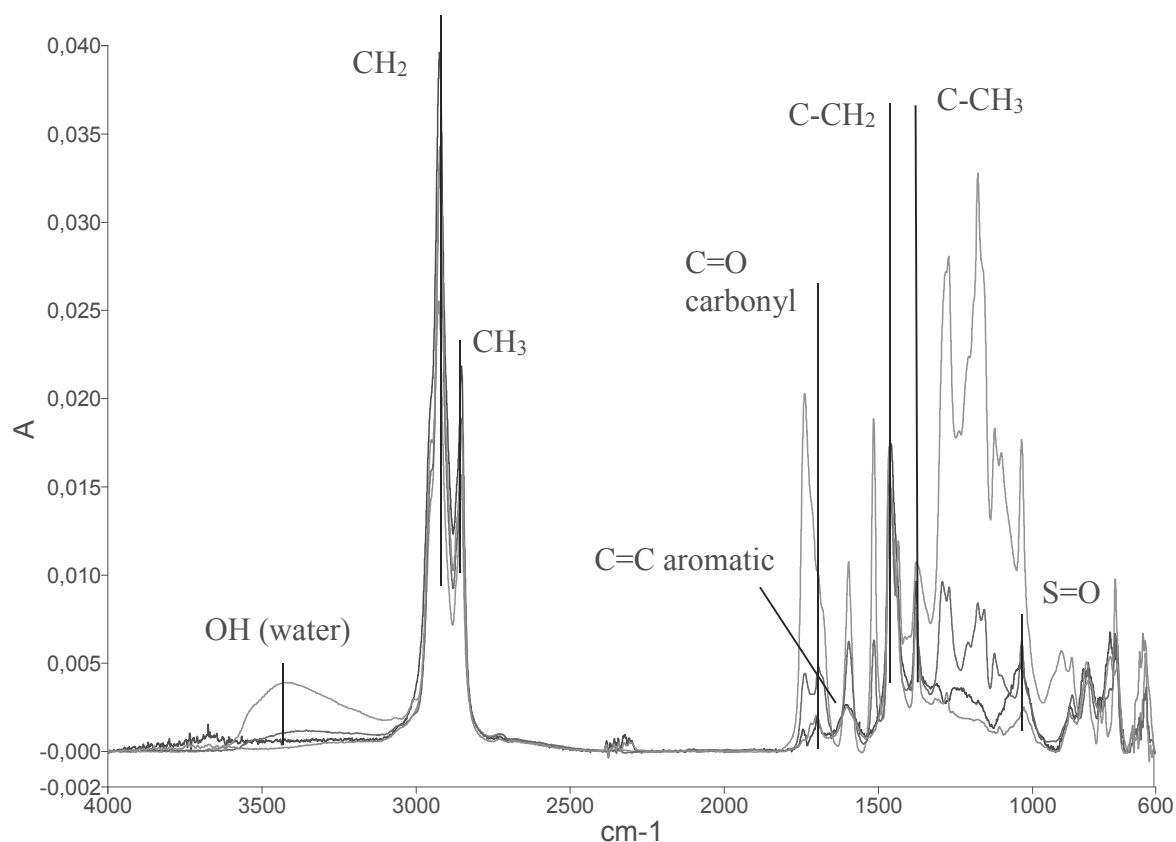


Figure 4-42 FTIR spectra for bitumen oven aged 14 days (black), the aged bitumen rejuvenated by B1 at 20%w (blue), the rejuvenated bitumen oven aged 14 days (green) and the rejuvenating agent B1 (red)

The spectra of the B1 agent corresponded to the spectra found for polyols by Lligadas et al. (2006), including a hydroxyl peak around 3450cm<sup>-1</sup>, an aliphatic ester carbonyl peak around 1750cm<sup>-1</sup> from approximately 1600-1000cm<sup>-1</sup>. The presence of peaks around that also corresponded to the oxidation indicators C=O and S=O resulted in difficulty determining the rejuvenation by the agent, especially for the rejuvenated samples (blue in Figure 4-42). The rejuvenated sample aged again for 14 d (green spectra) produced a lower intensity peak for S=O than for the aged bitumen (black

spectra). Conversely, the C=O peak was increased for the aged rejuvenated bitumen compared to the aged virgin bitumen, although this was likely due to the large peak for C=O in B1.

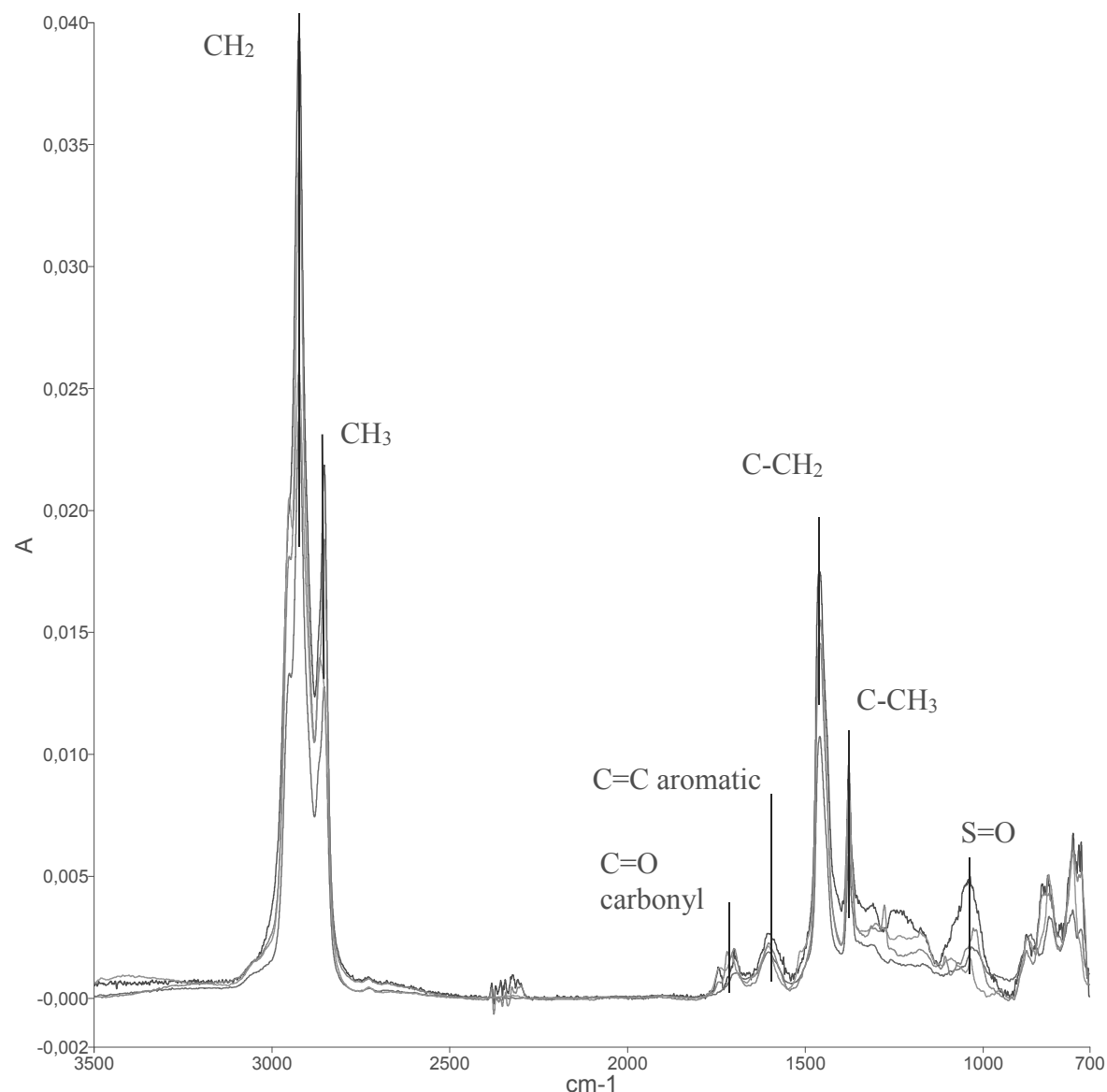


Figure 4-43 FTIR spectra for bitumen oven aged 14 days (black), the aged bitumen rejuvenated by P1 at 20%w (blue), the rejuvenated bitumen oven aged 14 days (green) and the rejuvenating agent P1 (red)

The rejuvenating agents P1 and P2 are petroleum-based like bitumen, and so have very similar FTIR spectra. Despite being much more liquid than bitumen, they produce small C=O and S=O signatures. Nevertheless, the signature for S=O is greatly reduced relative to the aged virgin binder with bitumen rejuvenation (blue spectra in Figure 4-43, Figure 4-44). This S=O is increased for the rejuvenated bitumen aged 14 d, but not to the degree of the aged virgin binder (green spectra).

The reduction of the C=O band is inconclusive, as rejuvenation with P1 and P2 does not appear to significantly decrease this band, although the band does increase when the rejuvenated bitumen is aged.

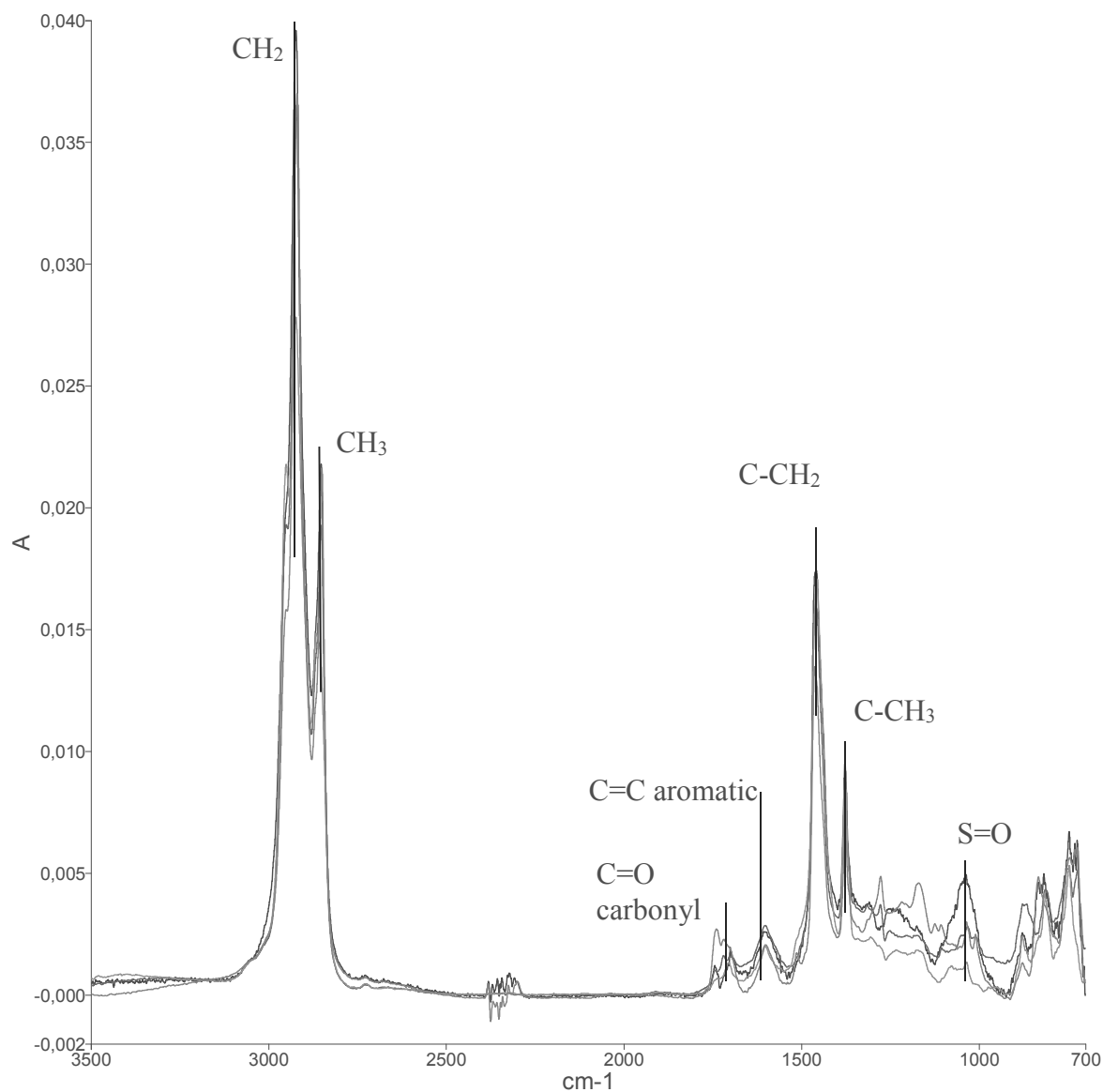


Figure 4-44 FTIR spectra for bitumen oven aged 14 days (black), the aged bitumen rejuvenated by P2 at 20%w (blue), the rejuvenated bitumen oven aged 14 days (green) and the rejuvenating agent P2 (red)

#### 4.2.2.5 Bitumen aging and rejuvenation with FTIR microscope imaging

Samples of mastic observed with FTIR-ATR imaging including (i) unaged mastic, (ii) mastic oven aged 14 d and (iii) mastic oven aged 14 d with 7.5%w of the rejuvenating agent B1, P1 or P2 added after aging.

The images were extrapolated by taking the band ratios for oxidation from the spectra. While the C=O peaks were difficult to observe, the S=O peaks appeared consistently, and thus the band ratio from Equation 2-8 was used.

The images (150x150  $\mu\text{m}$ , pixel size 1.56  $\mu\text{m}$ ) for unaged mastic and mastic aged for 14 d in an oven are shown in Figure 4-45, while the aged mastic with the rejuvenating agent B1 (at 7.5%w) is shown in Figure 4-46. The S=O index is indicated by the colour bar on the right of the images from values 0-0.1. The white regions on the graph would indicate a ration of greater than 0.1, while black regions indicate an index close to 0.

A higher  $I_{S=O}$  index (Equation 2-8) indicates a higher degree of oxidation, which is color coordinated with the legend to the right of the tables. The images show a significant increase in oxidation from the mastic oven aging for 14 d. The samples rejuvenated by B1 however, show a decrease in the S=O indicators, although not to the extent that they would resemble the virgin bitumen.

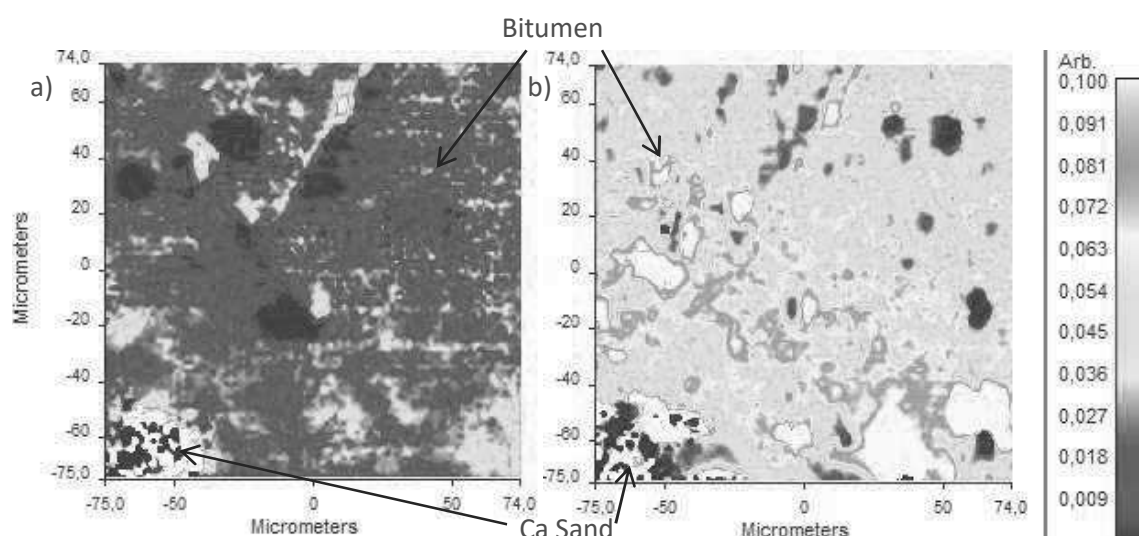


Figure 4-45 FTIR-ATR Microscope 1030 $\text{cm}^{-1}$ /(1460 +1376  $\text{cm}^{-1}$ ) band ratio images 150x150 $\mu\text{m}$ , pixel size 1.56 $\mu\text{m}$  for: a) unaged mastic and b) mastic aged for 14 days in oven (right)

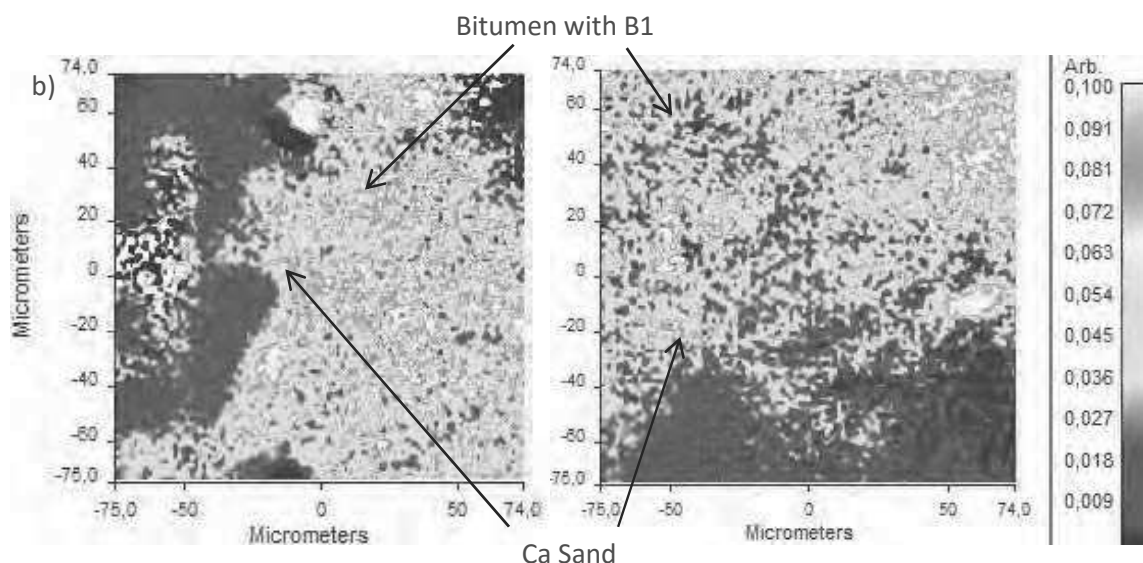


Figure 4-46 FTIR-ATR Microscope  $1030\text{cm}^{-1}/(1460 + 1376\text{ cm}^{-1})$  band ratio images  $150 \times 150\mu\text{m}$ , pixel size  $1.56\mu\text{m}$  for mastic aged for 14 days in oven WITH 7.5%w B1 added

For the mastic samples with the rejuvenating agents P1 and P2 at 7.5%w, the analysis proved more delicate as the samples melted far more easily. These difficulties required the reduction of the image acquisition time, and as such, the images were acquired with a  $6.25\mu\text{m}$  pixel size, reducing the image acquisition time approximately 3 times.

This analysis observed the unaged mastic compared with the one aged fourteen days (Figure 4-47), along with the rejuvenated samples (Figure 4-48).

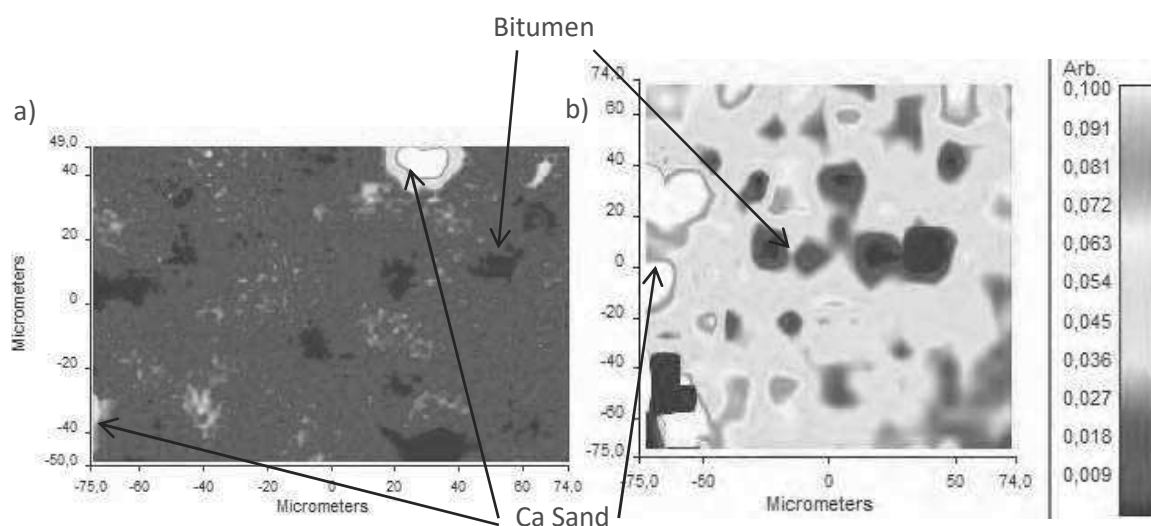


Figure 4-47 FTIR-ATR Microscope  $1030\text{cm}^{-1}/(1460 + 1376\text{ cm}^{-1})$  band ratio images pixel size  $6.25\mu\text{m}$  for: a) unaged mastic and b) mastic aged for 14 days in oven



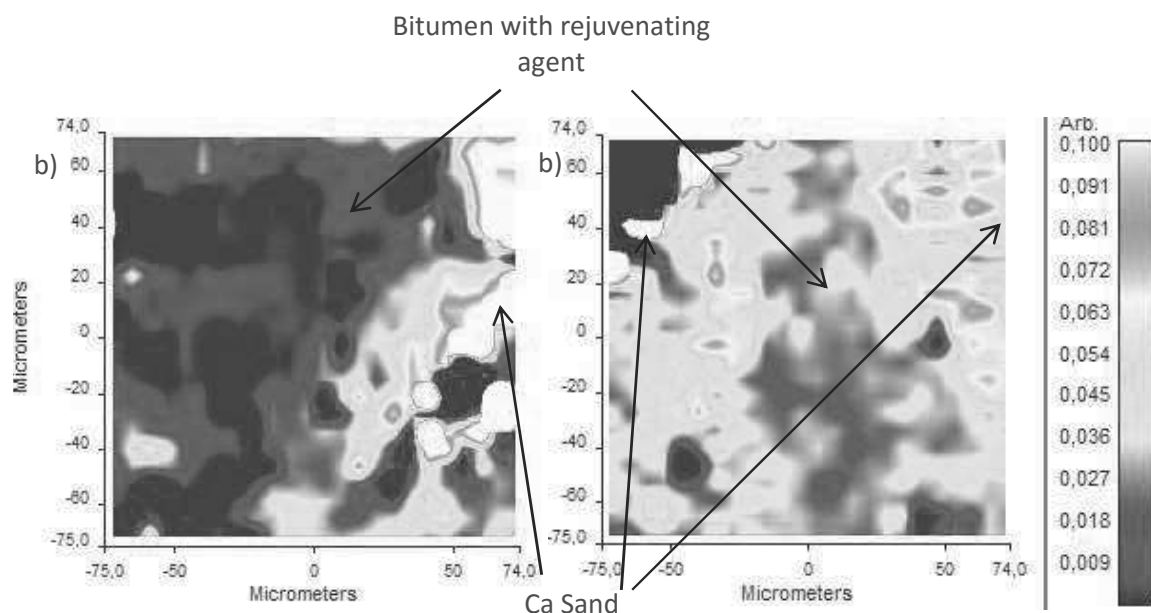


Figure 4-48 FTIR-ATR Microscope 1030cm<sup>-1</sup>/(1460 +1376 cm<sup>-1</sup>) band ratio image pixel size 6.25μm for mastic aged for 14 days in oven with a) 7.5%w P1 added and b) 7.5%w P2

As for the previous samples the bitumen aging increases the S=O band relative to the 1460 and 1376cm<sup>-1</sup> aliphatic bands. This band is decreased in the rejuvenated samples, especially for the samples with P1. The S=O band appears to increase the closer it is to the aggregate. Reduction of the  $I_{S=O}$  by the rejuvenating agents is much more significant away from the aggregates than next to them.

In the final analysis, the S=O indices proved to be a clearer indication of oxidation than the C=O indices, which possible showed a need to increase the accuracy of the FTIR analysis by having more scans per analysis for example, or improving the surface polishing. The band ratio for  $I_{S=O}$  allowed for the distinction of the bitumen zones from the aggregates. The mastic aged for 14 d indicated significantly higher oxidation than the unaged mastic, having zones exceeding 0.05 for the most part and a significant quantity of zones exceeding 0.1, while the unaged mastic was around 0.02-0.03. The bitumen showed higher oxidation around the sand, due to the oxidation that is induced by the hot aggregates on the bitumen during mixing (Atkins, 2003; Chen et al., 2007). However, in general, the pattern of oxidation was not consistent, similar to the experience of El Béze (2008). The addition of the rejuvenating agents resulted in a decrease in the oxidation overall, having a lower quantity of zones above 0.1, although it is not certain whether it is from a dilution effect or from chemical changes. This effect was even more significant for the agents P1 and P2. The fact that the quantity of

the agents was only 7.5%w could indicate that this was not solely a dilution effect. The spots of +0.1 absorbance for B1 also appear to be much less coagulated than for the aged bitumen.

The melting of the bitumen during the test was found to be a serious problem with FTIR microscopy in terms of getting a clear analysis, especially for the samples with P1 and P2, which significantly liquefied the bitumen.

#### ***4.2.2.6 Rheology of rejuvenated bitumen***

A parallel study (Malet, 2015) observed the viscosity studied the rheology of bitumen aged by RTFOT+PAV (Section 2.3.1.1.1) along with bitumen rejuvenated; with P1, P2 and B1 mixed with the RTFOT+PAV aged binder at the quantity (%w) needed for the aged binder to have a penetration equivalent to a 35/50 binder.

This was compared to virgin binder as shown in Figure 4-49. As observed in Figure 4-41, the aging of bitumen has a tendency to produce lower values for phase angle on the Black curve, indicating amore elastic and stiffer bitumen. The rejuvenating agents made the bitumen more viscous and less stiff, with agents P1 and B1 modifying the rheology somewhat more than P2 at their respective dosages. Nevertheless, these dosages were not enough to restore the aged bitumen rheology to that of a virgin 35/50 bitumen for the same penetration. This indicated that these agents served more as softeners than rejuvenators, although some degree of both is likely present.

This confirms as found by (Loeber et al., 1998), that the rheology of a bitumen does not necessarily correspond to the penetration, as the rejuvenating agents were able to restore the penetration of the aged bitumen more effectively than the rheology.

Something else to consider is the higher dispersion of the points with the rejuvenating agents. This indicates that the rejuvenated bitumen has more phases than the virgin and aged binder (Peralta, 2009). This dispersion is especially significant for the samples with the bio-sourced agent, which appears to have more difficulty in blending with the new binder than the petroleum-based agents. This can be attributed to the chemistry of the bio-sourced agents being having less in common with the chemistry of the petroleum based bitumen.

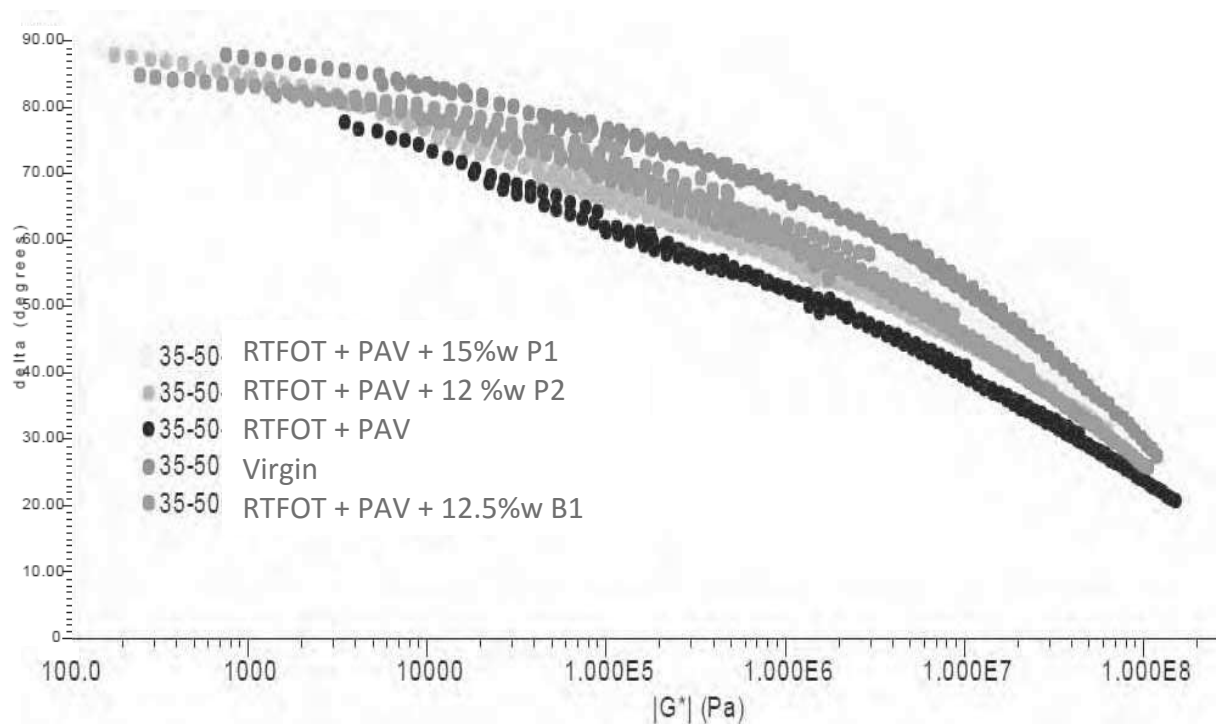


Figure 4-49 Black curves for virgin 35/50 bitumen, 35/50 bitumen aged by RTFOT+PAV, 35/50 bitumen aged by RTFOT+PAV with 15%w P1, 35/50 bitumen aged by RTFOT+PAV with 12%w P2, 35/50 bitumen aged by RTFOT+PAV with 12.5%w B1

### 4.3 Conclusions on bitumen aging, rejuvenation and remobilization

The principal findings of the study on bitumen aging, rejuvenation and remobilization are:

- The testing of bitumen samples in SEM at ambient temperature melts the bitumen. This also floods the chamber with C particles from their contact with the electron beam that in turn, altered the EDS analysis;
- The use of a Peltier device for cooling the bitumen sample prevented the melting of the sample, and reduced the fluorescence of C by the electron beam. Nevertheless, the potential damage to the SEM from bitumen observation is still present, meaning that this study was not able to observe the remobilization of aged bitumen by this technique;
- TGA bitumen found the bitumen is less volatile the more oven aging it has undergone;
- The decomposition of bitumen in Argon produces one large DTG peak, while decomposition of bitumen in air produces two;
- Silicone was an adequate material for aging bitumen due to the fact that it does not adhere to the bitumen;

- The volatilization of bitumen (mass loss), occurred for the most part during the first 24h of aging;
- In the FTIR-ATR analysis of oven-aged bitumen, the spectra for C=O and especially S=O were found to be the most consistent indicators of bitumen aging;
- An oven-aging time of 14 days was found to be appropriate aging duration due to the correspondence of oven aging to RTFOT+PAV at 11 d for penetration and 18 d for rheology;
- FTIR imaging found that the oxidation of bitumen is higher closer to the aggregate;
- Rejuvenating agents have shown a capacity to reduce oxidation ( $I_{S=O}$ ). This effect is reduced the closer the bitumen is to the aggregate. The rejuvenating agents were also capable of restoring the penetration and rheology of aged bitumen, however, they were more effective in restoring the penetration than rheology;
- The bio-sourced agent restores the penetration of aged bitumen at a similar level to the petroleum based P2 and more effectively than P1. For the same penetration, B1 restored bitumen rheology more effectively than P2 and about as effectively as P1. Nevertheless, B1 had more difficulty in blending with the bitumen than the petroleum based agents as revealed by a relatively larger phase variety in rheology relative to bitumen rejuvenated by petroleum-based agents.

## 5 General conclusions and perspectives

The use of petroleum based products as construction products such as asphalt release agents and rejuvenating agents has become more difficult to justify as there is new evidence emerges of the danger they pose to both workers' health and the environment. This has resulted in the banning of diesel from construction sites as an asphalt release agent.

The need for bio-sourced alternatives has been met with increased research in bio-sourced alternatives, especially in terms of asphalt rejuvenating agents, although these have yet to see significant use in the industry. On the other hand, there has been a number of bio-sourced commercial asphalt release agents developed, although some have been damaging to asphalt

In the scope of the AGRIBTP project objective to develop the production of bio-sourced agents for the construction industry, this work was focused around the developed of agents for the asphalt industry: an asphalt release agent (in the context of which a bitumen remover was developed) and a rejuvenating agent.

Due to a lack of available test methods for our agents, in order to determine of the performance and understand the methods of action of the ARAs and bitumen removers (BRs), several methods were developed. This was followed by the evaluation of commercial ARAs and BRs in order to understand how they function and establish a baseline for their performance. This was completed with the development and evaluation of bio-sourced candidate formulations as ARAs and BRs.

For the rejuvenating agents, it was also necessary to develop test methods, with particular focus on the understanding of bitumen oxidation and its reduction by the addition of a rejuvenating agent as well as bitumen remobilization, although the latter was not fully explored. The development of these techniques – which also included an oven-aging method – allowed the evaluation of a bio-sourced agent developed for this project and its evaluation compared to commercial petroleum based agents.

Asphalt release agents (ARAs) are sprayed on surfaces used in asphalt construction (truck beds, pavers, finishers, tools) in order to prevent bitumen from sticking to them. For ARAs, the traditional product, diesel fuel, has seen a significant reduction in its use due to its interdiction as an ARA in many countries such as France and the USA as well as the development of new bio-sourced agents. These ARAs are said to function as surfactants, creating a barrier between the asphalt and the surface of application. While these agents have been shown to be less harmful than diesel to the environment, they have been found at times to be less effective than diesel in reducing the adhesion

of bitumen to surfaces. ARAs that have been based on organic C18 esters are seeing wide use in France. While the damage to the asphalt that they can has been shown to be less than that for diesel, the results have been varied, with some agents causing significant bitumen degradation.

While there does exist a testing program for the performance and damage to asphalt for ARAs (NTPEP, 2014), its results are subjective. For bitumen removers, no such testing program exists for BRs. It was therefore necessary to develop a testing program for the performance of ARAs and BRs than can provide qualitative results, with the further goals of the classification of the agents available on the market and the development of superior performing agents.

The bitumen, which is classified by its penetration value, is affected by aging. The aging of bitumen occurs in the short term during its storage and mixing in asphalt pavement, and long term, through oxidation and exposure to outdoor conditions. This makes the bitumen hard and brittle, forming cracks in the road and necessitating the road replacement. This road can further be recycled to form RAP, which can in turn be incorporated into asphalt pavement.

The laboratory aging of bitumen can be performed with thin-film oven and convection oven methods. The aging can be observed through several physical and mechanical techniques. The principle mechanical properties of bitumen affected by aging are penetration, viscosity, rheology, ductility and low-temperature cracking the same properties that are affected in the hardened bitumen of RAP aggregates. The performance of the RAP-bitumen relative to these properties are improved with the use of rejuvenating agents, which can be sourced from petroleum or bio-based.

There are several techniques for chemically observing bitumen aging. These include FTIR, SARA classification and AFM. FTIR imaging is of particular interest relative to RAP in bitumen due to the possibility of observing bitumen oxidation signatures relative to the position of the binder and the aggregates. It remains to be seen if FTIR can also be applied to bitumen rejuvenation. This research project aimed to further develop these techniques.

### **Determination of the performance and damage to asphalt of bio-sourced asphalt release agents and bitumen removers**

Test methods for the determination of the performance and damage to asphalt of bio-sourced ARAs were developed and optimized in the frame of this study. The development of these test methods would allow for the evaluation of the biodegradable commercial ARAs available to the authors, including C18 ester based agents and a silicone in water emulsion with the addition of a surfactant.

The asphalt slide test aims to evaluate the performance of ARA. The test consists of sliding hot asphalt on an inclined steel plate where an ARA has been applied. It provides two indicators of ARA performance including mass of asphalt residue (residual mass of ARA for the barrier agents), and time for mixture to begin sliding after inclination (retention time). It was shown that the residual mass for the asphalt slide test (AST) has less variability and likely a more significant indicator of performance than the retention time. For the AST, heating under the plate is needed for the mixture to begin sliding on the ARA-PEA.

The testing of asphalt mix degradation was based on determining the reduction in resistance of asphalt in contact with ARAs, where the agent is applied in the middle of the flat side of a cylindrical sample with a pipette. The samples subject to CBR-loading did not produce reproducible or coherent results. The testing of asphalt mix degradation by ARAs with indirect tensile strength (ITS) testing produced reproducible results and was able to differentiate the damage from ARAs and BRs. A dosage of 1mL for the asphalt mix degradation by ARAs with ITS produced results that enabled the discrimination of agents that are intended to degrade asphalt mix and those that are not. Compaction of the asphalt mix by compression as opposed to proctor produced more consistent samples in terms of density distribution for the testing of damage to asphalt.

A third type of test, bitumen degradation test (BDT), was implemented. It consisted in submerging a bitumen sample in an agent for 24 h. From this, the change in mass of the bitumen sample was measured, and the residual liquid analyzed in BDT. It was found to be a measure of both (i) the safety of the ARAs vis-à-vis asphalt and (ii) a measure of performance for BRs.

The reduction in resistance for asphalt mix by ITS showed a strong correlation with BDT, with the C18 based ARAs degrading the asphalt more in ITS than a commercial agent functioning as substrate. The latter was adsorbed by the bitumen to a small degree, and the ITS indicated that it weakened the bitumen to an extent, though to a lower degree than the other C18 based ARAs.

The bitumen degradation test at 1 day was able to differentiate the damage from ARAs and BRs on bitumen with low variability, proving this to be a simple and efficient test for bitumen degradation from ARAs and BRs.

The most effective BRs among the C18 based agents corresponded to those that had the highest ester concentrations. Shorter chained esters are strong candidates for use as BRs due to their high degradation performance in BDT, significantly higher than the best performing commercial BRs in this study, as well as diesel fuel.

In terms of FTIR-ATR analysis for the interaction between bitumen and C18 ester based ARAs and BRs (as found by GC analysis), the presence of a  $1600\text{cm}^{-1}$  aromatics peak in the BDT solution correlates with bitumen degradation.

Two ARA modes of functioning were highlighted: as a bitumen softener (diesel C18 ester based agents) and as a substrate (surfactant in water emulsion). Although the C18 based ARAs were the best performing ARAs in AST in terms of time to beginning of slide, the results of the AST with the agents that act as a substrate indicated that the most important criteria for this test was the nature of the residual mass. Since the use of substrate agents leaves a plate that does not contain any bitumen residue, it is hypothesized that it is a superior performing ARA. Furthermore, since the residual mass is the agent itself, it does not need to be cleaned off, adding an economic benefit. The substrate agents, particularly the commercial barrier agent, are significantly less damaging to asphalt. In-field testing is needed to confirm this hypothesis.

Two surfactant-based ARA candidate formulations were developed in the context of the AGRIBTP project that were based on chemicals sourced from byproducts of agroindustry: glycerol undecenoate (MUG) and diglycerol undecenoate (MUDG). The glycerol based agents were mixed with both water and these formulations produced results comparable to the commercial substrate agent in terms of being adsorbed by the bitumen and having only the agent left on the plate after the AST.

MUG appeared to be a more effective substrate than MUDG when the agents were used mixed with water. MUDG was more adsorbed in the bitumen than MUG when both were mixed with water. However MUDG mixed with acetone was a more effective substrate than the latter mixed with MUG.

The performance characteristics in AST of MUG with water at 20% were superior to the commercial substrate in having a higher residual mass and lower time to beginning of slide. Never the less, the commercial substrate agent was less degrading to the asphalt in ITS.

### **Physico-chemical characterization of bitumen aging, rejuvenation and remobilization by rejuvenating agent**

The goal of this part of the study was to develop methods for bitumen aging (oven aging, adapted from RILEM method for aging asphalt) along with the evaluation of remobilization (SEM) and rejuvenating (FTIR, TGA). These methods were to be used to evaluate the performance of a bio-sourced rejuvenating agent compared to petroleum sourced commercial ones.



The testing of bitumen samples in SEM at ambient temperature melted the bitumen, which was a problem due to the bitumen moving during the analysis. Additionally, this flooded the SEM chamber with C particles from the bitumen from their contact with the electron beam that in turn, altered the EDS analyses of the bitumen, sand and tracers added in the bitumen with the goal of analyzing remobilization. The use of a Peltier device for cooling the bitumen sample prevented the melting of the sample, and reduced the fluorescence of C by the electron beam. Nevertheless, the potential damage to the SEM from bitumen observation was still present, meaning that this study was not able to observe the remobilization of aged bitumen by this technique.

TGA bitumen found the bitumen is less volatile the more oven-aging it has undergone. The volatilization of bitumen (mass loss), occurred for the most part during the first 24h of aging.

In the FTIR-ATR analysis of oven-aged bitumen, the spectra for C=O and especially S=O were found to be the most consistent indicators of bitumen aging.

An oven-aging time of 14 days was found to be appropriate aging duration due to the correspondence of oven aging to RTFOT+PAV at 10d for penetration and 18d for rheology.

FTIR imaging found that the oxidation of bitumen is higher closer to the aggregate.

Rejuvenating agents have shown a capacity to reduce oxidation ( $I_{S=O}$ ). This effect is reduced the closer the bitumen is to the aggregate. The bio-based rejuvenating agents were also capable of restoring the penetration and rheology of aged bitumen at a level similar or better than the petroleum-based agents, although there was less blending with the aged binder resulting in more phases. All of the agents were more effective in restoring the penetration than rheology.

The work for asphalt remobilization and rejuvenation by rejuvenating agents was unfortunately not carried through all the way. For the remobilization, the damage to the SEM apparatus itself is the limiting factor.

## **Perspectives**

With this research completed, a number of interesting conclusions have been drawn from it. Nevertheless, there remained a considerable amount of space for further development.

With regards to ARAs, the method of testing how weakened the asphalt pavement is from contact with the ARAs could be improved through pre-cutting the sample at the tensile place, possibly improving the consistency of the ITS results.

The testing of the ARA performance could be built upon if the barrier agents were tested for multiple asphalt loads. This would make the AST test more dynamic in adding an agent lifespan component. This should also be combined with testing in the field.

For the analysis of bitumen remobilization, an ESEM would have been more appropriate in this type of analysis than a SEM. The structures from the SEM beam have been studding with aging by others. This could be built upon by observing the structures for the aged bitumen rejuvenated.

The work with rejuvenating agents could have benefited from the rejuvenated samples tested in FTIR-ATR imaging and rheology being aged again at 14 days in order to better evaluate their resistance to aging.



## References

- Acton, Q.A., 2013. *Silicones—Advances in Research and Application*. Scholarly Editions, Atlanta, Georgia.
- Aguiar-Moya, J.P., Villegas-Villegas, R.E., Loria-Salazar, L.G., Salazar-Delgado, J., 2013. Use of Waste Products as Bitumen Modifiers in Costa Rica.
- Airey, G.D., 2003. State of the art report on ageing test methods for bituminous pavement materials. *Int. J. Pavement Eng.* 4, 165–176.
- Al-Qadi, I.L., Elseifi, M., Carpenter, S.H., 2007. Reclaimed Asphalt Pavement – A Literature Review. *Urbana* 51, 61801.
- Altgen, K.H., Harle, O.L., 1975. The effect of asphaltenes on asphalt viscosity. *Ind. Eng. Chem. Prod. Res. Dev.* 240–247.
- Anagnos, J.N., Kennedy, T.W., 1972. Practical method of conducting the indirect tensile test. Center for Highway Research University of Texas at Austin.
- Araújo, M.F. a. S., Lins, V.F.C., Pasa, V.M.D., 2011. EFFECT OF AGEING ON POROSITY OF HOT MIX ASPHALT. *Braz. J. Pet. Gas* 5. doi:10.5419/bjpg.v5i1.145
- Aravind, K., Das, A., 2007. Pavement design with central plant hot-mix recycled asphalt mixes. *Constr. Build. Mater.* 21, 928–936. doi:10.1016/j.conbuildmat.2006.05.004
- Artamendi, I., Allen, B., Ward, C., Phillips, P., 2012. Differential Thermal Contraction of Asphalt Components, in: Scarpas, A., Kringos, N., Al-Qadi, I., A, L. (Eds.), 7th RILEM International Conference on Cracking in Pavements, RILEM Bookseries. Springer Netherlands, pp. 953–962.
- Atkins, H.N., 2003. *Highway materials, soils, and concretes*. Prentice Hall, Upper Saddle River.
- Bahia, H.U., Coenen, A., Tabatabaee, N., 2013. Mixture Design and Compaction, in: *Advances in Interlaboratory Testing and Evaluation of Bituminous Materials*. Springer, pp. 361–428.
- Ballenger, W.T., Jr., Light, T.J., Sr., 1993. Method of prevention of adhesion of hot-mix asphalt to containers and equipment. U.S. Patent 5186979.
- Barman, B.N., Cebolla, V.L., Membrado, L., 2000. Chromatographic techniques for petroleum and related products. *Crit. Rev. Anal. Chem.* 30, 75–120.
- Benbouzid, M., Hafsi, S., 2008. Thermal and kinetic analyses of pure and oxidized bitumens. *Fuel* 87, 1585–1590. doi:10.1016/j.fuel.2007.08.016

Bergmann, U., Mullins, O.C., Cramer, S.P., 2000. X-ray Raman Spectroscopy of Carbon in Asphaltene: Light Element Characterization with Bulk Sensitivity. *Anal. Chem.* 72, 2609–2612. doi:10.1021/ac990730t

Boussambe, G.N.M., 2015. Utilisation d'une composition comprenant un mono- ou di-alkylénate en C7-C15 de mono- à tétra- (trialkanol en C3-C6) comme auxiliaire de mise en œuvre de produits bitumineux et/ou de béton. Doctoral Thesis, Laboratoire de Chimie Agro-industrielle, INRA, Toulouse, France.

Brownridge, J., 2010. The role of an asphalt rejuvenator in pavement preservation: use and need for asphalt rejuvenation, in: First International Conference on Pavement Preservation.

Bymaster, D.L., Smith, K., 2009. Asphalt Release Agent and Method of Use, U.S. Patent Application 2009/0038503.

Carbonneau, X., 2003. Evaluation of the indirect tensile stiffness modulus test. RILEM Publications SARL, pp. 308–315. doi:10.1617/2912143772.038

Carpenter, S.H., Wolosick, J.R., 1980. Modifier influence in the characterization of hot-mix recycled material. *Transp. Res. Rec.*

Cataldo, F., Keheyani, Y., Baccaro, S., 2004. The effect of gamma-irradiation of anthracite coal and oil bitumen. *J. Radioanal. Nucl. Chem.* 262, 443–450. doi:10.1023/B:JRNC.0000046775.43731.5d

Chávez-Valencia, L.E., Manzano-Ramírez, A., Alonso-Guzmán, E., Contreras-García, M.E., 2007. Modelling of the performance of asphalt pavement using response surface methodology—the kinetics of the aging. *Build. Environ.* 42, 933–939. doi:10.1016/j.buildenv.2005.10.013

Chen, J.S., Huang, C.C., Chu, P.Y., Lin, K.Y., 2007. Engineering characterization of recycled asphalt concrete and aged bitumen mixed recycling agent. *J. Mater. Sci.* 42, 9867–9876. doi:10.1007/s10853-007-1713-8

Chen, X., Huang, B., 2008. Evaluation of moisture damage in hot mix asphalt using simple performance and superpave indirect tensile tests. *Constr. Build. Mater.* 22, 1950–1962.

Chesky, S.R., 2001. Bituminous substance removal composition, PCT International Application WO2002008379.

Chesky, S.R., 2003. Bituminous substance removal composition. U.S. Patent App. 10/375,956.

Crum, J., 2008. Asphalt release agent automated spray system. US20080185455 A1.

Curtis, C.W., 1992. Investigation of asphalt-aggregate interactions in asphalt pavements. *Am. Chem. Soc. Fuel* 37, 1292–1297.

Dave, E.V., Braham, A.F., Buttlar, W.G., Paulino, G.H., 2011. Development of a flattened indirect tension test for asphalt concrete. *J. Test. Eval.* 39.

Davidson, D.D., Canessa, W., Escobar, S.J., 1978. Single additive recycling for asphalt pavements. Civ. Eng.-ASCE.

Davies, G., 2005. Release agent formulas and methods, U.S. Patent 6902606.

De Bock, L., Goncalves, A., 2006. Use of Recycled Materials. Rep. 30 Use Recycl. Mater.-Final Rep. RILEM Tech. Comm. 198-URM 45.

Dehouche, N., Kaci, M., Mokhtar, K.A., 2012. Influence of thermo-oxidative aging on chemical composition and physical properties of polymer modified bitumens. Constr. Build. Mater. 26, 350–356. doi:10.1016/j.conbuildmat.2011.06.033

De la Roche, C., Van de Ven, M., Planche, J.-P., Van den Bergh, W., Grenfell, J., Gabet, T., Mouillet, V., Porot, L., Farcas, F., Ruot, C., 2013. Hot Recycling of Bituminous Mixtures, in: Advances in Interlaboratory Testing and Evaluation of Bituminous Materials. Springer, pp. 361–428.

Delmas, G.-H., 2011. La Biolignine<sup>TM</sup> : Structure et Application à l'élaboration de résines époxy (phd).

DeLong, W.M., 1994. Asphalt release agent and system. U.S. Patent 5322554.

DeLong, W.M., 1996. Asphalt release agent. U.S. Patent 5494502.

Di Benedetto, H., Gabet, T., Grenfell, J., Perraton, D., Sauzéat, C., Bodin, D., 2013. Mechanical Testing of Bituminous Mixtures, in: Partl, M.N., Bahia, H.U., Canestrari, F., Roche, C. de la, Benedetto, H.D., Piber, H., Sybilski, D. (Eds.), Advances in Interlaboratory Testing and Evaluation of Bituminous Materials, RILEM State-of-the-Art Reports. Springer Netherlands, pp. 143–256.

Dituro, M.A., Lockwood, F.E., Dotson, D.J., Fang, J., 2002. Asphalt release agent, U.S. Patent 648624926.

Dunning, R., Mendenhall, R., 1978. Design of Recycled Asphalt Pavements and Selection of Modifiers, in: Recycling of Bituminous Pavements: A Symposium. ASTM International.

Durand, M., Mouret, A., Molinier, V., Féron, T., Aubry, J.-M., 2010a. Bitumen fluxing properties of a new class of sustainable solvents: The isosorbide di-alkyl ethers. Fuel 89, 2729–2734. doi:10.1016/j.fuel.2010.03.027

Durand, M., Mouret, A., Molinier, V., Féron, T., Aubry, J.-M., 2010b. Bitumen fluxing properties of a new class of sustainable solvents: The isosorbide di-alkyl ethers. Fuel 89, 2729–2734. doi:10.1016/j.fuel.2010.03.027

Durrieu, F., 1977. Influence des produits polaires des bitumes routiers sur leurs propriétés interfaciales. Bull liaison lab ponts chauss.

Durrieu, F., Farcas, F., Mouillet, V., 2007. The influence of UV aging of a Styrene/Butadiene/Styrene modified bitumen: Comparison between laboratory and on site aging. Fuel 86, 1446–1451. doi:10.1016/j.fuel.2006.11.024

- Edwards, Y., 2005. Influence of waxes on bitumen and asphalt concrete mixture performance. KTH.
- Eisenberg, D.S., Kauzmann, W., 1969. The Structure and Properties of Water. Oxford University Press.
- El Béze, L., 2008. Recyclage à chaud des agrégats d'enrobés bitumineux: Identification de tra-ceurs d'homogénéité du mélange entre bitume vieilli et bitume neuf d'apport. Doctoral Thesis, Université Paul Cézanne Aix-Marseille III, Marseille.
- El Béze, L., Rose, J., Mouillet, V., Farcas, F., Masion, A., Chaurand, P., Bottero, J.-Y., 2012. Location and evolution of the speciation of vanadium in bitumen and model of reclaimed bituminous mixes during ageing: Can vanadium serve as a tracer of the aged and fresh parts of the reclaimed asphalt pavement mixture? *Fuel* 102, 423–430. doi:10.1016/j.fuel.2012.06.080
- Escadeillas, G., Jackubowski, M., Ringot, E., Lelarge, A., Limon, S., Mazars, M., Navarre, P.H., Tiraby, H., 2011. Recherche d'un produit anti-adhérent pour les bitumes à chaud. Report for USIRF, Université Paul Sabatier, Toulouse, France. 2011.
- Escadeillas, G., Ringot, E., 2011. Qualification des anti-adhérents pour enrobés. Report for USIRF, Université Paul Sabatier, Toulouse, France. 2011.
- Eschbach, A.R., 1993. Dynamic shear rheometer and method. US5271266 A.
- Esteban, B., Riba, J.-R., Baquero, G., Puig, R., Rius, A., 2012. Characterization of the surface tension of vegetable oils to be used as fuel in diesel engines. *Fuel* 102, 231–238. doi:10.1016/j.fuel.2012.07.042
- Farcas, F., 1996. Etude d'une methode de simulation du vieillissement sur route des bitumes. Doctoral Thesis, Universit de Paris VI, Paris.
- Farcas, F., Mouillet, V., Besson, S., Battaglia, V., Petiteau, C., Le Cunff, F., 2009. Identifica-tion et dosage par spectrometrie infrarouge a transformee de Fourier des copolymeres SBS et EVA dans les liants bitumineux. *ME 71*, LCPC, Paris.
- Fernández-Gómez, W.D., Quintana, H.R., Lizcano, F.R., 2013. A review of asphalt and asphalt mixture aging. *Ing. E Investig.* 33, 5–12.
- Finlayson, D., Nicoletti, C., Pilkington, I., Sharma, V., Teufele, B., 2011. British Columbia's Success with Hot-In-Place Recycling—A 25 year History, in: CTAA Annual Conference Proceedings-Canadian Technical Asphalt Association. p. 185.
- Firoozifar, S.H., Foroutan, S., Foroutan, S., 2011. The effect of asphaltene on thermal properties of bitumen. *Chem. Eng. Res. Des.* 89, 2044–2048. doi:10.1016/j.cherd.2011.01.025
- Flego, C., Carati, C., Gaudio, L.D., Zannoni, C., 2013. Direct Mass Spectrometry of tar sands: A new approach to bitumen identification. *Fuel*. doi:10.1016/j.fuel.2013.04.010
- Fritsche, H., 1994. Zur Bestimmung des Paraffingehaltes in Bitumen. *Bitumen* 176–178.

Fuentes-Audén, C., Sandoval, J.A., Jerez, A., Navarro, F.J., Martínez-Boza, F.J., Partal, P., Gallegos, C., 2008. Evaluation of thermal and mechanical properties of recycled polyethylene modified bitumen. *Polym. Test.* 27, 1005–1012. doi:10.1016/j.polymertesting.2008.09.006

Garcia-Morales, M., Partal, P., Navarro, F.J., Gallegos, C., 2006. Effect of waste polymer addition on the rheology of modified bitumen. *Fuel* 85, 936–943.

Gasthauer, E., Mazé, M., Marchand, J.P., Amouroux, J., 2008. Characterization of asphalt fume composition by GC/MS and effect of temperature. *Fuel* 87, 1428–1434.

Gawrys, K.L., Kilpatrick, P.K., 2004. Asphaltene aggregation: Techniques for analysis. *Instrum. Sci. Technol.* 32, 247–253.

Golubev, Y.A., Kovaleva, O.V., Yushkin, N.P., 2008. Observations and morphological analysis of supermolecular structure of natural bitumens by atomic force microscopy. *Fuel* 87, 32–38. doi:10.1016/j.fuel.2007.04.005

Grant, T.P., 2001. Determination of asphalt mixture healing rate using the Superpave indirect tensile test. Doctoral Thesis, University of Florida.

Hajj, E.Y., Souliman, M.I., Alavi, M.Z., Loría Salazar, L.G., 2013. Influence of Hydrogreen Bioasphalt on Viscoelastic Properties of Reclaimed Asphalt Mixtures. *Transp. Res. Rec. J. Transp. Res. Board* 2371, 13–22.

Hansen, C.M., 2012. *Hansen Solubility Parameters: A User's Handbook*, Second Edition. CRC Press.

Harrison, J., 2012. *Les Enrobés Bitumineux*.

Higgins, F., 2012. Gasoline and Diesel Fuel Quality Confirmation and Composition by FTIR.

Hihara, L.H., Adler, R.P.I., Latanision, R.M., 2014. Environmental degradation of advanced and traditional engineering materials. Taylor & Francis, Boca Raton.

Hofko, B., Hospodka, M., Blab, R., Eberhardsteiner, L., Füssl, J., Grothe, H., Handle, F., 2014. Impact of field ageing on low-temperature performance of binder and hot mix asphalt, in: *Asphalt Pavements*. CRC Press, pp. 381–395.

Huber, G.A., Decker, D.S., 1995. *Engineering Properties of Asphalt Mixtures and the Relationship to Their Performance*. ASTM International.

IDRRIM, 2013. Matériels pour le recyclage en installations de production d'enrobés (Note d'information No. 26). Institut de s Routes, des Rues et des Infrastructures pour la Mobilité, Paris, France.

Jamshidi, A., Hamzah, M.O., Shahadan, Z., 2012. Selection of reclaimed asphalt pavement sources and contents for asphalt mix production based on asphalt binder rheological properties, fuel requirements and greenhouse gas emissions. *J. Clean. Prod.* 23, 20–27. doi:10.1016/j.jclepro.2011.10.008



Johnson, R., 1998. Environmental Scanning Electron Microscopy. Robert Johnson Associates, El Dorado Hills, CA, USA.

Jullien, A., Monéron, P., Quaranta, G., Gaillard, D., 2006. Air emissions from pavement layers composed of varying rates of reclaimed asphalt. *Resour. Conserv. Recycl.* 47, 356–374. doi:10.1016/j.resconrec.2005.09.004

Jung, S.H., 2006. The Effects of Asphalt Binder Oxidation on Hot Mix Asphalt Concrete Mixture Rheology and Fatigue Performance. Texas A&M University.

Kandhal, P.S., Chakraborty, S., 1996. Effect of asphalt film thickness on short-and long-term aging of asphalt paving mixtures. *Transp. Res. Rec. J. Transp. Res. Board* 1535, 83–90.

Katman, H.Y., Ibrahim, M.R., Matori, M.Y., Norhisham, S., Ismail, N., 2013. Effects of reclaimed asphalt pavement on indirect tensile strength test of foamed asphalt mix tested in dry condition. *IOP Conf. Ser. Earth Environ. Sci.* 16, 012091. doi:10.1088/1755-1315/16/1/012091

Kim, Y., 2014. Asphalt Pavements. CRC Press.

Kinnaird, M.G., 2000. Method of releasing asphalt from equipment using surfactant solutions, U.S. Patent 6126757.

Knapp, D.R., 1979. Handbook of Analytical Derivatization Reactions. John Wiley & Sons.

Kodali, D.R., Mahoney, F.G., Olson, R.H., 1997. Release agent composition for industrial application.

Koots, J.A., Speight, J.G., 1975. Relation of petroleum resins to asphaltenes. *Fuel* 54, 179–184.

Kriech, A.J., Osborn, L.V., Snawder, J.E., Olsen, L.D., Herrick, R.F., Cavallari, J.M., McCLEAN, M.D., Blackburn, G.R., 2011. Study Design and Methods to Investigate Inhalation and Dermal Exposure to Polycyclic Aromatic Compounds and Urinary Metabolites from Asphalt Paving Workers: Research Conducted through Partnership. *Polycycl. Aromat. Compd.* 31, 243–269. doi:10.1080/10406638.2011.586398

Kultala, M., 2000. Release Oil.

Kuszewski, J.R., Gorman, W.B., Kane, E.G., 1997. Characterization of asphalt volatility using TGA and iatroscan analyses. *Proc Roof. Tech* 285–291.

Lamontagne, J., Dumas, P., Mouillet, V., Kister, J., 2001a. Comparison by Fourier transform infrared (FTIR) spectroscopy of different ageing techniques: application to road bitumens. *Fuel* 80, 483–488.

Lamontagne, J., Durrieu, F., Planche, J.P., Mouillet, V., Kister, J., 2001b. Direct and continuous methodological approach to study the ageing of fossil organic material by infrared microspectrometry imaging: application to polymer modified bitumen. *Anal. Chim. Acta* 444, 241–250.

Lavin, P., 2003. Asphalt Pavements: A Practical Guide to Design, Production and Maintenance for Engineers and Architects. CRC Press.

Lee, M.S., 2012. Mass Spectrometry Handbook. John Wiley & Sons.

Lee, S.-J., Amirkhanian, S.N., Kim, K.W., 2009. Laboratory evaluation of the effects of short-term oven aging on asphalt binders in asphalt mixtures using HP-GPC. *Constr. Build. Mater.* 23, 3087–3093. doi:10.1016/j.conbuildmat.2009.03.012

Lee, S.-J., Amirkhanian, S.N., Shatanawi, K., Kim, K.W., 2008. Short-term aging characterization of asphalt binders using gel permeation chromatography and selected Superpave binder tests. *Constr. Build. Mater.* 22, 2220–2227. doi:10.1016/j.conbuildmat.2007.08.005

Le Guern, M., Chailleux, E., Farcas, F., Dreessen, S., Mabilie, I., 2010. Physico-chemical analysis of five hard bitumens: Identification of chemical species and molecular organization before and after artificial aging. *Fuel* 89, 3330–3339. doi:10.1016/j.fuel.2010.04.035

Leoneti, A.B., Aragão-Leoneti, V., de Oliveira, S.V.W.B., 2012. Glycerol as a by-product of biodiesel production in Brazil: Alternatives for the use of unrefined glycerol. *Renew. Energy* 45, 138–145. doi:10.1016/j.renene.2012.02.032

Lesueur, D., 2009. The colloidal structure of bitumen: Consequences on the rheology and on the mechanisms of bitumen modification. *Adv. Colloid Interface Sci.* 145, 42–82. doi:10.1016/j.cis.2008.08.011

Lesueur, D., Youtcheff, J., 2014. Asphalt Pavement Durability, in: *Environmental Degradation of Advanced and Traditional Engineering Materials*. Taylor & Francis, Boca Raton.

Lins, V.F.C., Araújo, M.F.A.S., Yoshida, M.I., Ferraz, V.P., Andrada, D.M., Lameiras, F.S., 2008. Photodegradation of hot-mix asphalt. *Fuel* 87, 3254–3261. doi:10.1016/j.fuel.2008.04.039

Litzka, J., Strobl, R., Pass, F., Augustin, H., 1998. *Gebrauchsvhaltensorientierte Bitumenprüfung (No. 9)*. Mitteilungen ISTU.

Lligadas, G., Ronda, J.C., Galià, M., Biermann, U., Metzger, J.O., 2006. Synthesis and characterization of polyurethanes from epoxidized methyl oleate based polyether polyols as renewable resources. *J. Polym. Sci. Part Polym. Chem.* 44, 634–645. doi:10.1002/pola.21201

Lockwood, F., Dituro, M., Dotson, D., Fang, J., 1999. Asphalt Release Agent. *Asphalt Release Agent*, WO1999054413.

Loeber, L., Muller, G., Morel, J., Sutton, O., 1998. Bitumen in colloid science: a chemical, structural and rheological approach. *Fuel* 77, 1443–1450. doi:10.1016/S0016-2361(98)00054-4

Loeber, L., Sutton, O., Morel, J., Valleton, J.-M., Muller, G., 1996. New direct observations of asphalts and asphalt binders by scanning electron microscopy and atomic force microscopy. *J. Microsc.* 182, 32–39. doi:10.1046/j.1365-2818.1996.134416.x

- Lucena, M. da C.C., Soares, S. de A., Soares, J.B., 2004. Characterization and thermal behavior of polymer-modified asphalt. *Mater. Res.* 7, 529–534.
- Lu, X., Isacsson, U., 2002. Effect of ageing on bitumen chemistry and rheology. *Constr. Build. Mater.* 16, 15–22. doi:10.1016/S0950-0618(01)00033-2
- Madrid, R.C., Davison, R.R., Glover, C.J., 2000. Compositional Evaluation of Asphalt Binder Recycling Agents. *Pet. Sci. Technol.* 18, 153–175. doi:10.1080/10916460008949838
- Ma, F., Hanna, M.A., 1999. Biodiesel production: a review. *Bioresour. Technol.* 70, 1–15. doi:10.1016/S0960-8524(99)00025-5
- Mahr, G., Okabe, T., Ito, K., 2003. Release agents for bituminous substances. U.S. Patent 6506444.
- Malet, 2015. Pré - rapport d'étude de la tâche 4 du lot 4. AGRIBTP, Toulouse.
- Marchal, R., Penet, S., Solano-Serena, F., Vandecasteele, J.P., 2003. Gasoline and diesel oil biodegradation. *Oil Gas Sci. Technol.* 58, 441–448.
- Martín-Alfonso, M.J., Partal, P., Navarro, F.J., García-Morales, M., Bordado, J.C.M., Diogo, A.C., 2009. Effect of processing temperature on the bitumen/MDI-PEG reactivity. *Fuel Process. Technol.* 90, 525–530. doi:10.1016/j.fuproc.2009.01.007
- Martin, E.R., 1978. Release composition for bituminous materials. U.S. Patent 4078104.
- Martin, E.R., Coffey, M.L., 2000. Asphalt release agents and use thereof. U.S. Patent 6143812.
- Mastrofini, D., Scarsella, M., 2000. The application of rheology to the evaluation of bitumen ageing. *Fuel* 79, 1005–1015. doi:10.1016/S0016-2361(99)00244-6
- Mathews, J.P., Eser, S., Rahimi, P., 1999. Preliminary results on the molecular structures of the Athabasca and Cold Lake asphaltenes., in: ABSTRACTS OF PAPERS OF THE AMERICAN CHEMICAL SOCIETY. AMER CHEMICAL SOC 1155 16TH ST, NW, WASHINGTON, DC 20036 USA, pp. U626–U626.
- Mathew, T.V., 2009. Pavement materials: Bitumen.
- McCarron, B., Yu, X., Tao, M., Burnham, N., 2012. The Investigation of “Bee-Structures” in Asphalt Binders. Worcester Polytechnic Institute, Worcester, MA, USA.
- McNally, T., 2011. Polymer Modified Bitumen: Properties and Characterisation. Elsevier.
- Mikhailenko, P., 2012. Durability of Cement Paste with Metakaolin. Ryerson University.
- Mikhailenko, P., Ringot, E., Bertron, A., 2015a. Determination of the performance and damage to asphalt of bio-sourced asphalt release agents (ARAs) Part II: Evaluation of biodegradable products for use as ARAs and bitumen removers (BR). *Mater. Struct.*

Mikhailenko, P., Ringot, E., Bertron, A., Escadeillas, G., 2015b. Determination of the performance and damage to asphalt of bio-sourced asphalt release agents (ARAs) Part I: Developing test methods. *Mater. Struct.* doi:10.1617/s11527-015-0585

Mikhailenko, P., Ringot, E., Bertron, A., Escadeillas, G., 2014. Developing test methods for the determination of the performance and safety of bio-sourced Asphalt Release Agents (ARAs), in: *Asphalt Pavements*. CRC Press, pp. 1713–1723.

Mojet, B.L., Ebbesen, S.D., Lefferts, L., 2010. Light at the interface: the potential of attenuated total reflection infrared spectroscopy for understanding heterogeneous catalysis in water. *Chem. Soc. Rev.* 39, 4643–4655. doi:10.1039/C0CS00014K

Mortazavi, M., Moulthrop, J.S., 1993. The SHRP Materials Reference Library. Strategic Highway Research Program, National Research Council.

Mouazen, M., Poulesquen, A., Bart, F., Masson, J., Charlot, M., Vergnes, B., 2013. Rheological, structural and chemical evolution of bitumen under gamma irradiation. *Fuel Process. Technol.* 114, 144–153. doi:10.1016/j.fuproc.2013.03.039

Mouillet, V., Lamontagne, J., Durrieu, F., Planche, J.-P., Lapalu, L., 2008. Infrared microscopy investigation of oxidation and phase evolution in bitumen modified with polymers. *Fuel* 87, 1270–1280. doi:10.1016/j.fuel.2007.06.029

Murgich, J., Rodríguez, J., Aray, Y., 1996. Molecular recognition and molecular mechanics of micelles of some model asphaltenes and resins. *Energy Fuels* 10, 68–76.

Nahar, S.N., Mohajeri, M., Schmetts, A.J., Scarpas, A., van de Ven, M.F., Schitter, G., 2013. First Observation of Blending-Zone Morphology at Interface of Reclaimed Asphalt Binder and Virgin Bitumen. *Transp. Res. Rec. J. Transp. Res. Board* 2370, 1–9.

Nakanishi, K., 1962. *Infrared absorption spectroscopy, practical*. San Francisco,.

Naskar, M., Reddy, K.S., Chaki, T.K., Divya, M.K., Deshpande, A.P., 2013. Effect of ageing on different modified bituminous binders: comparison between RTFOT and radiation ageing. *Mater. Struct.* 46, 1227–1241. doi:10.1617/s11527-012-9966-3

National Asphalt Pavement Association, 2012. *History of Asphalt*, [www.asphaltpavement.org](http://www.asphaltpavement.org).

Navaro, J., Bruneau, D., Drouadaine, I., Colin, J., Dony, A., Cournet, J., 2012. Observation and evaluation of the degree of blending of reclaimed asphalt concretes using microscopy image analysis. *Constr. Build. Mater.* 37, 135–143. doi:10.1016/j.conbuildmat.2012.07.048

Navaro, J.C., 2011. *Cinétique de mélange des enrobés recyclés et influence sur les performances mécaniques*. Doctoral Thesis, Arts et Métiers ParisTech, Paris.

Neves, J., Correia, A.G., 2005. Evaluation of the stiffness modulus of bituminous mixtures using laboratory tests (NAT) validate by field back-analysis.

Nguyen, M.T., Lee, H.J., Baek, J., 2013. Fatigue Analysis of Asphalt Concrete under Indirect Tensile Mode of Loading Using Crack Images. *J. Test. Eval.* 41, 104589. doi:10.1520/JTE104589

Nivet, A., Alliot, C., 2011. Validation d'un essai de qualification de produits anti-adhérents utilisés en technique routière, Master's Report, Université Paul Sabatier, Toulouse, France.

Nomura, M., Kidane, K., Murata, S., Su, Y., Artok, L., Miyatani, Y., 1999. Structure and reactivity of the asphaltene fraction of an Arabian light-medium crude mixture, in: *Proceedings of the 218th ACS National Meeting*. pp. 22–26.

NTPEP, 2014. Standard Practice for NTPEP Evaluation of Asphalt Release Agents, AASHTO.

Olard, F., 2003. Comportement thermomécanique des enrobés bitumineux à basses températures Relations entre les propriétés du liant et de l'enrobé. Institut National des Sciences Appliquées de Lyon, Lyon, France.

Olson, R.H., Mahoney, F.G., Kodali, D.R., 1999. Release agent composition for industrial application, U.S. Patent 5900048.

Oyekunle, L.O., 2006. Certain relationships between chemical composition and properties of petroleum asphalts from different origin. *Oil Gas Sci. Technol.-Rev. IFP* 61, 433–441.

Partl, M.N., 2003. PRO 28: 6th International RILEM Symposium on Performance Testing and Evaluation of Bituminous Materials (PTEBM'03). RILEM Publications.

Partl, M.N., Bahia, H.U., Canestrari, F., 2013. *Advances in Interlaboratory Testing and Evaluation of Bituminous Materials: State-Of-the-Art Report of the RILEM Technical Committee 206-ATB*. Springer.

Pauli, A.T., 2014. Chemomechanics of Damage Accumulation and Damage-Recovery Healing in Bituminous Asphalt Binders. Doctoral Thesis, TU Delft, Delft University of Technology.

Peralta, E.J.F., 2009. Study of the Interaction between Bitumen and Rubber.

Petersen, J.C., 2009. A Review of the Fundamentals of Asphalt Oxidation: Chemical, Physicochemical, Physical Property, and Durability Relationships. *Transp. Res. E-Circ.*

Porot, L., 2007. Laboratory investigation of recycled binder performance.

Porot, L., Nigen-Chaidron, S., 2007. Laboratory investigation of recycled binder performance. Presented at the 6th International Conference on Sustainable Aggregates, Asphalt Technology and Pavement Engineering, Liverpool, UK.

Qing, W., Baizhong, S., Aijuan, H., Jingru, B., Shaohua, L., 2007. Pyrolysis characteristics of Huadian oil shales. *Oil Shale* 24, 147.

Randrianarimanana, A., 2010. Recherche d'un produit anti-adhérent pour bitume à chaud, Université Paul Sabatier, Master's Report, Toulouse, France.

Read, J., Whiteoak, D., 2003. The Shell Bitumen Handbook. Thomas Telford.

Redelius, P., 2000. Solubility parameters and bitumen. *Fuel* 79, 27–35. doi:10.1016/S0016-2361(99)00103-9

Reinke, G., Glidden, S., Listberger, S., Stauduhar, S., 2014. Reduction of low temperature asphalt binder stiffness using a Renewable Additive, in: *Asphalt Pavements*. CRC Press, pp. 1707–1712.

Rodríguez-Valverde, M.A., Ramón-Torregrosa, P., Páez-Dueñas, A., Cabrerizo-Vílchez, M.A., Hidalgo-Álvarez, R., 2008. Imaging techniques applied to characterize bitumen and bituminous emulsions. *Adv. Colloid Interface Sci.* 136, 93–108. doi:10.1016/j.cis.2007.07.008

Romera, R., Santamaría, A., Peña, J., Muñoz, M., Barral, M., García, E., Jañez, V., 2006. Rheological aspects of the rejuvenation of aged bitumen. *Rheol. Acta* 45, 474–478. doi:10.1007/s00397-005-0078-7

Rosner, G., World Health Organization, International Programme on Chemical Safety, International Labour Organisation, United Nations Environment Programme, 1996. Diesel fuels and exhaust emissions. World Health Organization, Geneva.

Rozeveld, S.J., Shin, E.E., Bhurke, A., France, L., Drzal, L.T., 1997. Network morphology of straight and polymer modified asphalt cements. *Microsc. Res. Tech.* 38, 529–543. doi:10.1002/(SICI)1097-0029(19970901)38:5<529::AID-JEMT11>3.0.CO;2-O

Salmonsens, S.T., Frailey, M.D., Proctor, J.J., Krantz, L.P., Crooks, S.M., 1999. Asphalt release agent for truck beds. U.S. Patent 5888279.

Santos Jr., V.O., Oliveira, F.C.C., Lima, D.G., Petry, A.C., Garcia, E., Suarez, P.A.Z., Rubim, J.C., 2005. A comparative study of diesel analysis by FTIR, FTNIR and FT-Raman spectroscopy using PLS and artificial neural network analysis. *Anal. Chim. Acta* 547, 188–196. doi:10.1016/j.aca.2005.05.042

Santucci, L., 2007. Recycling asphalt pavements— A strategy revisited. *Tech Top. Technol. Transf. Program Univ. Calif. Berkley*.

Scardina, M., 2007. An Introduction to Asphalt Release Agent. *Asph. RAP* 7(1).

Schumacher, R.F., Workman, R.J., Edwards, T.B., 2000. Calibration and Measurement of the Viscosity of DWPF Start-Up Glass.

Schvallinger, M., 2011. Analyzing trends of asphalt recycling in France.

Seddik, H., Emery, J., 1997. Moisture Damage of Asphalt Pavements. Presented at the XIIIth IRF World Meeting, Toronto, Ontario, Canada.

Siddiqui, M.N., Ali, M.F., 1999. Studies on the aging behavior of the Arabian asphalts. *Fuel* 78, 1005–1015. doi:10.1016/S0016-2361(99)00018-6

Siddiqui, M.N., Ali, M.F., 1999. Investigation of chemical transformations by NMR and GPC during the laboratory aging of Arabian asphalt. *Fuel* 78, 1407–1416.

Silva, H.D., 2003. Comparison between tensile, stiffness and fatigue life tests results. RILEM Publications SARL, pp. 205–211. doi:10.1617/2912143772.024

Silva, H.M.R.D., Oliveira, J.R.M., Jesus, C.M.G., 2012. Are totally recycled hot mix asphalts a sustainable alternative for road paving? *Resour. Conserv. Recycl.* 60, 38–48. doi:10.1016/j.resconrec.2011.11.013

Sirota, E.B., 2005. Physical Structure of Asphaltenes. *Energy Fuels* 19, 1290–1296. doi:10.1021/ef049795b

SITTM Asphalt Release Agent Field Trial, 2010.

Smith, H.R., Edwards, A.C., 2001. Recycling of bituminous materials: final report.

Sobus, J.R., Mcclean, M.D., Herrick, R.F., Waidyanatha, S., Onyemauwa, F., Kupper, L.L., Rappaport, S.M., 2009. Investigation of PAH Biomarkers in the Urine of Workers Exposed to Hot Asphalt. *Ann. Occup. Hyg.* 53, 551–560. doi:10.1093/annhyg/mep041

Soenen, H., Redelius, P., 2014. The effect of aromatic interactions on the elasticity of bituminous binders. *Rheol. Acta* 53, 741–754. doi:10.1007/s00397-014-0792-0

Sonibare, O., Egashira, R., Adedosu, T., 2003. Thermo-oxidative reactions of Nigerian oil sand bitumen. *Thermochim. Acta* 405, 195–205. doi:10.1016/S0040-6031(03)00192-8

Srivastava, A., van Rooijen, R., 2000. Bitumen performance in hot and arid climates. Presented at the Pavement Seminar for the Middle East and North Africa Region, Amman, Jordan.

Stangle, K., Jager, A., Lackner, R., 2006. Microstructure-based identification of bitumen performance. *Road Mater. Pavement Des. Int. J.* 7, 111–142.

Tachon, N., 2008. Nouveaux types de liants routiers a hautes performances, a teneur en bitume reduite par addition de produits organiques issus des agroressources. Doctoral Thesis, L’Institut National Polytechnique de Toulouse, Toulouse, France.

Tahirou, M., 2009. Influence of Bitumen Ageing on Asphalt Quality, Comparison between Bitumen and Asphalt Ageing. Doctoral Thesis, Universiteit Gent Vrije Universiteit Brussel, Belgium.

Tang, B., 2008. Applications of Solid-Phase Microextraction to Chemical Characterization of Materials Used in Road Construction. Doctoral Thesis, Division of Highway Engineering, Royal Institute of Technology. 2008.

Tang, B., Isacson, U., 2006. Chemical characterization of oil-based asphalt release agents and their emissions. *Fuel* 85, 1232–1241. doi:10.1016/j.fuel.2005.11.002

- Tang, B., Isacson, U., 2005. Determination of aromatic hydrocarbons in asphalt release agents using headspace solid-phase microextraction and gas chromatography–mass spectrometry. *J. Chromatogr. A* 1069, 235–244. doi:10.1016/j.chroma.2005.02.011
- Terrel, R.L., Epps, J.A., 1989. Using additives and modifiers in hot mix asphalt. National Asphalt Pavement Association, USA.
- The Asphalt Paving Industry: A Global Perspective, 2nd ed, 2011. . National Asphalt Pavement Association European Asphalt Pavement Association,.
- The Bitumen Industry - A Global Perspective, 2nd ed, 2011. . Asphalt Institute, Eurobitume.
- Tran, J., Van Loon, H., 2009. Indirect tensile strength of asphalt mixes in South Australia.
- Valentin, R., Mouloungui, Z., 2013. Superhydrophilic surfaces from short and medium chain solvo-surfactants. *Ol. Corps Gras Lipides* 20, 33–44.
- Van den bergh, W., Van de Ven, M.F.C., 2012. The Influence of Ageing on the Fatigue and Healing Properties of Bituminous Mortars. *Procedia - Soc. Behav. Sci., SIIV-5th International Congress - Sustainability of Road Infrastructures* 2012 53, 256–265. doi:10.1016/j.sbspro.2012.09.878
- Vargas, X.A., Afanasjeva, N., Álvarez, M., Marchal, P.H., Choplin, L., 2008. Asphalt rheology evolution through thermo-oxidation (aging) in a rheo-reactor. *Fuel* 87, 3018–3023. doi:10.1016/j.fuel.2008.04.026
- Wagnoner, M.P., Buttlar, W.G., Paulino, G.H., 2005. Disk-shaped compact tension test for asphalt concrete fracture. *Exp. Mech.* 45, 270–277.
- Wang, Y., Wen, Y., Zhao, K., Wei, J., Wang, H., Wong, A., 2014. Oxidative aging of long-life asphalt pavements in Hong Kong, in: *Asphalt Pavements*. CRC Press, pp. 191–200.
- Wood, L.E., 1978. Recycling of Bituminous Pavements: A Symposium. ASTM International.
- Woods, J.R., Kung, J., Pleizier, G., Kotlyar, L.S., Sparks, B.D., Adjaye, J., Chung, K.H., 2004. Characterization of a coker gas oil fraction from athabasca oilsands bitumen. *Fuel* 83, 1907–1914. doi:10.1016/j.fuel.2003.08.024
- Yao, H., You, Z., Li, L., Goh, S.W., Lee, C.H., Yap, Y.K., Shi, X., 2013. Rheological properties and chemical analysis of nanoclay and carbon microfiber modified asphalt with Fourier transform infrared spectroscopy. *Constr. Build. Mater.* 38, 327–337. doi:10.1016/j.conbuildmat.2012.08.004
- Zaki, N.N., Troxler, R.E., 2013. . Asphalt Release Agent. U.S. Patent Application 2013/0156962.
- Zanzotto, L., 2003. Dynamic and transient testing of asphalt binder and paving mix. RILEM Publications SARL, pp. 66–73. doi:10.1617/2912143772.005



Zargar, M., Ahmadinia, E., Asli, H., Karim, M.R., 2012. Investigation of the possibility of using waste cooking oil as a rejuvenating agent for aged bitumen. *J. Hazard. Mater.* 233, 254–258. doi:10.1016/j.jhazmat.2012.06.021

Zaumanis, M., Mallick, R.B., Poulikakos, L., Frank, R., 2014. Influence of six rejuvenators on the performance properties of Reclaimed Asphalt Pavement (RAP) binder and 100% recycled asphalt mixtures. *Constr. Build. Mater.* 71, 538–550. doi:10.1016/j.conbuildmat.2014.08.073

Zhang, H., Yu, J., Wang, H., Xue, L., 2011. Investigation of microstructures and ultraviolet aging properties of organo-montmorillonite/SBS modified bitumen. *Mater. Chem. Phys.* 129, 769–776. doi:10.1016/j.matchemphys.2011.04.078

Zhang, J., Wang, J., Wu, Y., Wang, Y., Wang, Y., 2008. Preparation and properties of organic palygorskite SBR/organic palygorskite compound and asphalt modified with the compound. *Constr. Build. Mater.* 22, 1820–1830.

## List of Tables

Table 2-1 Typical bitumen chemical composition for Europe ( <i>The Bitumen Industry</i> , 2011).....	16
Table 2-2 Typical compositions by mass of SARA fractions (Lesueur, 2009) .....	20
Table 2-3 Hydrocarbon compositions by structural model of bitumen (Tachon, 2008) .....	24
Table 2-4 SARA composition and penetration values for bitumens corresponding to Figure 2-15 (Loeber et al., 1998) .....	30
Table 2-5 Elemental analysis (ASTM D 5291) by weight of asphaltene fractions after RTFOT aging (Mastrofini and Scarsella, 2000) .....	47
Table 2-6 FTIR bands with bitumen aging.....	52
Table 2-7 SARA Classification of recycling agents used in Chen et al. (2007).....	65
Table 3-1 General information and physical properties for commercial ARAs and BRs .....	73
Table 3-2 Chemical composition for commercial ARAs and BRs .....	73
Table 3-3 General information and physical properties for the candidate formulations .....	74
Table 3-4 Chemical composition of candidate formulations.....	75
Table 3-5 Typical composition of asphalt mixture.....	76
Table 3-6 Parameters for Asphalt Slide Test.....	83
Table 3-7 Images of plates after Asphalt Slide Test No. 1 .....	83
Table 3-8 Results for Asphalt Slide Test No.1 .....	84
Table 3-9 Results for Asphalt Slide Test no. 2.....	84
Table 3-10 Images of plates after Asphalt Slide Test no. 4.....	85
Table 3-11 Results for Asphalt Slide Test no. 4.....	85
Table 3-12 Images of plates after Asphalt Slide Test final (asphalt mass: 1200±10 g, ARA: 65 mL/m <sup>2</sup> , cooling time: 30min, heating of plate: 60°C, inclination angle of plate: 45°).....	85
Table 3-13 Results for Asphalt Slide Test final (asphalt mass: 1200±10 g, ARA: 65 mL/m <sup>2</sup> , cooling time: 30 min, heating of plate: 60°C, inclination angle of plate: 45°) .....	86
Table 3-14 Asphalt samples compacted by compression.....	90
Table 3-15 Parameters for Asphalt Degradation Testing.....	94
Table 3-16 Comparison of CBR Loading Trial No. 1&2.....	95
Table 3-17 Proctor-CBR loading Test No. 1 samples showing leaching of bitumen onto moulds.....	95
Table 3-18 Proctor-CBR loading Test No. 1 samples showing flow of ARA towards the side of the sample.....	96
Table 3-19 Resistance reduction % for ITS Trial No. 3 ITS (5mL ARA applied after compaction), ITS Trial No. 4 (2mL ARA applied before compaction) and ITS Final Test (1mL ARA applied before compaction) .....	97
Table 3-20 Bitumen Degradation Test results .....	102
Table 3-21 Bitumen Degradation Test results for commercial ARAs and BRs.....	106
Table 3-22 Images of plates after Asphalt Slide Test.....	112
Table 3-23 Results for Asphalt Slide Test.....	113

Table 3-24 Resistance Reduction for ITS Testing .....	113
Table 3-25 Composition of glycerol-based formulations (Boussambe, 2015).....	119
Table 3-26 Chemical structure for MUG and MUDG components (Boussambe, 2015) .....	119
Table 3-27 ARA formulations featuring glycerol-based formulations mixed with water .....	121
Table 3-28 Bitumen Degradation Test results for bio-sourced candidate formulations .....	122
Table 3-29 Images of plates after Asphalt Slide Test for RD 1, RD 2, RD 4 and RD 7.....	125
Table 3-30 Results of Asphalt Slide Test for RD 1, RD 2, RD 4 and RD 7 .....	125
Table 3-31 Images of plates after Asphalt Slide Test for MUG-based formulations .....	127
Table 3-32 Results of Asphalt Slide Test for MUG-based formulations.....	127
Table 3-33 Images of plates after Asphalt Slide Test for MUDG-based formulations.....	128
Table 3-34 Results of Asphalt Slide Test for MUDG-based formulations .....	128
Table 3-35 Resistance Reduction for ITS Testing (MUG 20 H 80) .....	134
Table 4-1 Properties of tracers for bitumen .....	143
Table 4-2 Summary of samples prepared for this study of bitumen aging and rejuvenation.....	154
Table 4-3 Properties of rejuvenating agents.....	157
Table 4-4 FTIR bands with bitumen aging.....	159
Table A-1 Pavement grade bitumen specifications (NF EN 12591) .....	213
Table B-1 Gradations for Asphalt.....	218

## List of Figures

Figure 2-1 Pavement roller .....	14
Figure 2-2 Simplified model of bitumen structure (asphaltenes suspended in maltenes) (Lesueur, 2009) .....	16
Figure 2-3 Trends of bitumen components by aromatic content and polarity .....	17
Figure 2-4 Formation of dimer, trimer and tetramer for an asphaltene molecule (Lesueur, 2009) ....	18
Figure 2-5 Asphaltene molecules, micelles and aggregations [Yuen et al. (1972) cited by El Béze (2008)].....	19
Figure 2-6 Asphaltene aggregates observed by SANS (Gawrys and Kilpatrick, 2004).....	19
Figure 2-7 Saturate molecules ( <i>The Bitumen Industry</i> , 2011) .....	20
Figure 2-8 Aromatic/ Naphthene Aromatic molecules ( <i>The Bitumen Industry</i> , 2011) .....	21
Figure 2-9 Resin molecule ( <i>The Bitumen Industry</i> , 2011) .....	22
Figure 2-10 SOL (top) and GEL (bottom) bitumen models (Read and Whiteoak, 2003) .....	23
Figure 2-11 GEL bitumen model (Stangle et al., 2006) .....	24
Figure 2-12 GEL bitumen structure observed by AFM (Loeber et al., 1996) .....	26
Figure 2-13 SEM observation of bitumen x250 (Rozeveld et al., 1997).....	26
Figure 2-14 SEM observation of asphaltenes x15000 (Rozeveld et al., 1997).....	27
Figure 2-15 Black curve representation of different bitumens, varying in composition from testing with rheometer from frequencies 0.06-10Hz at 5 to 60°C (Loeber et al., 1998).....	30
Figure 2-16 Application of ARA on truck bed (left); part of field Trial showing effectiveness of two ARAs (right) ("SITTM Asphalt Release Agent Field Trial," 2010).....	33
Figure 2-17 Damage to asphalt observed from the use of vegetable based ARA on new pavement..	35
Figure 2-18 Asphalt in EN 13297-30 proctor moulds after compaction (left) and CBR test on asphalt sample (right).....	36
Figure 2-19 Various solvents according to their HSD values with good solvents shown in grey (Hansen, 2012).....	39
Figure 2-20 Breaking up of old asphalt slabs for use as RAP (bitumen.info, 2009).....	40
Figure 2-21 Rolling Thin Film Oven Test (Jet Materials) .....	42
Figure 2-22 Example of Pressurized Aging Vessel (ASTM D 6521).....	43
Figure 2-23 Possible representation of reaction types in a hypothetical asphalt structure on laboratory aging (Siddiqui and Ali, 1999b).....	48
Figure 2-24 DTG curve for SARA fractions of bitumen (Pauli, 2014) .....	53
Figure 2-25 DTG curves for unoxidized (40/50, left) and oxidized (20/30, right) bitumen (Benbouzid and Hafsi, 2008) .....	54
Figure 2-26 SEM observation of bitumen x350 (Rozeveld et al., 1997).....	56
Figure 2-27 SEM observation of 50/70 bitumen a-new/ b-RTFOT aging / c-RTFOT + PAV aging (Stangle et al., 2006) .....	57
Figure 2-28 RAP in contact with new bitumen (El Beze, 2008) .....	58

Figure 2-29 XANES cartography of S=O content in RAP asphalt (El Béze, 2008) .....	61
Figure 2-30 FTIR-ATR imaging of bitumen – limestone sample (El Béze, 2008) .....	62
Figure 2-31 AFM tapping mode for topography (left) and phase (right) revealing the microstructure morphology of (a) virgin bitumen (b) RAP-binder and (c) blending zone of virgin and RAP-binder (Nahar et al., 2013). .....	63
Figure 2-32 Asphalt recycling agent blending guide according to ASTM D 4887 (Chen et al., 2007)... 66	
Figure 2-33 Typical changes in chemical composition via the Rostler method with aging of a typical asphalt pavement (Brownridge, 2010) .....	68
Figure 3-1 Schema for deriving glycerol from biodiesel production (Leoneti et al., 2012) .....	75
Figure 3-2 M&O Type 182 asphalt mixer .....	77
Figure 3-3 Addition of bitumen (at 160°C) to aggregates in mixer (left) and asphalt after mixing (right) .....	77
Figure 3-4 Asphalt after being placed into aluminum containers for storage.....	78
Figure 3-5 ARA Performance Evaluation Apparatus (ARA-PEA) .....	79
Figure 3-6 Details on the ARA Performance Evaluation Apparatus (ARA-PEA) .....	80
Figure 3-7 Features of ARA-PEA: laser temperature sensor; laser thickness sensor; gage for setting the angle of inclination .....	81
Figure 3-8 Asphalt Slide Test: 1) applying ARA, 2) asphalt spread on the plate, 3) load of 2.5kPa distributed on top of the asphalt and 4) the inclination of the plate on ARA-PEA at 45° .....	82
Figure 3-9 Influence du compaction on the resistance of control samples with CBR loading .....	89
Figure 3-10 Demolding asphalt sample .....	89
Figure 3-11 Compaction of asphalt sample by hydraulic compressor (left) and damaged surface of sample from the use of a cold piston (right) .....	90
Figure 3-12 State of surfaces for asphalt samples compacted by compression corresponding to Table 3-14 .....	91
Figure 3-13 Application of ARA in the center of the sample .....	92
Figure 3-14 CBR loading press and a sample being loaded in CBR .....	92
Figure 3-15 Asphalt samples after CBR loading .....	93
Figure 3-16 ITS loading.....	93
Figure 3-17 CBR Loading Test No. 1 Resistance Curves for Control Samples .....	95
Figure 3-18 Compressor compacted ITS samples showing leaching of bitumen with 5mL ARA applied after compaction (left) and 2mL ARA applied before compaction (right).....	98
Figure 3-19 Loading curves for ITS Final Test control sample.....	99
Figure 3-20 Loading curves for ITS Final Test Diesel (left) and BR 1 (right) .....	99
Figure 3-21 Loading curves for ITS Final Test ARA 1(left) and ARA 2 (right).....	99
Figure 3-22 BDT silicon sample moulds (top left), sample submerged in ARA product (top right and bottom left) and beakers after test (bottom right) .....	101
Figure 3-23 FTIR-ATR analysis of the residual liquid from the BDT .....	102
Figure 3-24 PVC and crumb rubber samples for testing BR degradation of construction materials .	103

Figure 3-25 BDT sample showing i) light degradation of bitumen after 1d exposure to ARA 2 (left) and ii) heavy degradation after 1d exposure to BR 5 (right) .....	107
Figure 3-26 ARA 4 in glass beaker (left), with bitumen sample after 1 d contact with ARA 4 in BDT (right) .....	107
Figure 3-27 FTIR-ATR spectra (1800-1130 $\text{cm}^{-1}$ ) for ester-based commercial ARAs and BRs: ARA 1, ARA 2, ARA 3, BR 1, BR 2, BR 3 and BR 4 along with diesel and 35/50 bitumen .....	108
Figure 3-28 FTIR-ATR spectra (3050-2800 $\text{cm}^{-1}$ ) for ester-based commercial ARAs and BRs: ARA 1, ARA 2, ARA 3, BR 1, BR 2, BR 3 and BR 4 along with diesel and bitumen.....	109
Figure 3-29 FTIR-ATR spectra (1650-1550 $\text{cm}^{-1}$ ) of BDT solution for ester-based commercial ARAs: ARA 3, BR 1, BR 2, BR 3, BR 4, bitumen, and diesel fuel .....	110
Figure 3-30 FTIR-ATR Spectra ARA 4 for BDT solution (blue), agent (red), bitumen sample after test (green) and 35/50 bitumen (black) .....	111
Figure 3-31 FTIR-ATR Spectra BR 5 for BDT solution (blue), agent (red) and 35/50 bitumen (black) .....	112
Figure 3-32 Ester content of commercial ARAs and BRs compared to their mass loss in BDT.....	114
Figure 3-33 Characteristic mechanisms of ARA performance .....	116
Figure 3-34 Chemical transformations involved in the production of MUG and MUDG .....	118
Figure 3-35 Esterification reactions of glycerol and diglycerol with undecylenic acid (Boussambe, 2015) .....	118
Figure 3-36 MUG (left) and MUDG (right) compounds at room temperature .....	120
Figure 3-37 BDT sample showing i) no degradation of bitumen after 1d exposure to water (left) and ii) sample deformation after 1d exposure to acetone (right).....	123
Figure 3-38 BDT sample showing bitumen after 1d exposure to MUG 50 ARA2 50; the bitumen has been degraded by the solution and the solution has coagulated .....	123
Figure 3-39 Bitumen degradation test results of RD formulations at 1 and 7 days .....	124
Figure 3-40 FTIR-ATR spectra (1800-1100 $\text{cm}^{-1}$ ) for candidate ARA and BR formulations: C7, RD 1, RD 2, RD 4, RD 5, RD 6, RD 7.....	129
Figure 3-41 FTIR-ATR spectra (3050-2800 $\text{cm}^{-1}$ ) for candidate ARA and BR formulations: C7, RD 1, RD 2, RD 4, RD 5, RD 6, RD 7.....	130
Figure 3-42 FTIR-ATR spectra around the peak at 1600 $\text{cm}^{-1}$ for candidate ARA and BR (C7, RD 5, RD 6, RD 7) BDT solutions compared to bitumen.....	131
Figure 3-43 FTIR-ATR spectra (3250-700 $\text{cm}^{-1}$ ) for RD 4 (red) and RD 4 BDT solution (blue); the small peak around 2350 $\text{cm}^{-1}$ is carbon dioxide from the air and is not part of the sample .....	132
Figure 3-44 FTIR-ATR spectra MUG 20 H 80 (red), MUG 20 H 80 BDT solution (blue), MUDG 20 H 80 (pink) and MUDG 20 H 80 BDT solution (green) .....	133
Figure 3-45 FTIR-ATR spectra (3750-950 $\text{cm}^{-1}$ ) MUG 20 H 80 BDT bitumen sample (green), MUDG 20 H 80 BDT bitumen sample (pink) and 35/50 bitumen (black) .....	134
Figure 3-47 AST Performance of MUG and MUDG formulations with water in terms of residual mass compared to ARA 4 .....	137
Figure 3-48 AST Performance of MUG and MUDG formulations with water in terms of time to beginning of slide compared to ARA 4.....	137

Figure 4-1 : Préparation the samples for SEM analysis including the addition of TiO <sub>2</sub> tracer (left) and the mixing with a Heidoph RZR mixer (right).....	143
Figure 4-2 Bitumen samples stored in silicone moulds .....	144
Figure 4-3 Bitumen sample for SEM being cut with a diamond saw .....	144
Figure 4-4 Bitumen and Ti rutile tracer sample melted by the electron beam .....	145
Figure 4-5 Peltier effect device with mastic sample inside the chamber and on the device (left) and the device coming out of the SEM chamber to the water source cooling the device (right).....	146
Figure 4-6 SEM observation of bitumen 35/50 sample with Peltier device cooling at -10°C. The EDS chemical analysis (in %w of oxide) for the area of the image is shown in the table on the right .....	146
Figure 4-7 SEM observation of bitumen with structures caused by the beam at x500 (left) and x700 (right) .....	147
Figure 4-8 SEM observation of bitumen with structures caused by the electron beam at x200 (HD image with special acquisition mode).....	147
Figure 4-9 SEM observation of bitumen with structures caused by the electron beam at magnifications of x200, x500 x750, x1000 and x2000 .....	148
Figure 4-10 : Particles of TiO <sub>2</sub> rutile (2%w of bitumen, left) and TiO <sub>2</sub> anatase (2%w of bitumen, right) observed by SEM in ambient temperature.....	149
Figure 4-11 : Observation of a rutile particle in bitumen by SEM at ambient temperature with EDS analysis of the area inside the blue circle.....	150
Figure 4-12 Limestone sand particle (0-0.315 mm) SEM image x500 with EDS analysis (in blue circle) observed at ambient temperature .....	151
Figure 4-13 Silica sand particle (0-0.315 mm) SEM image x500 with EDS analysis (in blue circle) observed at ambient temperature .....	151
Figure 4-14 Limestone sand particle (0.315-1 mm) in bitumen SEM image x200 observed with the aid of a Peltier effect device at -10°C .....	152
Figure 4-15 EDS analysis cartography for calcium (blue dots) of limestone sand (0.315-1 mm) mastic observed with the aid of a Peltier effect device at -10°C, corresponding to the SEM image in Figure 4-14 .....	152
Figure 4-16 EDS analysis line scan for C, S, Si and Ca of limestone sand (0.315-1 mm) mastic observed with the aid of a Peltier effect device at -10°C .....	153
Figure 4-17 Larronde – Ainhoa limestone sand graded to 0.315/1 mm .....	155
Figure 4-18 Preparation of mastic samples using Heidolph RZR mixer and Fisher Scientific Isotemp hot plate.....	156
Figure 4-19 Compaction of mastic sample with spatula after mixing .....	156
Figure 4-20 Oven aging of bitumen (left) and mastic (right) .....	158
Figure 4-21 PerkinElmer Spotlight 400 FTIR-ATR.....	159
Figure 4-22 Polishing of mastic samples with discs (left) and polishing at 180-200rpm (right).....	161
Figure 4-23 PerkinElmer Spotlight 400 coupled with a PerkinElmer Frontier Imager (left) and ZnSe ATR crystal (right).....	161

Figure 4-24 Mastic sample for FTIR imaging (left) and FTIR microscope analysis on mastic sample (right) .....	161
Figure 4-25 Nietzsche thermogravimetric analyzer coupled with a mass spectrometry attachment (right, not used) .....	162
Figure 4-26 Mass loss % for 0-17 days of bitumen aging.....	163
Figure 4-27 Change in $I_{C=O}$ for 0-17 days of bitumen aging.....	164
Figure 4-28 Change in $I_{S=O}$ for 0-17 days of bitumen aging.....	164
Figure 4-29 Change in $A_{1600}$ for 0-17 days of bitumen aging .....	165
Figure 4-30 Change in $I_{C=O}$ for 0-42 days of bitumen aging.....	165
Figure 4-31 Spectra $1730-1670\text{cm}^{-1}$ for 0-42 days of bitumen aging .....	166
Figure 4-32 Change in $I_{S=O}$ for 0-42 days of bitumen aging.....	166
Figure 4-33 Spectra $1110-970\text{cm}^{-1}$ for 0-42 days of bitumen aging .....	167
Figure 4-34 Change in $A_{1600}$ for 0-42 days of bitumen aging.....	167
Figure 4-35 Spectra $3100-2800\text{cm}^{-1}$ for 0-42 days of bitumen aging .....	168
Figure 4-36 Spectra $1510-1350\text{cm}^{-1}$ for 0-42 days of bitumen aging .....	168
Figure 4-37 DTG in air curves for bitumen aged from 0-42 days.....	169
Figure 4-38 Evolution of DTG peak in air at $450^{\circ}\text{C}$ for bitumen aging 0-42 days .....	170
Figure 4-39 Evolution of DTG peak in air at $575^{\circ}\text{C}$ for bitumen aged 0-42 days .....	170
Figure 4-40 DTG in argon curves for bitumen aged from 0-7 days.....	171
Figure 4-41 Black curved for virgin 35/50 bitumen, bitumen oven aged 0-18 d and bitumen recovered from asphalt aged with the RILEM method.....	172
Figure 4-42 FTIR spectra for bitumen oven aged 14 days (black), the aged bitumen rejuvenated by B1 at 20%w (blue), the rejuvenated bitumen oven aged 14 days (green) and the rejuvenating agent B1 (red).....	173
Figure 4-43 FTIR spectra for bitumen oven aged 14 days (black), the aged bitumen rejuvenated by P1 at 20%w (blue), the rejuvenated bitumen oven aged 14 days (green) and the rejuvenating agent P1 (red).....	174
Figure 4-44 FTIR spectra for bitumen oven aged 14 days (black), the aged bitumen rejuvenated by P2 at 20%w (blue), the rejuvenated bitumen oven aged 14 days (green) and the rejuvenating agent P2 (red).....	175
Figure 4-45 FTIR-ATR Microscope $1030\text{cm}^{-1}/(1460 + 1376 \text{ cm}^{-1})$ band ratio images $150 \times 150 \mu\text{m}$ , pixel size $1.56 \mu\text{m}$ for: a) unaged mastic and b) mastic aged for 14 days in oven (right).....	176
Figure 4-46 FTIR-ATR Microscope $1030\text{cm}^{-1}/(1460 + 1376 \text{ cm}^{-1})$ band ratio images $150 \times 150 \mu\text{m}$ , pixel size $1.56 \mu\text{m}$ for mastic aged for 14 days in oven WITH 7.5%w B1 added .....	177
Figure 4-47 FTIR-ATR Microscope $1030\text{cm}^{-1}/(1460 + 1376 \text{ cm}^{-1})$ band ratio images pixel size $6.25 \mu\text{m}$ for: a) unaged mastic and b) mastic aged for 14 days in oven .....	177
Figure 4-48 FTIR-ATR Microscope $1030\text{cm}^{-1}/(1460 + 1376 \text{ cm}^{-1})$ band ratio image pixel size $6.25 \mu\text{m}$ for mastic aged for 14 days in oven with a) 7.5%w P1 added and b) 7.5%w P2 .....	178



Figure 4-49 Black curves for virgin 35/50 bitumen, 35/50 bitumen aged by RTFOT+PAV, 35/50 bitumen aged by RTFOT+PAV with 15%w P1, 35/50 bitumen aged by RTFOT+PAV with 12%w P2, 35/50 bitumen aged by RTFOT+PAV with 12.5%w B1.....	180
Figure A-1 Bitumen softening point test – Ring and Ball (Mathew, 2009) .....	214
Figure A-2 Brookfield viscometer (Schumacher et al., 2000) .....	215
Figure A-3 Mouton pendulum (fr.wikipedia.org).....	216
Figure A-4 Bitumen ductility test (Mathew, 2009) .....	217
Figure B-1 Grading curve for asphalt .....	218
Figure C-1 Steel plate after bitumen flow test.....	220
Figure D-1 FTIR-ATR Spectra Diesel for BDT solution (blue), agent (red) and 35/50 bitumen (black).....	222
Figure D-2 FTIR-ATR Spectra ARA 1 for BDT solution (blue), agent (red) and 35/50 bitumen (black).....	222
Figure D-3 FTIR-ATR Spectra ARA 2 for BDT solution (blue), agent (red) and 35/50 bitumen (black).....	223
Figure D-4 FTIR-ATR Spectra ARA 3 for BDT solution (blue), agent (red) and 35/50 bitumen (black).....	223
Figure D-5 FTIR-ATR Spectra ARA 4 for BDT solution (blue), agent (red), bitumen sample after test (green) and 35/50 bitumen (black).....	224
Figure D-6 FTIR-ATR Spectra BR 1 for BDT solution (blue), agent (red) and 35/50 bitumen (black).....	224
Figure D-7 FTIR-ATR Spectra BR 2 for BDT solution (blue), agent (red) and 35/50 bitumen (black).....	225
Figure D-8 FTIR-ATR Spectra BR 3 for BDT solution (blue), agent (red) and 35/50 bitumen (black).....	225
Figure D-9 FTIR-ATR Spectra BR 4 for BDT solution (blue), agent (red) and 35/50 bitumen (black).....	226
Figure D-10 FTIR-ATR Spectra BR 5 for BDT solution (blue), agent (red) and 35/50 bitumen (black).....	226
Figure D-11 FTIR-ATR Spectra C7 for pure formulation (red), BDT solution (blue) and 35/50 bitumen (black).....	227
Figure D-12 FTIR-ATR Spectra RD 1 for pure formulation (red), BDT solution (blue) and 35/50 bitumen (black) .....	227
Figure D-13 FTIR-ATR Spectra RD 2 for pure formulation (red), BDT solution (blue) and 35/50 bitumen (black) .....	228
Figure D-14 FTIR-ATR Spectra RD 4 for pure formulation (red), BDT solution (blue) and 35/50 bitumen (black) .....	228
Figure D-15 FTIR-ATR Spectra RD 5 for pure formulation (red), BDT solution (blue) and 35/50 bitumen (black) .....	229
Figure D-16 FTIR-ATR Spectra RD 6 for pure formulation (red), BDT solution (blue) and 35/50 bitumen (black) .....	229
Figure D-17 FTIR-ATR Spectra RD 7 for pure formulation (red), BDT solution (blue) and 35/50 bitumen (black) .....	230
Figure D-18 FTIR-ATR Spectra MUG for pure formulation (pink), MUG 20 H 80 (red), MUG 20 H 80 BDT solution (blue), MUG 20 H 80 BDT bitumen sample (green) and 35/50 bitumen (black).....	230
Figure D-19 FTIR-ATR Spectra MUDG for pure formulation (pink), MUDG 20 H 80 (red), MUDG 20 H 80 BDT solution (blue), MUDG 20 H 80 BDT bitumen sample green and 35/50 bitumen (black).....	231
<b>Figure E-1 SEM Jeol JSM-6380LV .....</b>	<b>232</b>
<b>Figure E-2 SEM Signals (Johnson, 1998).....</b>	<b>233</b>





# Appendix

## Appendix A. Bitumen testing

The standard bitumen testing prescribed by NF EN 12591 are shown in Table A-1.

Table A-1 Pavement grade bitumen specifications (NF EN 12591)

Characteristic/ Test Method	Norm	20/30	30/45	35/50	40/60	50/70	70/100	100/150
<b>Penetration @ 25°C (mm)</b>	EN 1426	2-3	3-4.5	3.5-5	4-6	5-7	7-10	10-15
<b>Softening Point (°C)</b>	EN 1427	55-63	52-60	50-58	48-56	46-54	43-51	39-47
<b>Resistance to Hardening @ 163°C</b>	EN 12607-1							
<b>Retained Penetration (%)</b>		≥ 55	≥ 53	≥ 53	≥ 50	≥ 50	≥ 46	≥ 43
<b>Increase in Softening Point (°C)</b>		≤ 8 <sup>1</sup> ≤ 10 <sup>2</sup>	≤ 8 <sup>1</sup> ≤ 11 <sup>2</sup>	≤ 8 <sup>1</sup> ≤ 11 <sup>2</sup>	≤ 9 <sup>1</sup> ≤ 11 <sup>2</sup>	≤ 9 <sup>1</sup> ≤ 11 <sup>2</sup>	≤ 9 <sup>1</sup> ≤ 11 <sup>2</sup>	≤ 10 <sup>1</sup> ≤ 12 <sup>2</sup>
<b>Change in Mass (± %)</b>		≤ 0.5	≤ 0.5	≤ 0.5	≤ 0.5	≤ 0.5	≤ 0.8	≤ 0.8
<b>Flash Point (°C)</b>	EN ISO 2592	≥ 240	≥ 240	≥ 240	≥ 230	≥ 230	≥ 230	≥ 230
<b>Solubility (%)</b>	EN 12592	≥ 99	≥ 99	≥ 99	≥ 99	≥ 99	≥ 99	≥ 99
<b><sup>a</sup>Dynamic Viscosity @ 60°C (Pa*s)</b>	EN 12596	≥ 440	≥ 260	≥ 225	≥ 175	≥ 145	≥ 90	≥ 55
<b><sup>a</sup>Fraass Breaking Point (°C)</b>	EN 12593		≤ -5	≤ -5	≤ -7	≤ -8	≤ -10	≤ -12
<b><sup>a</sup>Kinematic Viscosity @ 135 °C (mm<sup>2</sup>/s)</b>	EN 12595	≥ 530	≥ 400	≥ 370	≥ 325	≥ 295	≥ 230	≥ 175

<sup>1</sup> Severity 1

<sup>2</sup> Severity 2

<sup>a</sup> Properties required to meet specific regional conditions. Associated with regulatory or other regional requirements.

### Softening point

The softening point (ASTM D36-EN 1427) or ring and ball test is a method (Figure A-1) to determine the point where bitumen reaches a certain softness point, arbitrary to the standard. The test is generally conducted at a temperature range of 30 to 157°C. Two horizontal disks of bitumen are heated at a controlled rate in a liquid bath while each of them supports a steel ball. The softening point is taken as the average of the temperatures at which the two disks soften enough to allow each ball, enveloped in bitumen, to fall a distance of 25 mm.

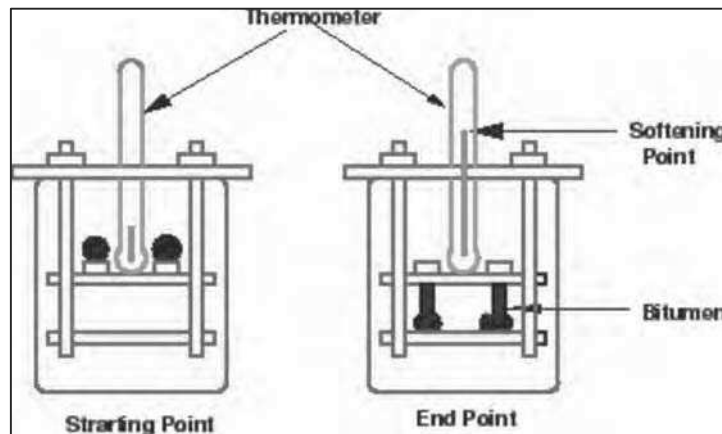


Figure A-1 Bitumen softening point test – Ring and Ball (Mathew, 2009)

### Penetration index

The penetration index ( $I_p$ ) is an evaluation of bitumen that combines the values attained from the penetration test ( $P$ ) and the softening point ( $t_{RnB}$ ) at 25°C, as shown in Equation A-1.

Equation A-1

$$I_p = \frac{20 * t_{RnB} + 500 * \log P - 1952}{t_{RnB} - 50 * \log P + 120}$$

### Flash point

The flash point test (EN ISO 2592) is used to determine the flammability of bitumen. The test exposes a sample of bitumen to an open flame while increasing the temperature. This test is used as a benchmark for the safety of the bitumen, as bitumen work is generally done at high temperatures, creating dangers from accidental ignition. A higher flash point indicates less flammable and thereby safer bitumen. This test can also be used to gage the amount of impurities in the bitumen as impurities will change the flammability temperature. The Cleveland Open-Cup method (ASTM D92) is used on asphalt cements or asphalts with relatively higher flash points, while the Tag Open-Cup (ASTM D1310) method is used on cutback asphalts or asphalts with flash points of less than 79°C.

### Viscosity

An example of a viscometer is shown in Figure A-2. The viscosity testing of bitumen has been described in Section 2.1.4.2.

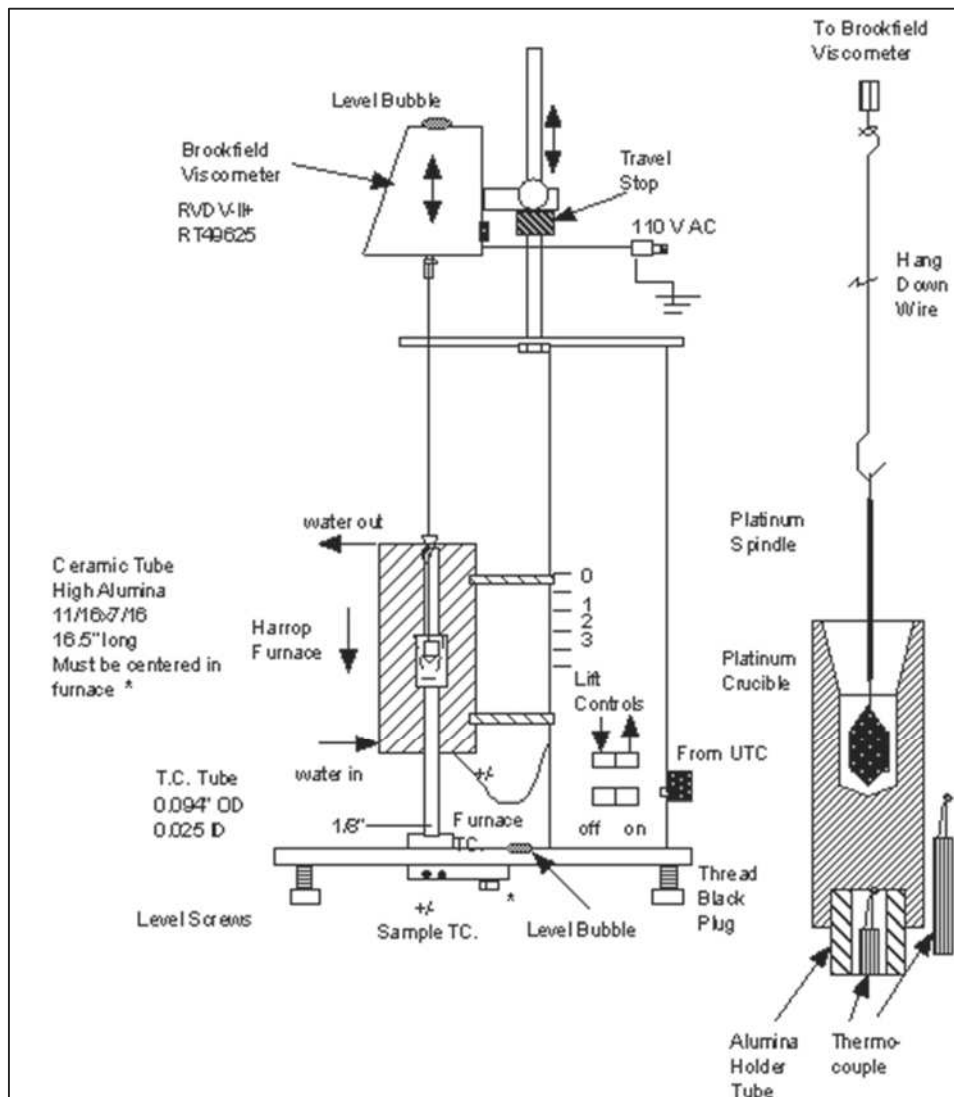


Figure A-2 Brookfield viscometer (Schumacher et al., 2000)

### Fraas breaking point

The Fraass breaking point (EN 12593) determines the brittleness of bitumen at low temperatures, using a Fraass breaking point tester.

### Solubility

The solubility test (EN 12592- ASTM D2042) is used to determine the bitumen purity by measuring its solubility in toluene. The bitumen content is the part that is not soluble in toluene and EN 12592 sets a minimum content for this at 99%. The production and transportation processes of asphalt can allow for the possibility of bitumen contamination.

### Density / specific gravity

The density and specific gravity of the bitumen at 25 °C can be found by EN 15326. It involves filling a volumetric pyknometer with bitumen and adding water on top to fill in the volume.

### Cohesion

The cohesion of bitumen is determined by the pendulum test (EN 13588). The principle of this test is to swing a pendulum (Mouton pendulum, Figure A-3) at a cube of bitumen and observe how the bitumen is able to cut through the sample. It is conducted at three temperatures within 10°C of each other. The cohesion (C) is defined as energy per unit area required to fully detach a cube from the support and is measured in J/cm<sup>2</sup> from Equation A-2.

Equation A-2

$$C = mgr(\cos \alpha - \cos \alpha')/s$$

Where,  $m$  is the mass of the pendulum (2 kg),

$g$  is the force of gravity (9.81 m/s<sup>2</sup>),

$\alpha$  (test with bitumen) and  $\alpha'$  (test without bitumen) are the maximum angles attained by the pendulum head after this swing, and  $s$  is the area of the sample, or the area of contact with the pendulum head (1 cm<sup>2</sup>).

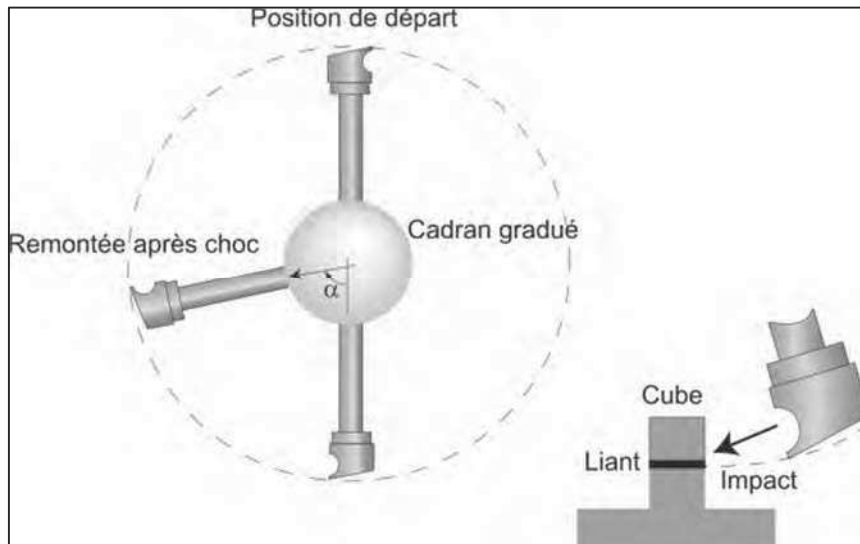


Figure A-3 Mouton pendulum (fr.wikipedia.org)

### Ductility test

The ductility test (EN 13589-ASTM D 113) is used to determine the tensile deformation properties of the bitumen. The ductility of bitumen has a significant effect on the deformation properties of the

corresponding asphalt, being an indicator of the resistance to cracking. The test consists of stretching a sample of bitumen (Figure A-4) at room temperature and measuring the point at which the bitumen breaks. The sample of bitumen is kept in a water bath at  $27^{\circ}\text{C}$  for  $90 \pm \text{min}$ . The sample (at  $25^{\circ}\text{C}$ ) is then pulled axially ( $50 \pm 2.5 \text{ mm/min}$ ) until the bitumen breaks. The ductility (in cm) is taken as the horizontal deformation of the bitumen during the stretching (Mathew, 2009).

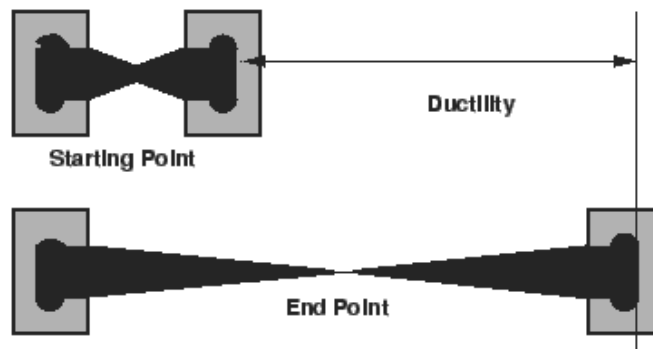


Figure A-4 Bitumen ductility test (Mathew, 2009)

#### **Adherence of bitumen to aggregates**

The adhesion of bitumen to aggregates has a very significant effect on the performance of asphalt (Curtis, 1992. Seddik and Emery, 1997). The adherence of bitumen to aggregates can be found using the ASTM D 5100 for Adhesion of Mineral Aggregate to Hot Bitumen. Although this test is intended for roofing applications, it is based on the same mechanism of bitumen-aggregates adhesion that applies to road pavements.

The test consists of applying an even layer ( $2.9\text{-}3.7 \text{ kg/m}^2$ ) of sand to hot bitumen ( $177\text{-}232^{\circ}\text{C}$ ). After 30 minutes of cooling, the sample is flipped over and the weight of the loose sand is measured. The mass of adhered aggregates ( $\text{kg/m}^2$ ) is found by subtracting the mass of loose aggregates from the original mass of aggregates.



## Appendix B. Asphalt gradation and fabrication

### Gradation of asphalt

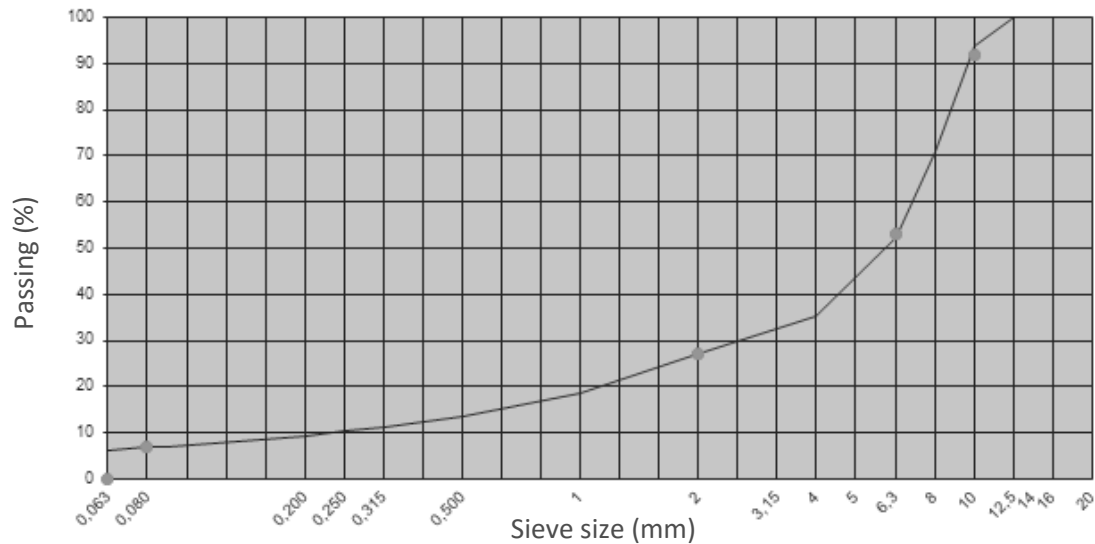


Figure B-1 Grading curve for asphalt

Table B-1 Gradations for Asphalt

Sieve size (mm)	Mass retained (%)				
	Aggregates 6.3/10 mm	Aggregates 2/6.3 mm	Sand 0/2 mm	Limestone filler (< 80 µm)	Total
20	100.0	100.0	100.0	100	100.0
16	100.0	100.0	100.0	100	100.0
14	100.0	100.0	100.0	100	100.0
12.5	100.0	100.0	100.0	100	100.0
10	88.4	100.0	100.0	100	93.9
8	44.7	100.0	100.0	100	70.7
6.3	12.4	93.9	100.0	100	52.4
4	2.0	36.6	100.0	100	35.3
2	1.6	4.3	94.2	100	27.1
1	1.6	2.6	62.4	100	18.5
0.5	1.6	2.2	43.9	100	13.7
0.315	1.6	1.9	34.8	100	11.3
0.25	1.6	1.9	31.0	100	10.3
0.2	1.6	1.7	27.0	100	9.3
0.08	1.6	1.5	17.9	93	6.8
0.063	1.6	1.4	16.2	76.0	6.2

### **Equipement for the fabrication of asphalt mix**

- Convection oven
- Aluminum containers
  - With cardboard covers
- Safety equipment
  - Oven gloves
  - Breathing mask
- Scoop
- Trowel
- Spatula
- Balance ( $\pm 1$  g)
- Plastic droppers 5 mL
- Proctor moulds (EN 13297-30)
- Compaction equipment
  - Proctor
  - Compressor with piston
- IR Thermometer
  - With thermocouple
- Cleaning equipment
  - Rags
  - Ethanol
  - BRs

## Appendix C. Bitumen Flow Test

The bitumen flow test measures the ability of the asphalt release agent to prevent the adherence between bitumen and a steel plate. There is a similar test in (NTPEP, 2014) called the “asphalt performance test”. As with the “mixture slide test”, it can be subjective and it is a pass/fail test.

The principle of the bitumen flow test is to measure the flow of hot bitumen along an inclined and ARA covered steel plate with the ARA-PEA (Figure C-1).

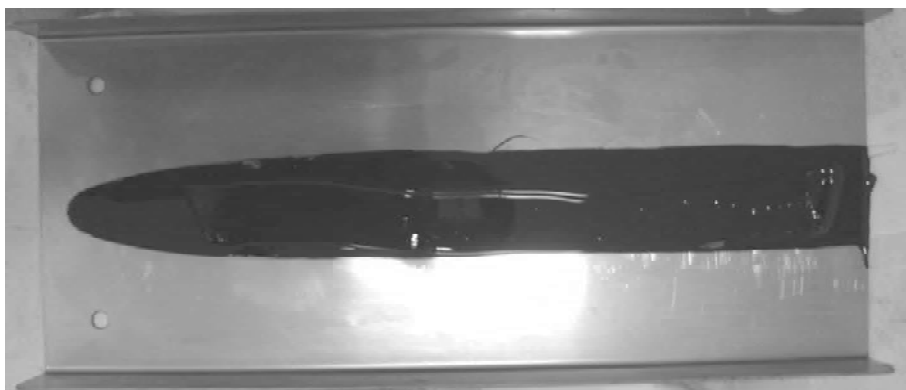


Figure C-1 Steel plate after bitumen flow test

Bitumen is heated in the oven for 120 min before the test so that it is at 160°C before the test. A steel plate is placed on the ARA-PEA and pre-heated to a certain temperature, it is inclined to a certain angle and an ARA is applied to it with a spray bottle (at around 75 g/m<sup>2</sup>). A certain quantity of bitumen is then poured from a container on top of the apparatus. As the bitumen flows down the middle of the plate and the following parameters could potentially be monitored:

- The temperature of the bitumen;
- The shape and speed of the bitumen flow from the image acquisition of the camera;
- The depth of the bitumen flow.

The bitumen flows down the plate and the speed is measured from the photos taken at 50Hz with the aid of the camera fixed on the ARA-PEA and a computer program Bituflow. The area of the bitumen at each image can then be quantified with the program.

Although this is measure of performance to a certain degree in terms of the ARA reduction in contact between steel and bitumen, the results correspond less to the field conditions than for AST as the latter is performed with asphalt. The application of ARAs to the field was shown to increase the velocity of the bitumen flow, although not enough testing was done to compare ARA performance. The depth of flow measurements were difficult to calibrate as well due to the rapidity

of the test. The principle reason the test was not developed further were the enormous difficulties in i) cleaning the bitumen off the plate after a test and ii) cleaning the bitumen of tools used in the test. The AST was far simpler in this aspect, even considering the fact that the AST requires the fabrication of asphalt.

## Appendix D. Bitumen Degradation Test FITR-ATR results

### Commercial agents

The solution in the beaker after the BDT is represented in blue, the agent by itself in red and the 35/50 bitumen used in the BDT in black.

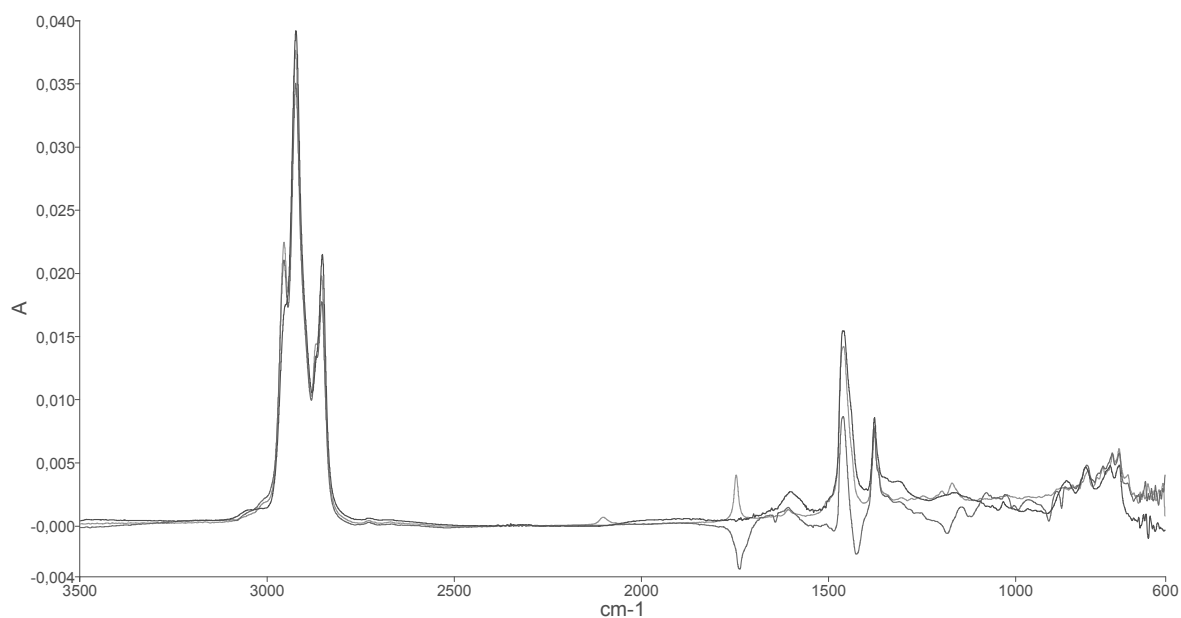


Figure D-1 FTIR-ATR Spectra Diesel for BDT solution (blue), agent (red) and 35/50 bitumen (black)

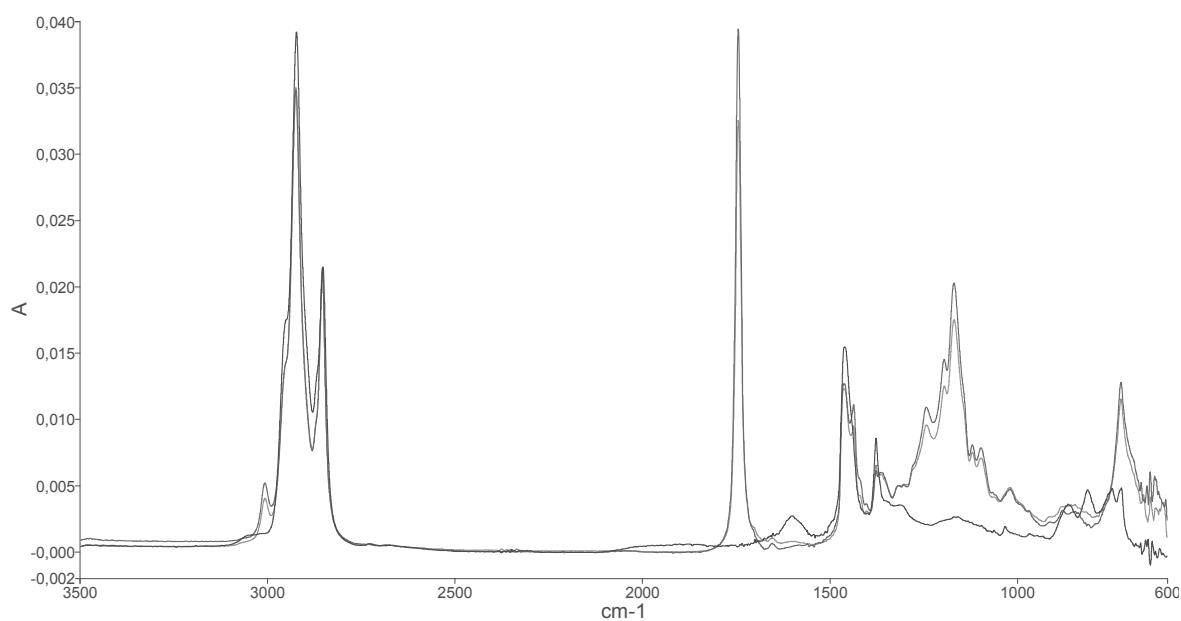


Figure D-2 FTIR-ATR Spectra ARA 1 for BDT solution (blue), agent (red) and 35/50 bitumen (black)

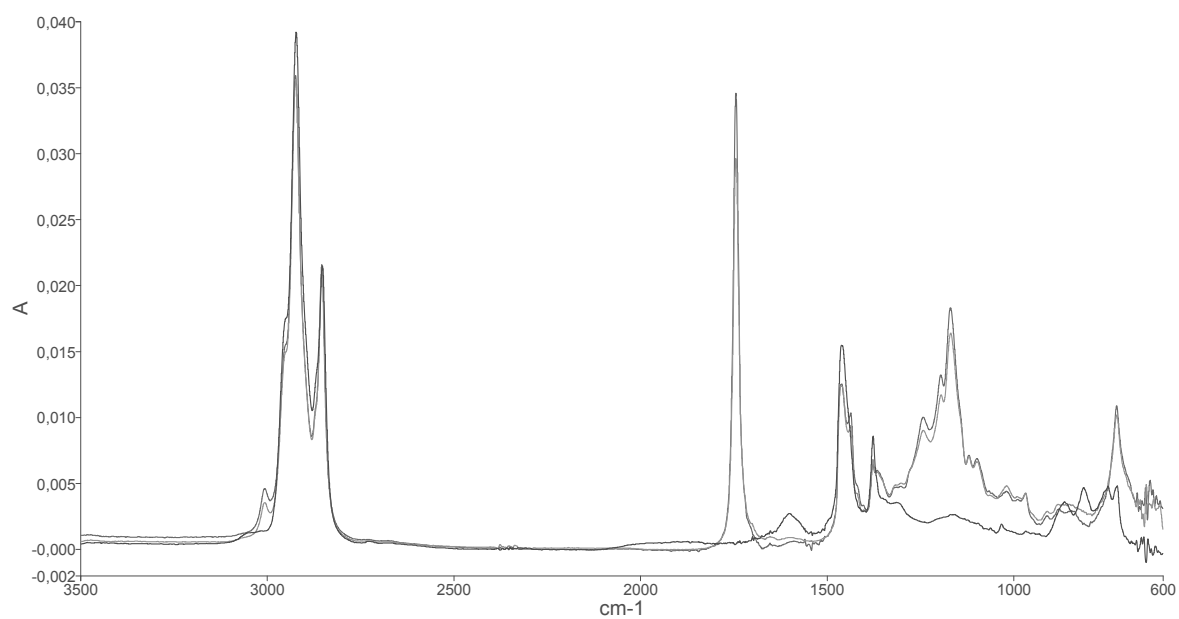


Figure D-3 FTIR-ATR Spectra ARA 2 for BDT solution (blue), agent (red) and 35/50 bitumen (black)

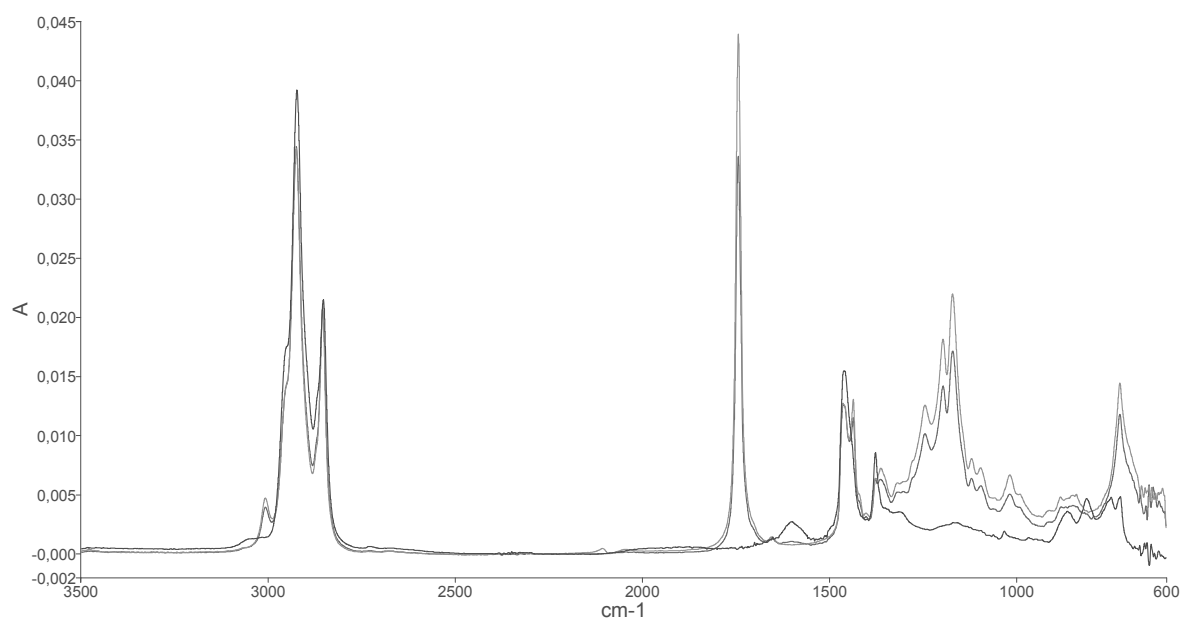


Figure D-4 FTIR-ATR Spectra ARA 3 for BDT solution (blue), agent (red) and 35/50 bitumen (black)

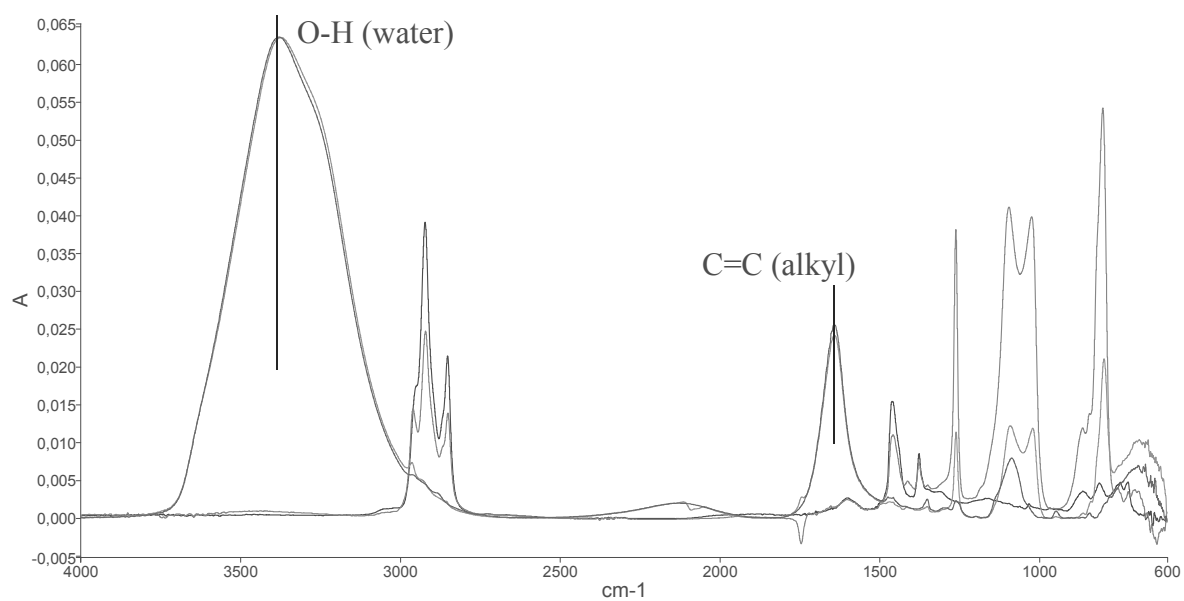


Figure D-5 FTIR-ATR Spectra ARA 4 for BDT solution (blue), agent (red), bitumen sample after test (green) and 35/50 bitumen (black)

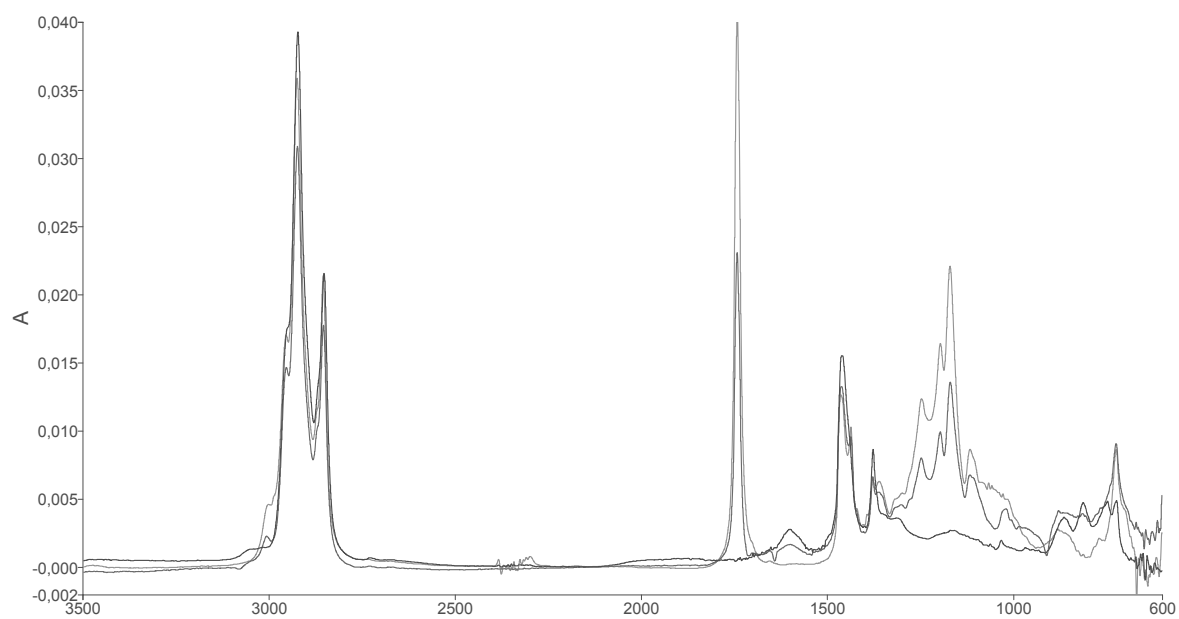


Figure D-6 FTIR-ATR Spectra BR 1 for BDT solution (blue), agent (red) and 35/50 bitumen (black)

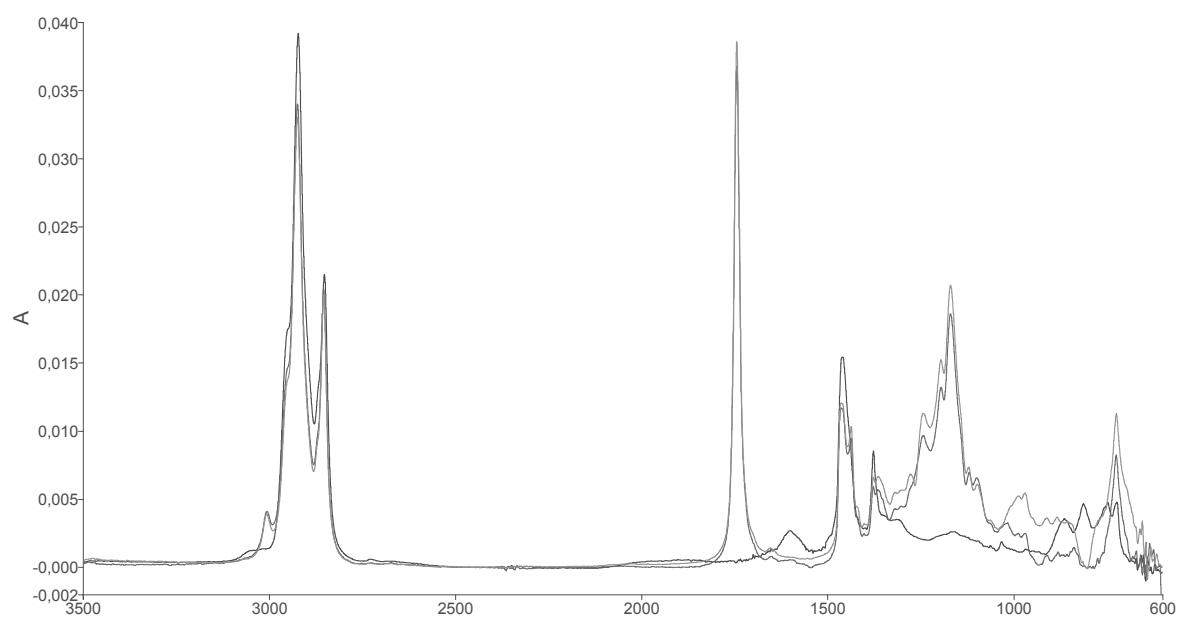


Figure D-7 FTIR-ATR Spectra BR 2 for BDT solution (blue), agent (red) and 35/50 bitumen (black)

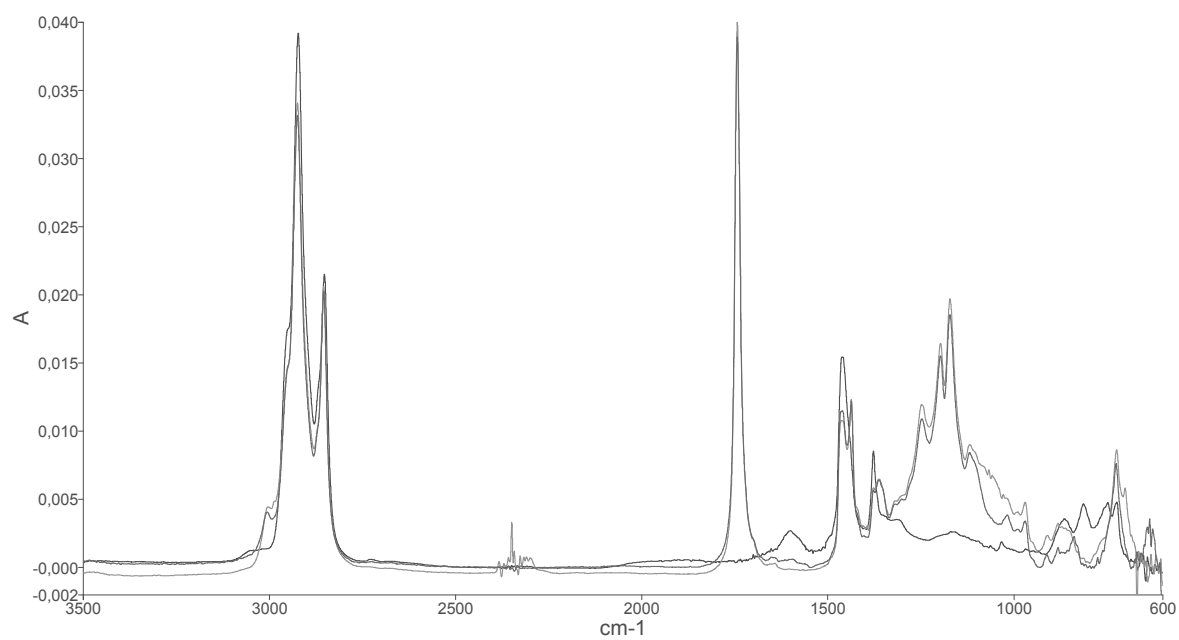


Figure D-8 FTIR-ATR Spectra BR 3 for BDT solution (blue), agent (red) and 35/50 bitumen (black)



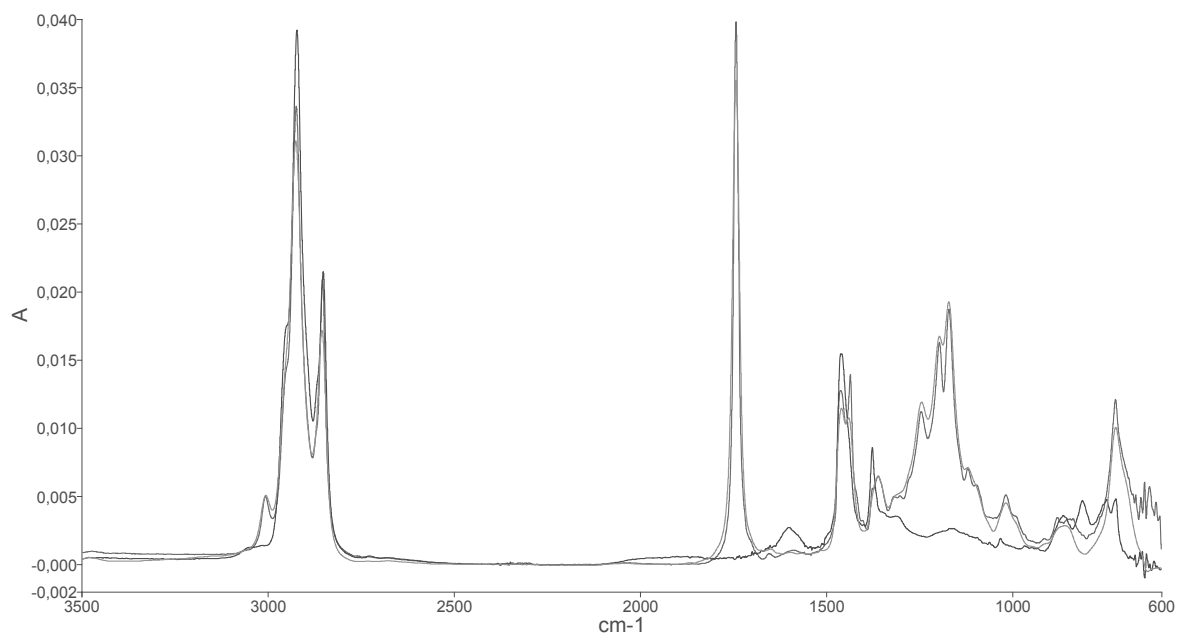


Figure D-9 FTIR-ATR Spectra BR 4 for BDT solution (blue), agent (red) and 35/50 bitumen (black)

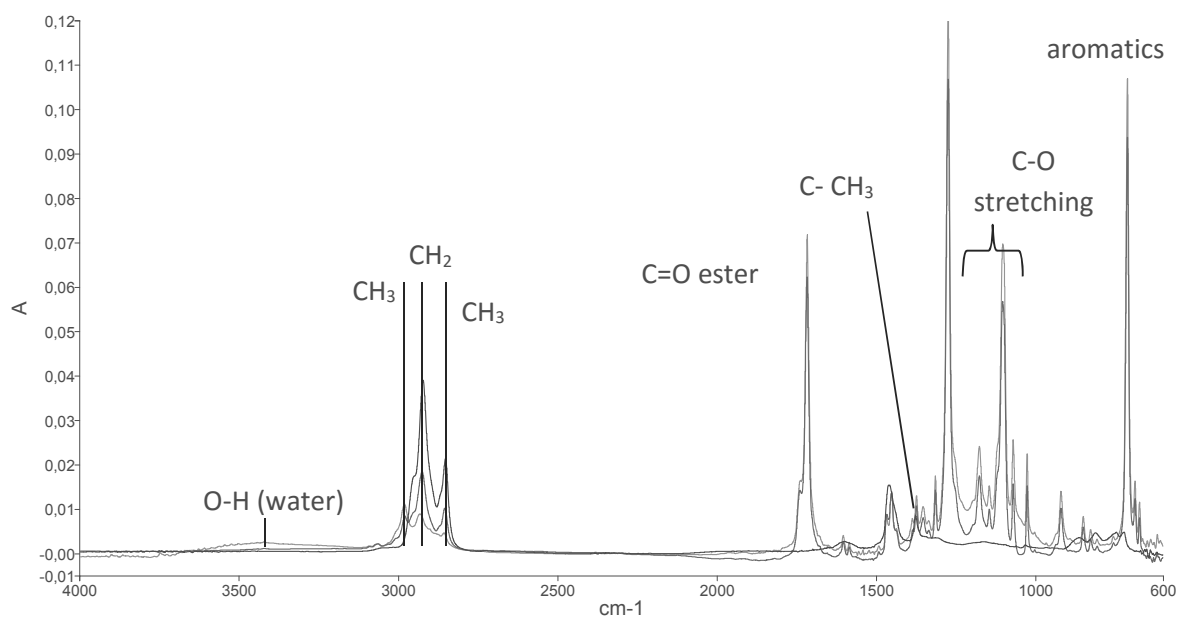


Figure D-10 FTIR-ATR Spectra BR 5 for BDT solution (blue), agent (red) and 35/50 bitumen (black)

### Candidate formulations

The solution in the beaker after the BDT is represented in blue, the agent by itself in red and the 35/50 bitumen used in the BDT in black.

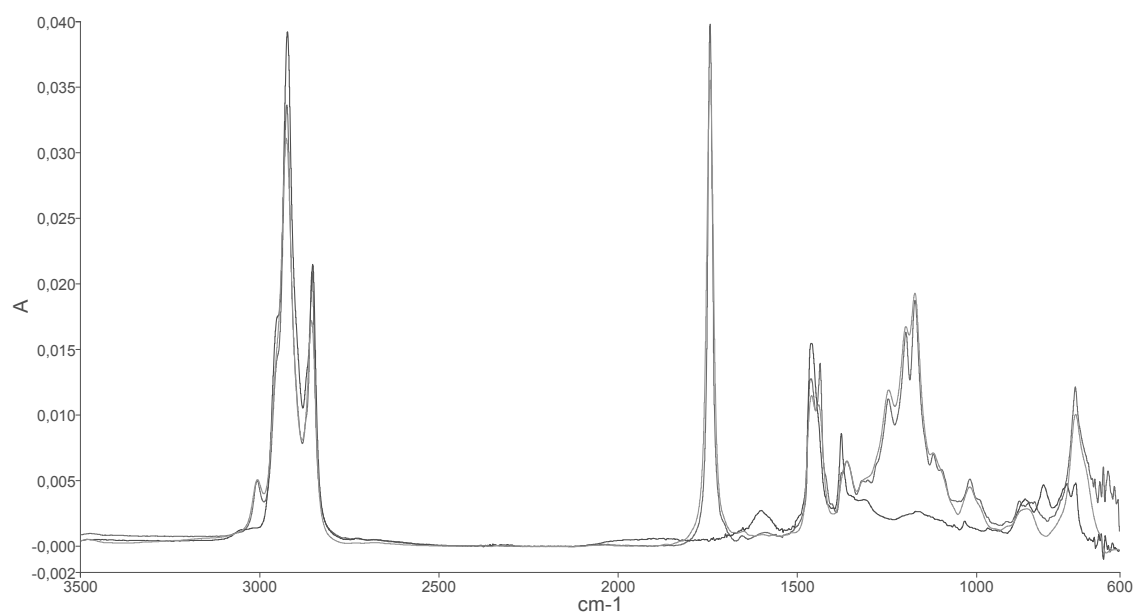


Figure D-11 FTIR-ATR Spectra C7 for pure formulation (red), BDT solution (blue) and 35/50 bitumen (black)

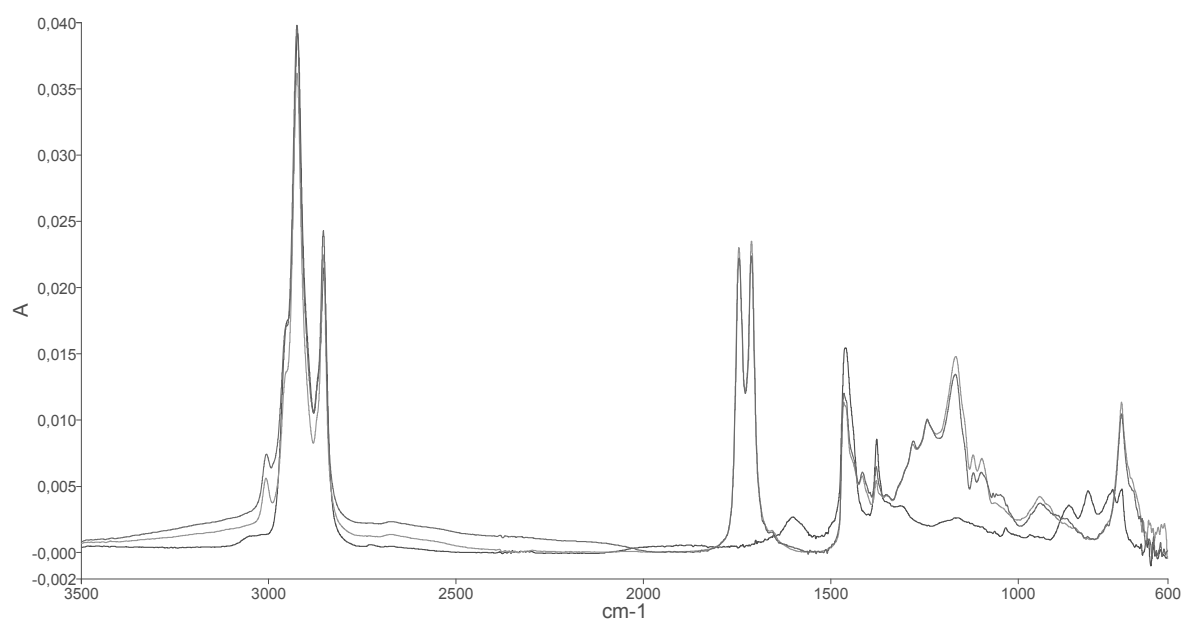


Figure D-12 FTIR-ATR Spectra RD 1 for pure formulation (red), BDT solution (blue) and 35/50 bitumen (black)

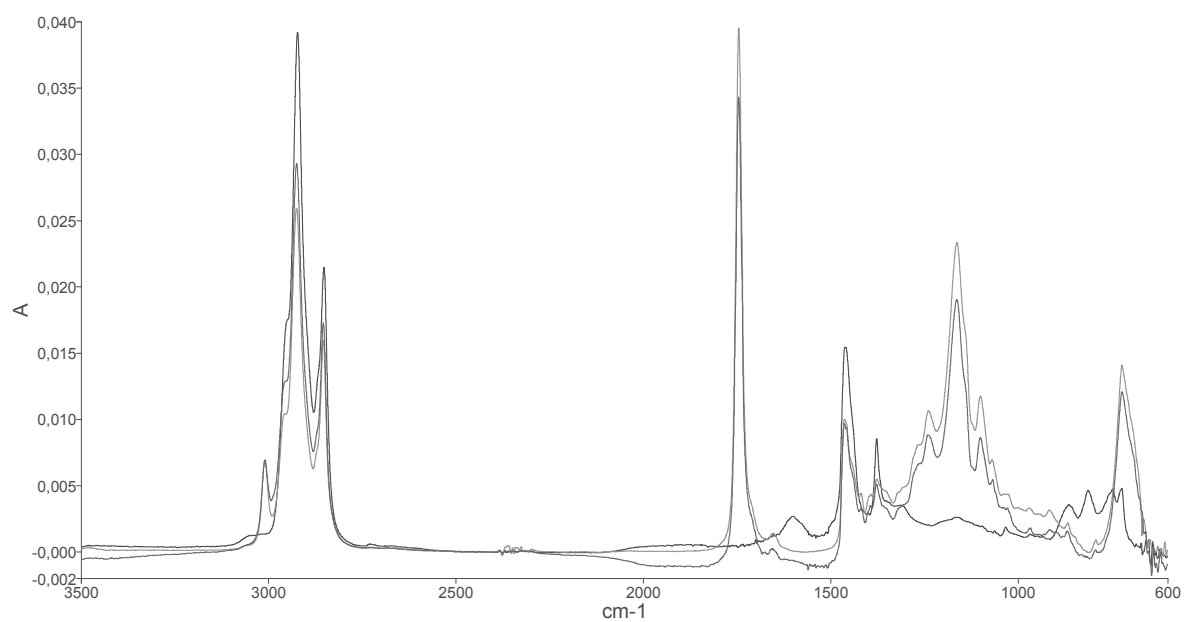


Figure D-13 FTIR-ATR Spectra RD 2 for pure formulation (red), BDT solution (blue) and 35/50 bitumen (black)

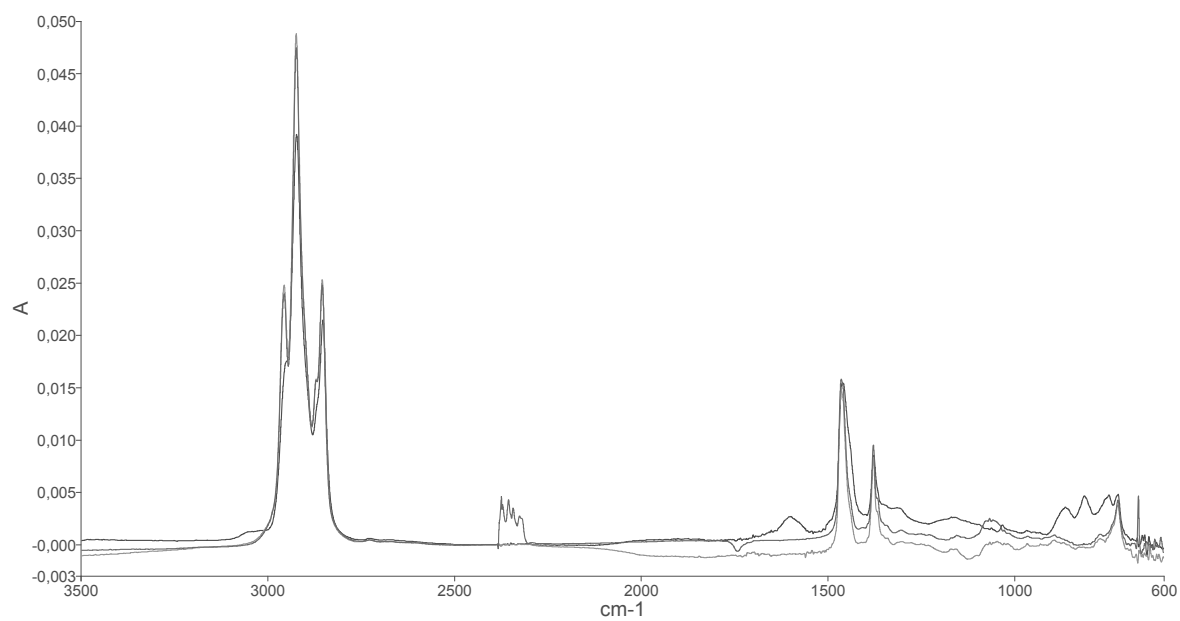


Figure D-14 FTIR-ATR Spectra RD 4 for pure formulation (red), BDT solution (blue) and 35/50 bitumen (black)

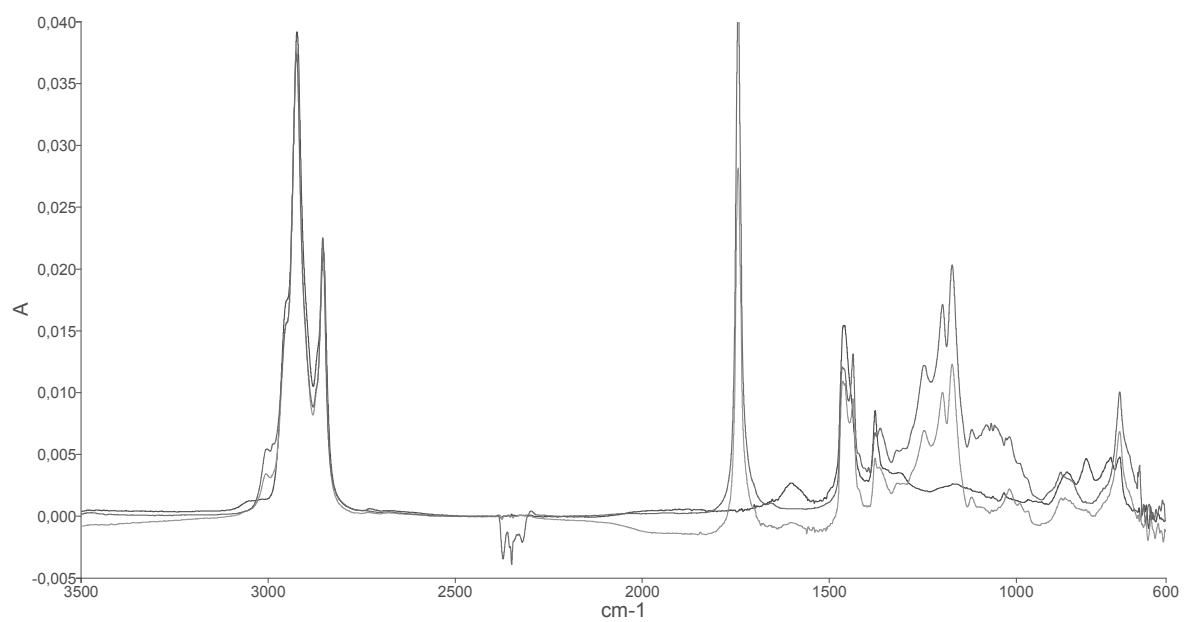


Figure D-15 FTIR-ATR Spectra RD 5 for pure formulation (red), BDT solution (blue) and 35/50 bitumen (black)

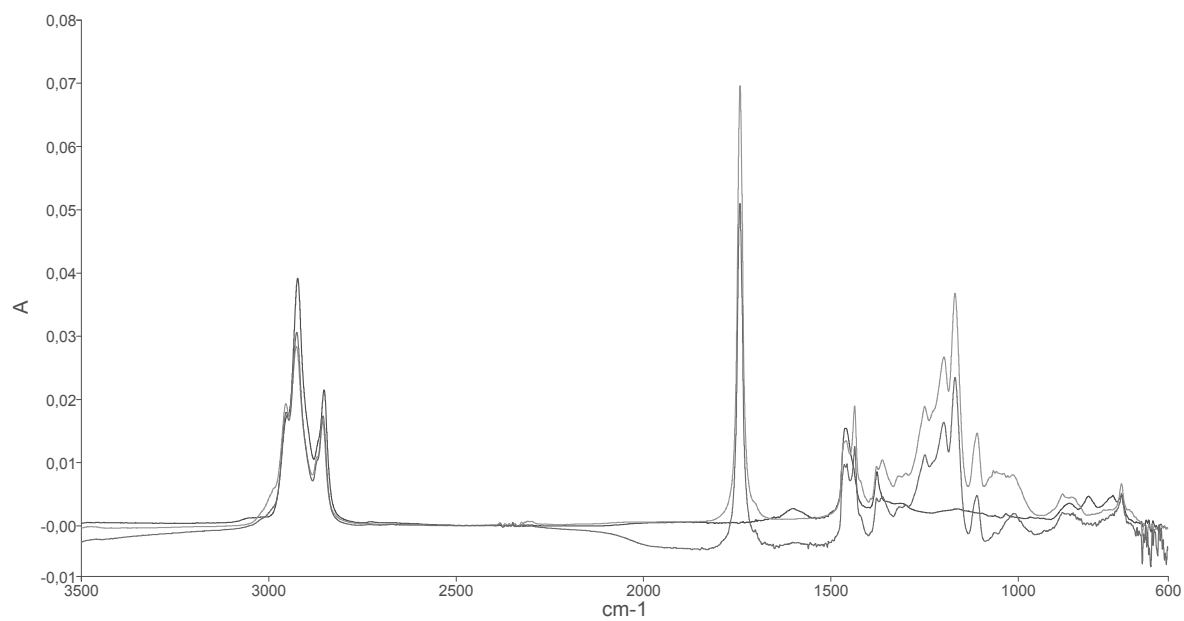


Figure D-16 FTIR-ATR Spectra RD 6 for pure formulation (red), BDT solution (blue) and 35/50 bitumen (black)

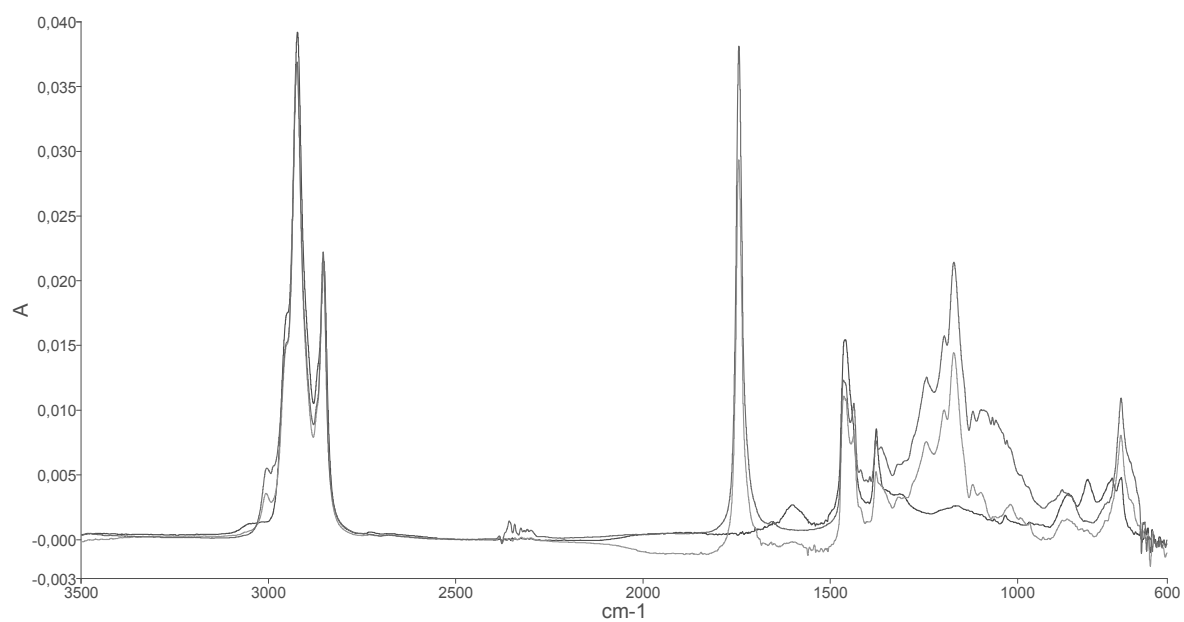


Figure D-17 FTIR-ATR Spectra RD 7 for pure formulation (red), BDT solution (blue) and 35/50 bitumen (black)

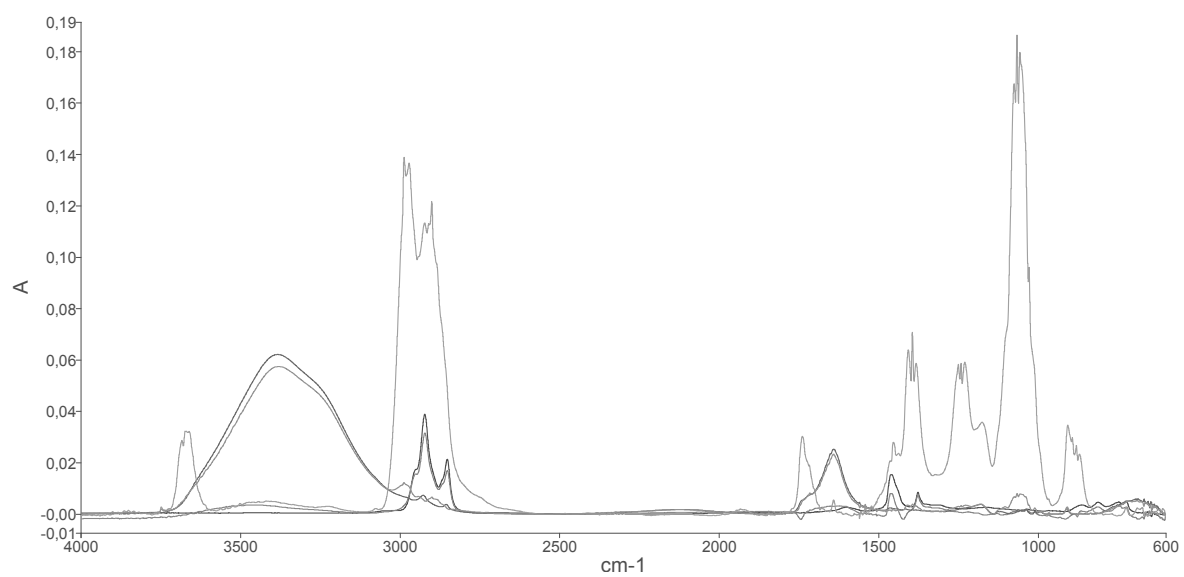


Figure D-18 FTIR-ATR Spectra MUG for pure formulation (pink), MUG 20 H 80 (red), MUG 20 H 80 BDT solution (blue), MUG 20 H 80 BDT bitumen sample (green) and 35/50 bitumen (black)

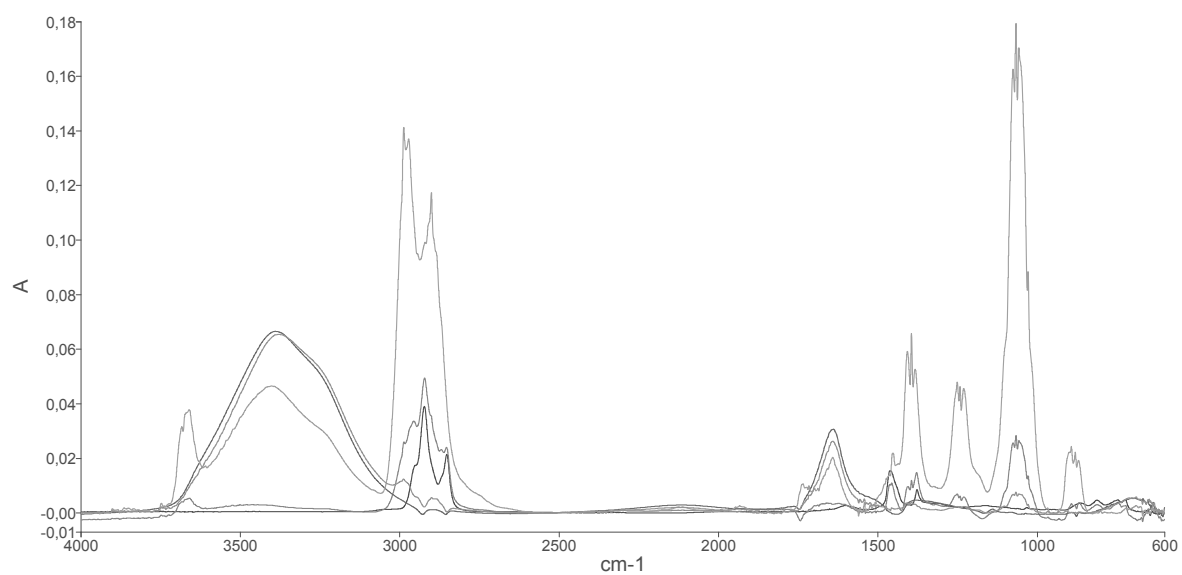


Figure D-19 FTIR-ATR Spectra MUDG for pure formulation (pink), MUDG 20 H 80 (red), MUDG 20 H 80 BDT solution (blue), MUDG 20 H 80 BDT bitumen sample green and 35/50 bitumen (black)

## **Appendix E. Bitumen microscopy**

The Scanning Electron Microscope (SEM) as shown in Figure E-1, began to appear commercially in the mid nineteen-sixties (Johnson, 1998). It can observe a sample with a focused beam of electrons. The interaction of the SEM electrons with those on the sample surface allows for a wide range of signals to be interpreted allowing the analysis of the sample's chemistry and topography (Figure E-2). The SEM can take pictures of a sample's surface at very high magnification, up to 100,000 times, although this exceeds the magnification we need for the purpose of this study. The SEM is able to scan a sample in two ways, through backscatter electron and through secondary electron scanning. Imaging through secondary electrons (SEI) is ideal for examining the texture of a surface. Backscatter electron scanning (BES) is ideal for identifying the elements that are present in the sample.

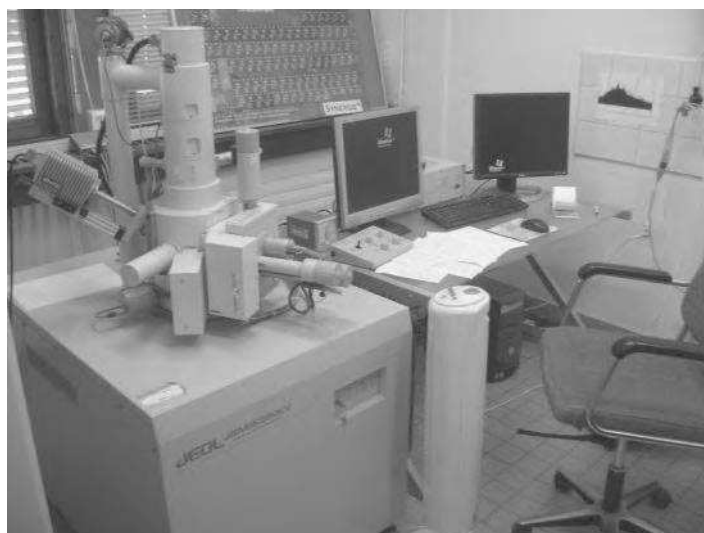


Figure E-1 SEM Jeol JSM-6380LV

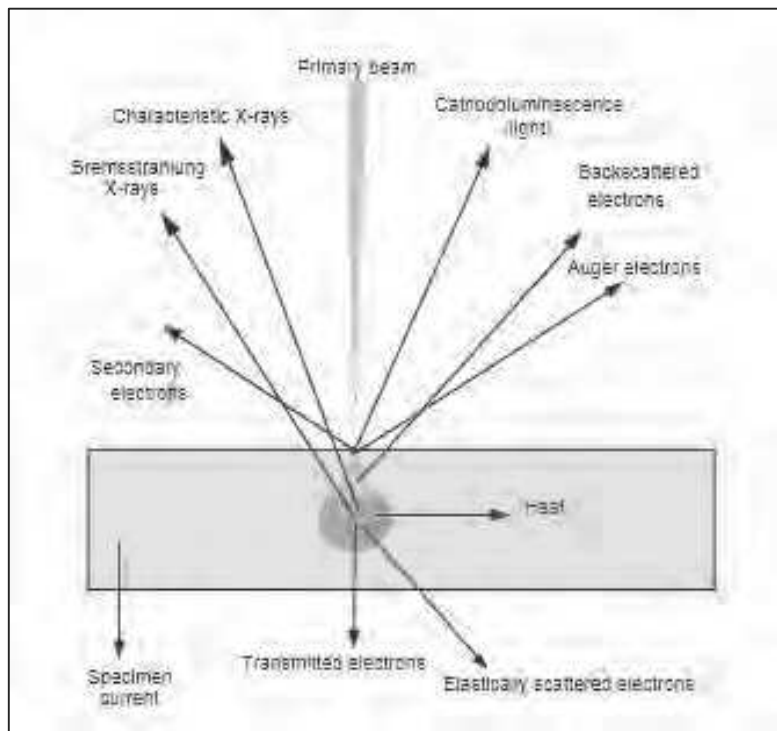


Figure E-2 SEM Signals (Johnson, 1998)

Through a feature called Energy Dispersive Spectroscopy (EDS) it is possible to perform elemental analysis on the samples, quantifying the elemental ratios of a certain point on the sample. This also allows for chemical analysis of a whole area as well, allowing the user to take a representative portion (although small) of the sample. There are also many other options available with the EDS program analysis, including line and area colour mapping. However it should be noted that that elemental quantification with elements lighter than Na generally does not provide an accurate representation (Rozeveld et al., 1997).